

DEVELOPMENT OF HUMAN VISUAL CORTEX

Development of human visual cortex:

A neurobiological approach

By Caitlin Rae Siu, B.Sc

A Thesis Submitted to the School of Graduate Studies in Partial Fulfillment of the
Requirements for the Degree Doctor of Philosophy

McMaster University

© Copyright by Caitlin Rae Siu, August 2017

DOCTOR OF PHILOSOPHY (2017)

(Neuroscience)

McMaster University

Hamilton, Ontario

TITLE: Development of Human Visual Cortex: A neurobiological
approach

AUTHOR: Caitlin Rae Siu, B.Sc (University of Windsor)

SUPERVISOR: Dr. Kathryn M. Murphy

NUMBER OF PAGES: xiii, 277

Lay Abstract

The ability to see the world constantly changes from birth to old age, and depends on the health and function of our brain. The visual cortex is the part of the brain that processes vision, and it is made up of millions of cells that connect to each other through billions of synapses. Fine-tuning those connections and networks in the brain leads to better vision. The ability for connections to be fine-tuned by experience is called plasticity, and it is necessary for developing good vision. This thesis addresses the development of plasticity in the human brain by measuring levels of proteins that are responsible for controlling plasticity and vision. My findings suggest that humans have a longer period of plasticity for developing good vision than previously thought. These findings will help identify new targets to rescue vision loss that occurs in aging or visual disorders across the lifespan.

Abstract

Human visual perception changes across the lifespan that relies on changes in synaptic plasticity in the visual cortex. Anatomical studies of the visual cortex, however, suggest human V1 develops early and remains relatively constant from childhood and on. Animal models have pinpointed specific neurobiological mechanisms that are necessary for the development of visual plasticity and receptive field properties in the visual cortex. Very little is known, however, about how those synaptic mechanisms develop in the human visual cortex to support plasticity and perception across the lifespan.

This thesis addresses this gap by providing new studies on the development of those neurobiological mechanisms in postmortem human visual cortex cases that range in age from 20 days to 79 years. The main findings from this thesis support prolonged development of plasticity mechanisms in human V1 that could be characterized in 5 stages of change across the lifespan: booting up synaptic function in infancy, high neural variability in young childhood, peaks of development in older childhood, prolonged plasticity in adulthood, and return to juvenile-like state in aging. In addition, I show a contrasting development of synaptic plasticity mechanisms in V1 and extrastriate areas that suggest higher order visual perception is processed differently. I also highlight a modernized technique for isolating synaptoneuroosomes in human brain that helps quantify synaptic proteins using postmortem human tissue. Together these findings aid in the translation of neurobiological mechanisms in animal models for identifying new therapeutic targets for recovery in human visual disorders and vision loss.

Acknowledgements

Thank you to my parents Cathy and Rory, my sisters Kirstin and Jillian, my Mah Mah, Yeh Yeh, Nana, Grampy, the rest of my family and the Balsor family for your patience, support, and comfort I needed to succeed. Thank you to my supervisory committee, Dr. Deda Gillespie and Dr. Pat Bennet for guidance and wisdom while navigating graduate school and preparing this thesis. Thank you to Dr. David Jones, for your mathematical insight. Thank you to Dr. Simon Beshara, for keeping me on my toes and being a good friend. Thank you to Dr. Kathryn Murphy, for teaching me with all of your energy and passion, and for leading me into a career I love. Thank you to Justin Balsor, for everything else.

Table of Contents

Chapter 1. General Introduction	1
1.1 Early development of the human visual cortex	2
1.2 Prolonged development of visual perception and plasticity of human visual cortex	8
1.3 Aging human visual cortex	10
1.4 Neurobiological mechanisms for plasticity and perception in animal models	11
Preamble for Chapter 2	21
Preamble for Chapter 3	22
Preamble for Chapter 4	24
Preamble for Chapter 5	26
Preamble for Chapter 6	27
Chapter 2. Use of synaptoneurosome samples to study development and plasticity of human cortex	29
2.1 Introduction	31
2.2 Materials	34
2.3 Methods	38
2.4 Notes	50
2.5 References	56
Chapter 3. Classic and Golli Myelin Basic Protein have distinct developmental trajectories in human visual cortex	60
3.1 Introduction	62
3.2 Materials and Methods	64
3.3 Results	69

3.4 Discussion	77
3.5 References	84
Chapter 4. Development of glutamatergic proteins in human visual cortex across the lifespan	90
4.1 Introduction	93
4.2 Materials and Methods	95
4.3 Results	103
4.4 Discussion	115
4.5 References	122
Chapter 5. Development of the tetrapartite synapse in human primary visual cortex (V1)	129
5.1 Introduction	131
5.2 Materials and Methods	135
5.3 Results	141
5.4 Discussion	148
5.5 References	155
Chapter 6. Development of synaptic mechanisms in human extrastriate cortex	162
6.1 Introduction	164
6.2 Materials and Methods	168
6.3 Results	176
6.4 Discussion	214
6.5 References	227
Chapter 7. General Discussion	238
7.1 Summary of Main Findings	238

7.2 Stages of Human Visual Cortex Development and Clinical Implications	241
7.3 Future Directions	251
References	252

List of Figures

Chapter 2

Figure 1	33
Figure 2	34

Chapter 3

Figure 1	70
Figure 2	73
Figure 3	75
Figure 4	76

Chapter 4

Figure 1	105
Figure 2	107
Figure 3	109
Figure 4	110
Figure 5	112
Figure 6	114
Figure 7	116

Chapter 5

Figure 1	132
Figure 2	142
Figure 3	143
Figure 4	145
Figure 5	147

Chapter 6

Figure 1	177
Figure 2	179
Figure 3	181
Figure 4	183
Figure 5	185
Figure 6	187
Figure 7	189

Figure 8	192
Figure 9	195
Figure 10	198
Figure 11	200
Figure 12	202
Figure 13	203
Figure 14	206
Figure 15	209
Figure 16	211
Figure 17	213
Figure 18	224
Figure 19	225
Figure 20	226

Chapter 7

Figure 1	241
Figure 2	243

List of Tables

Chapter 3

Table 1	65
---------------	----

Chapter 4

Table 1	95-96
---------------	-------

Chapter 5

Table 1	135-136
---------------	---------

Chapter 6

Table 1	168-169
---------------	---------

List of Abbreviations

2A	GluN2A
2B	GluN2B
AMPA	α -amino-3-hydroxy-5-methyl-4-isoxazolepropionic acid receptor
ANOVA	analysis of variance
β -tubulin	beta-tubulin
BCA	bicinchinchoic acid
BDNF	brain derived neurotrophic factor
CP	critical period
CSPG	chondroitin sulfate proteoglycan
DTT	dithiothreitol
E-I	excitatory/inhibitory
ECM	extracellular matrix
EDTA	ethylenediaminetetraacetic acid
EGTA	ethylene glycol tetra-acetic acid
fMRI	functional magnetic resonance imaging
GABA	gamma-aminobutyric acid
GAPDH	glyceraldehyde 3-phosphate dehydrogenase
GFAP	glial fibrillary acidic protein
GluA	glutamate receptor ionotropic AMPA receptor
GluN	glutamate receptor ionotropic NMDA receptor
HEPES	4-(2-hydroxyethyl)-1-piperazineethanesulfonic acid
LTD	long term potentiation
LTP	long term depression
MD	monocular deprivation
MBP	myelin basic protein
MT	medial temporal
NMDAR	N-methyl-D-aspartate receptor
ODC	ocular dominance column
ODP	ocular dominance plasticity
PBS	phosphate-buffered saline
PET	positron emission tomography
PMI	postmortem interval
PMSF	phenylmethylsulfonyl fluoride
PNNs	perineuronal nets
PSD-95	post-synaptic density protein 95
PV	parvalbumin
PVDF-FL	polyvinylidene difluoride
RF	receptive field
SDS-PAGE	sodium dodecyl sulfate polyacrylamide gel electrophoresis
SEM	standard error of the mean

Ube3A	ubiquitin protein ligase E3A
V1	primary visual cortex
V2d	dorsal second visual area cortex
V3	third visual area cortex
V4	fourth visual area cortex
VMR	variance-to-mean ratio

Declaration of Academic Achievement

Chapter 2 is a chapter that was submitted for publication in Springer Nature Protocol in Neuroscience Series under the section ‘Development and Disease’. This chapter was a collaboration between myself, Dr. Simon Beshara, Justin Balsor, Steven Mancini, and Dr. Kathryn Murphy. I was the lead on organizing the content of the chapter, and I wrote the chapter with Dr. Simon Beshara and Dr. Kathryn Murphy.

Chapter 3 is a paper that was published in Frontiers in Neuroscience. This chapter was a collaboration between myself, Justin Balsor, Dr. David Jones, and Dr. Kathryn Murphy. Justin Balsor and I are co-authors on this paper. I was the lead on designing and performing the experiments, analyzing the data, and I wrote the manuscript with Justin Balsor and Dr. Kathryn Murphy.

Chapter 4 is a paper that was published in Journal of Neuroscience. This chapter was a collaboration between myself, Dr. Simon Beshara, Dr. David Jones, and Dr. Kathryn Murphy. Dr. Simon Beshara and I are co-authors on this paper. I was the lead on performing the experiments, analyzing the data, and I wrote the manuscript with Dr. Simon Beshara and Dr. Kathryn Murphy.

Chapter 5 was a collaboration between myself, Justin Balsor, and Dr. Kathryn Murphy. I was the lead on designing and performing the experiments, analyzing the data, and I wrote the manuscript.

Chapter 6 was a collaboration between myself, Dr. David Jones, and Dr. Kathryn Murphy. I was the lead on designing the experiments, analyzing the data, and I wrote the manuscript.

Chapter 3 Citation

Siu, C. R., Balsor, J. L., Jones, D. G., & Murphy, K. M. (2015). Classic and Golli Myelin Basic Protein have distinct developmental trajectories in human visual cortex. *Frontiers in Neuroscience*, 9, 138–10. <http://doi.org/10.3389/fnins.2015.00138>

Chapter 4 Citation

Siu, C. R., Beshara, S. P., Jones, D. G., & Murphy, K. M. (2017). Development of Glutamatergic Proteins in Human Visual Cortex across the Lifespan. *The Journal of Neuroscience : the Official Journal of the Society for Neuroscience*, 37(25), 6031–6042. <http://doi.org/10.1523/JNEUROSCI.2304-16.2017>

Chapter 1. General Introduction

Preamble

Visual perception changes across the lifespan and is characterized by many developmental visual milestones as well as changes in vision in aging. Perceptual, physiological, and anatomical studies have pointed to the visual cortex as the source of visual processing necessary for the normal development of human vision. Despite decades of research, however, our understanding of how the human visual cortex develops remains conflicted. Many vision scientists rely on animal models to help identify the neurobiological mechanisms in the cortex that underlie visual perceptual abilities. Animal research has significantly moved the field forward in understanding mechanisms of basic visual perception and neuroplasticity. Human vision is complex, however, and the translation of those neurobiological mechanisms for understanding human visual development has been slow. Thus, there is a call-to-action for investigating the neurobiological mechanisms of visual perception in the developing human brain. Studies in this thesis provide a link between those animal models and human visual development by characterizing the development of neurobiological mechanisms for visual plasticity and perception in the human visual cortex across the lifespan. In this introduction, I will discuss the foundation of research on the human visual cortex that has led to our modern understanding of visual perception and my hypotheses about the development of the human visual cortex.

1.1 Early development of the human visual cortex

The dominant view of human visual cortex development originates from early studies in postmortem human brain samples that showed cytoarchitectonic features, including myelination, lamination, and dendritic axonal processes of the human visual cortex, appear immature at birth but become adult-like within the first few years (Conel, 1939-1967; Huttenlocher et al., 1982).

However, animal studies showed that the development of the visual cortex is regulated by visual experience. Dr. David Hubel and Dr. Torsten Wiesel discovered organization of the cat visual cortex is dependent on binocular vision (Wiesel and Hubel, 1963), and that neurons in the visual cortex have specific response properties for stimuli in the visual field (Hubel and Wiesel, 1959; 1962). Those studies inspired many investigations of structure and function in the human visual cortex that underlie the development of vision.

Early visual milestones are dependent on visual experience

Although the single-cell receptive field (RF) properties studied in animal models are difficult to measure in human visual cortex, both visual evoked potentials (VEP) and perceptual thresholds have been used to estimate the development of neuronal RF properties in humans. VEP recorded at the scalp over the visual cortex have revealed neurons with response selectivity to different characteristics of visual stimuli, like orientation and spatial frequency (Campbell and Maffei, 1970). VEP measurements in infants showed that contrast sensitivity (Allen et al., 1996; Pirchio et al., 1978), spatial frequency selectivity (Norcia and Tyler, 1985; Sokol and Jones, 1979) and orientation selectivity (Morrone and Burr, 1986) develop within the first year of life. Behavioural studies that use perceptual thresholds also provide evidence for visual development in the first year of life. For example, such studies have tracked the development of grating acuity (Gwiazda et al., 1980), orientation selectivity (Campbell and Kulikowski, 1966; Hood et al., 1992), stereoacuity (Held et al., 1980), and binocular convergence (Thorn et al., 1994) during infancy.

Matched binocular visual experience is necessary for development of visual perception, especially binocularity. In children, the sensitive period for binocularity begins with the onset of

binocular vision at 4-6 months of age (Gwiazda et al., 1980) and peaks between 1 and 3 years of age (Banks et al., 1975; Hohmann and Creutzfeldt, 1975). Abnormal binocular vision caused by misalignment, unequal refraction (Birch et al., 2010), or opacity in one or both eyes (Leinfelder, 1962) during this sensitive period can result in amblyopia (Levi et al., 2011; McKee et al., 2003; Mitchell et al., 1973). Amblyopia is marked by central visual field acuity loss (Agervi et al., 2010), and deficits in visual evoked responses (Arden et al., 1974; Levi, 1975), contour processing (Levi et al., 2007), motion processing (Luu and Levi, 2013; Tychsen and Lisberger, 1986), contrast sensitivity (Polat et al., 1997) and hyper acuity (Levi and Klein, 1982). Some of those perceptual deficits can recover rapidly if binocular vision is restored in infancy. For example, improvements in visual acuity occur in as little as 1 hour after cataract removal (Maurer et al., 1999), although higher-level visual deficits persist into adulthood (Segalowitz et al., 2017).

Structural development of human visual cortex

During prenatal development, axons of bipolar cells and pyramidal cells develop with long and thin dendritic spines at around 14 weeks gestation. At 20 to 24 weeks gestation, the 6 cortical layers in human V1 are differentiated (Takashima et al., 1980), while layers III and V mature through prenatal development (Becker et al., 1984). Neuronal density is initially high with over 1 million cells/mm³ at 21 weeks gestation, then decreases to about 90,000 cells/mm³ at birth, and reaches adult levels of about 40,000 cells/mm³ by 4 months postnatally (Leuba and Garey, 1987). Vertical intracolumnar connections develop 26-29 weeks gestation, and become adult-like in patchiness around 8 weeks postnatal, while long-range horizontal intercolumnar connections in layers IVB and V emerge later around 37 weeks gestation, and show adult-like patchiness around

15 months postnatal (Burkhalter et al., 1993). Pyramidal neurons develop progressively by layer, expressed in infragranular layers (V and VI) by the 1st postnatal day, expressed in layer IVB by 5 months, in supragranular layer III by 15 months, and reach adult levels of expression by 3 years of age (Ang et al., 1991).

Postnatally, the human visual cortex is further refined, as visual experience begins to shape functional organization. The number of synapses in human V1 is highest between 8 months and 2 years then declines to adult levels (Huttenlocher et al., 1982). This trajectory is paralleled by counts of dendritic spines across development that peak around 5 months of age and decrease to adult levels by 2 years (Michel and Garey, 1984). Measures of total neuronal density show the same overshooting with neuron production increasing up to 8 months, with the highest rate of loss found in layers II-IVA (Klempfner et al., 1991).

Human primary visual cortex (V1) carries feedforward signal to the second visual area V2, called feedforward projections that mature 4 months of age (Burkhalter, 1993). Feedback matures later, at around 2 years of age (Burkhalter, 1993). Thus, anatomical studies of the development the human visual cortex suggested the majority of development in the primary visual cortex (V1) matures within the first few years.

Noninvasive in vivo imaging of human cortex shows functional organization and prolonged cortical development

The development of noninvasive high-resolution functional imaging allowed for in vivo anatomical studies of the human cortex. In vivo imaging provided maps of functional organization in the human visual cortex, as well as evidence for prolonged trajectories of

development beyond the first few years. Positron-emission tomography (PET) scanning using cerebral blood flow has been used to map the retinotopic receptive field (RF) in the visual cortex, revealing individual functional zones that are separated by less than 3mm (Fox et al., 1986). PET was used to map the higher-order dorsal and ventral visual pathways (Grady et al., 1992; Haxby et al., 1991a; 1994), and showed those functional maps tied to higher-order visual percepts in the human cortex were analogous to maps in nonhuman primates (Haxby et al., 1991b). Spatial organization of higher order visual areas, such as the fusiform gyrus and lateral occipital cortex, is present in the human brain by 4-6 months of age (Deen et al., 2017), but the subsequent pace of maturation for both dorsal and ventral visual streams into adulthood are still debated (Simic & Rovet, 2016).

Functional magnetic resonance imaging (fMRI) provides finer resolution for mapping RFs in human visual cortex, revealing functional zones separated by less than 1.4mm (Engel, 1994). fMRI was used to further refine retinal eccentricity maps on the visual cortex (Engel, 1994), and patterns of response properties such as colour selectivity (Engel et al., 1997). RF sizes vary by cortical areas, as the smallest RFs are located in V1 and become increasingly larger in each higher order visual area, as well as with increasing retinal eccentricity (Smith et al., 2001). fMRI has been used to measure single-cell visual summation of cortical neurons in human V1 that is similar to mechanisms found in macaques (Nurminen et al., 2009).

Imaging studies show that intracortical myelin in human visual cortex develops well into adulthood, peaking around 30 to 40 years of age (Rowley et al., 2017). Postmortem analysis of human visual cortex supports the evidence for prolonged myelination into the third decade of life

that is unique to humans (Miller et al., 2012). Gray matter density mapping shows a slow linear decline of cortical thinning with age in the occipital cortex (Sowell et al., 2003; 2004), that regression appears to mature sequentially across the cortical areas, with primary areas maturing before higher-order association areas (Gogtay et al., 2004). This hierarchical development of human cortical areas was revealed by synapse counting where synaptic density reaches adult levels first in V1, then in the middle frontal gyrus, and finally in frontal cortex by 16 years (Huttenlocher, 1990). Even within the visual cortical areas, there is still much debate on the pace of development for the dorsal and ventral visual streams in humans, largely due to discrepancy in development of those higher order visual abilities.

Dorsal and ventral visual streams are largely differentiated by thalamic magno- and parvocellular visual input (Livingstone and Hubel, 1987), respectively, from segregated layers in the lateral geniculate nucleus (LGN) (Denison et al., 2014). Those feedforward receptive field properties that contribute to their functional organization in 2 visual processing streams in higher order visual cortex (Livingstone and Hubel, 1988). In nonhuman primates the two pathways of extrastriate visual processing exhibit functional specialization: The ventral stream, including striate and inferior temporal areas, is important for object and form perception (Desimone and Schein, 1987; Mishkin et al., 1983), whereas the dorsal stream, including striate and inferior parietal areas, is important for motion and spatial processing (Albright et al., 1984; Distler et al., 1996; Goodale and Milner, 1992; Mishkin et al., 1983; Van Essen and Gallant, 1994).

Imaging studies have provided evidence for higher-order visual abilities align with those extrastriate areas that together develop later into adolescence and adulthood . fMRI shows that

extrastriate areas that have functional specialization like face and scene processing actually emerge within a few months after birth, but are not adult-like (Deen et al., 2017). The development of face processing in the fusiform gyrus matures through childhood as fMRI responses decrease to non-preferred visual categories (Cantlon et al., 2010). fMRI of the fusiform gyrus, however, shows substantial increases of cortical tissue volume into adulthood (Golarai et al., 2010), that could be explained by cortical proliferation and is linked to late development of face processing (Gomez et al., 2017). In human extrastriate, the magno- and parvo-cellular streams remain segregated throughout the cortical areas (V2, V3, V3a, V4) (Tootell and Nasr, 2017). Some of the discrepancy between developmental delays in the dorsal and ventral visual streams may be due to extrastriate cortical reorganization of visual processing from infancy to adulthood, as global motion processing in infants is processed by area V5 (MT), but in adults global motion is dominated by areas V3 and V6 (Wattam-Bell et al., 2010).

1.2 Prolonged development of visual perception and plasticity of human visual cortex

Many aspects of human visual perception develop beyond the first few years of life, although specific ages of maturity largely depend on the approach to measuring vision. For example, a broad age range of maturity has been suggested for visual acuity between 5-15 years, and contrast sensitivity between 8 and 19 years of age (Leat et al., 2010). Spatial contrast sensitivity using vertical sine-wave gratings is adult-like by 7 years, and grating acuity adult-like by 6 years, whereas temporal contrast sensitivity at high frequency is adult-like by 4 years, but at lower-frequencies is adult-like around 7 years (Elleberg et al., 1999). Global and biological motion (Bogfjellmo et al., 2014; Bucher et al., 2006; Hadad et al., 2015; Hadad et al., 2011; Meier and

Giaschi, 2017; Schrauf et al., 1999), as well as spatial integration of contours (Kovacs et al., 1999) is mature in adolescence (i.e., 14-15 years of age). Face perception shows a slower pace of maturation, developing through childhood and adolescence (Gao et al., 2010). Mondloch et al., suggest the slow development of face perception depends on configural face processing, or the spacing between facial features rather than the shapes or contours of the features themselves (Mondloch et al., 2002). Face learning and face recognition matures nearly a decade later than that of motion perception, into mid 30s (Germine et al., 2011; Hartshorne and Germine, 2015; Susilo et al., 2013).

Perceptual learning in adulthood: plasticity in adult vision

There is significant evidence for visual plasticity that extends into adulthood. The end of susceptibility to developing amblyopia ends in humans between 6-10 years, however there are sensitive periods for multiple aspects of visual development, including the sensitive period for visually-driven normal development, and the sensitive period for recovery from amblyopia (Lewis and Maurer, 2005). Although children older than 7 years of age have been found to be less responsive to amblyopia treatment (Holmes, 2011), visual plasticity persists in the adult visual cortex, depending on the type and amount of visual training, making treatment for amblyopia possible and effective throughout adulthood (Karni and Bertini, 1997; Levi and Li, 2009; Sasaki et al., 2009). For example, perceptual learning of low-level perceptual abilities like contrast sensitivity and letter-recognition can be learned in adulthood of amblyopic patients whom did not develop these abilities during childhood (Polat et al., 2004). The perceptual learning is persistent, that suggests long-term plastic changes in the underlying neural mechanisms.

Perceptual learning is effective using monocular high-contrast sine-wave gratings visual training, but takes thousands of trials for improvement (Ding and Levi, 2011). In normal binocular adults, perceptual learning of specific orientations can refine selectivity in V1 and the early extrastriate areas (V2-V4), but takes up to 10,000 trials (Jehee et al., 2012). It has been suggested that higher order visual areas participate strongly in perceptual learning, as perceptual learning for complex stimuli, like faces are rapidly learned (McMahon and Leopold, 2012), and with significantly fewer trials (Hussain et al., 2009) compared to simpler stimuli like orientated gratings. These findings may be attributed to theories of attention in perceptual learning for higher order stimuli (Doshier and Lu, 2006), suggesting differences in underlying neuroplasticity mechanisms between V1 and extrastriate areas. Together with the prolonged development of visual perception, perceptual learning in adulthood suggests significant experience-dependent plasticity remains in the visual cortex well beyond the critical period in humans.

1.3 Aging human visual cortex

Aging in the visual cortex is characterized by changes in both structural and functional abnormalities. Structurally, there is a significant loss of dendrite number and changes in morphology of somata and dendritic arborizations of pyramidal cells in human visual cortex (Mavroudis et al., 2015). Intracortical myelin in the visual cortex remyelinate with less compact and with shorter segments that can negatively affect efficiency axonal conduction (Peters and Sethares, 2003; Peters et al., 2000; Peters et al., 2008). Many animal studies have pointed to the loss of intracortical inhibition as a mechanism of age-related losses in visual function, as treating old monkeys with GABA improved degraded orientation selectivity in V1 (Leventhal, 2003).

Functionally, many studies have shown loss of visual function through a variety of age-related changes in visual receptive field properties. In normal healthy aging, there is an increase in population receptive field size in foveal representations of V1 and V2 (Brewer and Barton, 2014), that could contribute to collective age-related changes in visual acuity. There are age-related losses in basic visual perceptual abilities like visual acuity (Sekuler et al., 1980), contrast sensitivity (Allard et al., 2013b; Owsley et al., 1983), and orientation selectivity (Betts et al., 2007). There is however, a large effect of aging on higher-order visual stimuli (Habak and Faubert, 2000), including face processing (Germine et al., 2011; Konar et al., 2013; Rousselet et al., 2010; Wilson et al., 2011), and motion processing (Allard et al., 2013a; Bennett et al., 2007; Betts et al., 2005; Fernandez et al., 2013; Kavcic et al., 2013).

1.4 Neurobiological mechanisms for plasticity and perception in animal models

Despite the advances that human research has provided for understanding the complexity of human vision, it is the animal studies of visual perception and plasticity that have moved the field of visual neuroscience forward over the last 30 years. Those animal studies have provided specific mechanisms that underlie fine-scale aspects of visual plasticity and perception that are necessary for development of vision. The knowledge gained from animal models of visual plasticity and perception that have inspired each of the chapters in my thesis to better understand the development of those neurobiological mechanisms in the human visual cortex.

Neurobiological mechanisms that regulate critical period plasticity

The timing of the critical period (CP) for ocular dominance plasticity (ODP) is regulated by development and visual experience that triggers changes in excitatory and inhibitory neurons.

Inhibitory GABAergic transmission is necessary for experience-dependent plasticity during the critical period (Hensch et al., 1998). It is the increase of GABAergic transmission that must reach an inhibitory threshold in the visual cortex that activates the CP for monocular deprivation in mice (Fagiolini and Hensch, 2000). When this inhibitory threshold is reached, there is an excitatory-inhibitory (E-I) balance in the cortex that allows for synaptic consolidation. The E-I balance is regulated at the individual cell level (Xue et al., 2014), and can be onset by many factors including scaffolding proteins (Prange et al., 2004), visual experience (Beston et al., 2010), cell adhesion molecules like polysialic acid and neuroligin (Di Cristo et al., 2007; Prange et al., 2004). During development, binocular vision functionally organizes the visual cortex into ocular dominance columns (ODC), that can be disrupted with monocular deprivation (Wiesel and Hubel, 1963). During the CP, this disruption can result in a strengthening of the ‘good eye’ and weakening of the deprived eye, resulting in the experimental model for CP plasticity (Hubel and Wiesel, 1970). This experience-dependent strengthening or weakening affects many levels of the visual cortex circuitry and has demonstrated 3 major types of plasticity in the visual system: Hebbian plasticity (Kirkwood and Bear, 1994), homeostatic plasticity (Turrigiano and Nelson, 2004), and metaplasticity (Philpot et al., 2007). Those types of plasticity are not mutually-exclusive in visual circuits, and together contribute to maintaining an efficient synaptic function and visual processing. Furthermore, each of those models of plasticity rely on glutamatergic and GABAergic mechanisms that I will describe in more detail below.

Glutamatergic synaptic plasticity and perception

α -amino-3-hydroxy-5-methyl-4-isoxazolepropionate receptors (AMPA) and N-methyl-D-aspartate receptors (NMDAR) are the 2 primary excitatory glutamatergic receptors, and have individual roles in regulating plasticity and perception in the visual cortex.

AMPA is an ionotropic glutamate receptor that regulates fast, excitatory transmission at the post-synaptic membrane (Gan et al., 2014; Henley and Wilkinson, 2016). AMPARs are diheteromeric tetramer glutamate receptors that are made up out of 4 possible subunits (GluA1, GluA2, GluA3, and GluA4) that each regulate different binding properties, kinetics, and downstream second-messenger pathways (Herguedas et al., 2016). Different AMPAR subunit combinations can make up AMPAR that are dependent on development and brain area. Most AMPARs, however, are made up of either GluA2/GluA1 or GluA2/GluA3 combinations (Herguedas et al., 2016; Rosenmund et al., 1998; Shepherd and Huganir, 2007), as GluA1/GluA3 AMPAR receptors are poorly translocated to the synaptic membrane (Sans et al., 2003).

The GluA2 subunit is Ca^{2+} -impermeable, a unique property compared to the other AMPAR subunits. GluA2-containing AMPAR are located on both pyramidal cells (Gutierrez-Igarza et al., 1996), and parvalbumin-positive (PV+) inhibitory interneurons (He et al., 2001; Kooijmans et al., 2014) in V1, predominately in layers II/III and V/VI (Van Damme et al., 2003). AMPAR inclusion into the post-synaptic membrane is necessary for activating NMDAR-dominated silent synapses (Liao et al., 2001). Furthermore, AMPAR receptor subunit composition may be developmentally regulated as the number of Ca^{2+} permeable AMPAR decreases with development (Pellegrini-Giampietro et al., 1992), that is caused by a developmental increase in

GluA2-containing AMPAR (Kumar et al., 2002). Furthermore, GluA2-containing AMPAR are required for homeostatic synaptic scaling (Gainey et al., 2009; Sun and Turrigiano, 2011).

Transcription of GluA2 is regulated by neuronal activity (Bai and Wong-Riley, 2003) and transcription factors specificity protein 4 (Sp4), NRF-1 (Dhar et al., 2009), and NRF-2 (Priya et al., 2014a; 2014b) and is coupled with cytochrome oxidase c (CO) in the visual cortex (Dhar et al., 2009; Wong-Riley, 2002). In V1 and V2 GluA2/GluA3 clusters are colocalized strongly with CO-rich regions (Xu et al., 2003). CO blobs are located in the center of ocular dominance columns in monkey (Horton and Hubel, 1981) and in human visual cortex (Duffy et al., 2007). In human V1, CO labelling is dense in layer IVc and light in layer V, with patches about 1mm apart in layers II/III (Horton and Hedley-Whyte, 1984). In human V2, CO labelling forms stripes (Burkhalter and Bernardo, 1989). The functional significance of CO blobs are under investigation, with evidence for overlapping with colour domains, but not with orientation selective regions (Lu and Roe, 2008). CO organization functionally compartmentalizes the visual cortex, and GluA2 may be an important part of this neuronal activity.

GluA2 expression can be regulated by many other neuronal factors, including suppressed by the immature NMDAR subunit GluN2B (Hall et al., 2007), endocytosed via activity through ECM-ligand receptors β 3-integrins (Cingolani et al., 2008; Pozo et al., 2012), and also through early immediate gene Arc (Shepherd et al., 2006). GluA1 is necessary for open-eye potentiation during monocular deprivation in the CP (Ranson et al., 2013). Finally, the interaction of GluA2 and GAPDH, a cellular housekeeping protein, is necessary for axon and dendritic development in neonatal brain (Lee et al., 2016).

NMDAR receptors are heteromeric tetramers that bind glutamate and co-agonists glycine or D-serine to allow for excitatory transmission into both pre- and post-synaptic membranes (Banerjee et al., 2016; Bouvier et al., 2015; Carter and Jahr, 2016; Corlew et al., 2007). NMDAR subunits include the obligatory subunit GluN1, and developmentally regulated subunits GluN2A, GluN2B, GluN2C, GluN2D, GluN3A and GluN3B (Paoletti et al., 2013). In this thesis, I focus on 3 of these receptor subunits: GluN1, GluN2A, and GluN2B in the scope of understanding development in the human visual cortex. GluN1 is an obligatory NMDAR subunit (Monyer et al., 1994; Monyer et al., 1992), and therefore is a good marker for all NMDAR. GluN1 shows that NMDAR have distinct lamination patterns, most densely labeled in layer IVC in human visual cortex (Huntley et al., 1994). The NMDAR tetramer always has two GluN1 subunits, and two other subunits, including options for two GluN2B subunits, two GluN2A subunits, or one GluN2A and one GluN2B (Paoletti et al., 2013). The specific combination of GluN2A and GluN2B subunits in the receptor controls the receptor kinetics, as well as the response selectivity of the neuron to visual stimuli.

GluN2A and GluN2B subunits are developmentally regulated subunits (Monyer et al., 1994; Sheng et al., 1994) that together regulate the potential for LTP and LTD in the synapse, or metaplasticity (Yashiro and Philpot, 2008). GluN2B is the immature subunit that regulates a slower EPSC and are highly expressed in early developing synapses (Sheng et al., 1994) and through the critical period (Erisir and Harris, 2003). GluN2B is highly mobile (Groc et al., 2006), and allows for NMDAR insertion to the synapses (Barria and Malinow, 2002). The upregulation of GluN2A subunits into the receptor is driven by development (Flint et al., 1997; Sheng et al., 1994) and by visual activity (Quinlan et al., 1999a; Quinlan et al., 1999b). The inclusion of even

one GluN2A subunit accelerates the EPSC of the receptor (Flint et al., 1997). Even 1 hour of visual experience can trigger the rapid inclusion of GluN2A-containing NMDAR (Quinlan et al., 1999b). The decline of GluN2B is paralleled by a decline of LTP (Yoshimura et al., 2003), and the end of the CP (Erisir and Harris, 2003). The expression of GluN2A, however, is not necessary for the timing of the CP, but is necessary for the maturation of orientation selectivity in V1 neurons (Fagiolini et al., 2003). The timing of the developmental switch from GluN2B to GluN2A has been associated with the onset of the CP in the ferret visual cortex (Roberts and Ramoa, 1999), at the peak of the CP in cat visual cortex (Chen et al., 2000). Interestingly, the ratio of 2A:2B is 5x higher on PV+ interneurons compared to pyramidal neurons, indicating the GluN2A is critical for the maintenance of PV+ function (Kinney et al., 2006).

The GluN2A:GluN2B (2A:2B) ratio is perhaps most famous for its role in regulating metaplasticity (Yashiro and Philpot, 2008). The ratio of 2A:2B subunits alters the ‘sliding modification threshold’ for a synapse, that can increase or decrease the probability for visual activity to elicit LTP or LTD (Philpot et al., 2007; Philpot et al., 2003; Philpot et al., 2001; Yashiro and Philpot, 2008). Specifically, increases in the GluN2A subunit increase the probability for eliciting LTD, while increases in GluN2B increase the probability for eliciting LTP (Philpot et al., 2007). The 2A:2B ratio regulates ocular dominance plasticity in the critical period, as monocularly deprived GluN2A-KO mice fail show to normal depression to the deprived eye (Cho et al., 2009). The amount of NMDARs decrease in aging (Chen et al., 2000), but the receptors that remain are sufficient to maintain LTP (Barnes et al., 1997). NMDAR activity is required for experience-dependent synaptic modifications in the visual cortex, not confined to the critical period (Kleinschmidt et al., 1987).

Both NMDAR and AMPAR are bound to the synaptic membrane with excitatory scaffolding protein post-synaptic density-95 (PSD-95) (Chen et al., 2015). The accumulation of PSD-95 is linked to the end of the critical period (Huang et al., 2015), and is positively correlated with synaptic strength and maturation (Chen et al., 2015). PSD-95 is also necessary for AMPAR mediated synaptic scaling (Sun and Turrigiano, 2011).

GABAergic synaptic plasticity and perception

Inhibitory transmission is regulated by GABA receptors found on both excitatory and inhibitory cells (Owens and Kriegstein, 2002). There are many pre- and post-synaptic GABAergic synaptic proteins that contribute to the precise timing of inhibitory transmission, however, in this thesis I focus on the GABA_A receptor. The majority of GABAergic transmission is received through either GABA_A and GABA_B receptors. GABA_A receptors mediate most of the inhibitory transmission in the cortex, as they are fast, ligand-gated, heteropentameric chloride channels that are typically assembled by 2 α , 2 β , and 1 γ subunit (Mele et al., 2016). Like the NMDAR and AMPAR receptors, the GABA_A receptor undergoes developmental subunit maturation that determines the receptors binding affinity, kinetic properties, and second messenger pathways (Chen et al., 2001). GABA_A subunits $\alpha 2$ and $\alpha 3$ are present in early developing brains then switch to predominantly more $\alpha 1$ subunits (Heinen et al., 2004) during the critical period (Chen et al., 2001; Dunning et al., 1999). The developmental switch to $\alpha 1$ is correlated with a significant acceleration in the decay of spontaneous IPSCs (Heinen et al., 2004; Vicini et al., 2001). $\alpha 1$ is upregulated in mature visual cortex, and has a significantly higher density (7x) on pyramidal cells innervated by PV⁺ interneurons than other types of synapses (Klausberger et al., 2002), where as the immature subunits $\alpha 2$ are predominately located on PV-negative synapses

(Nyíri et al., 2001). In addition, $\alpha 1$ subunit is necessary for the maturation of adult-like mushroom shaped dendritic spines in the visual cortex (Heinen et al., 2003).

In adult human visual cortex, GABA_A receptors are strongly expressed in layers IVc, with densest expression in layer IVC β , and lesser expression in layers IVC α , II/III, and VI (Hendry et al., 1994). Across the lifespan, expression of GABA_A $\alpha 1$ mRNA showed a 3-fold increase in development, and a 1.5-fold decrease in GABA_A $\alpha 2$ mRNA in the human prefrontal cortex (Duncan et al., 2010), that shows a similar developmental pattern in the genes as found in animal models, and found previously in human V1 (Pinto et al., 2010). Importantly, GABA transmission is necessary for monocular deprivation (Hensch et al., 1998), and the onset of GABA inhibition is necessary for the onset of the CP for ODP (Fagiolini and Hensch, 2000; Huang et al., 1999). Only $\alpha 1$ subunits, however, are necessary for driving cortical plasticity that produces an OD shift (Fagiolini et al., 2004), as the other GABA_A α subunits, participate in other aspects of regulating inhibitory transmission. For example, $\alpha 2$ subunits regulate neuronal firing around the axon-initial segment (Fagiolini et al., 2004).

Expression of GABA_A at the post-synaptic membrane are regulated by inhibitory scaffolding protein Gephyrin (Petrini et al., 2014), that clusters GABA_A to the post-synaptic membrane (Mukherjee et al., 2011; Tretter et al., 2008; 2011) and increases inhibitory synaptic strength and stability (Tyagarajan and Fritschy, 2014; Yu et al., 2007).

Extra-synaptic regulators of plasticity

The end of the CP is characterized by the consolidation of synapses, that become more resistant to experience-dependent change. A major contribution to this consolidation is by the increase of

structural boundaries physically limiting the plasticity of synapses, including intracortical myelination (McGee et al., 2005; Raiker et al., 2010) and extracellular matrix (ECM) (Dityatev and Schachner, 2006).

Myelin is composed of multiple layered membranes of oligodendrocyte sheaths that become tightly packed with lipids and many different proteins (Aggarwal et al., 2011), the most abundant proteins are proteolipid protein (PLP) and myelin basic protein (MBP) (Baumann and Pham-Dinh, 2001). Myelination is driven by action potentials (Wake et al., 2011), and forms around axons of pyramidal cells (Tomassy et al., 2014) and PV+ interneurons (Micheva et al., 2016). While the primary role of myelin is supporting fast axonal transmission, but can also communicate with axons with AMPAR (Kougioumtzidou et al., 2017) and NMDAR (Li et al., 2013; Lundgaard et al., 2013; Micu et al., 2005). MBP, a protein involved in the compaction of the myelin sheaths, increases in expression at the end of the CP in layers IV and V of mouse V1 (McGee et al., 2005). In addition, disruption to myelin-associated protein receptor Nogo-66, reinstates CP plasticity in adult mouse V1 (McGee et al., 2005), suggesting myelin is part of the brakes on plasticity (Bavelier et al., 2010). Interestingly, the myelin around PV+ axons are composed of 20% more MBP than non-GABA cells, showing significant differences in myelin composition of inhibitory and excitatory neurons in the cortex (Micheva et al., 2016). Myelin and ECM associated regulation of PV+ interneurons play a role in the closure of the CP (Erchova et al., 2017; Stephany et al., 2016).

The ECM is comprised of many molecules, including chondroitin proteoglycans (CSPG), that are secreted by neurons and astrocytes (Wiese et al., 2012) and form in the extracellular space

around synapses (Dityatev and Schachner, 2003; 2006). At the end of the CP, CSPGs aggregate at a high concentration around visual cortical synapses called perineuronal nets (PNNs) (Pizzorusso, 2002). Degrading these PNNs with a digestive enzyme, chondroitinase, reinstates ODP in the visual cortex (Pizzorusso, 2002), showing that the maturation of those ECM molecules into a net are part of what puts the brakes on CP plasticity (Carulli et al., 2010; Ye and Miao, 2013). Interestingly, PNNs strongly wrap around mature, fast-spiking PV+ interneurons, and play a role in protecting these cells from oxidative stress (Cabungcal et al., 2013). Astrocytes, together with the pre- and post-synaptic elements were dubbed the ‘tripartite synapse’ (Araque et al., 1999), that changed to the ‘tetrapartite’ synapse by including the ECM (Dityatev and Rusakov, 2011; Smith et al., 2015). The bidirectional communications between these synaptic elements are critical for regulation of both CP and adult plasticity necessary for visual perception across the lifespan.

These animal models are seminal for the basis of each of the questions investigated in my thesis. The physiological, behavioural, and anatomical characteristics of each of the synaptic and non-synaptic mechanisms that regulate plasticity and perception in those studies have helped elucidate some mechanisms of plasticity and perception in the human visual cortex, and are a necessary link for translation between animal and human models.

Preamble for Chapter 2

There is a gap in translation between mechanisms studied in animal models and use for humans. Despite the mass quantity of animal models producing new findings on neurobiological mechanisms that underlie specific aspects of visual system plasticity and visual receptive field properties, it is not well known when, where, or how these mechanisms regulate visual development in humans. While the resolution of most noninvasive imaging for human cortex remains low, there are approaches that can identify expression of synaptic proteins in human visual cortex including anatomy, but anatomical studies using postmortem human tissue are difficult and precocious. Thus the gap remains in finding an approach to identify synaptic plasticity mechanisms in the human visual cortex to translate important findings from animal models.

This chapter addresses the need for tools to translate neurobiological mechanisms studied in animal models for use in postmortem human tissue. This chapter describes in detail a method that my lab and I have modernized and refined, in order accurately quantify expression levels in synaptic proteins in postmortem human visual cortex. The chapter includes detailed protocols that have been used to modernize the making of human synaptoneurosomes, a technique that was used to study glutamatergic and GABAergic proteins in human visual cortex in Chapters 4 and 6. My contribution to this chapter was in collecting data, preparing and testing protocols, and writing the manuscript. This chapter is a collaboration with my colleagues Dr. Simon Beshara, Justin Balsor, Steve Mancini, and Dr. Kathryn Murphy.

Preamble for Chapter 3

Myelin is well-known as an insulator of axonal transmission, that contributes toward an efficient network of cortical processing. Recent studies have shown, however, that myelin plays more roles in regulating neural transmission and circuit function than just insulation. Even myelin basic protein (MBP) is translated into multiple isoforms, including Classic-MBP and Golli-MBP that contribute differently to neuronal function. In animal models, the upregulation of intracortical myelin in the visual cortex coincides with the end of the critical period for ocular dominance plasticity. Even though the sensitive period for susceptibility to amblyopia ends between 6-10 years of age, noninvasive imaging studies in humans show that intracortical myelin continues to develop across the lifespan. Thus the gap remains, when does intracortical myelin develop in the human visual cortex?

This chapter addresses the questions when does myelin expression peak in human visual cortex across the lifespan? Does the timing of the peak of myelin expression in human visual cortex coincide with the end of susceptibility to amblyopia in human vision? Do the two different developmentally regulated MBP proteins follow the same trajectory in human visual cortex?

The findings from this chapter suggest that the brakes on plasticity in human visual cortex are fully expressed late into adulthood, well beyond the end of susceptibility to developing amblyopia. We showed the two MBP proteins, Classic and Golli, develop with different and complementary trajectories across the lifespan. Furthermore, this chapter suggests there is prolonged potential for plasticity in the human visual cortex that extends well into adulthood.

This chapter is co-authored by my colleague Justin Balsor. My contribution for this chapter was collecting the tissue samples, running the experiments, collecting and analyzing the data, writing

the manuscript, making the figures. This chapter contributes to my thesis as my first study that projected the potential magnitude of plasticity across the lifespan in the human visual cortex.

Preamble for Chapter 4

There is a gap in understanding of the development of the human visual cortex, as structurally anatomical studies have found human V1 quickly gains synapses that are subsequently pruned to become adult-like within the first few years of life. Human vision, however, continues to develop across the lifespan as many receptive field properties and visual perceptual abilities mature in late childhood, adolescence and even into adulthood. Animal models have shown that many visual response properties of neurons in V1 are dependent on glutamatergic proteins, as well as being necessary for the critical period for ocular dominance plasticity, homeostatic synaptic scaling, and metaplasticity in the visual cortex. Little is known about how the glutamatergic proteins develop in the human visual cortex across the lifespan that could support the late developing vision. Thus the gap remains, when do glutamatergic proteins in human V1 mature across the lifespan?

This chapter addresses the questions of when do glutamatergic proteins that support synaptic plasticity and visual perception in animal models develop in human V1? Findings from this chapter showed that AMPAR and NMDAR glutamatergic proteins develop in multiple trajectories across the lifespan that can support plasticity across 5 stages of development. In particular, the GluN2A:GluN2B balance showed prolonged development into adulthood that suggests the trajectory for metaplasticity in human V1 development is extended well beyond the sensitive period for amblyopia in humans. This chapter also shows evidence for a switch back to a juvenile-like state of synaptic plasticity in older adulthood (>55 years) that may underlie age-related changes in vision.

This chapter is co-authored by my colleague Dr. Simon Beshara. My contribution to this study was collecting and analyzing the data, writing the manuscript, and making the figures. This chapter contributes to my thesis by showing evidence for prolonged glutamatergic plasticity across the lifespan in human V1.

Preamble for Chapter 5

The last chapter found evidence for prolonged glutamatergic synaptic development in human V1 that extends into adulthood. Those findings suggest that glutamatergic synaptic transmission is plastic across the lifespan in human visual cortex, that could support the late maturation of many visual perceptual abilities. Glutamatergic synapses are made up out of many components that regulate their expression and function, including components of the tetrapartite synapse that include the pre- and post-synaptic compartments, astrocytes and the extracellular matrix. Furthermore, excitatory synapses are predominately on dendritic spines, thus the question remains do components of the tetrapartite synapse and dendritic spines develop like glutamatergic mechanisms in human V1?

This short study was a step to address the development of some of the regulatory components of glutamatergic synapses that I previously showed develop across the lifespan. Although there are hundreds of proteins involved in tetrapartite synapse development, I chose to address this question by mapping the trajectories of just a few components of astrocyte expression, ECM-synapse signaling, and dendritic spine plasticity. The findings from this study suggest maturation of excitatory dendritic spines support the prolonged glutamatergic development found in Chapter 4.

Preamble for Chapter 6

According to anatomical studies, human cortical areas develop sequentially as primary sensory areas develop early and higher cortical areas develop in hierarchy as the most ‘complex’ prefrontal areas develop last. Despite this, evidence for synaptic protein development suggests that human primary visual cortex (V1) actually continues to mature well into adulthood, making it hard to believe that subsequent visual areas develop even later. Many higher-order visual abilities develop well into adulthood, including global motion and face processing that suggest dorsal and ventral visual areas develop later in humans. In addition, perceptual learning using higher-order visual stimuli elicit rapid training effects that suggest plasticity in the human extrastriate areas. The question remains, do synaptic plasticity mechanisms develop sequentially to human V1, as suggest by anatomical development?

This chapter addresses the development of glutamatergic, GABAergic, and presynaptic vesicle plasticity proteins in postmortem human extrastriate cortical areas V2d and V4 between childhood and older adults. The proteins studied in this chapter have each been previously quantified across development of human V1, that allowed me the opportunity to compare developmental trajectories in extrastriate to V1 to answer the question if those plasticity mechanisms develop in sequence across cortical areas. The findings in this chapter suggest that those synaptic plasticity mechanisms in human V2d and V4 do not follow one pattern of development, but can be distributed into 3 categories: mechanisms that follow the same developmental trajectory as V1, that are delayed, or that develop completely differently. In particular, the GluN2A:GluN2B balance followed a trajectory in human V2d and V4 that was

exactly opposite to the development in V1, suggesting mechanisms that support contrasting forms of plasticity between V1 and extrastriate areas.

Chapter 2. Use of synaptoneurosome samples to study development and plasticity of human cortex

Abstract

Translation from animal models of visual system development and plasticity to human studies is difficult due to many obstacles in comparing results. Animal models provide important data about the neurobiological mechanisms that support cortical function and behaviour, but identifying the same mechanisms in human cortex can be challenging. Many neurobiological techniques used in animal models cannot be used in humans, hindering our understanding of visual system development in the human brain. Western blotting using synaptoneurosomes prepared from post-mortem human tissue, however, is a simple and reliable way to study synaptic protein expression in both animal and human brains. Synaptic proteins are linked with specific aspects of visual system development and plasticity necessary to establish functional neural circuitry. Our lab has implemented a filtered synaptoneurosome preparation using human cortical tissue to study the development of human visual cortex. This approach provides human researchers with much needed information about neurobiological development and potential targets for treatments or therapies of visual disorders that have been previously tested in animal models. The protocol detailed in this chapter provides the step-by-step information needed for making synaptoneurosomes from human post-mortem brain tissue, testing and equating antibodies for Western blotting using human brain tissue, and studying the expression of synaptic proteins. We provide strengths and limitations for using synaptoneurosomes to link structure and function in the human brain. This chapter highlights Western blotting of human synaptoneurosomes as an effective tool for studying the human brain and helping to narrow the translation gap.

2.1 Introduction

A fundamental problem in neuroscience is the difficulty translating discoveries from animal models into clinical applications. One way to address this challenge is by using similar techniques across species; yet, few techniques are amenable to this goal. In animal models, especially rodents, there are many sophisticated neuroanatomical, neurophysiological, molecular and imaging techniques that allow precise experimental control and generate rich data sets. Most of those techniques, however, are either too invasive or impractical to use in human studies. One technique, however, quantifying neural proteins using synaptosomes or synaptoneurosome, has emerged as a reliable approach for studying neurodevelopment and plasticity in both animal and human brains.

Translation Challenges

In vivo single-cell neurophysiology provides unparalleled resolution for measuring the properties of individual neurons and their contributions to perception and behaviour. The critical period for ocular dominance plasticity and orientation columns in primary visual cortex (V1) were discovered using single-cell physiology [1, 2]. In humans, in vivo physiology has been used to study mirror-neurons [3], but is restricted to patients who are undergoing operations for pathological conditions, such as epilepsy, because it is too invasive for common use and subject to significant sampling bias. Pharmacological manipulation is another tool commonly used to study the role of receptors and cell types in the developing brain. For example, application of Diazepam, a GABA_A receptor agonist, revealed the role of that GABA_A receptors play in controlling the timing of the critical period [4, 5]. Pharmaceuticals have also been used in studies

of human visual perception to link specific receptors with visual behavior [6] but research in humans is restricted by dose, delivery method, and eligible participants, all of which adds to the translation challenge.

The emergence of precise genetic manipulations with in vivo control of neurons are revealing how the function of neural circuits gives rise to behaviour [e.g. 5, 7]. Furthermore, optogenetic manipulations allow for specific control of the membrane potential in a brain region, or single cell type or subcellular location. All of that can be done with millisecond precision leading to new insights into the role of different neural populations in V1 for visual perception [8-10]. This remarkable spatial and temporal specificity is accelerating our understanding of the neural basis of plasticity and function in animal models but it is not currently applicable for human studies. Thus, while genetic and optogenetic manipulations provide precise experimentation in animals, their findings are not readily translated to human cortical function.

Several imaging and neurophysiological recording techniques, like fMRI and EEG, have been designed and optimized for studying in vivo human cortical activity. Those tools have been used to make great strides linking structure [11, 12] with the function of human V1 [13-15]. There are translation challenges, however, because MRI and EEG techniques have poor spatial resolution, are indirect measures of the underlying neurobiology, and not commonly used in animal studies [16]. Those reasons have made it hard to link findings from human brain imaging with the modern high resolution imaging techniques (e.g. multiphoton) commonly used for animal studies.

Synaptic proteins link structure and function in animal and human models

Studying synaptic proteins has been a successful approach for linking development and plasticity in V1 of animal models with function [17-23]. Synaptic proteins are highly conserved across species making them ideal candidates for studying the human brain and comparing its development with animal models. This approach has been applied to different cohorts, including cases with neuropsychiatric disease [24-26], or cases representing different stages of the lifespan [27-29]. Synaptic proteins, however, are low abundance and can be difficult to quantify in a whole homogenate sample preparation hence the need to use a preparation such as filtered synaptoneuroosomes that enriches pre- and post-synaptic membranes 3-fold or more over homogenate samples [30, 31]. Finally, Western blotting using synaptoneurosome samples is a rapid, reliable, and relatively inexpensive technique to directly measure and compare synaptic protein expression across species.



Figure 1 -- An example image of a multi-species test blot using synaptoneurosome samples (25 μ g) from human, monkey, rat, and cat V1 that were loaded into adjacent wells in a gel. The blot was probed with an antibody for the pre-synaptic protein synaptophysin and the image shows the similar appearance of the bands among the 4 species.

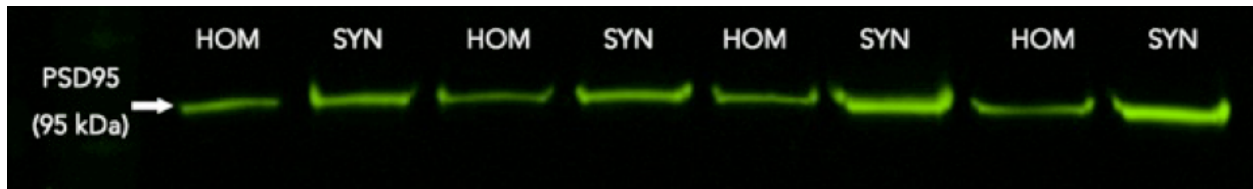


Figure 2 – An example blot showing the relative expression for a synaptic protein (PSD-95) in homogenate (HOM) versus synaptoneurosomes (SYN) samples. Visual inspection shows that the synaptoneurosomes bands are brighter than the homogenate bands. When the bands were quantified there was a 3-5 fold enrichment for synaptic proteins in synaptoneurosomes samples prepared following the protocol described in this Chapter.

2.2 Materials

2.1 Laboratory Equipment for Human Synaptoneurosomes Preparation and Western blotting

1. -80°C Freezer for storing human tissue samples
2. Benchtop Homogenizer (Fast Prep-24 Tissue and Cell Homogenizer, MP Biomedicals) located inside a Biosafety cabinet certified for using Human tissue (Note 5)
3. Scale
4. Coarse filters (100µm mesh pores) cut to fit holder and Swinnex Filter Holder (EMD Millipore, Billerica, MA)
5. 3ml Syringes and 18.5 gauge needle tips (at least 2 per tissue sample), labelled with sample code
6. Pipette (0.5-10µl) and Pipette tips (>25µl, gel loading) (Diamed Lab Services Inc., Mississauga, ON, Canada)
7. Centrifugal filter units (fine filters) (Ultrafree-CL Durapore PVDF 5.0 µm pore, EMD Millipore, Billerica, MA)

8. Scalpel, surgical blades, forceps, scoopula, 2ml centrifuge tubes, and weigh boats, all placed in cooler with dry ice for use with frozen tissue
9. Centrifuge, cooled to 4°C (E.g. Sorvall Legend Micro 21R)
10. Personal Protective Equipment for working with human tissue; including gloves, face masks, lab coats
11. 96-well microplate
12. iMark Microplate Absorbance Reader (Bio-Rad Laboratories, Hercules, CA, USA)
13. Incubator set to 45°C
14. Gel Tank & Gel Holder (Thermo Fisher Scientific, Carlsbad, CA, USA) and Power source (PowerPac 200)
15. Immobilon-FL PVDF Blot Membrane, Wool Transfer pads, and Transfer Filter Paper, all cut to approximately 6x8cm rectangles (Millipore Corporation, Billerica, MA, USA)
16. Plastic Square Petri Dishes for incubation of membranes in antibodies, PBS washing, antibody blocking and antibody stripping solutions
17. Aluminum foil to protect membranes from light
18. Orbital Shaker (Thermolyne Rotomix, Type 50800, Marshall Scientific, Hampton, NH, USA)
19. Transfer cassette and small glass vial to roll and flatten transfer layers
20. Large Styrofoam Box to house transfer tanks, filled with wet ice
21. Ice pack to place in transfer containers
22. Fluorescent Flatbed Scanner (Odyssey Infrared Scanner, Li-Cor, Lincoln, NE, USA)

2.2 Chemicals for Human Synaptoneurosome Prep, Tissue Homogenization and Western blotting

23. Dry & Wet Ice
24. Homogenization buffer (Note 4) chilled to 4°C
25. 10% Sodium Dodecyl Sulfate (SDS) at room temperature, 1% SDS boiling (100°C)
26. Sample loading buffer (M260 NextGel® Sample Loading Buffer 4x, Amresco LLC, Solon, OH, USA)
27. Laemmli buffer (Cayman Chemical Company, Ann Arbor, MI, USA)
28. BCA Protein Assay Reagents A & B (Pierce, ThermoFisher Scientific, Rockford, IL, USA)
29. Bovine Serum Albumin (BSA) protein standards, diluted for 4 concentrations: 2mg/ml, 1mg/ml, 0.5mg/ml, 0.25mg/ml (Pierce Bovine Serum Albumin Standard, 2mg/ml, Bio-Rad Laboratories, Hercules, CA, USA)
30. Novex WedgeWell 4-20% Tris-Glycome Mini Gels, 15-well (Thermo Fisher Scientific, Waltham, MA, USA)
31. Selected Primary and Secondary Antibodies
32. 10x Tris/Glycine/SDS Running Buffer, 10x Tris/Glycine Transfer Buffer (Bio-Rad Laboratories, Hercules, CA, USA)
33. Distilled Water
34. 99% Methanol
35. ProSieve QuadColor Protein Marker, 4.6-300 kDa (Lonza Group, Basel, Switzerland)
36. PBS (PBS tablets) and PBS-Tween
37. Blocking Buffer (Li-Cor, Lincoln, NE, USA)

38. Blot Restore Membrane Rejuvenation Kit, 10x (EDM Millipore, Temecula, CA, USA)

2.3 Methods

To use human synaptoneurosome samples for effective and efficient quantification of synaptic proteins, we have implemented a 3 stage approach to optimize consistency and reliability in our samples even before probing with antibodies. Here we outline our approach for 1) obtaining, 2) preparing, and 3) analyzing protein expression in human synaptoneurosomes for use in 4)

Western blotting.

3.1 Obtaining High quality human tissue samples

To ensure high-quality, reliable protein data from human synaptoneurosomes, it is important to obtain human cortical samples from a brain bank with rigorous protocols for quality and handling. Important considerations for postmortem tissue should maintain structural and cellular integrity. For these reasons, we obtained our human brain samples from the University of Maryland Brain and Tissue Bank, an organization that has a strong reputation for providing high-quality human brain samples for some of the most important human developmental brain studies over the last 20 years [7,17,22].

At the Brain and Tissue Bank, the brain and section of brainstem are carefully removed, typically within 24 hours postmortem, and cooled on wet ice for 30 minutes to increase ease of sectioning. The brain is then sectioned into right and left hemispheres; while the right hemisphere is preserved in 10% formalin, the left is flash frozen by freezing in isopentane/dry ice at -30°C to -40°C , and sectioned coronally in 1-cm intervals. Only the fresh frozen human tissue is suitable to be used for semi-quantitative SDS-PAGE Western blotting, since formalin fixation causes cross-linking of proteins, and this prevents proteins from being separated on gels based on linear molecular weight. Coronal sections are rinsed with water and gently blotted dry, before being

stored in a freezer at -80°C . This protocol is only modified if serious injury or disease prevents typical sectioning. This standard protocol ensures that human postmortem tissue has undergone minimal structural or cellular disruptions so that specific areas of interest can be easily examined, sectioned, and prepared according to sulcal and gyral landmarks.

Once frozen coronal sections are obtained, there are many considerations for further sectioning a suitable tissue piece to use for synaptoneurosome preparation. The coronal section must be transferred immediately from a -80°C freezer to a dry ice cutting block covered in aluminum foil, located inside a biosafety cabinet. Orient the coronal section and identify sulcal and gyral landmarks before cutting a small sample from the area of interest. Use a very sharp scalpel to cut through the frozen tissue and section a piece (about $1\text{cm} \times 1\text{cm} \times 1\text{cm}$, $\sim 50\text{-}100\text{mg}$). This piece must stay frozen until homogenization to avoid denaturing of proteins. To do this, freeze all tools before touching the tissue piece, including the weigh boat and Lysing Matrix D tube to weigh and homogenize the sample, respectively.

3.1.1 Human tissue collection protocol

All experiments with human tissues must be approved by the institute's guidelines set forth by the Standard Operating Protocols and Research Ethics Board.

1. Label all vials with respective sample ID for each human case and each type of tissue prepared (Homogenate, Synaptoneurosome, Supernatant), freeze all surgical tools, Lysing Matrix D tubes, centrifuge tubes, weigh boats in preparation for working with frozen tissue (Note 1)

2. Prepare inside of biosafety cabinet with a slab of dry ice covered in aluminum foil, frozen tools, tubes, weigh boats kept on dry ice, and scale. (Note 2)
3. Tare scale with empty frozen weigh boat to zero
4. Retrieve frozen coronal sections stored in sealed plastic bags from -80°C freezer and keep on crushed dry ice until ready to use.
5. Place whole coronal section on aluminum foil on top of the dry ice block. Determine the orientation of the coronal section, and identify gyral and sulcal landmarks. Draw a sketched map of the tissue, including gyral and sulcal landmarks and shape, and identify area needed for tissue collection (i.e. V1 primary visual cortex)
6. Identify the area of interest, and using surgical blade, scalpel, and forceps, carefully cut a 1cm x 1cm x 1cm tissue piece with frozen blade. Quickly place sectioned tissue piece in frozen weigh boat
7. Weigh frozen sample in weigh boat on the tared scale and record weight. If the sample is too small ($<50\text{mg}$) or too large ($>1\text{mg}$), make note, and if necessary cut another small piece or section tissue further (Note 3)
8. Using frozen forceps, place tissue piece into frozen Lysing Matrix D tube or frozen centrifuge tube, and keep on crushed dry ice (Note 4)
9. Return original coronal section of human tissue to a sealed plastic bag on dry ice, to be returned to the -80°C freezer
10. Repeat collection steps for each coronal sample, using a different frozen, labeled tube for each region of interest and case

11. If continuing synaptoneurosome preparation at a later time, keep tissues frozen by storing each tissue piece in -80°C freezer (See Note 11)

3.2 Preparing human synaptoneurosome samples

Human brain tissue is non-perfused, and requires an extra filtration step added to the synaptoneurosome preparation referred to in Chapter 1. Filtering the homogenized tissue sample through a coarse mesh pore filter ($100\mu\text{m}$), cut to fit into a Swinnex Filter Holder, easily captures large cellular debris like blood vessels that is otherwise perfused in an animal tissue preparation. All other steps in the synaptoneurosome preparation remain the same for human tissue as other tissues, including the subsequent use of $5\mu\text{m}$ mesh pore fine filtering to filter other non-synaptic components like organelles, which helps isolate for low abundance synaptic proteins.

3.2.1 Synaptoneurosome preparation for human tissues protocol

1. Prepare homogenization buffer according to recipe, enough for about 3ml per sample and keep chilled on ice (For buffer recipe see Note 5)
2. Transfer 1cm x 1cm x 1cm frozen tissue pieces into labeled Lysing Matrix D tubes.
3. Add the appropriate amount of homogenization buffer to each frozen sample (see Note 3)
4. Homogenize human tissue in the Fast Prep-24 benchtop homogenizer using Lysing Matrix D tubes for 40 seconds at 6m/s. If the tissue is not visibly homogenized, then run Fast Prep-24 again
5. Insert $100\mu\text{m}$ coarse filter into Swinnex filter holder
6. Add $10\mu\text{l}$ of %10 SDS to each of the centrifuge tubes labeled 'Homogenate' and 'Supernatant.'

7. Pipette 90 μ l of homogenized tissue into centrifuge tubes labeled 'Homogenate' and keep chilled on ice
8. Take up the remaining amount of homogenized tissue in 3ml syringe from the Lysing Matrix D tube, replace needle tip with prepared Swinnex filter holder
9. Using constant pressure, filter the tissue through the coarse filter into the centrifuge tube labeled "Supernatant" (see Note 6)
10. Once human homogenate tissue is filtered, follow the remainder of the synaptoneurosome preparation should exactly as listed in Chapter 1 beginning with the fine filtration step using fine filter Ultrafree Spin tubes (Chapter 1, 3.2.3)
11. Continue to protein assay step or store synaptoneurosome samples in -80°C freezer until ready to use (Note 12)

3.3 Synaptoneurosome tissue protein assay

Synaptic proteins are the machinery that executes the function of a synapse in the cortex.

Accurate measurements of these low abundance proteins can be difficult, however, especially in human samples that have inherent variability. Synaptoneurosome preparation of postmortem cortical tissue is one way to address measuring meaningful changes in synaptic proteins in humans. As outlined in this book, however, there are many ways to make synaptoneurosomes, and many places for variability that can allow for misleading quantifications of synaptic proteins. One important way to assess the reliability and efficiency of the synaptoneurosome protocol is to test for protein concentration in a bicinchoninic acid (BCA) assay against known albumin protein standards. BCA assay is an important control for ensuring each sample has equal amounts of protein before being loaded into a gel for Western blotting. To ensure a high-quality

measurement, the experimenter must be a high-quality pipetter, using a high-quality pipette (Note 10). The correlation between expected and observed ($R^2=0.99$) protein standard concentration expression must be met to consider the protein assay data reliable (Note 18). Validation of protein concentration through the BCA assay ensures that Western blotting data can be reliably quantified, an otherwise difficult task. These steps can take the place of a traditional loading control for Western blotting with human synaptoneurosome tissue. The synaptoneurosome preparation rids the sample of large amounts of typical 'loading controls' such as cytoskeletal or housekeeping proteins found predominately in the cell body (See 3.5 for more details on loading controls in synaptoneurosomes).

3.3.1 Protein assay protocol

1. Collect diluted BSA protein standards (2.0, 1.0, 0.5, 0.25 $\mu\text{g/ml}$) and synaptoneurosome protein samples out of the freezer to thaw (See Note 12 & 13)
2. Organize an assay map so that each sample, including the protein standards and synaptoneurosomes, are loaded three separate times. Also, include a full column of blank wells for control (See Note 14)
3. Prepare BCA assay solution for about 300 μl /sample loaded + blank lanes (See Note 15)
4. Vortex and load 3 μl of each protein standard and synaptoneurosome sample into well-plate according to the assay map organization
5. Add 300 μl of BCA solution to each of the wells that have samples, standards, and also to the designated 'blank' wells (See Note 16)
6. Incubate plate for 45 minutes in an incubator set to 45°C. (See Note 17)

7. After incubation, insert plate into Microplate Absorbance Reader and obtain absorbance measurement values for each well
8. Record absorbance values for protein standards, calculate the average of the three runs for each standard, and calculate the correlation of observed absorbance values against expected.
9. Obtain the correlation (R^2) value for a standard curve fit to the data points. The R^2 value of the standard curve must be equal or greater than 0.99 to proceed with quantification of assay results. If the R^2 value is not 0.99 then the plate with protein standards must be run again. (See Note 18)
10. Calculate the average absorbance of each synaptoneurosome samples loaded into the three wells, and using the slope and y-intercept of the protein standards to calculate the protein concentration with the following equation: [(average sample absorbance/slope) + y-intercept] (See Note 19)
11. Calculate and add the appropriate amounts of 4x Sample buffer and Laemmli buffer to each sample to equal $1\mu\text{g}/\mu\text{l}$ protein concentration (See Note 20)
12. Continue to Western blotting protocol, or store prepared samples in -20°C freezer. (See Note 11)

3.4 Post mortem interval quantification of human synaptoneurosome samples

The postmortem interval, or length of time from death until tissue collection can range significantly, and can affect the quality of the tissue; including synaptic protein integrity, cytoskeletal levels and receptor binding stability [41,42,11]. To ensure that variability in protein expression across samples is not affected by the length of postmortem interval, the total protein

concentration from each sample can be tested against postmortem interval in hours. We found that neither total protein expression or individual synaptic protein expression is affected by postmortem interval within 24 hours in the visual cortex of human synaptoneurosome samples obtained from specimens prepared at the Human Brain and Tissue Bank [32,43].

3.5 Western blotting using human synaptoneurosomes

Western blotting can provide robust quantitative data on protein expression from synaptoneurosome samples if careful considerations are made when planning the experiment, including amount of protein loaded, antibody concentrations, and control samples.

Experimenter loading error is typically controlled for by probing with antibodies for ubiquitous cellular housekeeping or cytoskeletal proteins that ensure the amount of protein in each well is loaded consistently across a gel, and was transferred to membranes evenly. If the same amount of protein is loaded into each well, the expression of the loading control does not change across different samples or lanes, as these housekeeping and cytoskeletal proteins are assumed to be stable under various conditions as well as ages.

Synaptoneurosomes, however, are enriched for the pre- and post-synaptic membranes and adjacent synaptic compartments, and do not express high levels of housekeeping or cytoskeletal proteins that are mostly found in cell bodies. Diminishing large amounts of housekeeping proteins by eliminating cell bodies in the synaptoneurosome preparation will reduce the expression and therefore increase sensitivity to otherwise negligible changes in loading control proteins. Normalizing the expression level of synaptic proteins to the expression of housekeeping proteins in the synapse may lead to misleading results by artificially inflating synaptic protein

enrichment. Even in homogenous tissue, these loading controls often display high variability [19]. The size and shape of dendritic spines and synapses change across development [25,30] and aging, [4] which compounds this artificial enrichment when studying developmental trajectories of synaptic proteins [33]. Therefore, it is necessary to be cautious when choosing a loading control for Western blotting with human synaptoneurosome tissue and to collect and prepare the tissue with a highly reliable and thoughtful protocol to limit the potential of variability in loading.

A control sample of human tissue must be made by mixing a small amount of each human synaptoneurosome sample and running one lane on each gel. Expression of protein from each sample on the blot is divided by the expression of the control sample to allow for comparison samples run on different blots.

Lastly, Western blotting requires the use of antibodies as a means of quantifying protein expression. These antibodies cannot be validated by traditional knock-out methods typically available to animal models, but can be validated through other means; including, testing the antibodies on a multi-species blot to ensure consistency across species for molecular weight and expression (See Note 21). We also ensure accurate protein quantification by titrating a range of primary and secondary antibody concentrations on each sample to identify bands within a linear dynamic range (see Note 22). Also, many of the antibodies used in our human studies are verified antibodies in the Human Protein Atlas ([38] www.proteinatlas.org). The blots are imaged on a sensitive near-infrared scanner (Odyssey Infrared Scanner, Li-Cor, Lincoln, NE, USA) to ensure low background and a high linear dynamic range.

3.5.1 *Western Blotting with human synaptoneurosomes protocol*

1. Organize gel maps, to use as a guide for loading each gel (i.e., Protein ladder, Control Sample, Sample 1, Sample 2...)
2. Prepare transfer, running, and blocking buffers for the desired number of blots
3. Load gels into tank and fill with running buffer, inside and outside of the gels, and open the wells by aspirating some running buffer into each well, ensuring there are no bubbles
4. Pipette 1.5µl of protein ladder into the first well
5. Pipette 25-30µg of control sample into the second well
6. Pipette the same amount (titrated between 20-30µg) of each sample into the following wells, using a gel loading tipped pipette with a slow speed setting, according to the gel map. The last lane is typically not loaded to ensure to equal transfer among all lanes
7. Cover the gel box with the lid and plug leads into the power source set to 150V for about 1 hour, watching to ensure the bands do not run off the gel, add more time if the bands have not run far enough or if you are interested in heavier proteins.
8. Cut PVDF (Immobilon-FL) membranes into rectangular squares large enough to fit a gel (typically about 6x8cm), soak in methanol for 10 seconds and put in Transfer buffer for 10 minutes under agitation
9. Soak wool pads and transfer paper in Transfer buffer and prepare transfer sandwiches for gels in the following order: Wool pad, transfer paper, gel, PVDF membrane, transfer paper, wool pad. This step helps eliminate bubbles between layers.

10. Close the transfer sandwich in the cassette and fit into the transfer tank according to tank specifications. Fill with transfer buffer, an ice pack, and surrounded completely by ice, as the tank and contents will become hot while it is running.
11. Connect the transfer box to a power source and start the transfer at 40V for 2 hours.
12. Once transfer is over, remove the blot membrane from the cassette, place in methanol for 10 seconds, then PBS for 10 minutes to prepare for the blocking process.
13. Add 20ml of blocking buffer and place blot on Orbital Shaker for 1 hour. Take primary antibody out of -20°C freezer to thaw at this time. After 1 hour, pour the blocking buffer back into the original container as it can be reused for approximately one month.
14. Add ~20ml of primary antibody diluted to a working concentration (Note 23), place on orbital shaker plate in the 4°C fridge and incubate for 14-18 hours or overnight.
15. Take off primary antibody, rinse and wash blots with PBS-Tween 3 x 10min, on an orbital shaker. Primary antibody can be reused typically about 4-6 times.
16. Rinse with PBS, and add 20ml of secondary antibody diluted to a working concentration (Note 23). Cover petri dish with aluminum foil to shield from the light (Note 24), and place on an orbital shaker for 1 hour at room temperature.
17. Take off secondary antibody; it can be reused typically about 6-10 times. Rinse and wash blots with PBS-Tween 3 x 10min on an orbital shaker, under aluminum foil to keep blots in the dark.
18. Rinse with PBS and then bring covered blots to scanner
19. Scan blots according to specifications of the scanner, and using the corresponding wavelength of laser appropriate for the secondary antibody. Identify the molecular weight

of the band(s) against the ladder loaded in lane 1, making sure this band represents the protein of interest. Quantify the integrated intensity value of each band, divided by the width of the lane. Normalize the expression value of each sample to the value of the control band on the same blot.

20. Blots can be stripped using a membrane blot restore stripping solution, and re-probed with additional antibodies typically 4-6 times without any decrease in the quality of the blot.

2.4 Notes

1. Labeling all of the vials is an important part of planning the experiment. Before any tissue is disturbed from the -80 freezer, organize all tools and equipment, so tissue is not lost due to unnecessary thaw. Before beginning tissue collection, ensure that all experimenters are prepared with lab notebooks to record notes and that checkpoints are in place in case it is necessary to stop the procedure and start again at another time.

Typically, the tissue collection (3.1) can be done on a separate day from preparing the tissue (3.2) and protein assay (3.3), and subsequently, Western blotting (3.5) can be done at a later time . We recommend, however, that the tissue preparation (3.2) and protein assay (3.3) be completed on the same day to avoid an additional freeze-thaw cycle that might damage the proteins.
2. The tools used to dissect a piece of human tissue from the larger block should be cooled using dry-ice to avoid the scalpel blade or forceps from thawing the tissue when cutting or picking up the small tissue samples. Keeping the tissue frozen preserves the integrity of the proteins to be analyzed by Western blotting.
3. It is important to record the weight of the sample to determine how much homogenization buffer to add. The amount of homogenization buffer added to the sample depends on the weight of the excised piece. For example, approximately 1ml buffer for 50mg, 1.25ml buffer for 75mg, 1.5ml buffer for 100mg.

4. If continuing to homogenization step, then frozen tissue pieces can be put into frozen Lysing Matrix D tubes. Otherwise, put samples into 2ml centrifuge tubes and store in the -80°C freezer.
5. Homogenization buffer recipe, makes 50mL (see more details in Chapter 1):
 - 5mL, 10mM HEPES
 - 5mL, 2mM EDTA
 - 5mL, 2mM EGTA
 - 125µL, 0.5mM DTT
 - 500µL, 10mg/L Leupeptin
 - 500µL, 50mg/L Soybean Trypsin Inhibitor
 - 50µL, 100nM Microcystin 24
 - 33.825mL Water
6. Filtering non-perfused homogenate tissue may require replacing the coarse filter with a new one as a filter may become clogged with debris. As the filter becomes clogged the force needed to push the syringe plunger will increase indicating that it is time to change the filter. The filter may have to be changed multiple times even for one sample.
7. Novex WedgeWell 4-20% Tris-Glycine Mini Gels can easily accommodate large volumes of tissue, which is necessary when loading synaptoneurosome tissue. A single gel contains 15 wells and each well can hold up to 35µl of sample, which minimizes the amount (and hence cost) of chemical reagents and saves on experimenter time.
8. When making the transfer sandwiches, use a small glass vial to pour small amounts of transfer buffer between the layers; this ensures there are no bubbles. Between each layer,

except for the gel, roll the glass tube horizontally across the layer with equal pressure to facilitate a smooth transfer surface.

9. Biosafety cabinet must be certified by the establishments' biosafety office for use with human brain tissue, the type of cabinet may vary depending on the kind of experiment and must be apart of the labs Standard Operating Procedures for using human tissue in the lab.
10. To ensure that the experimenter can dispense a consistent volume from the pipette, it is useful to practice pipetting and calibrating the experimenter. This is done by pipetting small volumes of dH₂O into a weight-boat sitting on an analytic balance, then recording the weight of each amount pipetted and analyzing the variability to ensure that it is within the error specifications from the pipette manufacturer. The pipette should also be sent out annually for servicing that includes certification. Our lab has tried various pipettes and concluded that the Picus Electronic Pipette (Sartorius, Goettingen, Germany) is optimal for this application.
11. Human brain tissue samples must be stored in a -80°C freezer before they are prepared with Sample loading and Laemmli buffers. Once the samples have been prepared with the correct amounts of buffers, they may be stored in the -20°C freezer for up to 1 month, and in the -80°C freezer for longer periods.
12. It is best to limit the number of freeze/thaw cycles for each synaptoneurosome sample. Therefore, if possible it is ideal to plan to homogenize, prepare the tissue, and perform a western blot all on the same day.

13. Albumin Protein standards are bovine serum albumin (BSA) protein solutions that provide reference standards for use in most protein assays. This standard is typically supplied with a concentration of 2mg/ml (Pierce Bovine Serum Albumin Standard Ampules, ThermoFisher Scientific) and must be diluted with homogenization buffer to make the following concentrations: 1.0, 0.5, 0.25mg/ml to use in the assay. These standards can be stored in -20°C freezer for future use.
14. Assay map must show a diagram of a 96 well-plate with each sample, including protein standards, labeled in 3 different wells, and must also contain one blank column of wells.
15. The BCA solution provides selective colorimetric detection that produces an intense purple-coloured reaction dependent on the amount of protein concentration in the sample, for more details refer to <https://www.thermofisher.com/order/catalog/product/23225>
16. Blank wells loaded with BCA solution only and no protein will provide a lane of controls that establish a baseline for zero protein concentration. If the blank wells show some amount of protein after the assay is complete, the BCA solution must be re-made, and the assay must be completed again.
17. The length of time and temperature of incubation determine the rate of colour development of the BCA solution with the proteins in the sample. Ensure the spectrophotometer in the microplate reader is set to a wavelength of 562nm, or the appropriate wavelength for your solution.
18. Calculate a standard curve by plotting the average absorbance of each protein standard on a scatter plot, with expected protein concentration (0.25, 0.5, 1.0, 2.0) on the x-axis and observed concentration on the y-axis. Fit a linear trend-line to the points and use this to

identify the slope, y-axis and R^2 of the fit. The correlation value R^2 must be at least 0.99 to be used as a protein standard for the assay. If R^2 is not >0.99 , the entire assay must be run again. This value can be difficult to achieve and is usually dependent on the experience of the experimenter in pipetting and titration of samples.

19. Once the average protein concentration is obtained for each sample, calculate the amount of samples buffers needed to dilute the sample to $1\mu\text{g}/\mu\text{l}$ (see Note 20). Calculate how many runs (of $25\mu\text{g}$) are possible for each human synaptoneurosome sample to be used in Western blotting.
20. Sample loading buffer (M260 NextGel® Sample Loading Buffer 4x, Amresco LLC, Solon, OH, USA) and Laemmli Buffer (Cayman Chemical Company, Ann Arbor, MI, USA) are added sample buffers for protein denaturation, as well as adding a dye and density to the sample to make them easier to run on SDS-PAGE. Sample loading buffer must be diluted 1 part buffer: 3 parts protein sample. After that, enough Laemmli buffer is added to dilute the sample to $1\mu\text{g}/\mu\text{l}$ protein concentration. Do not dilute the samples to less than $1\mu\text{g}/\mu\text{l}$.
21. One way to verify antibodies used on human synaptoneurosome tissue is to probe on a multi-species blot. To do this, prepare a single blot with at least three different species run (twice each). For example, we run a multi-species blot with 2 control samples of cortical tissue from each: rat, cat, rabbit, monkey, human. This blot is run with multiple different antibodies at different concentrations to test that a band(s) of the same molecular weights are found across species. If the band is found in the human tissue at the same molecular

weight and expression as the other species, it is considered a reliable antibody to use to quantify accurate data.

22. Different primary and secondary antibodies can work within their linear dynamic range at many different concentrations depending on the type of tissue, protein concentration, the age of antibody or even amount of freeze/thaw cycles. It is important to test the dilution factor of each antibody before use by performing a titration starting with the suggested working dilution. It is possible and helpful to mix primary antibodies that probe for proteins of differing molecular weights or correspond to different secondary antibodies to create a 'cocktail'. This is most useful when testing a new antibody to mix with a known antibody that shows dependable antigenicity so that any error in the new antibody will not be mistaken for sample error, as the known antibody will show consistent expression.
23. Keep secondary antibody in the dark at all times. The aluminum foil is used as a cover to protect the blots from the light of the room; an option is to also turn the lights off or down in the lab to further protect the fluorescence of the secondary antibody from light exposure.

2.5 References

1. Atallah, B. V., Bruns, W., Carandini, M., & Scanziani, M. (2012). Parvalbumin-expressing interneurons linearly transform cortical responses to visual stimuli. *Neuron*, 73(1), 159–170. <http://doi.org/10.1016/j.neuron.2011.12.013>
2. Barksdale, K. A., Lahti, A. C., & Roberts, R. C. (2014). Synaptic Proteins in the Postmortem Anterior Cingulate Cortex in Schizophrenia: Relationship to Treatment and Treatment Response, 39(9), 2095–2103. <http://doi.org/10.1038/npp.2014.57>
3. Curley, A. A., Arion, D., Volk, D. W., Asafu-Adjei, J. K., Sampson, A. R., Fish, K. N., & Lewis, D. A. (2011). Cortical deficits of glutamic acid decarboxylase 67 expression in schizophrenia: clinical, protein, and cell type-specific features. *The American Journal of Psychiatry*, 168(9), 921–929. <http://doi.org/10.1176/appi.ajp.2011.11010052>
4. Dickstein, D. L., Weaver, C. M., Luebke, J. I., & Hof, P. R. (2013). Dendritic spine changes associated with normal aging. *Neuroscience*, 251, 21–32. <http://doi.org/10.1016/j.neuroscience.2012.09.077>
5. ENGEL, S. A. (1994). Fmri of Human Visual-Cortex (Vol 369, Pg 525, 1994). *Nature*, 370(6485), 106–106.
6. Engel, S., Zhang, X. M., & Wandell, B. (1997). Colour tuning in human visual cortex measured with functional magnetic resonance imaging. *Nature*, 388(6637), 68–71. <http://doi.org/10.1038/40398>
7. Ernst, A., Alkass, K., Bernard, S., Salehpour, M., Perl, S., Tisdale, J., et al. (2014). Neurogenesis in the Striatum of the Adult Human Brain. *Cell*, 156(5), 1072–1083. <http://doi.org/10.1016/j.cell.2014.01.044>
8. Fagiolini, M., & Hensch, T. K. (2000). Inhibitory threshold for critical-period activation in primary visual cortex. *Nature*, 404(6774), 183–186. <http://doi.org/10.1038/35004582>
9. Fagiolini, M., Katagiri, H., Miyamoto, H., Mori, H., Grant, S. G. N., Mishina, M., & Hensch, T. K. (2003). Separable features of visual cortical plasticity revealed by N-methyl-D-aspartate receptor 2A signaling. *Proceedings of the National Academy of Sciences*, 100(5), 2854–2859. <http://doi.org/10.1073/pnas.0536089100>
10. Gainey, M. A., Hurvitz-Wolff, J. R., Lambo, M. E., & Turrigiano, G. G. (2009). Synaptic Scaling Requires the GluR2 Subunit of the AMPA Receptor. *Journal of Neuroscience*, 29(20), 6479–6489. <http://doi.org/10.1523/JNEUROSCI.3753-08.2009>
11. Glantz, L. A., Gilmore, J. H., Hamer, R. M., Lieberman, J. A., & Jarskog, L. F. (2007). Synaptophysin and postsynaptic density protein 95 in the human prefrontal cortex from mid-gestation into early adulthood. *Neuroscience*, 149(3), 582–591. <http://doi.org/10.1016/j.neuroscience.2007.06.036>

12. Glantz, L. A., Gilmore, J. H., Overstreet, D. H., Salimi, K., Lieberman, J. A., & Jarskog, L. F. (2010). Pro-apoptotic Par-4 and dopamine D2 receptor in temporal cortex in schizophrenia, bipolar disorder and major depression. *Schizophrenia Research*, *118*(1-3), 292–299. <http://doi.org/10.1016/j.schres.2009.12.027>
13. Haynes, J.-D., & Rees, G. (2005). Predicting the orientation of invisible stimuli from activity in human primary visual cortex. *Nature Neuroscience*, *8*(5), 686–691. <http://doi.org/10.1038/nn1445>
14. Hensch, T. K., & Fagiolini, M. (2005). Excitatory-inhibitory balance and critical period plasticity in developing visual cortex. *Progress in Brain Research*, *147*, 115–124. [http://doi.org/10.1016/S0079-6123\(04\)47009-5](http://doi.org/10.1016/S0079-6123(04)47009-5)
15. Hensch, T. K., Fagiolini, M., Mataga, N., Stryker, M. P., Baekkeskov, S., & Kash, S. F. (1998). Local GABA circuit control of experience-dependent plasticity in developing visual cortex. *Science*, *282*(5393), 1504–1508. <http://doi.org/10.1126/science.282.5393.1504>
16. HUBEL, D. H., & WIESEL, T. N. (1968). Receptive fields and functional architecture of monkey striate cortex. *The Journal of Physiology*, *195*(1), 215–243.
17. Huttenlocher, P. R., & Dabholkar, A. S. (1997). Regional differences in synaptogenesis in human cerebral cortex. *The Journal of Comparative Neurology*, *387*(2), 167–178.
18. Larsen, R. S., Smith, I. T., Miriyala, J., Han, J. E., Corlew, R. J., Smith, S. L., & Philpot, B. D. (2014). Synapse-Specific Control of Experience-Dependent Plasticity by Presynaptic NMDA Receptors. *Neuron*, *83*(4), 879–893. <http://doi.org/10.1016/j.neuron.2014.07.039>
19. Lee, H.-G., Jo, J., Hong, H.-H., Kim, K. K., Park, J.-K., Cho, S.-J., & Park, C. (2016). State-of-the-art housekeeping proteins for quantitative western blotting: Revisiting the first draft of the human proteome. *Proteomics*, *16*(13), 1863–1867. <http://doi.org/10.1002/pmic.201500344>
20. Lee, S.-H., Kwan, A. C., Zhang, S., Phoumthipphavong, V., Flannery, J. G., Masmanidis, S. C., et al. (2012). Activation of specific interneurons improves V1 feature selectivity and visual perception. *Nature Publishing Group*, *488*(7411), 379–383. <http://doi.org/10.1038/nature11312>
21. Levelt, C. N., & Hübener, M. (2012). Critical-Period Plasticity in the Visual Cortex, *35*(1), 309–330. <http://doi.org/10.1146/annurev-neuro-061010-113813>
22. Lu, T., Pan, Y., Kao, S. Y., Li, C., Kohane, I., Chan, J., & Yankner, B. A. (2004). Gene regulation and DNA damage in the ageing human brain. *Nature*, *429*(6994), 883–891. <http://doi.org/10.1038/nature02661>
23. Lunghi, C., Berchicci, M., Morrone, M. C., & Di Russo, F. (2015). Short-term monocular deprivation alters early components of visual evoked potentials. *The Journal of Physiology*, *593*(19), 4361–4372. <http://doi.org/10.1113/JP270950>
24. Meuwese, J. D. I., van Loon, A. M., Scholte, H. S., Lirk, P. B., Vulink, N. C. C., Hollmann, M. W., & Lamme, V. A. F. (2013). NMDA Receptor Antagonist Ketamine Impairs Feature Integration in Visual Perception. *PLoS ONE*, *8*(11), e79326–12. <http://doi.org/10.1371/journal.pone.0079326>

25. Michel, A. E., & Garey, L. J. (1984). The development of dendritic spines in the human visual cortex. *Human Neurobiology*, 3(4), 223–227.
26. Mirsattari, S. M., Bihari, F., Leung, L. S., Menon, R. S., Wang, Z., Ives, J. R., & Bartha, R. (2005). Physiological monitoring of small animals during magnetic resonance imaging. *Journal of Neuroscience Methods*, 144(2), 207–213. <http://doi.org/10.1016/j.jneumeth.2004.11.019>
27. Mukamel, R., Ekstrom, A. D., Kaplan, J., Iacoboni, M., & Fried, I. (2010). Single-Neuron Responses in Humans during Execution and Observation of Actions. *Current Biology*, 20(8), 750–756. <http://doi.org/10.1016/j.cub.2010.02.045>
28. Murphy, K. M., Balsor, J., Beshara, S., Siu, C., & Pinto, J. G. A. (2014). A high-throughput semi-automated preparation for filtered synaptoneurosomes, 235, 35–40. <http://doi.org/10.1016/j.jneumeth.2014.05.036>
29. Murphy, K. M., Beston, B. R., Boley, P. M., & Jones, D. G. (2005). Development of human visual cortex: a balance between excitatory and inhibitory plasticity mechanisms. *Developmental Psychobiology*, 46(3), 209–221. <http://doi.org/10.1002/dev.20053>
30. Petanjek, Z., Judaš, M., Šimic, G., Rasin, M. R., Uylings, H. B. M., Rakic, P., & Kostovic, I. (2011). Extraordinary neoteny of synaptic spines in the human prefrontal cortex. *Proceedings of the National Academy of Sciences of the United States of America*, 108(32), 13281–13286. <http://doi.org/10.1073/pnas.1105108108>
31. Philpot, B. D., Sekhar, A. K., Shouval, H. Z., & Bear, M. F. (2001). Visual experience and deprivation bidirectionally modify the composition and function of NMDA receptors in visual cortex. *Neuron*, 29(1), 157–169.
32. Pinto, J. G. A., Hornby, K. R., Jones, D. G., & Murphy, K. M. (2010). Developmental changes in GABAergic mechanisms in human visual cortex across the lifespan. *Frontiers in Cellular Neuroscience*, 4, 16. <http://doi.org/10.3389/fncel.2010.00016>
33. Pinto, J. G. A., Jones, D. G., & Murphy, K. M. (2013). Comparing development of synaptic proteins in rat visual, somatosensory, and frontal cortex. *Frontiers in Neural Circuits*, 7, 97. <http://doi.org/10.3389/fncir.2013.00097>
34. Polonsky, A., Blake, R., Braun, T., & Heeger, D. J. (2000). Neuronal activity in human primary visual cortex correlates with perception during binocular rivalry. *Nature Neuroscience*, 3(11), 1153–1159. <http://doi.org/10.1038/80676>
35. Quinlan, E. M., Olstein, D. H., & Bear, M. F. (1999). Bidirectional, experience-dependent regulation of N-methyl-D-aspartate receptor subunit composition in the rat visual cortex during postnatal development. *Proceedings of the National Academy of Sciences*, 96(22), 12876–12880.
36. Ramoa, A. S., Mower, A. F., Liao, D., & Jafri, S. (2001). Suppression of cortical NMDA receptor function prevents development of orientation selectivity in the primary visual cortex. *Journal of Neuroscience*, 21(12), 4299–4309.
37. Rivadulla, C., Sharma, J., & Sur, M. (2001). Specific roles of NMDA and AMPA receptors in direction-selective and spatial phase-selective responses in visual

- cortex. *The Journal of Neuroscience : the Official Journal of the Society for Neuroscience*, 21(5), 1710–1719.
38. Uhlen, M. (2007). Mapping the human proteome using antibodies. *Molecular & Cellular Proteomics*, 6(8), 1455–1456.
 39. WIESEL, T. N., & HUBEL, D. H. (1963). SINGLE-CELL RESPONSES IN STRIATE CORTEX OF KITTENS DEPRIVED OF VISION IN ONE EYE. *Journal of Neurophysiology*, 26, 1003–1017.
 40. Wilson, N. R., Runyan, C. A., Wang, F. L., & Sur, M. (2012). Division and subtraction by distinct cortical inhibitory networks in vivo. *Nature Publishing Group*, 488(7411), 343–348. <http://doi.org/10.1038/nature11347>
 41. Blair, J. A., Wang, C., Hernandez, D., Siedlak, S. L., Rodgers, M. S., Achar, R. K., ... & Casadesus, G. (2016). Individual case analysis of postmortem interval time on brain tissue preservation. *PloS one*, 11(3), e0151615.
 42. Kontur, P., Al-Tikriti, M., Innis, R. B., & Roth, R. H. (1994). Postmortem Stability of Monoamines, Their Metabolites, and Receptor Binding in Rat Brain Regions. *Journal of neurochemistry*, 62(1), 282-290.
 43. Siu, C. R., Beshara, S. P., Jones, D. G., & Murphy, K. M. (2017). Development of glutamatergic proteins in human visual cortex across the lifespan. *Journal of Neuroscience*, 37(25), 6031-6042.

Chapter 3. Classic and Golli Myelin Basic Protein have distinct developmental trajectories in human visual cortex

Publication Reference

Siu, C. R., Balsor, J. L., Jones, D. G., & Murphy, K. M. (2015). Classic and Golli Myelin Basic Protein have distinct developmental trajectories in human visual cortex. *Frontiers in Neuroscience*, 9, 138–10. <http://doi.org/10.3389/fnins.2015.00138>

Abstract

Traditionally, myelin is viewed as insulation around axons, however, more recent studies have shown it also plays an important role in plasticity, axonal metabolism, and neuroimmune signaling. Myelin is a complex multi-protein structure composed of hundreds of proteins, with Myelin Basic Protein (MBP) being the most studied. MBP has two families: Classic-MBP that is necessary for activity driven compaction of myelin around axons, and Golli-MBP that is found in neurons, oligodendrocytes, and T-cells. Furthermore, Golli-MBP has been called a 'molecular link' between the nervous and immune systems. In visual cortex specifically, myelin proteins interact with immune processes to affect experience-dependent plasticity. We studied myelin in human visual cortex using Western blotting to quantify Classic- and Golli-MBP expression in post-mortem tissue samples ranging in age from 20 days to 80 years. We found that Classic- and Golli-MBP have different patterns of change across the lifespan. Classic-MBP gradually increases to 42 years and then declines into aging. Golli-MBP has early developmental changes that are coincident with milestones in visual system sensitive period, and gradually increases into aging. There are 3 stages in the balance between Classic- and Golli-MBP expression, with Golli-MBP dominating early, then shifting to Classic-MBP, and back to Golli-MBP in aging. Also Golli-MBP has a wave of high inter-individual variability during childhood. These results about cortical MBP expression are timely because they compliment recent advances in MRI techniques that produce high resolution maps of cortical myelin in normal and diseased brain. In addition, the unique pattern of Golli-MBP expression across the lifespan suggests that it supports high levels of neuroimmune interaction in cortical development and in aging.

3.1 Introduction

The last decade has seen renewed interest in studying myelin in the cortex because it is involved in neuroplasticity, neurodegeneration and neuroinflammation. As maturation of cortical myelin limits developmental plasticity (McGee et al., 2005), changes in aging are linked with cognitive decline (Peters et al., 2008), and myelin abnormalities contribute to neurodegenerative and neuropsychiatric disease (Roussos and Haroutunian, 2014; Mighdoll et al., 2015). Novel brain imaging techniques are producing high resolution maps of myelin in human cortex (Shafee et al., 2015; Grydeland et al., 2013; Glasser and Van Essen, 2011) that can follow these changes in cortical myelin during adaptive or maladaptive plasticity. Myelin, however, is a complex multi-protein structure and we need to know more about the expression of proteins that make up myelin in the human cortex to link these new brain imaging techniques with disease-related changes in myelin proteins.

In the cortex, oligodendrocytes are the second most abundant type of neuroglial cell and they form myelin. Myelin is made up of hundreds of proteins, many of which have multiple families and isoforms. The most commonly used marker for myelin expression is Myelin Basic Protein (MBP). MBP makes up about 30% of all myelin proteins and is composed of two families, Classic- and Golli-MBP, each with multiple isoforms and post-translational modifications (Pribyl et al., 1996; Harauz et al., 2009; Harauz and Boggs, 2013) that individually contribute to myelination (Jacobs et al., 2005; 2009; Harauz et al., 2009). Classic-MBP isoforms (18.5 - 21.5 kDa in human) are found in mature oligodendrocytes and myelin sheaths, and have a key role in activity driven compaction of myelin around axons (Wake et al., 2011). Expression of Classic-MBP increases during cortical development (Miller et al., 2012) and immunohistochemical

labeling of Classic-MBP is correlated with traditional myelin staining. In contrast, Golli-MBP isoforms (33 – 35 kDa) are found in early developing oligodendrocytes, neurons and immune cells, with functions that extend beyond the myelin sheath and include regulating oligodendrocyte proliferation and migration (Paez et al., 2011). Golli-MBP is highly expressed prenatally in neurons and oligodendrocytes, even before the process of myelination begins (Tosic et al., 2002) and has been called a ‘molecular link’ between the nervous and immune systems (Pribyl et al., 1993).

The primary sensory cortices are heavily myelinated (Geyer et al., 2011) and are good cortical regions to study developmental changes in expression of both families of MBP. Expression of MBP and myelination in the visual cortex is affected by neuropsychiatric disease and genetic manipulation of Golli-MBP. In schizophrenia, there is reduced MBP mRNA in human visual cortex, as well as other cortical areas, suggesting that MBP expression in visual cortex is vulnerable to neuropsychiatric disease (Matthews et al., 2012). Furthermore, abnormalities in genes that code for Golli-MBP are linked with significant risk for schizophrenia (Baruch et al., 2009). Although Golli-MBP is not part of the myelin sheath, it is necessary for normal development of myelination (Jacobs et al., 2005). Golli-MBP knockout (KO) mice have an abnormal balance between Golli- and Classic-MBP that leads to profound hypomyelination restricted to the visual cortex (Jacobs et al., 2005). While Golli-MBP overexpressing mice have delayed development of myelination (Jacobs et al., 2009). Several lines of evidence have linked myelin (McGee et al., 2005) and neuroimmune signaling (Syken et al., 2006) with the end of the sensitive period in the visual cortex. Since Golli-MBP has been called a ‘molecular link’ between

the nervous and immune systems (Pribyl et al., 1993) it is timely to characterize its expression in human visual cortex.

To address how the two families of MBP proteins change across the lifespan, we used Western blotting to quantify expression of Classic- and Golli-MBP in post-mortem tissue samples from human primary visual cortex. We used model fitting to characterize developmental trajectories that capture how Classic- and Golli-MBP change across the lifespan. We analyzed changes in the relative expression of Classic- and Golli-MBP to determine how the balance between these families of MBP vary in human visual cortex. Finally, we compared inter-individual variability in expression of Classic- and Golli-MBP to determine if there are times in development with higher inter-individual variability.

3.2 Materials and Methods

Samples and Tissue

Tissue samples from human primary visual cortex were obtained from the Brain and Tissue Bank for Developmental Disorders at the University of Maryland (Baltimore, MD, USA) and were approved for use by the McMaster University Research Ethics Board. Samples were taken from the posterior pole of the left hemisphere of human visual cortex, and included both superior and inferior portions of the calcarine fissure, according to the gyral and sulcal landmarks. Cortical samples were obtained from individuals with no history of mental health or neurological disorders, and all causes of death were natural, or with minimal trauma. Samples were obtained within 23 hours post-mortem, and were rapidly frozen at the Brain and Tissue Bank after being sectioned coronally in 1-cm intervals, rinsed with water, blotted dry, placed in a quick-freeze

bath (dry ice and isopentane), and stored frozen (-80°C). A total of 31 cases were used in this study, ranging in age from 20 days to 79 years (Table 1).

Table 1. Cases used in the study.

Age Group	Age	Post-mortem Interval (Hrs)	Sex
Neonatal	20 days	9	M
Neonatal	20 days	14	F
Neonatal	86 days	23	F
Neonatal	96 days	12	M
Neonatal	98 days	16	M
Neonatal	119 days	22	M
Neonatal	120 days	23	M
Infant	133 days	16	M
Infant	136 days	11	F
Infant	273 days	10	M
Young Children	1 year 123 days	21	M
Young Children	2 years 57 days	21	F
Young Children	2 years 75 days	11	F
Young Children	3 years 123 days	11	F
Young Children	4 years 203 days	15	M
Young Children	4 years 258 days	17	M
Older Children	5 years 144 days	17	M
Older Children	8 years 50 days	20	F
Older Children	8 years 214 days	20	F
Older Children	9 years 46 days	20	F
Teens	12 years 164 days	22	M
Teens	13 years 99 days	5	M
Teens	15 years 81 days	16	M
Teens	19 years 76 days	16	F
Young Adults	22 years 359 days	4	M
Young Adults	32 years 223 days	13	M
Young Adults	50 years 156 days	8	M
Young Adults	53 years 330 days	5	F
Older Adults	69 years 110 days	12	M
Older Adults	71 years 333 days	9	F
Older Adults	79 years 181 days	14	F

Tissue-Sample Preparation

Small pieces of tissue samples (75-150 mg) were cut from 1-cm thick coronal slices of primary visual cortex (area V1), and suspended in cold homogenization buffer (1 ml buffer:50 mg tissue; 0.5 mM DTT, 1 mM EDTA, 2 mM EGTA, 10 mM HEPES, 10 mg/L leupeptin, 100 nM microcystin, 0.1 mM PMSF, 50 mg/L soybean trypsin inhibitor). Samples were homogenized using the FastPrep®-24 Tissue and Cell Homogenizer (MP Biomedicals, Solon, OH, USA) by placing the piece of tissue and buffer in a lysing matrix D homogenization tube (MP Biomedicals, Solon, OH, USA) and homogenizing for 40s at 6/ms. After homogenization, sodium-dodecyl-sulfate 10% (SDS) was added to each sample to further unravel proteins in preparation for gel electrophoresis. Total protein concentrations were determined using a bicinchonic acid (BCA) assay (Pierce, Rockford, IL, USA). A control sample was made by combining a small amount of the homogenized tissue sample from each case.

Immunoblotting

Homogenized tissue samples (20µg) were separated on SDS polyacrylamide gels (SDS-PAGE) and transferred to polyvinylidene difluoride (PVDF-FL) membranes (Millipore, Billerica, MA, USA) using electroblotting in BupH Tris Glycine Transfer Buffer (Thermo Scientific, Waltham, MA, USA). Each sample was run 3 times. Each blot was loaded with a protein standards ladder and a control sample. Blots were pre-incubated for 1 hour in blocking buffer (Odyssey Blocking Buffer 1:1 with PBS; Li-cor Biosciences; Lincoln, NE, USA), then in primary antibody overnight at 4°C using the following concentrations: Anti-GAPDH, 1:8000 (Imgenex, San Diego, CA); Anti-β-Tubulin, 1:4000 (Imgenex, San Diego, CA); Anti-Myelin Basic Protein (MBP), 1:4000 [AB62631] (Abcam, Cambridge, MA, USA). The blots were

washed with PBS containing 0.05% Tween (Sigma, St. Louis, MO, USA) (3 x 10min), and incubated for 1 hour with the appropriate secondary antibody (1:8000 IRDye, Li-cor Biosciences, Lincoln, NE, USA). The blots were washed again in PBS-Tween (3 x 10min) and bands were visualized using the Odyssey scanner (Li-cor Biosciences, Lincoln, NE, USA). The blots were stripped (Blot Restore Membrane Rejuvenation kit, Millipore, Billerica, MA, USA) and then reprobbed with another primary antibody.

Analyses

To quantify protein expression, blots were scanned using Odyssey Infrared Imaging System (Li-cor Biosciences, Lincoln, NE, USA) and the bands were quantified using densitometry (Li-cor Odyssey Software Version 3.0, Li-cor Biosciences, Lincoln, NE, USA). The density of each band was determined by subtracting the background, integrating the pixel intensity of the band, and dividing that intensity by the width of the band to control for variations in lane width. GAPDH was used as the loading control in this study after determining that GAPDH expression was not affected by either age or length of post-mortem interval (PMI, see Results). The expression of Classic- and Golli-MBP in each lane of the blot was divided by GAPDH expression in the same lane. To compare protein expression levels across blots, a control sample (mixture of all samples) was run on every gel, and for each sample on a blot the density was normalized to the density of the control sample. Finally, for each MBP protein, expression levels across runs were normalized using the average expression of the protein.

To analyze the developmental changes in Classic- and Golli-MBP we began by plotting scatterplots, showing the results from every run (grey dots) as well as the average for each sample (black dots), and histograms binning all the data into different age groups. We applied a

model-fitting approach (Christopoulos and Lew, 2000) to determine the best fitting curve to the data presented in the scatterplots (grey dots) using Matlab. Significant curve fits are plotted on the scatterplots. We found that quadratic functions were good fits to each data set ($y = \text{PeakExp} + A \cdot (x - \text{PeakAge})^2$) and the best fitting curves were determined by least squares giving the goodness-of-fit (R), statistical significance of the fit (p), and 95% confidence interval (CI) for the age at the peak of the function. The age when mature levels of protein expression were reached was calculated from the parameters of the curve-fits and was defined as the age when protein expression first reached 90% of peak expression.

We compared differences among developmental stages by binning the data into the following age groups: neonatal (< 0.4 years), infants (0.4 - 1 years), young children (1-4 years), older children (5-11 years), teens (12-20 years), young adults (21-55 years), and older adults (>55 years). Histograms were plotted using the mean and standard error of the mean (SEM) for each age bin. Statistical comparisons among age groups were made using an analysis of variance (ANOVA) and when significant ($p < 0.05$), Tukey's post-hoc comparisons were done to determine which age groups were significantly different.

We quantified changes in the relative expression of Classic- to Golli-MBP by calculating an index using the formula $(\text{Classic-MBP} - \text{Golli-MBP}) / (\text{Classic-MBP} + \text{Golli-MBP})$. The two families of MBP are genetically and functionally related so this index provides information about their combined development. The index can vary from -1 to +1 and this type of contrast index is commonly used in signal processes to reduce noise. Here we applied the index to analyze the balance between Classic- and Golli-MBP across the lifespan, where negative values represent more Golli-MBP and positive values more Classic-MBP. The index was plotted as described

above. Briefly, a quadratic function was fit to all the index data and an analysis of variance was done to compare changes in the index among age bins.

In a previous study, we identified stages in cortical development when there was high inter-individual variability in the expression of various synaptic proteins (Pinto et al., 2015). We applied the same approach in this study to examine changes in inter-individual variability in expression of Classic- and Golli-MBP by calculating the Fano Factor (Variance-to-Mean Ratio, VMR) for each MBP protein. The VMR at each age was calculated using the average protein expression for each case and determining the mean and variance in expression within a window that included the case and the two adjacent ages. The VMRs for Classic- and Golli-MBP were plotted as scatterplots to visualize whether there are ages in development with high inter-individual variability.

3.3 Results

Loading control and postmortem interval

Our first step was to determine the best loading control for this study by quantifying expression of the two most commonly used loading controls, GAPDH and β -Tubulin. We were looking for a loading control that had similar expression in human visual cortex across all ages. We found that β -Tubulin declined across the lifespan (Fig 1A; $R=0.5669$, $p<0.0001$; Fig 1B; ANOVA, $F=18.71$, $p<0.0001$). In contrast, GAPDH expression did not change across the lifespan as neither the ANOVA or curve-fits were significant (Fig 1C,D), therefore we selected GAPDH to use as the loading control. Next, we compared GAPDH expression with PMI and found no effect of the length of PMI on GAPDH expression ($R=0.05$, n.s.). Finally, we assessed

the effect of PMI on expression of Classic- and Golli-MBP to determine if any samples needed to be removed because the PMI was too long. We found no correlation with PMI for either myelin protein (Classic: $R=0.307$, n.s.; Golli: $R=0.143$, n.s.) so all samples were included in the study.

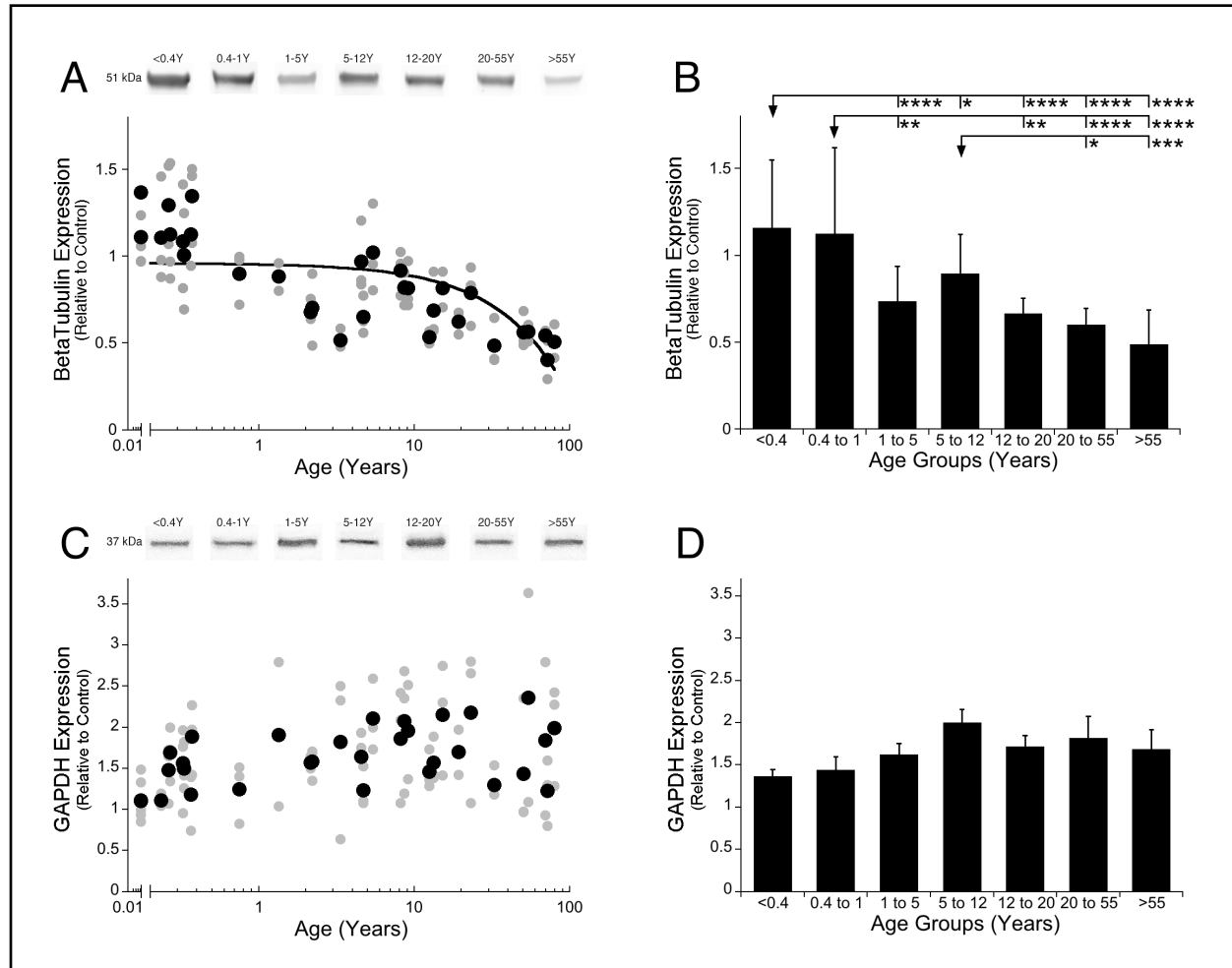


Figure 1. Developmental changes in β -Tubulin (A,B) and GAPDH (C,D) expression in human visual cortex. (A, C) Scatterplots show grey dots for the results from each run, with significant curve fits, and black dots for the average expression for each sample. Example bands from the Western blots are displayed above the graphs. (B, D) Histograms show group means and the standard error for each developmental group. (A) A quadratic function was fit to the β -Tubulin data points ($R=0.567$, $p < 0.0001$). (B) There was a significant difference in expression of β -Tubulin (ANOVA, $F=18.715$, $p < 0.0001$) and Tukey's post-hoc comparisons were made between groups ($*p < 0.05$, $**p < 0.01$, $***p < 0.001$, $****p < 0.0001$). (C) There was no significant change in GAPDH expression across the lifespan. (D) There was no significant difference in expression of GAPDH between the developmental age groups.

Developmental of Classic- and Golli-MBP

To study Classic- and Golli-MBP expression in human visual cortex, we used two approaches: model fitting to describe the developmental trajectories, and age binning of the data to compare among stages of development. We found a gradual increase in expression of Classic-MBP that continued into adult years, before a roll off in aging. That trajectory was well fit by a quadratic function ($y=1.999-0.0008182*(x-42.01)^2$; $R=0.59$, $p<0.0001$) showing that Classic-MBP rose through development, increasing about 4-fold to the peak of expression at 42 years (95% CI +/- 4.26 years)(Fig 2A). We defined the age when Classic-MBP matures as the age when expression reached 90% of the peak. For Classic-MBP that occurred at about 38 years of age showing the very slow and prolonged development of this myelin protein in human visual cortex.

We compared expression of Classic-MBP across developmental stages and found significant differences among the various stages (ANOVA; $F=10.25$; $p<0.0001$)(Fig 2B). Classic-MBP expression in neonates (<0.4 years) was less than all of the other age groups (Fig 2B; p values range 0.0001 - 0.01). There was a jump in expression between neonates and infants (0.4-1 year) ($p < 0.01$), another significant increase between children (5-12 years) and young adults (20-55 years)($p < 0.01$), followed by a trend to decline into aging (>55 years)($p = 0.14$). Together, the curve-fitting and developmental stage comparisons showed that Classic-MBP in human visual cortex had prolonged development and substantial increase in expression.

The developmental trajectory for Golli-MBP was very different from Classic-MBP. Golli-MBP expression was very low in neonates (<0.4 years) and increased abruptly in slightly older infants. This early postnatal jump in Golli-MBP could be seen in both the scatterplot and age binned histogram (Fig 2C,D). Because of this pattern, we chose to apply model fitting to analyze

development for cases older than 0.4 years of age. Expression of Golli-MBP expression for cases older than 0.4 years was well fit by an inverse quadratic function ($y=0.6301+0.15*(\log(x)-\log(10.31))^2$; $R=0.61$; $p<0.0001$) (Fig 2C). Golli-MBP expression dropped from high levels to reach a minimum at about 10 years of age (Fig 2C; minimum = 10.3 years 95% CI +/- 3.8) and then increased through adults into aging. Analysis of the age binned groups found similar results (Fig 2D; ANOVA; $F=10.95$, $p<0.0001$). Golli-MBP expression in infants (0.4 - 1 year) was significantly higher than all of the other age groups (Fig 2D; p values range $< 0.0001 - 0.01$). Children (5-12 years) had the lowest level of Golli-MBP followed by a 2-fold increase in expression into aging ($p<0.0001$). Thus, the rate of development of Golli- was faster than Classic-MBP, the peaks were at different ages, Golli- decreased while Classic-MBP increased through childhood, then they flipped and Golli- increased while Classic-MBP decreased into aging.

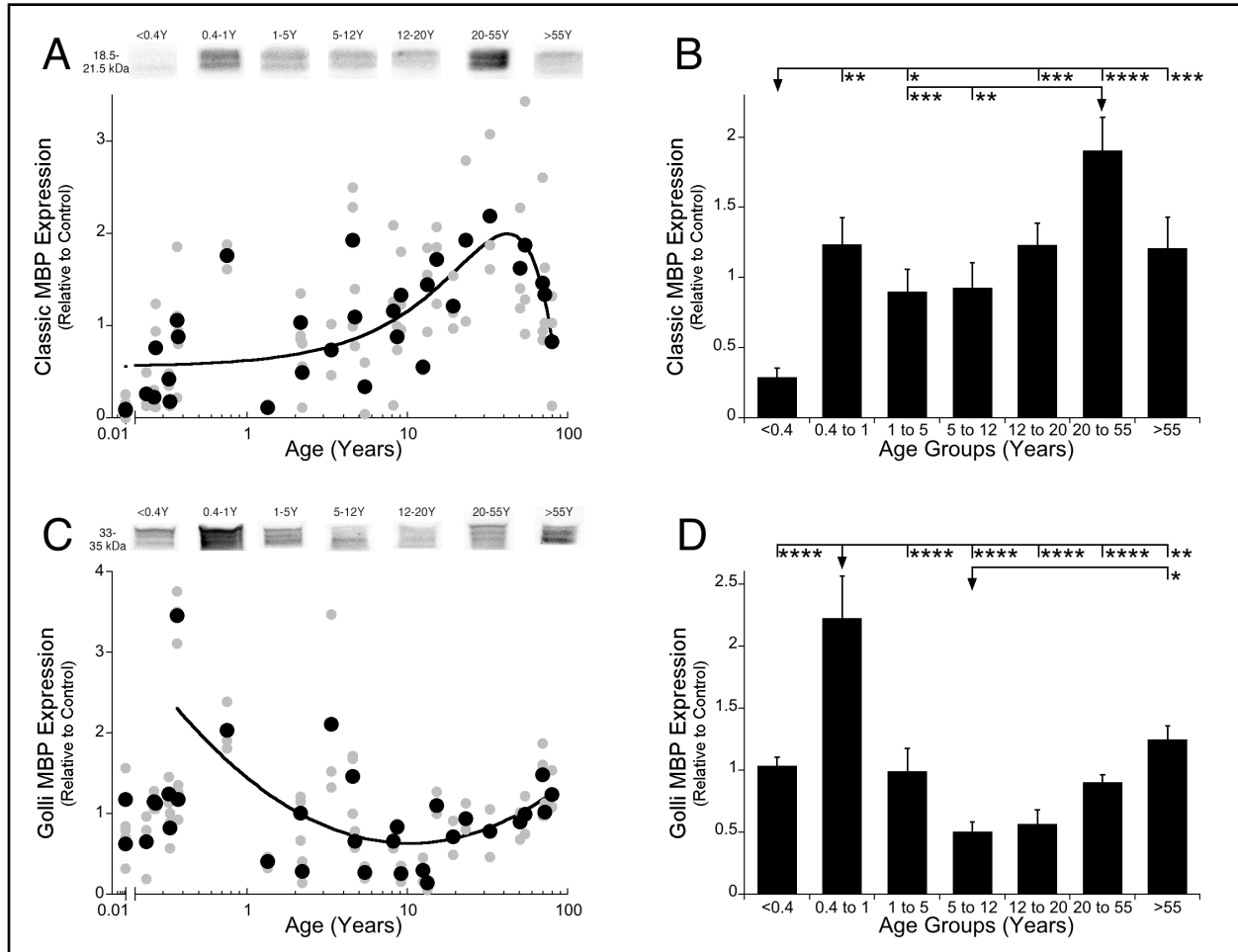


Figure 2. Developmental changes in Classic- (A,B) and Golli-MBP (C,D) expression across the lifespan in human visual cortex. (A, C) Scatterplots show grey dots for the results from each run, with significant curve fits, and black dots for the average expression for each sample. Example bands from the Western blots are displayed above the graphs. (B, D) Histograms show group means and standard error for each developmental group. (A) A quadratic function was fit to all Classic-MBP data points ($R=0.59$, $p<0.0001$), and a peak in expression was reached at 42 years of age (peak = 42 years 95% CI +/- 4.26 years). (B) There was a significant difference in expression of Classic-MBP (ANOVA, $F=10.248$, $p < 0.0001$) and Tukey's post-hoc comparisons were made between groups ($*p<0.05$, $**p<0.01$, $***p<0.001$, $****p<0.0001$). (C) An inverse quadratic function was fit to all the Golli-MBP data points older than 0.4 years of age ($R=0.61$; $p<0.0001$), and reached minimum expression at about 10 years of age (minimum = 10.3 years 95% CI +/- 3.8). (D) There was a significant difference in expression of Golli-MBP (ANOVA, $F=10.955$, $p<0.0001$) and Tukey's post-hoc comparisons were made between groups ($*p<0.05$, $**p<0.01$, $***p<0.001$, $****p<0.0001$).

Balance between Classic- and Golli-MBP

Often changes in Classic- and Golli-MBP are described as moving in opposite directions. Even the current results, especially the histograms (Fig 2B,D) appeared to be complementary, but when we analyzed the relationship between Classic- and Golli-MBP we found no correlation ($R=0.177$, n.s.), suggesting that there is no simple linear relationship for the amount of protein expressed by these two MBP families. However, there is a functional link between Golli- and Classic-MBP through calcium signaling (Smith et al., 2011; Paez et al., 2009), and in addition Golli-MBP KO mice have profound hypomyelination in the visual cortex (Jacobs et al., 2005). Those two findings provide evidence of a relationship, and so we analyzed the relative expression of Classic-to-Golli-MBP. We calculated an index $((\text{Classic-MBP} - \text{Golli-MBP}) / (\text{Classic-MBP} + \text{Golli-MBP}))$ that could vary from -1 (only Golli-MBP) to +1 (only Classic-MBP) and provided information about how the balance between Classic- and Golli-MBP changed in human visual cortex across the lifespan. The scatterplot and age binned histogram of the Classic-to-Golli-MBP index showed gradual changes that continued across the entire lifespan (Fig 3 A,B). A quadratic function was a good fit to the index results ($y=0.6308-0.0006492*(x-38.92)^2$; $R=0.65$, $p<0.0001$) and captured the gradual shift from more Golli- to more Classic-MBP, then back to relatively more Golli-MBP in older adults (Fig 3A). The function crossed from more Golli- to more Classic-MBP at 7.6 years of age, reached a peak with more Classic-MBP at about 38 years of age (38.3 years, 95% CI +/- 2.7 years) and crossed back to more Golli-MBP at about 68 years (Fig 3A). There were also significant differences among the developmental stages (Fig 3B; ANOVA, $F=16.35$, $p<0.0001$). Teens (12-20 years) and young adults (20-55 years) had relatively more Classic-MBP than the other age groups. The initial shift in the index was driven by the more rapid loss of Golli-MBP, then the switch to

Classic-MBP by the prolonged increase in Classic-, and the change into aging by complementary decrease and increase in Classic- and Golli-MBP, respectively. These results suggest three phases of development, an early stage (<8 years) when Golli-MBP is changing, an intermediate stage (8 - 67 years) when Classic-MBP changes and a late stage (>68 years) when both families of MBP change.

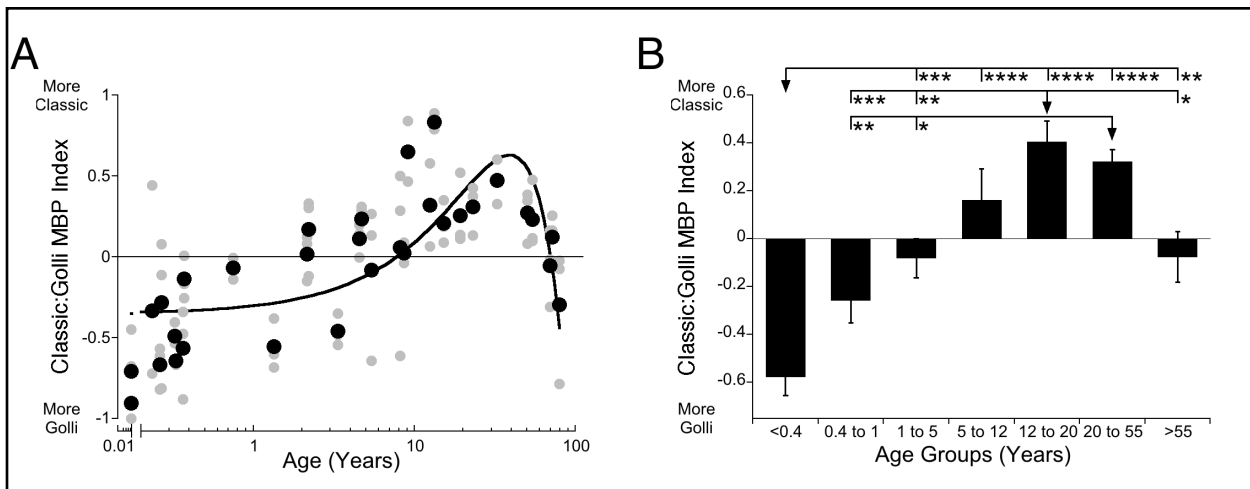


Figure 3. Developmental changes of Classic- to Golli-MBP index across the lifespan in human visual cortex. (A) Scatterplot shows grey dots for the index results from each run, with a significant curve fit, and black dots for the average value for each sample. (B) Histogram shows group means and standard errors for each developmental group. (A) A quadratic function was fit to all the Classic:Golli index data points ($R= 0.653$, $p<0.0001$) and showed relatively more Classic-MBP at 7.6 years, showed peak Classic-MBP expression at 38 years (38.3 years, 95% CI ± 2.7 years) then showed more Golli-MBP at 68 years of age. (B) There was a significant difference in the Classic:Golli MBP index expression (ANOVA, $F=16.35$, $p<0.0001$) and Tukey's post-hoc comparisons were made between groups ($*p<0.05$, $**p<0.01$, $***p<0.001$, $****p<0.0001$).

Inter-individual variability

In our recent paper, we discovered stages in development of human visual cortex when there was a high degree of inter-individual variability in expression of synaptic proteins (Pinto et al., 2015). To assess if Classic- or Golli-MBP had similar waves of inter-individual variability we

calculated the Fano factor (Variance-to-Mean Ratio, VMR) for a running window of 3 adjacent ages for each protein, and plotted the VMR across the lifespan. The VMR for Classic-MBP was low at all ages, suggesting that there was little inter-individual variability in expression of Classic-MBP in visual cortex (Fig 4A). In contrast, Golli-MBP had a period with higher inter-individual variability between about 0.4 and 5 years of age that peaked at 1.4 years ($y=0.920387*\exp(-0.285089/x-0.151975*x)$) (Fig 4B). These findings highlight another way that expression of the two families of MBP differ and raises the possibility that the wave of high inter-individual variability for Golli-MBP reflects a period of vulnerability in development of human visual cortex.

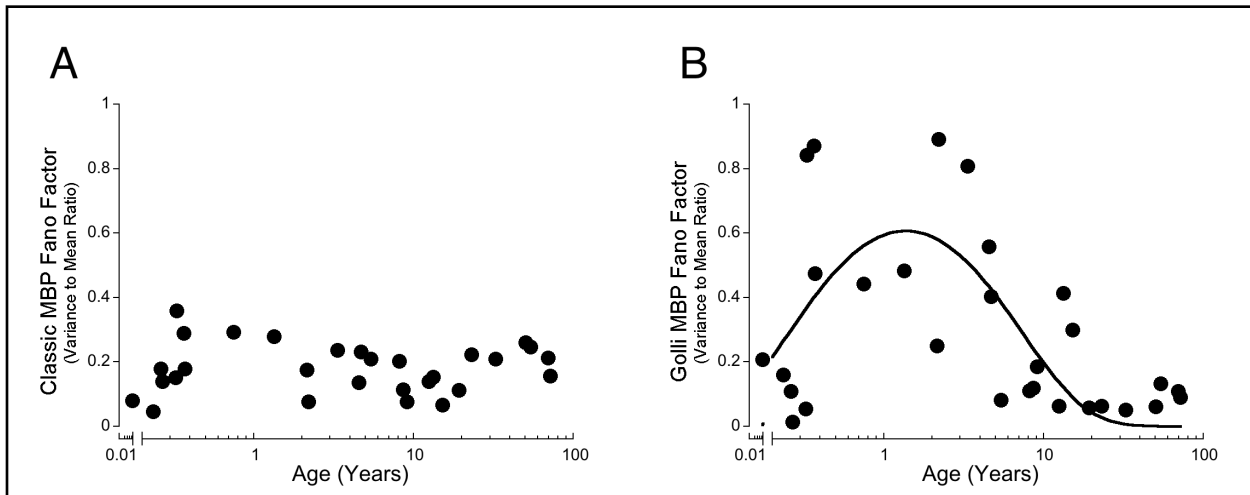


Figure 4. Development of the Variance-to-Mean Ratio (VMR) for Classic-MBP (A) and Golli-MBP (B). (A) Classic-MBP had no change in VMR across the lifespan. (B) A quadratic function was fit to all Golli-MBP VMR data points, and had a period of high VMR early on with a peak at about 1.4 years of age.

3.4 Discussion

The changes in Classic- and Golli-MBP found in this study of human visual cortex highlight the complex nature of myelin expression in the brain. We found that these two families of MBP follow different developmental trajectories, have 3 stages of a Classic:Golli balance, and only Golli-MBP has high inter-individual variability during childhood. We have 3 main conclusions from this study.

Different developmental trajectories for Classic- and Golli-MBP in human visual cortex

First, Classic- and Golli-MBP follow different trajectories during development and aging of human visual cortex. Classic-MBP had a prolonged period of development that extended well into adulthood and then declined into aging. The pattern of prolonged development is consistent with findings from anatomical and brain imaging studies of myelin in human cortex. Anatomical measurements of myelin sheath density from postmortem human cortex showed that maturation continued well into the third decade of life (Miller et al., 2012). Brain imaging of myelin content in human cortex also showed that grey matter myelin continued to increase into adulthood (Grydeland et al., 2013; Shafee et al., 2015). Together, those results confirm that myelin development in human visual cortex extends well beyond the window of time (6-10 years of age) that represents the end of the sensitive period for development of lazy-eye (amblyopia) (Epelbaum et al., 1993; Keech and Kutschke, 1995; Lewis and Maurer, 2005). Our study also identified that Classic-MBP expression continued to change in older adults by declining into aging. The loss of Classic-MBP into aging is similar to findings from in vivo imaging of cortical myelin (Grydeland et al., 2013) and may be related to degeneration of myelin sheath integrity in aging monkey visual cortex (Peters et al., 2008).

The development of Golli-MBP was different from Classic-MBP providing additional evidence that the various myelin proteins follow different developmental trajectories (Miller et al., 2012). We found an abrupt increase in Golli-MBP at about 4-6 months of age, a peak around 1 year followed by a decline to the minimum level at about 10 years, and then a gradual increase into aging. The abrupt increase in Golli-MBP corresponds with the start of the sensitive period for development of binocular vision (Banks et al., 1975) and matches the timing of rapid changes in the balances among pre- and post-synaptic proteins in human visual cortex (Pinto et al., 2015). Perhaps the coincidence in timing of abrupt changes in Golli-MBP and synaptic proteins helps to trigger the start of a period of heightened plasticity when visual experience readily sculpts maturation of circuits in the visual cortex.

It is interesting to consider how the early changes in Golli-MBP could contribute to mechanisms that facilitate and limit experience-dependent plasticity in the developing visual cortex. We chose to study Golli-MBP because it has been called a 'molecular link' between the nervous and immune systems (Pribyl et al., 1993), and its functions during neural development are consistent with Golli-MBP contributing to sensitive period plasticity. Golli-MBP is found in developing oligodendrocytes (Campagnoni et al., 1993), neurons (Landry et al., 1996), T-cells (Feng et al., 2000; 2004) and macrophages (Papenfuss et al., 2007), and is a major regulatory protein for calcium influx into both oligodendrocytes (Paez et al., 2007) and T-cells (Feng et al., 2004). Its expression during early development increases cell migration, proliferation, extension, and retraction which contributes to maturation of neuroglia (Paez et al., 2009) and is consistent with supporting developmental plasticity. Golli-MBP is an intrinsically disordered protein that

provides many sites for protein-protein interactions (Ahmed et al., 2007) that may be candidate sites to mediate experience-dependent plasticity.

At the other end of the lifespan, we found an age-related increase of Golli-MBP in visual cortex. Golli-MBP plays an important role in myelin repair, since Golli over-expressing mice have increased survival and proliferation of remyelinating oligodendrocytes (Paez et al., 2012). The age-related increase in Golli-MBP may reflect an increase in oligodendrocytes and changes in myelination such as thicker and shorter myelin segments that have been found in visual cortex of old monkeys (Peters et al., 2001; Peters and Sethares, 2004; Peters et al., 2008). Therefore, as a molecular link between the nervous and immune systems, Golli-MBP may bridge those systems and contribute to neuroimmune driven neurodegenerative diseases. Unfortunately, there have been no studies of Golli-MBP function in the aging brain and to the best of our knowledge our finding of increased Golli-MBP expression in human visual cortex is the first report of Golli-MBP in the aging brain. Clearly, more studies are needed to determine how Golli-MBP functions in the aging cortex and what role it plays in neuroimmune processes involved in neurodegeneration.

Three stages of MBP development

Our second conclusion is that the balance between Classic- and Golli-MBP in human visual cortex has 3 stages. We found an early stage during childhood (<8 years) when Golli-MBP dominated, an intermediate stage (8 - 67 years) when there was more Classic-MBP, and a late stage (>68 years) that shifted back to more Golli-MBP. The 3 stages were driven by the different trajectories for Classic- and Golli-MBP. The early stage was marked by rapid changes in Golli-MBP expression while the intermediate stage had relatively constant Golli- and gradually

increasing Classic-MBP. Finally, the aging stage reflected both an increase of Golli- and loss of Classic-MBP. Examining the balance between Classic- and Golli-MBP is a new way to study MBP changes across the lifespan and although these proteins do not interact directly, Golli-MBP can affect expression of Classic-MBP. For example, over-expression of Golli-MBP significantly delays expression of Classic-MBP and the process of myelination, (Jacobs et al., 2009) while knocking out Golli causes permanent hypomyelination of the visual cortex (Jacobs et al., 2005). Perhaps, higher expression of Golli-MBP during development of human visual cortex delays myelination, thereby holding off one of the brakes on critical period plasticity (McGee et al., 2005).

The timing of the shift to more Classic-MBP corresponds with the end of the sensitive period for development of amblyopia in children (Epelbaum et al., 1993; Keech and Kutschke, 1995; Lewis and Maurer, 2005). That stage of the Classic-:Golli-MBP balance may contribute to a period of stability in the visual cortex as Classic-MBP expression increases into adulthood. Traditionally, myelination is viewed as supporting signal transduction by enabling saltatory propagation of neural impulses. More recently, myelin has been shown to be important for supporting (Fields, 2005; 2014) or limiting synaptic plasticity (McGee et al., 2005), and transporting metabolites to axons (Saab et al., 2013; Nave and Werner, 2014). Glutamate release promotes formation of the myelin sheath around axons and increases synthesis of Classic-MBP thereby linking myelination with electrically active axons (Wake et al., 2011). In our recent study of synaptic proteins in human visual cortex (Pinto et al., 2015), we found that the glutamate receptor scaffolding protein, PSD-95, increases during late childhood at a similar point in development when Classic-MBP expression takes off. Interestingly, Classic-MBP has an SH3

ligand that can bind to the SH3 binding site on PSD-95 (Polverini et al., 2008), thereby providing a mechanism where Classic-MBP may contribute to SH3-mediated establishment of a stable lattice of PSD-95 molecules at the post-synaptic density (Sturgill et al., 2009). Myelin also functions to supply axons with metabolites and neurotrophic factors that are necessary to maintain healthy neural connections (Nave and Werner, 2014). These 2 lines of evidence suggest that the stage when Classic-MBP dominates is driven by an increase in excitatory activity and supports a period of optimal axonal energy metabolism.

The late stage of the Classic-Golli-MBP balance was the shift to relatively more Golli-MBP. There have been no studies of Golli-MBP function in the aging cortex, but its roles in demyelination and remyelination (Paez et al., 2012), and multiple sites for protein-protein interactions make it an ideal candidate for regulating changes to myelination in the aging cortex. In addition, this loss of Classic-MBP suggests that one component of impaired circuit function in the aging cortex may be reduced metabolic support for axons.

A wave of Golli-MBP inter-individual variability during childhood

Our third conclusion is that Golli-MBP goes through a period of high inter-individual variability in childhood. In our previous study of synaptic protein development in human visual cortex, we found protein specific waves of high inter-individual variability throughout childhood (Pinto et al., 2015). In the current study, only Golli-MBP had a wave of high inter-individual variability in childhood, while Classic-MBP had low variability across the lifespan. The timing of the wave of Golli-MBP variability was similar to the wave for PSD-95 (Pinto et al., 2015) with both being low in neonates, high during infancy and childhood, then dropping to low levels in adults. The difference in variability between Golli- and Classic-MBP suggests that Golli-

MBP expression is more dynamic than myelin structural proteins such as Classic-MBP. Since Golli-MBP is involved in signaling between neurons, oligodendrocytes, and immune cells, the wave of variability in childhood is likely a complex interaction reflecting a period of vulnerability between neural and immune systems. Perhaps it is linked to the high risk of infection during childhood. In contrast, we were surprised by the lack of inter-individual variability for Golli-MBP in aging, especially since neuroimmune regulation is impaired in age-related neurodegeneration (Frank-Cannon et al., 2009).

Studying myelin in visual cortex

Myelin proteins bind to Nogo and PirB receptors to inhibit axon regeneration (Hu and Strittmatter, 2004; Atwal et al., 2008), and in the visual cortex both of those receptors limit experience-dependent plasticity (McGee and Strittmatter, 2003; Syken et al., 2006). Mutations to or blocking either Nogo-66 or PirB receptors allow ocular dominance plasticity to continue into adulthood (McGee et al., 2005; Syken et al., 2006; Bochner et al., 2014) showing a link between myelin proteins, neuroimmune processes, and visual experience-dependent plasticity. Over-expression of Golli-MBP significantly delays myelination (Jacobs et al., 2009) while knocking out Golli-MBP causes profound hypomyelination that is restricted to the visual cortex (Jacobs et al., 2005). Thus, both too much or no Golli-MBP affect myelination. The specific effect of knocking out Golli-MBP on myelination of the visual cortex suggests that it plays a special role in maturation of that cortical area.

In this study, we found that the shift from more Golli- to more Classic-MBP in human visual cortex coincides with the end of the sensitive period for development of amblyopia.

Furthermore, MBP mRNA is reduced in the visual cortex of patients with schizophrenia

(Matthews et al., 2012) suggesting that it may contribute to the pathophysiology underlying changes in their visual perception. Thus, the visual cortex is an interesting cortical area for studying the role of myelin proteins in disease.

Previous studies of myelin in the human brain have focused on white matter maturation (e.g. Guleria and Kelly, 2014; Paus, 2010) and diseases related to changes in the white matter (Fields, 2008). In contrast, our study quantified Classic- and Golli-MBP expression in human visual cortex. The findings are timely because novel MRI techniques are driving renewed interest in the role of myelin function in human cortex (Glasser et al., 2014). Furthermore, the changes in Golli-MBP expression in human visual cortex raise new questions about its role as a molecular link between neural and immune systems at different stages of the lifespan.

3.5 References

- Ahmed, M. A. M., Bamm, V. V., Harauz, G., and Ladizhansky, V. (2007). The BG21 isoform of Golli myelin basic protein is intrinsically disordered with a highly flexible amino-terminal domain. *Biochemistry* 46, 9700–9712. doi:10.1021/bi700632x.
- Atwal, J. K., Pinkston-Gosse, J., Syken, J., Stawicki, S., Wu, Y., Shatz, C., and Tessier-Lavigne, M. (2008). PirB is a functional receptor for myelin inhibitors of axonal regeneration. *Science* 322, 967–970. doi:10.1126/science.1161151.
- Banks, M. S., Aslin, R. N., and Letson, R. D. (1975). Sensitive period for the development of human binocular vision. *Science* 190, 675–677.
- Baruch, K., Silberberg, G., Aviv, A., Shamir, E., Bening-Abu-Shach, U., Baruch, Y., Darvasi, A., and Navon, R. (2009). Association between golli-MBP and schizophrenia in the Jewish Ashkenazi population: are regulatory regions involved? *Int. J. Neuropsychopharmacol.* 12, 885–894. doi:10.1017/S1461145708009887.
- Bochner, D. N., Sapp, R. W., Adelson, J. D., Zhang, S., Lee, H., Djuricic, M., Syken, J., Dan, Y., and Shatz, C. J. (2014). Blocking PirB up-regulates spines and functional synapses to unlock visual cortical plasticity and facilitate recovery from amblyopia. *Sci Transl Med* 6, 258ra140–258ra140. doi:10.1126/scitranslmed.3010157.
- Campagnoni, A. T., Pribyl, T. M., Campagnoni, C. W., Kampf, K., Amur-Umarjee, S., Landry, C. F., Handley, V. W., Newman, S. L., Garbay, B., and Kitamura, K. (1993). Structure and developmental regulation of Golli-mbp, a 105-kilobase gene that encompasses the myelin basic protein gene and is expressed in cells in the oligodendrocyte lineage in the brain. *Development* 120, 4930–4938.
- Christopoulos, A., and Lew, M. J. (2000). Beyond eyeballing: Fitting models to experimental data. *Crit. Rev. Biochem. Mol. Biol.* 35, 359–391. doi:10.1080/10409230091169212.
- Epelbaum, M., Milleret, C., Buisseret, P., and Dufier, J. L. (1993). The sensitive period for strabismic amblyopia in humans. *Ophthalmology* 100, 323–327.
- Feng, J. M., Givogri, I. M., Bongarzone, E. R., Campagnoni, C., Jacobs, E., Handley, V. W., Schonmann, V., and Campagnoni, A. T. (2000). Thymocytes express the golli products of the myelin basic protein gene and levels of expression are stage dependent. *J. Immunol.* 165, 5443–5450.
- Feng, J.-M., Fernandes, A. O., Campagnoni, C. W., Hu, Y.-H., and Campagnoni, A. T. (2004). The golli-myelin basic protein negatively regulates signal transduction in T lymphocytes. *J. Neuroimmunol.* 152, 57–66. doi:10.1016/j.jneuroim.2004.03.021.

- Fields, R. D. (2005). Myelination: an overlooked mechanism of synaptic plasticity? *Neuroscientist* 11, 528–531. doi:10.1177/1073858405282304.
- Fields, R. D. (2014). Neuroscience. Myelin--more than insulation. *Science* 344, 264–266. doi: 10.1126/science.1253851.
- Fields, R. D. (2008). White matter in learning, cognition and psychiatric disorders. *Trends in Neurosciences* 31, 361–370. doi:10.1016/j.tins.2008.04.001.
- Frank-Cannon, T. C., Alto, L. T., McAlpine, F. E., and Tansey, M. G. (2009). Does neuroinflammation fan the flame in neurodegenerative diseases? *Mol Neurodegener* 4, 47. doi:10.1186/1750-1326-4-47.
- Geyer, S., Weiss, M., Reimann, K., Lohmann, G., and Turner, R. (2011). Microstructural Parcellation of the Human Cerebral Cortex - From Brodmann's Post-Mortem Map to in vivo Mapping with High-Field Magnetic Resonance Imaging. *Front Hum Neurosci* 5, 19. doi:10.3389/fnhum.2011.00019.
- Glasser, M. F., and Van Essen, D. C. (2011). Mapping Human Cortical Areas In Vivo Based on Myelin Content as Revealed by T1- and T2-Weighted MRI. *Journal of Neuroscience* 31, 11597–11616. doi:10.1523/JNEUROSCI.2180-11.2011.
- Glasser, M. F., Goyal, M. S., Preuss, T. M., Raichle, M. E., and Van Essen, D. C. (2014). Trends and properties of human cerebral cortex: Correlations with cortical myelin content. *NeuroImage* 93, 165–175. doi:10.1016/j.neuroimage.2013.03.060.
- Grydeland, H., Walhovd, K. B., Tamnes, C. K., Westlye, L. T., and Fjell, A. M. (2013). Intracortical Myelin Links with Performance Variability across the Human Lifespan: Results from T1-and T2-Weighted MRI Myelin Mapping and Diffusion Tensor Imaging. *Journal of Neuroscience* 33, 18618–18630. doi:10.1523/JNEUROSCI.2811-13.2013.
- Guleria, S., and Kelly, T. G. (2014). Myelin, myelination, and corresponding magnetic resonance imaging changes. *Radiol. Clin. North Am.* 52, 227–239. doi:10.1016/j.rcl.2013.11.009.
- Harauz, G., and Boggs, J. M. (2013). Myelin management by the 18.5-kDa and 21.5-kDa classic myelin basic protein isoforms. *J. Neurochem.* 125, 334–361. doi:10.1111/jnc.12195.
- Harauz, G., Ladizhansky, V., and Boggs, J. M. (2009). Structural polymorphism and multifunctionality of myelin basic protein. *Biochemistry* 48, 8094–8104. doi:10.1021/bi901005f.
- Hu, F., and Strittmatter, S. M. (2004). Regulating axon growth within the postnatal central nervous system. *Semin. Perinatol.* 28, 371–378.

- Jacobs, E. C., Pribyl, T. M., Feng, J.-M., Kampf, K., Spreur, V., Campagnoni, C., Colwell, C. S., Reyes, S. D., Martin, M., Handley, V., et al. (2005). Region-specific myelin pathology in mice lacking the golli products of the myelin basic protein gene. *J. Neurosci.* 25, 7004–7013. doi:10.1523/JNEUROSCI.0288-05.2005.
- Jacobs, E. C., Reyes, S. D., Campagnoni, C. W., Irene Givogri, M., Kampf, K., Handley, V., Spreuer, V., Fisher, R., Macklin, W., and Campagnoni, A. T. (2009). Targeted overexpression of a golli-myelin basic protein isoform to oligodendrocytes results in aberrant oligodendrocyte maturation and myelination. *ASN Neuro* 1, 213–226. doi: 10.1042/AN20090029.
- Keech, R. V., and Kutschke, P. J. (1995). Upper age limit for the development of amblyopia. *J Pediatr Ophthalmol Strabismus* 32, 89–93.
- Landry, C. F., Ellison, J. A., Pribyl, T. M., Campagnoni, C., Kampf, K., and Campagnoni, A. T. (1996). Myelin basic protein gene expression in neurons: developmental and regional changes in protein targeting within neuronal nuclei, cell bodies, and processes. *Journal of Neuroscience* 16, 2452–2462.
- Lewis, T. L., and Maurer, D. (2005). Multiple sensitive periods in human visual development: evidence from visually deprived children. *Dev Psychobiol* 46, 163–183. doi:10.1002/dev.20055.
- Matthews, P. R., Eastwood, S. L., and Harrison, P. J. (2012). Reduced myelin basic protein and actin-related gene expression in visual cortex in schizophrenia. *PLoS ONE* 7, e38211. doi:10.1371/journal.pone.0038211.
- McGee, A. W., and Strittmatter, S. M. (2003). The Nogo-66 receptor: focusing myelin inhibition of axon regeneration. *Trends in Neurosciences* 26, 193–198. doi:10.1016/S0166-2236(03)00062-6.
- McGee, A. W., Yang, Y., Fischer, Q. S., Daw, N. W., and Strittmatter, S. M. (2005). Experience-driven plasticity of visual cortex limited by myelin and Nogo receptor. *Science* 309, 2222–2226. doi:10.1126/science.1114362.
- Mighdoll, M. I., Tao, R., Kleinman, J. E., and Hyde, T. M. (2015). Myelin, myelin-related disorders, and psychosis. *Schizophr. Res.* 161, 85–93. doi:10.1016/j.schres.2014.09.040.
- Miller, D. J., Duka, T., Stimpson, C. D., Schapiro, S. J., Baze, W. B., McArthur, M. J., Fobbs, A. J., Sousa, A. M. M., Sestan, N., Wildman, D. E., et al. (2012). Prolonged myelination in human neocortical evolution. *Proc. Natl. Acad. Sci. U.S.A.* 109, 16480–16485. doi: 10.1073/pnas.1117943109.

- Nave, K.-A., and Werner, H. B. (2014). Myelination of the nervous system: mechanisms and functions. *Annu. Rev. Cell Dev. Biol.* 30, 503–533. doi:10.1146/annurev-cellbio-100913-013101.
- Paez, P. M., Cheli, V. T., Ghiani, C. A., Spreuer, V., Handley, V. W., and Campagnoni, A. T. (2012). Golli myelin basic proteins stimulate oligodendrocyte progenitor cell proliferation and differentiation in remyelinating adult mouse brain. *Glia* 60, 1078–1093. doi:10.1002/glia.22336.
- Paez, P. M., Fulton, D. J., Spreuer, V., Handley, V., Campagnoni, C. W., Macklin, W. B., Colwell, C., and Campagnoni, A. T. (2009). Golli myelin basic proteins regulate oligodendroglial progenitor cell migration through voltage-gated Ca²⁺ influx. *J. Neurosci.* 29, 6663–6676. doi:10.1523/JNEUROSCI.5806-08.2009.
- Paez, P. M., Fulton, D., Spreuer, V., Handley, V., and Campagnoni, A. T. (2011). Modulation of canonical transient receptor potential channel 1 in the proliferation of oligodendrocyte precursor cells by the golli products of the myelin basic protein gene. *J. Neurosci.* 31, 3625–3637. doi:10.1523/JNEUROSCI.4424-10.2011.
- Paez, P. M., Spreuer, V., Handley, V., Feng, J.-M., Campagnoni, C., and Campagnoni, A. T. (2007). Increased expression of golli myelin basic proteins enhances calcium influx into oligodendroglial cells. *J. Neurosci.* 27, 12690–12699. doi:10.1523/JNEUROSCI.2381-07.2007.
- Papenfuss, T. L., Thrash, J. C., Danielson, P. E., Foye, P. E., Hillbrush, B. S., Sutcliffe, J. G., Whitacre, C. C., and Carson, M. J. (2007). Induction of Golli-MBP expression in CNS macrophages during acute LPS-induced CNS inflammation and experimental autoimmune encephalomyelitis (EAE). *ScientificWorldJournal* 7, 112–120. doi:10.1100/tsw.2007.251.
- Paus, T. (2010). Growth of white matter in the adolescent brain: myelin or axon? *Brain Cogn* 72, 26–35. doi:10.1016/j.bandc.2009.06.002.
- Peters, A., and Sethares, C. (2004). Oligodendrocytes, their progenitors and other neuroglial cells in the aging primate cerebral cortex. *Cereb. Cortex* 14, 995–1007. doi:10.1093/cercor/bhh060.
- Peters, A., Sethares, C., and Killiany, R. J. (2001). Effects of age on the thickness of myelin sheaths in monkey primary visual cortex. *J. Comp. Neurol.* 435, 241–248.
- Peters, A., Verderosa, A., and Sethares, C. (2008). The neuroglial population in the primary visual cortex of the aging rhesus monkey. *Glia* 56, 1151–1161. doi:10.1002/glia.20686.

- Pinto, J. G., Jones, D. G., Williams, K., and Murphy, K. M. (2015). Characterizing synaptic protein development in human visual cortex enables alignment of synaptic age with rat visual cortex. *Frontiers in neural circuits* 9, 1–16. doi:10.3389/fncir.2015.00003/abstract.
- Polverini, E., Rangaraj, G., Libich, D. S., Boggs, J. M., and Harauz, G. (2008). Binding of the proline-rich segment of myelin basic protein to SH3 domains: spectroscopic, microarray, and modeling studies of ligand conformation and effects of posttranslational modifications. *Biochemistry* 47, 267–282. doi:10.1021/bi701336n.
- Pribyl, T. M., Campagnoni, C. W., Kampf, K., Ellison, J. A., Landry, C. F., Kashima, T., McMahon, J., and Campagnoni, A. T. (1996). Expression of the myelin basic protein gene locus in neurons and oligodendrocytes in the human fetal central nervous system. *J. Comp. Neurol.* 374, 342–353. doi:10.1002/(SICI)1096-9861(19961021)374:3<342::AID-CNE3>3.0.CO;2-1.
- Pribyl, T. M., Campagnoni, C. W., Kampf, K., Kashima, T., Handley, V. W., McMahon, J., and Campagnoni, A. T. (1993). The human myelin basic protein gene is included within a 179-kilobase transcription unit: expression in the immune and central nervous systems. *Proc. Natl. Acad. Sci. U.S.A.* 90, 10695–10699.
- Roussos, P., and Haroutunian, V. (2014). Schizophrenia: susceptibility genes and oligodendroglial and myelin related abnormalities. *Front Cell Neurosci* 8, 5. doi:10.3389/fncel.2014.00005.
- Saab, A. S., Tzvetanova, I. D., and Nave, K.-A. (2013). The role of myelin and oligodendrocytes in axonal energy metabolism. *Curr. Opin. Neurobiol.* 23, 1065–1072. doi:10.1016/j.conb.2013.09.008.
- Shafee, R., Buckner, R. L., and Fischl, B. (2015). Gray matter myelination of 1555 human brains using partial volume corrected MRI images. *NeuroImage* 105, 473–485. doi:10.1016/j.neuroimage.2014.10.054.
- Smith, G. S. T., Paez, P. M., Spreuer, V., Campagnoni, C. W., Boggs, J. M., Campagnoni, A. T., and Harauz, G. (2011). Classical 18.5- and 21.5-kDa isoforms of myelin basic protein inhibit calcium influx into oligodendroglial cells, in contrast to golli isoforms. *J. Neurosci. Res.* 89, 467–480. doi:10.1002/jnr.22570.
- Sturgill, J. F., Steiner, P., Czervionke, B. L., and Sabatini, B. L. (2009). Distinct domains within PSD-95 mediate synaptic incorporation, stabilization, and activity-dependent trafficking. *J. Neurosci.* 29, 12845–12854. doi:10.1523/JNEUROSCI.1841-09.2009.
- Syken, J., Grandpre, T., Kanold, P. O., and Shatz, C. J. (2006). PirB restricts ocular-dominance plasticity in visual cortex. *Science* 313, 1795–1800. doi:10.1126/science.1128232.

Tosic, M., Rakic, S., Matthieu, J. M., and Zecevic, N. (2002). Identification of Golli and myelin basic proteins in human brain during early development. *Glia* 37, 219–228. doi:10.1002/glia.10028.

Wake, H., Lee, P. R., and Fields, R. D. (2011). Control of local protein synthesis and initial events in myelination by action potentials. *Science* 333, 1647–1651. doi:10.1126/science.1206998.

Chapter 4. Development of glutamatergic proteins in human visual cortex across the lifespan

Publication Reference

Siu, C. R., Beshara, S. P., Jones, D. G., & Murphy, K. M. (2017). Development of Glutamatergic Proteins in Human Visual Cortex across the Lifespan. *The Journal of Neuroscience : the Official Journal of the Society for Neuroscience*, 37(25), 6031–6042. <http://doi.org/10.1523/JNEUROSCI.2304-16.2017>

Abstract

Traditionally, human primary visual cortex (V1) has been thought to mature within the first few years of life, based on anatomical studies of synapse formation, and establishment of intra- and inter-cortical connections. Human vision, however, develops well beyond the first few years. Previously, we found prolonged development of some GABAergic proteins in human V1 (Pinto et al., 2010). Yet as over 80% of synapses in V1 are excitatory, it remains unanswered if the majority of synapses regulating experience-dependent plasticity and receptive field properties develop late like their inhibitory counterparts. To address this question, we used Western blotting of post-mortem tissue from human V1 (12 female, 18 male) covering a range of ages. Then quantified a set of post-synaptic glutamatergic proteins (PSD-95, GluA2, GluN1, GluN2A, GluN2B), calculated indices for functional pairs that are developmentally regulated (GluA2:GluN1; GluN2A:GluN2B), and determined inter-individual variability. We found early loss of GluN1, prolonged development of PSD-95 and GluA2 into late childhood, protracted development of GluN2A until ~40 years and dramatic loss of GluN2A in aging. The GluA2:GluN1 index switched at ~1 year but the GluN2A:GluN2B index continued to shift until ~40 year before changing back to GluN2B in aging. We also identified young childhood as a stage of heightened inter-individual variability. The changes show that human V1 develops gradually through a series of 5 orchestrated stages, making it likely that V1 participates in visual development and plasticity across the lifespan.

Significance

Anatomical structure of human V1 appears to mature early, but vision changes across the lifespan. This discrepancy has fostered 2 hypotheses: either other aspects of V1 continue changing, or later changes in visual perception depend on extrastriate areas. Previously, we showed that some GABAergic synaptic proteins change across the lifespan but most synapses in V1 are excitatory leaving unanswered how they change. So we studied expression of glutamatergic proteins in human V1 to determine their development. Here we report prolonged maturation of glutamatergic proteins, with 5 stages that map onto life-long changes in human visual perception. Thus, the apparent discrepancy between development of structure and function may be explained by life-long synaptic changes in human V1.

4.1 Introduction

Anatomical development of human visual cortex (V1) proceeds quickly over the first few years (Huttenlocher et al., 1982; Zilles et al., 1986; Burkhalter, 1993; Burkhalter et al., 1993) but maturation of vision is slow, changing through childhood, adolescence, adulthood and aging (Kovács et al., 1999; Lewis and Maurer, 2005; Germine et al., 2011; Owsley, 2011). The discrepancy between development of structure and function led to the idea that prolonged maturation of vision might depend on features of V1 not captured by anatomical studies (Taylor et al., 2014). For example, some GABAergic and myelin proteins involved with plasticity continue developing into adulthood in human V1 (Pinto et al., 2010; Siu et al., 2015). Most V1 synapses, however, are excitatory (Beaulieu et al., 1992) and glutamatergic receptors regulate experience-dependent plasticity (Hensch, 2004; Turrigiano and Nelson, 2004; Cooper and Bear, 2012; Levelt and Hübener, 2012) and receptive field properties (Ramoá et al., 2001; Rivadulla et al., 2001; Fagiolini et al., 2004; Self et al., 2012). Currently, little is known about expression of glutamatergic proteins in human V1 (Huntley et al., 1994; Scherzer et al., 1998) and less about how they change across the lifespan (Pinto et al., 2015).

Animal models found that activation of glutamate receptors, NMDA (N-methyl-D-aspartate) and AMPA (α -amino-3-hydroxy-5-methyl-4-isoxazolepropionic acid), regulate plasticity in V1 (Kleinschmidt et al., 1987; Daw et al., 1992; Turrigiano and Nelson, 2004; Yashiro and Philpot, 2008; Smith et al., 2009; Cooke and Bear, 2014; Turrigiano, 2017). The recruitment of AMPARs to silent synapses starts the critical period (CP) (Rumpel et al., 1998) and an increase in the glutamate receptor scaffolding protein, PSD-95, consolidates synapses to end the CP (Huang et al., 2015). The composition of AMPARs and NMDARs regulates juvenile ocular dominance plasticity starting with weakening of deprived eye responses by the rapid loss of GluA2 (Heynen et al., 2003; Lambo and Turrigiano, 2013) and increase of GluN2B (Chen and Bear, 2007).

Next, open eye responses are strengthened by an increase of GluA2 (Lambo and Turrigiano, 2013) and decrease of GluN2A (Smith et al., 2009). The developmental shift from more GluN2B to more GluN2A (2A:2B balance) regulates metaplasticity since GluN2B allows more Ca²⁺ to enter the synapse and activate LTP mechanisms (Yashiro and Philpot, 2008). The 2A:2B balance shifts during the CP (Sheng et al., 1994) when visual experience drive a loss of GluN2B (Philpot et al., 2001), an increase of GluN2A (Quinlan et al., 1999a; 1999b), and reduces ocular dominance plasticity (Philpot et al., 2003; 2007).

Receptive field properties in V1 are also regulated by glutamate receptors. The dense expression of glutamate receptors in layers 2/3 and 4 (Huntley et al., 1994; Kooijmans et al., 2014) supports AMPARs dominated feed-forward and NMDARs dominated feed-back drive (Self et al., 2012). Furthermore, development of orientation preference is prevented by suppressing NMDARs (Ramoia et al., 2001) and requires the GluN2A subunit (Fagiolini et al., 2003).

Here, we investigate development of glutamate receptors in human V1 (PSD-95, GluN1, GluN2A, GluN2B and GluA2) from birth to 80 years of age. We find changes that could contribute to visual processing and plasticity throughout the lifespan.

4.2 Materials and Methods

Samples

The post-mortem tissue samples from human visual cortex used in this study were obtained from the Brain and Tissue Bank for Developmental Disorders at the University of Maryland (Baltimore, MD, USA) and the study was approved by the McMaster University Research Ethics Board. Cortical samples were from individuals with no history of brain disorders, and all causes of death were with minimal trauma. Samples were collected within 23 hours post-mortem, sectioned coronally in 1cm intervals, flash frozen at the Brain and Tissue Bank, and stored at -80°C. Visual cortex samples were taken from the posterior pole of the left hemisphere and included both superior and inferior portions of the calcarine fissure. A total of 30 cases were used and ranged in age from 20 days to 79 years (Table 1).

Age	Age Group	Sex	PMI (Hours)
20 days	Neonate	M	9
86 days	Neonate	F	23
96 days	Neonate	M	12
98 days	Neonate	M	16
119 days	Neonate	M	22
120 days	Neonate	M	23
133 days	Infant	M	16
136 days	Infant	F	11
273 days	Infant	M	10
1 year 123 days	Young Children	M	21
2 years 57 days	Young Children	F	21
2 years 75 days	Young Children	F	11
3 years 123 days	Young Children	F	11

4 years 203 days	Young Children	M	15
4 years 258 days	Young Children	M	17
5 years 144 days	Older Children	M	17
8 years 50 days	Older Children	F	20
8 years 214 days	Older Children	F	20
9 years 46 days	Older Children	F	20
12 years 164 days	Teens	M	22
13 years 99 days	Teens	M	5
15 years 81 days	Teens	M	16
19 years 76 days	Teens	F	16
22 years 359 days	Young Adults	M	4
32 years 223 days	Young Adults	M	13
50 years 156 days	Young Adults	M	8
53 years 330 days	Young Adults	F	5
69 years 110 days	Older Adults	M	12
71 years 333 days	Older Adults	F	9
79 years 181 days	Older Adults	F	14

Table 1. Human V1 tissue samples used in this study. Each case is identified by their age in years and days, age group assignment, sex, and post-mortem interval (PMI).

Sample preparation

A small piece of tissue (50-100mg) was cut from the calcarine fissure of each frozen block of human V1, suspended in cold homogenization buffer (1ml buffer: 50mg tissue, 0.5mM DTT, 2mM EDTA, 2mM EGTA, 10mM HEPES, 10mg/L leupeptin, 100nM microcystin, 0.1mM PMSF, 50mg/L soybean trypsin inhibitor), and homogenized in a glass-glass Dounce hand homogenizer (Kontes, Vineland, NJ, USA). To enrich for synaptic proteins, we used a synaptoneurosome preparation. Homogenate samples were filtered through coarse (100 μ g) and

fine (5 μ g) pore hydrophilic mesh filters (Millipore, Bedford, MA, USA), and then centrifuged at 1000 x g for 10 minutes to obtain the synaptic fraction. The synaptoneurosome pellet was resuspended in boiling 1% sodium-dodecyl-sulfate (SDS), heated for 10 minutes and stored at -80°C.

Synaptoneurosome protein measurement and equating

Low abundance synaptic proteins are enriched 3- to 5-fold by the synaptoneurosome preparation (Murphy et al., 2014) which facilitates the reliable detection of synaptic proteins by Western blot analysis. In contrast, housekeeping proteins used as loading controls, such as GAPDH or β -tubulin, are reduced about 10-fold in a synaptoneurosome preparation because the small synaptoneurosome volume is dominated by synaptic proteins (Balsor & Murphy, unpublished observation). Moreover, those loading controls are known to exhibit high variability (Lee et al., 2016) and change under many conditions including experience (Dahlhaus et al., 2011) and development (Pinto et al., 2015). For these reasons, normalizing an enriched synaptoneurosome preparation with a diminished loading control can lead to the undesirable outcome of inflating the apparent expression of synaptic proteins, especially early in development. It is important, however, for Western blot analyses to accurately quantify total protein and to load equivalent amounts. To achieve these, we used a stringent 3 stage protocol to measure and equate protein concentrations among the samples and then load equivalent volumes into each gel.

To measure and equate protein concentration for each synaptoneurosome sample, we used a bicinchoninic acid (BCA) assay (Pierce, ThermoFisher Scientific, Rockford, IL, USA) and compared the samples with a set of protein standards (0.25, 0.5, 1.0, 2.0 mg/ml) (Bovine Serum Albumin (BSA) protein standards, Bio-Rad Laboratories, Hercules, CA, USA). We mixed a small amount of each sample and standard (9 μ l) with BCA assay solution (1:100), and loaded 3

aliquots (each 300 μ l) into separate wells of a 96-well microplate. The plate was incubated at 45°C for 45 minutes to activate the reaction, then scanned in an iMark Microplate Absorbance Reader (Bio-Rad Laboratories, Hercules, CA, USA) to quantify the colorimetric change. Next, we plotted the absorbance values of the standards relative to their known concentrations, and fit a linear correlation to the data. The fit for the correlation had to be $R^2 > 0.99$, and if it did not reach that level, the BCA assay was re-run. The absorbance of the human samples was measured and averaged for the 3 aliquots. This sample absorbance value and the linear equation fit to the standards were used to determine the amount of Laemmli buffer (Cayman Chemical Company, Ann Arbor, MI, USA) and sample buffer (M260 Next Gel Sample loading buffer 4x, Amresco LLC, Solon, OH, USA) needed to achieve protein concentrations of 1 μ g/ μ l. Finally, to ensure loading of equivalent volumes into each well of the gel we used a high-quality pipette (e.g. Picus, Sartorius Corp Bohemia, NY USA) and performed regular calibrations.

Immunoblotting

Synaptoneurosome samples (20 μ g) were separated on 4-20% SDS-polyacrylamide gels (SDS-PAGE) and transferred to polyvinylidene difluoride (PVDF) membranes (Immobilon-FL PVDF, EMD Millipore, Billerica, MA, USA). Each sample was run multiple times and a control sample, made by combining a small amount of the synaptoneurosome preparation from each of the 30 cases, was run on each gel. Blots were pre-incubated in blocking buffer for 1 hour (Odyssey Blocking Buffer 1:1 with phosphate buffer saline (PBS)) (Li-Cor Biosciences; Lincoln, NE, USA), then incubated in primary antibody overnight at 4°C using these primary antibodies: Anti-NMDAR1, 1:4000 (RRID: AB_396353, BD Pharmingen, San Jose, CA); Anti-NR2A, 1:1000 (RRID: AB_95169, EMD Millipore, Billerica, MA, USA); Anti-NMDAR2B, 1:1000 (RRID: AB_2112925, EMD Millipore, Billerica, MA, USA); Anti-GluA2, 1:1000 (RRID: AB_2533058, Invitrogen, Waltham, MA, USA); Anti-PSD95, 1:16000 (RRID: AB_94278, EMD Millipore, Billerica, MA, USA). These antibodies were selected after testing them on a multi-

species blot that included samples from human, monkey, cat, and rat to ensure that the human samples had bands comparable with the other species. The blots were washed with PBS-Tween (0.05% PBS-T, Sigma, St. Louis, MO, USA) (3x10 minutes) and incubated for 1 hour at room temperature with the appropriate IRDye labeled secondary antibody, (Anti-Mouse, 1:8000, RRID: AB_10956588; Anti-Rabbit, 1:10,000, RRID: AB_621843; Li-Cor Biosciences, Lincoln, NE, USA), and washed again in PBS-Tween (3x10 minutes). The bands were visualized using the Odyssey scanner (Li-Cor Biosciences; Lincoln, NE, USA) and we determined that the amount of protein loaded into each well and the antibody concentrations were within the linear range of the Odyssey scanner. After scanning, the blots were stripped using a Blot Restore Membrane Rejuvenation Kit (EMD Millipore, Billerica, MA, USA), re-scanned to ensure complete stripping, and then re-probed with another antibody.

Band analysis

To analyze the bands, blots were scanned on an Odyssey infrared scanner and quantified using densitometry (Li-Cor Odyssey Software version 3.0; Li-Cor Biosciences; Lincoln, NE, USA). A density profile for each band was calculated by performing a subtraction of the background, integrating the pixel intensity across the area of the band, and dividing the intensity by the width of the band to control for variations in lane width. A control sample, made by combining a small amount from each sample, was run on each gel and the density of each sample was quantified relative to the control (sample density/control density).

Band image manipulation

Bands shown on figures are representative samples and were added to the figures in Photoshop (Adobe Systems Inc, San Jose, CA, USA, RRID:SCR_014199). Horizontal and vertical transformations were applied to size and orient the bands for each figure. A linear adjustment layer was applied uniformly to all bands for each protein, preserving the relative intensities among bands.

Receptor subunit index

To quantify the balance between functional pairs of proteins, we calculated a difference ratio, often called a contrast index, that is commonly used in signal processing to determine the quality of a signal. We calculated 2 indices that reflect the balance between pairs of proteins that are developmentally regulated: AMPA:NMDA index -- $(\text{GluA2}-\text{GluN1})/(\text{GluA2}+\text{GluN1})$; and NMDAR subunit 2A:2B index -- $(\text{GluN2A}-\text{GluN2B})/(\text{GluN2B}+\text{GluN2A})$. These indices can have values between -1 and +1.

Curve-fitting and statistical analyses

The results were plotted in two ways to visualize and analyze changes in expression across the lifespan. First, to describe the time course of changes in protein expression, scatterplots were made for each protein showing the expression level from each run (grey dots) and the average of the runs (black dots). To determine the trajectory of changes across the lifespan we used a model-fitting approach (Christopoulos and Lew, 2000) and found the best curve-fit to the data using Matlab (The MathWorks, Inc, Natick, MA, RRID: SCR_001622). A single-exponential decay function ($Y=A*\exp(-(x/\tau))+B$) was fit to the data for GluN1. A Gaussian function ($Y=A*\exp(-((\log(x/\mu)^2)/(2*(\sigma^2))))+B$) was fit to the data for PSD-95, GluA2, GluN2B, and the 2A:2B index. A quadratic function was fit to the AMPA:NMDA balance ($Y=A+B*\log(x)+C*\log(x)^2$). Finally, a weighted average was used to describe the trajectory for GluN2A. The fits were found by least squares, and the goodness-of-fit (R^2) and statistical significance of the fit (p) were determined. For the decay function, we calculated the time constants (τ) and defined 3τ (when 87.5% of the change in expression had occurred) as the age when mature expression was reached with the 95% confidence interval (95% CI) around that age. For Gaussian functions, the age at the peak was calculated and the 95% CI determined.

Second, to compare changes among different stages across the lifespan, samples were binned into age groups (<0.3 years, Neonates; 0.3-1 year, Infants; 1-4 years, Young Children; 5-11 years,

Older Children; 12-20 years, Teens; 21-55 years, Young Adults; >55 years, Older Adults) and histograms were plotted showing the mean and standard error of the mean (SEM) for each group. We used bootstrapping to make statistical comparisons among the groups since this method provides robust estimates of standard error and CI, which are especially useful for human studies constrained to smaller sample sizes. The statistical software R (R Core Team (2014), R: A language and environment for statistical computing. R Foundation for Statistical Computing, Vienna, Austria, URL <http://www.R-project.org/>, RRID: SCR_001905) was used for the bootstrapping and we began by simulating a normally distributed dataset (1,000,000 points) with the same mean and standard deviation of the group being compared. We used this normally distributed dataset to determine if the observed means for the other age groups were significantly different. A Monte Carlo simulation was used to randomly sample from the simulated dataset N times, where N was the number of cases in the other age groups. This simulation was run 10,000 times to generate an expected distribution for the N number of cases. Confidence intervals (CI) were calculated for that simulated distribution (i.e. 95%, 99% CI) and compared with the observed group means. The age groups were considered to be significantly different (i.e. $p < 0.05$) when the observed mean was outside the 95% CI.

Analysis of Inter-individual variability

Previously we identified ages during infancy and childhood with waves of high inter-individual variability (Pinto et al., 2015; Siu et al., 2015). To analyze if the glutamatergic proteins studied here have similar waves of inter-individual variability we calculated the Fano-Factor (Variance-to-Mean Ratio - VMR) for each protein and examined how it changed across the lifespan. The VMR around each case was determined by calculating the mean and variance for the protein expression within a moving box that included 3 adjacent ages and then dividing the variance by the mean. Scatter plots were made to show how the VMRs changed across the life span and functions were fit to those data to identify ages when there was high inter-

individual variability. The VMRs were fit with the same Gaussian function described above, and a wave of higher inter-individual variability was identified when 4 or more points at the peak fell above the 95% CI for lower bound of the curve.

4.3 Results

Postmortem interval

We examined whether glutamate protein expression levels were affected by post-mortem interval (PMI). First, we verified that immunoreactivity was present and then analyzed the correlation between PMI and protein expression. There were no significant correlations between PMI and expression of the 5 glutamatergic proteins (PSD-95: $R=0.05$, $p=0.66$; GluA2: $R=0.17$, $p=0.13$; GluN1: $R=0.26$, $p=0.11$; GluN2A: $R=0.17$, $p=0.41$; GluN2B: $R=0.16$, $p=0.24$) so all of the data was included in the following analyses.

Slow development of PSD-95, earlier but opposite development of GluA2 and GluN1

We began analyzing development of glutamate proteins in human V1 by measuring expression of PSD-95, a scaffolding protein involved in anchoring AMPA and NMDA receptors (Kim and Sheng, 2004), controlling visual developmental plasticity (Yoshii et al., 2003), and ending the CP for ocular dominance plasticity (Huang et al., 2015). We found a steady increase in expression of PSD-95 in the synaptoneurosome preparation used in this study and analyzed the results in two ways (Fig. 1). First, by model-fitting to all the data to determine the best curve to capture changes across the lifespan, and second, by binning the data into age groups and using bootstrapping for statistical comparisons between groups. Development of PSD-95 peaked at 9.6 years (± 4.1 years; $R^2=0.457$, $p<0.0001$) (Fig. 1A). This result was similar to our previous findings using whole homogenate samples (Pinto et al., 2015). The magnitude of the peak in the synaptoneurosome, however, was about half that found using the whole homogenate ((Pinto et al., 2015) figure 3), suggesting there could be a large mobile pool of PSD-95 during late childhood. Comparing the age-binned results showed a 3-fold increase in PSD-95 expression during development that reached a peak in older children (5-11 years, $p<0.001$) before dropping about 30% into aging ($p<0.001$) (Fig. 1B). The PSD-95 peak corresponded with the age when children are no longer susceptible to amblyopia (Lewis and Maurer, 2005) and may signify that

PSD-95 contributes to ending the CP for ocular dominance plasticity in humans similar to its role in mouse V1 (Huang et al., 2015).

Next, we quantified development of GluA2 and GluN1, which identify the 2 main classes of ionotropic glutamate receptors AMPARs and NMDARs, respectively. Development of these subunits followed a similar pattern to that found in animal studies, where GluA2 increased, while GluN1 decreased during development (Fig. 1C-F). GluA2 expression increased about 40% during childhood and then declined a similar amount into adulthood and aging. The GluA2 developmental trajectory peaked at 3.1 years (± 1.8 years, $R^2=0.131$, $p<0.01$) (Fig. 1C). Comparison of GluA2 expression among the age groups, however, identified a slightly later peak during late childhood (5-11 years) (Fig. 1D). The uncertainty about the peak for GluA2 probably reflects variability in expression during childhood and the modest increase between neonates and older children.

The trajectory of GluN1 expression started high under 1 year of age, then rapidly decreased to a relatively constant level for the rest of the lifespan (Fig. 1E,F). The change in GluN1 expression was fit with an exponential decay function ($R^2=0.482$, $p<0.0001$) that fell to mature levels (3τ) by 4.2 years (± 1.7 years) (Fig. 1E). The same pattern was found when we compared among age groups where GluN1 levels were higher under 1 year and dropped by almost half during young childhood (1-4 years) ($p<0.001$) and remained at that level for the rest of the lifespan (Fig. 1F).

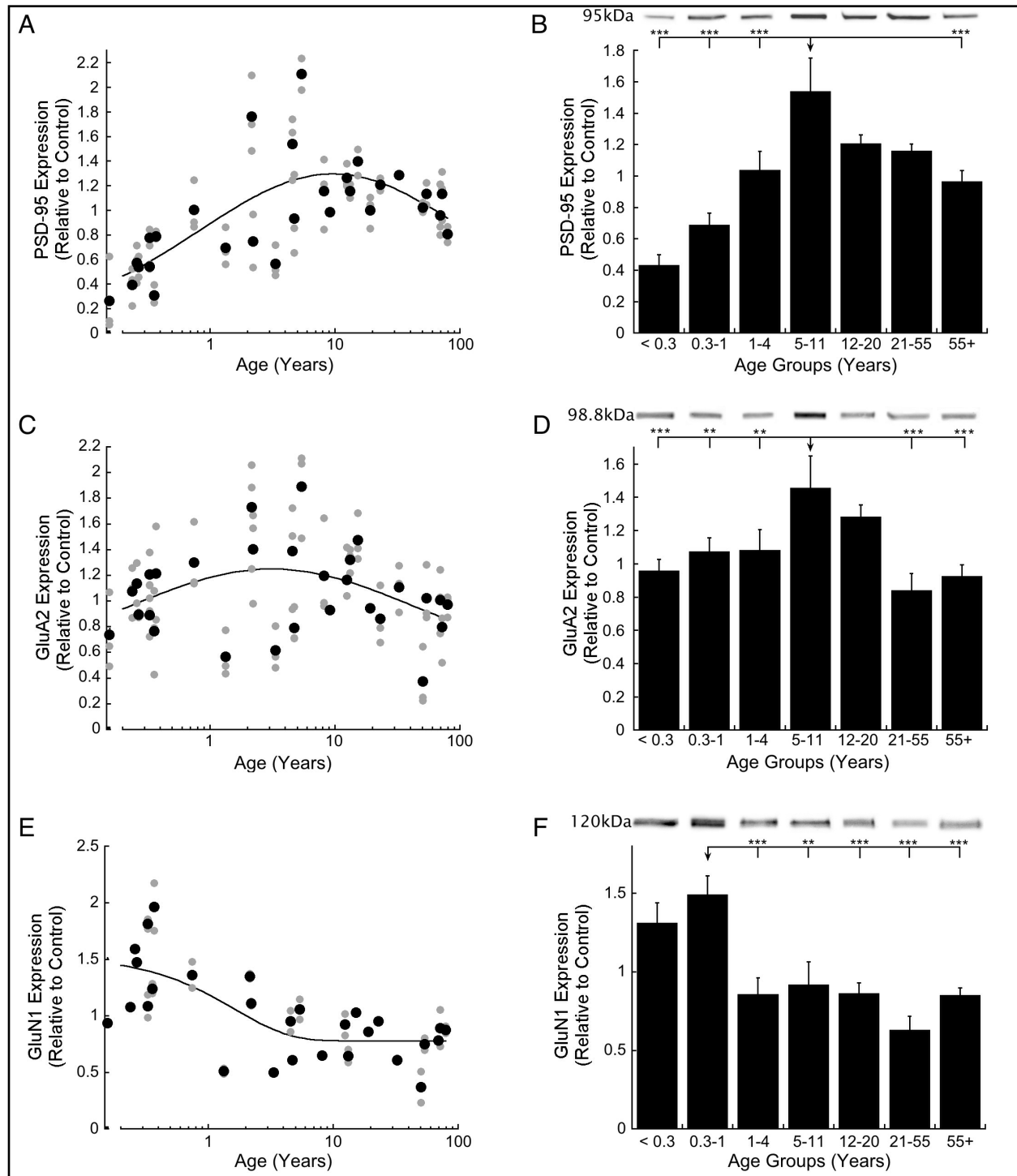


Figure 1 - Development of PSD-95, GluA2, and GluN1 expression in human V1. (A) A scatterplot of PSD-95 expression across the lifespan fit with a Gaussian function ($R^2=0.457$, $p<0.0001$) with peak expression at 9.6 years (± 4.1 years). (B) Age-binned results for PSD-95 expression. (C) A scatterplot of GluA2 expression across the lifespan fit with a Gaussian function ($R^2=0.131$, $p<0.01$), with peak expression at 3.1 years (± 1.8 years). (D) Age-binned results for GluA2 expression. (E) A scatterplot of GluN1 expression across the lifespan fit with

an exponential decay function ($R^2=0.482$, $p<0.0001$), and fell to mature levels (3τ) at 4.2 years (± 1.7 years). (F) Age-Binned results for GluN1 expression. For the scatterplots, grey dots represent each run, black dots represent the average for each case and age was plotted on a logarithmic scale. For the histograms, protein expression was binned into age groups (< 0.3 years, Neonates; 0.3-1 year, Infants; 1-4 years, Young Children; 5-11 years, Older Children; 12-20 years, Teens; 21-55 years, Young Adults; >55 years, Older Adults) showing the mean and SEM. Representative bands are shown above each age group. (* $p<0.05$, ** $p<0.01$, *** $p<0.001$).

Comparing the changes across the lifespan for PSD-95, GluA2, and GluN1 we found different timing (GluA2 and GluN1 matured before PSD-95), different directions (PSD-95 and GluA2 increased while GluN1 decreased), and different amounts of protein change. Thus, even these 3 tightly associated proteins had different developmental trajectories.

Early shift from more NMDA to more AMPA in human V1

Animal studies have shown that there is an early developmental shift from NMDAR-dominated silent synapses to functional synapses with AMPARs (Isaac et al., 1997; Rumpel et al., 1998). Here we examined development of the AMPA:NMDA balance in human V1 as an indication of functional maturation of glutamatergic transmission. We calculated an AMPA:NMDA index where a value of -1 indicated only GluN1 expression, 0 indicated equal expression, and +1 indicated only GluA2 expression. We found an early switch from more GluN1 under 1 year of age to more GluA2 after 1 year (Fig. 2). The AMPA:NMDA balance was fit with a quadratic function ($R^2=0.406$, $p<0.0001$) that captured the shift from GluN1 to GluA2 that peaked at 10.7 years (95%CI 4.8-23.7 years) before slowly returning to equal expression during aging (Fig. 2A). The age-binned results showed the same pattern of a significant switch at 1 year, GluA2 peaking during late childhood, and returning to balanced expression in older adults (Fig. 2B). The changes in this AMPA:NMDA balance suggest an early stage of human V1 development during infancy (<1 year) that may characterize unsilencing of glutamate synapses

followed by AMPAR dominated excitatory drive during childhood and young adults before regressing to balanced AMPAR and NMDAR expression in aging.

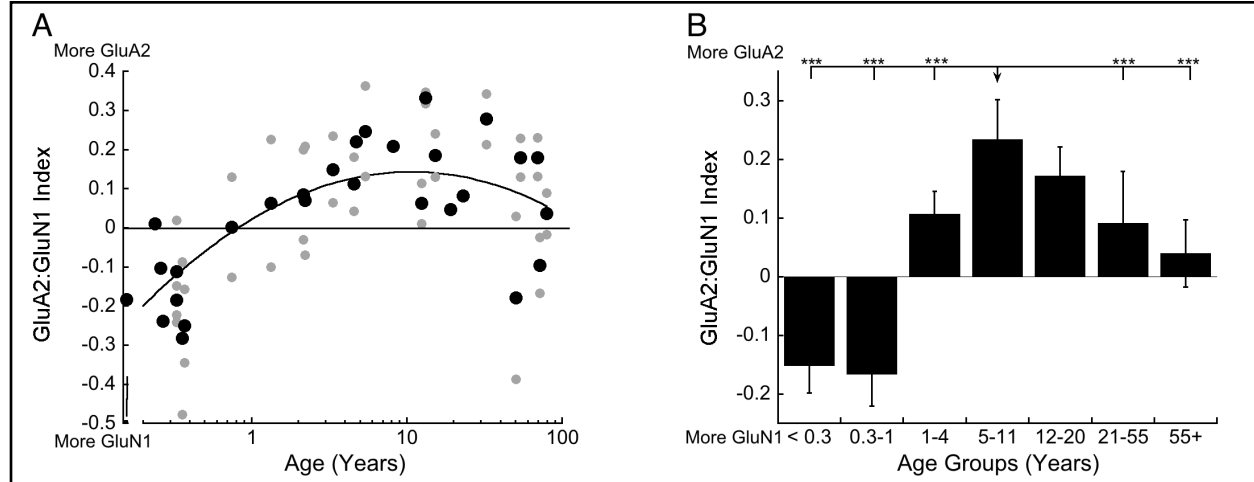


Figure 2 - Development of the AMPA:NMDA balance ($((\text{GluA2}-\text{GluN1})/(\text{GluA2}+\text{GluN1}))$) in human V1. (A) A scatterplot of the AMPA:NMDA balance across the lifespan fit with a quadratic function ($R^2=0.406$, $p<0.0001$), which peaked at 10.7 years (95% CI 4.8-23.7 years). (B) Age-Binned results for the AMPA:NMDA balance. Scatterplot, histogram and significance levels plotted using the conventions described in Figure 1.

GluN2A and GluN2B subunit expression in human V1

We examined developmental changes in expression of 2 NMDAR subunits, GluN2A and GluN2B because they affect development of receptive field tuning and ocular dominance plasticity. In particular, the rise of GluN2A and concomitant loss of GluN2B during the CP is one mechanism that causes reduced ocular dominance plasticity in adult cortex (Philpot et al., 2007). The scatterplot of GluN2B expression showed a modest peak during childhood and relatively constant expression through teens, young adults, and older adults (Fig. 3A&B). The GluN2B trajectory was fit by a Gaussian function ($R^2=0.176$, $p<0.01$) that peaked at 1.2 years (± 0.7 years) (Fig. 3A). We compared GluN2B expression among the age groups and found higher levels during childhood (5-11 years) relative to teens, young adults, and older adults (Fig. 3B) ($p<0.01$).

The developmental trajectory for GluN2A was different from GluN2B. Initially, GluN2A expression was low, then variable during childhood and teenage years (8 cases with low and 3 cases with high GluN2A expression) followed by high expression in young adults and ending with a large (~75%) decline into aging. The variability during childhood reduced the goodness-of-fit for a Gaussian function so instead we plotted a descriptive weighted curve (Fig. 3C). Interestingly, the 3 childhood cases with high GluN2A expression also had high GluN2B expression. Binning the results into age groups showed that young adults had more GluN2A expression than infants ($p < 0.001$), young children ($p < 0.01$), teens ($p < 0.01$), and older adults ($p < 0.001$) (Fig 3. D).

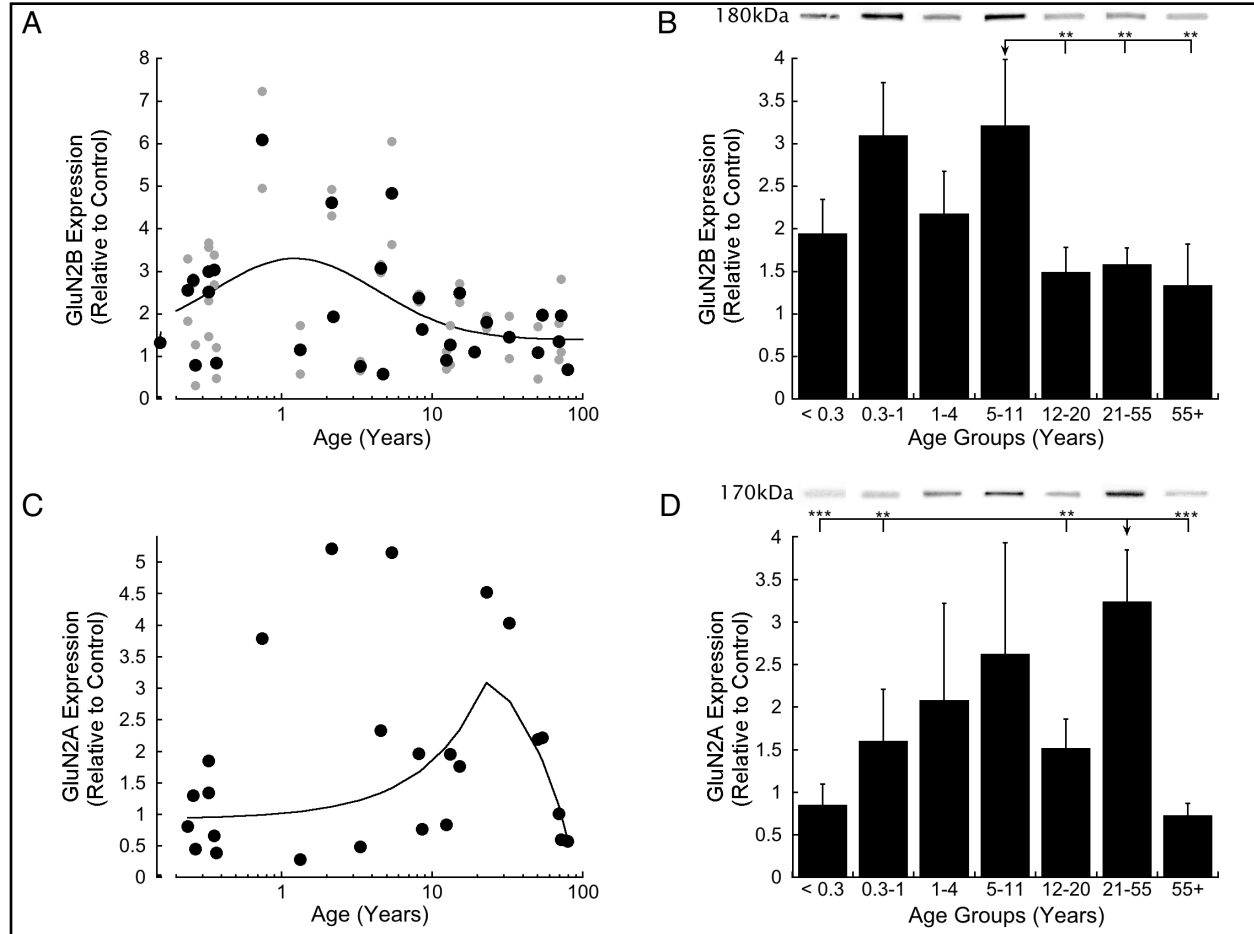


Figure 3 - Development of GluN2B and GluN2A in human V1. (A) A scatterplot of GluN2B expression across the lifespan fit with a Gaussian function ($R^2=0.176$, $p<0.01$), with peak expression at 1.2 years (± 0.7 years). (B) Age-Binned results for GluN2B expression. (C) A scatterplot of GluN2A expression across the lifespan fit with a weighted curve. (D) Age-Binned results for GluN2A expression. Scatterplots, histograms, and significance levels plotted using the conventions described in Figure 1.

NMDARs are tetrameric channels with diheteromeric nascent receptors comprised of GluN1/GluN2B that shift during development with the majority becoming triheteromers comprised of GluN1/GluN2A/GluN2B (Sheng et al., 1994). Since GluN1 is a component of all NMDARs we normalized expression of GluN2A and GluN2B to the expression of GluN1 to determine if high

variability during childhood was driven by variability in the total pool of NMDARs.

Normalizing with GluN1 expression reduced the variability for both GluN2A and GluN2B throughout childhood, it also enhanced the GluN2B peak in late childhood (Fig. 4 A&B) and the GluN2A peak in adulthood (Fig. 4 C&D). The GluN1 normalization, however, did not eliminate variability of GluN2A and GluN2B during childhood.

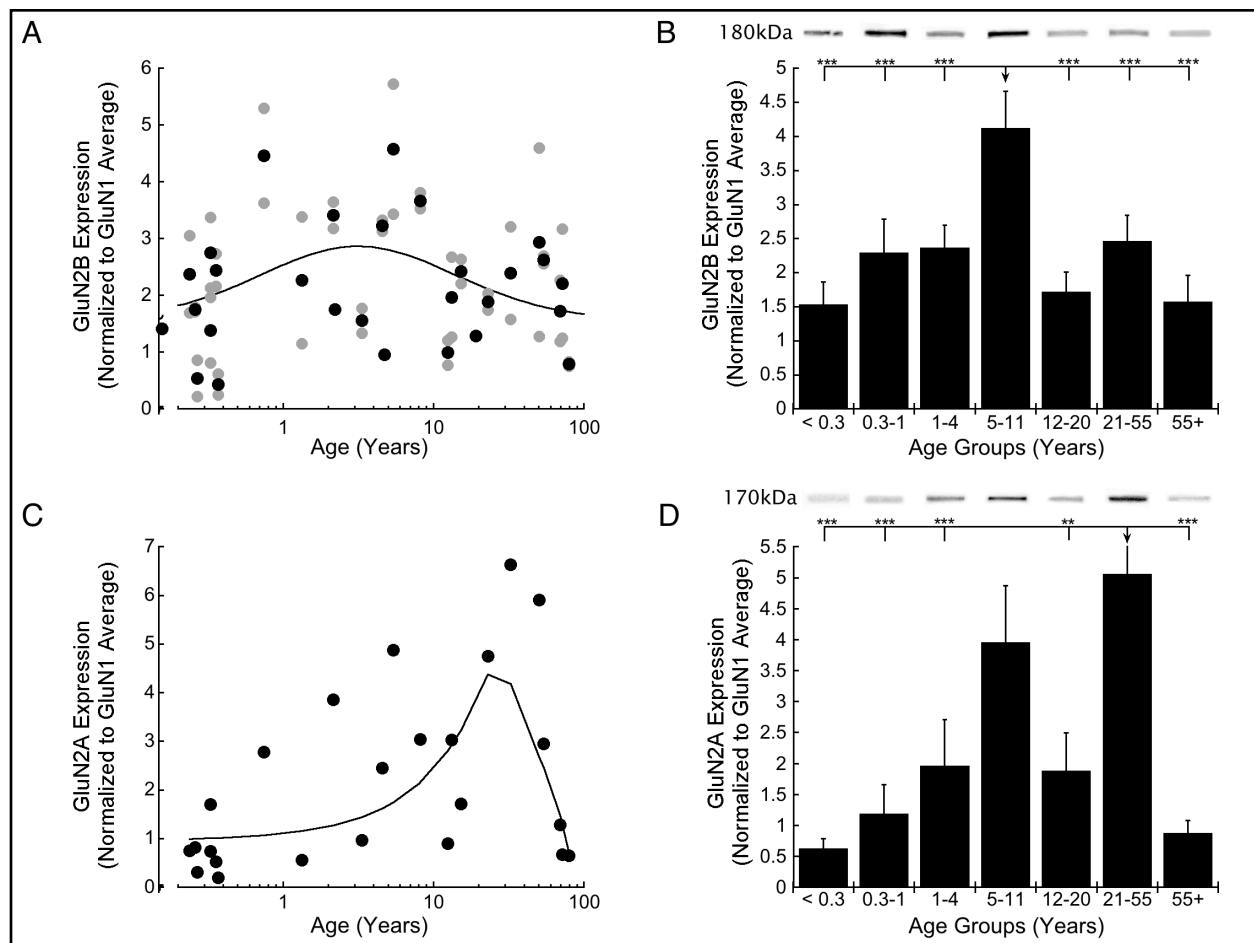


Figure 4 - Development of GluN2B and GluN2A normalized to GluN1 in human V1. (A) A scatterplot of GluN2B expression normalized to GluN1 across the lifespan fit with a Gaussian function ($R^2=0.106$, $p<0.05$), with peak expression at 3.2 years (± 1.8 years). (B) Age-Binned results for GluN2B normalized to GluN1 expression. (C) A scatterplot of GluN2A normalized to GluN1 expression across the lifespan fit with a weighted curve. (D) Age-Binned results for

GluN2A normalized to GluN1. Scatterplots, histograms, and significance levels plotted using the conventions described in Figure 1.

2A:2B balance: protracted change across the lifespan

Visual experience shifts the 2A:2B balance in favour of GluN2A (Quinlan et al., 1999a; 1999b) and that regulates the synaptic modification threshold for engaging long-term potentiation (LTP) versus long-term depression (LTD) (Philpot et al., 2007). Since the 2A:2B balance is a key mechanism regulating visual experience-dependent metaplasticity, we analyzed it for human V1 by calculating an index of 2A:2B expression for each case. Here we found an orderly progression from more GluN2B under 5 years of age, to roughly balanced GluN2B and GluN2A during the teen years, to a peak with more GluN2A during adulthood, followed by a shift back to more GluN2B in aging (Fig. 5 A&B). These changes in the 2A:2B balance were fit by a Gaussian function ($R^2=0.633$, $p<0.0001$) that peaked at 35.9 years (± 4.6 years) (Fig. 5A). The binned results illustrate the progressive shift towards significantly more GluN2A in adulthood and then shifting back to GluN2B in aging (Fig. 5B). The orderly shift in the 2A:2B balance, especially through childhood, was somewhat surprising since the individual subunits showed a lot of variability at that stage. The low variability of the 2A:2B index suggests that the balance between this pair of subunits, rather than the absolute amount of each, is a critical component for GluN2A and GluN2B regulation of developmental plasticity. Importantly, when compared with animal models where the shift to GluN2A is complete by the end of the CP (Sheng et al., 1994; Quinlan et al., 1999a; Beston et al., 2010), the 2A:2B shift in human V1 continued for 25 years beyond the age for susceptibility of developing amblyopia (Lewis and Maurer, 2005).

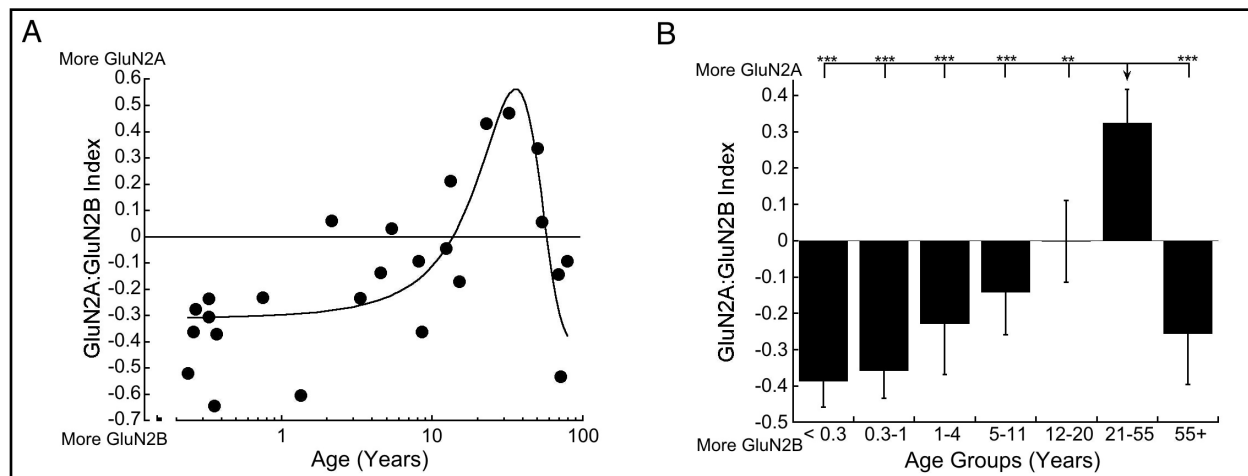


Figure 5 - Development of the 2A:2B balance ((GluN2A-GluN2B)/(GluN2A+GluN2B)) in human V1. (A) A scatter plot of the 2A:2B balance across the lifespan fit with a Gaussian function ($R^2=0.633$, $p<0.0001$), with peak expression around 35.9 years of age (± 4.6 years). (B) Age-Binned results for the 2A:2B balance. Scatterplot, histogram, and significance levels plotted using the conventions described in Figure 1.

Waves of inter-individual variability during childhood

Many studies of human brain development and function have found large inter-individual variations including our studies of synaptic and non-synaptic proteins in human V1. We analyzed inter-individual variability and found waves of higher variability in childhood (Pinto et al., 2015; Siu et al., 2015). Here we applied the same approach and calculated the Fano factor to determine how the variance-to-mean ratio (VMR) changed across the lifespan for the current set of glutamatergic proteins.

We found that each glutamatergic protein had a wave of higher inter-individual variability during childhood that was well fit by a Gaussian function (Fig. 6 A-E). There was a progression in the peak age of inter-individual variability (VMRs) that began with GluN1 and GluN2B at 1.1 years (GluN1, ± 0.2 years, $R^2= 0.8$, $p < 0.0001$)(GluN2B, ± 0.3 years, $R^2= 0.618$, $p < 0.0001$),

to GluN2A at 1.6 years (\pm 0.4 years, $R^2= 0.694$, $p < 0.0001$), to GluA2 at 2.1 years (\pm 0.6 years, $R^2= 0.641$, $p < 0.0001$), to PSD-95 at 2.5 years (\pm 0.5 years, $R^2= 0.778$, $p < 0.0001$) (Fig 6 A-E). We plotted the progression of peak ages for inter-individual variability with their 95% CIs to show that variability occurred between 1-3 years of age and the peaks started with GluN1 and GluN2B then progressed to GluN2A, GluA2 and ended with PSD-95 (Fig. 6F).

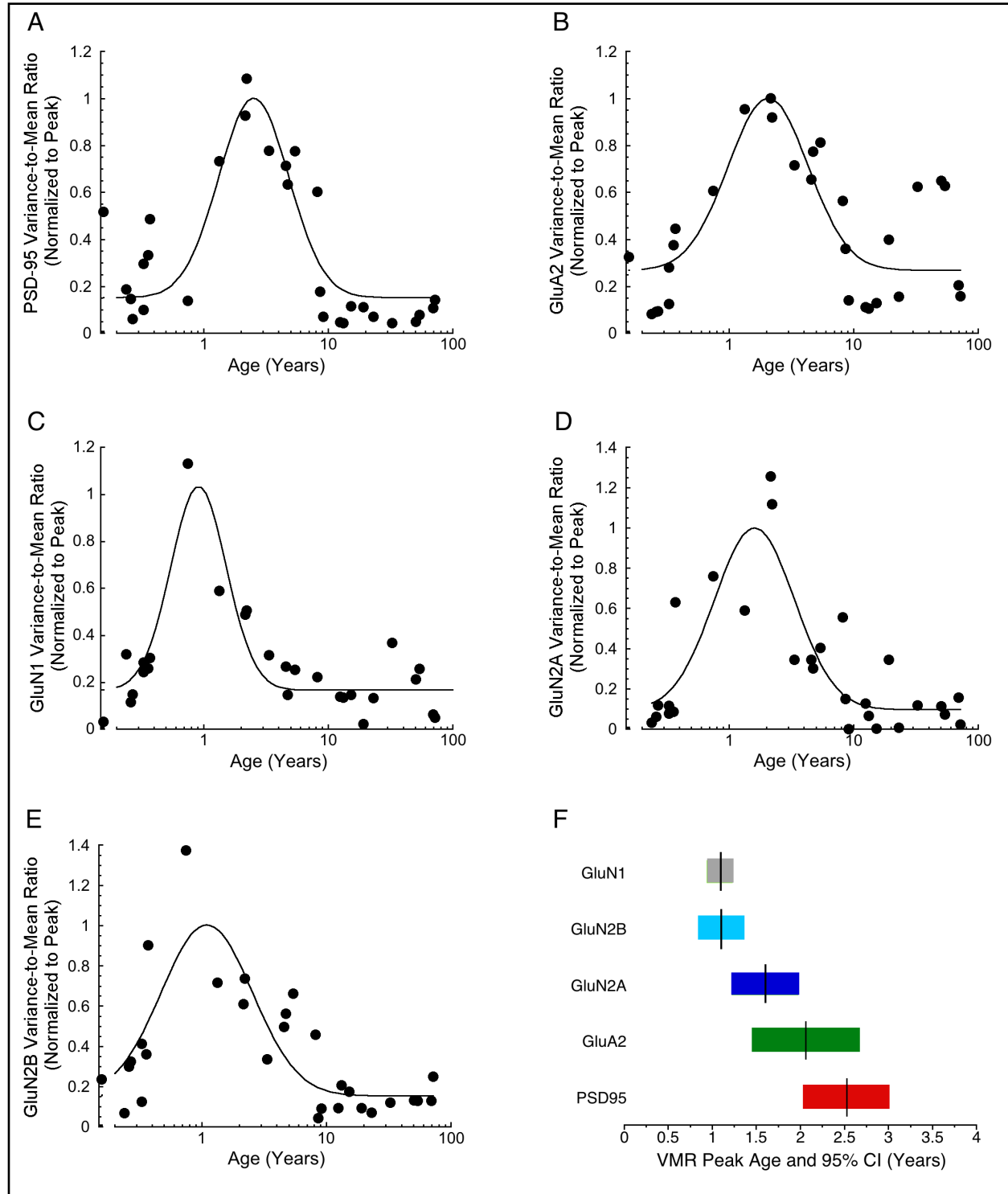


Figure 6 - Development of the VMR for PSD-95, GluA2, GluN1, GluN2A, and GluN2B in human V1. Black dots are the VMR for a moving window of 3 cases. Each protein's scatterplot were fit with a Gaussian function, and the data were normalized to the peak of the function. (A) PSD-95 VMR peaked at 2.5 years (± 0.5 years) ($R^2=0.778$, $p<0.0001$). (B) GluA2 VMR peaked at 2.1 years (± 0.6 years) ($R^2=0.641$, $p<0.0001$). (C) GluN1 VMR peaked at 1.1 years (± 0.2

years) ($R^2=0.8$, $p<0.0001$). (D) GluN2A VMR peaked at 1.6 years (± 0.4 years) ($R^2=0.694$, $p<0.0001$). (E) GluN2B VMR peaked at 1.1 years (± 0.3 years) ($R^2=0.618$, $p<0.0001$). (F) A summary chart showing the progression of peaks of inter-individual variability (vertical black line) and the 95% CI (colored bar) for each protein.

4.4 Discussion

Our results show that development of glutamatergic synaptic proteins in human V1 mirror changes in visual perception across the lifespan. Human visual perception matures in stages (Elleberg et al., 1999; Kovács et al., 1999; Braddick et al., 2005; Owsley, 2011; Hartshorne and Germine, 2015), and the glutamate receptor proteins studied here revealed 5 stages of development (Fig. 7). Those stages can support structural maturation of the intrinsic network, visually driven plasticity, closure of the CP, synaptic stability, and degeneration in human V1. These results are similar to the maturation of GABAergic proteins in human V1 (Pinto et al., 2010) and suggest that synaptic changes in V1 are likely to impact visual perception and plasticity across the lifespan.

		Stage 1 (<1 year)	Stage 2 (1-4 years)	Stage 3 (5-11 years)	Stage 4 (12-55 years)	Stage 5 (>55 years)
Individual Protein Development	GluN1	GluN1				
	GluN2B			GluN2B		
	GluA2			GluA2		
	PSD-95			PSD-95		
	GluN2A				GluN2A	
Index Development	2A:2B	GluN2B			GluN2A	GluN2B
	GluA2:GluN1	GluN1		GluA2		
Inter-Individual Variability Waves	GluN1		GluN1			
	GluN2B		GluN2B			
	GluA2		GluA2			
	PSD-95		PSD-95			
	GluN2A		GluN2A			

Figure 7 - Summary of the 5 stages of development for the glutamatergic proteins. Changes for the individual glutamatergic proteins are illustrated with grey-levels where black represents the maximum expression and lighter grey less expression. GluN1 peaked during the first year (stage 1), GluN2B, GluA2, and PSD-95 in late childhood (stage 3), and GluN2A at ~40 years (stage 4) before declining in aging (stage 5). Changes for the 2 indices (2A:2B, GluA2:GluN1) are color-coded. For the 2A:2B balance red indicates more GluN2B and green more GluN2A, and for the AMPA:NMDA balance red indicates more GluN1 and green more GluA2. The shift to more GluN2A peaked in adulthood (stage 4) and then returned to more GluN2B in aging (stage 5). The switch to more GluA2 happened at ~ 1 year and continued until late childhood (stage 3). The waves of inter-individual variability for each protein are present with dark blue identifying maximum variability that occurred in young childhood (stage 2) and lighter blue indicating stages with low variability.

Glutamatergic proteins regulate fundamental aspects of excitatory neurotransmission (Cull-Candy et al., 1998), visual plasticity (Turrigiano, 2008; Yashiro and Philpot, 2008; Cooke and Bear, 2014; Turrigiano, 2017), and receptive field properties in V1 (Ramoia et al., 2001; Rivadulla et al., 2001; Fagiolini et al., 2004; Self et al., 2012). Quantification of these proteins by Western blotting is one of the few methods that can track the maturation of human V1 to link changes in synaptic function, network structure, and visual perception. Protein analysis,

however, does not address the cell types, layers, and circuits that are changing. Nor does it separate pre- and post-synaptic NMDARs which play different roles in neurotransmission and experience-dependent plasticity (Banerjee et al., 2016). The current results may provide a blueprint to focus anatomical and other studies of human V1 on key stages of development.

Five stages of glutamatergic protein development in human V1

Stage 1: the first year -- structural maturation of the intrinsic network

Initially, GluN1 expression was high and then a rapid reduction at ~1 year caused a switch in the AMPA:NMDA balance to more GluA2. That pattern suggests initial dominance by NMDAR-containing silent synapses that are rapidly replaced by AMPAR-containing active synapses (Isaac et al., 1997; Rumpel et al., 1998). The loss of GluN1 at ~1 year coincides with a loss of the endocannabinoid receptor CB1 (Pinto et al., 2010) and since CB1 plays a central role in establishing excitatory connections (Harkany et al., 2008), the high levels of CB1 and GluN1 may contribute to the functional maturation of intra-cortical (Burkhalter et al., 1993) and inter-cortical connections (Burkhalter, 1993).

We found that GluN2B dominated the 2A:2B balance throughout stages 1 to 3. Many animal studies have shown that the 2A:2B balance contributes to developmental plasticity in V1 and emergence of visual function (Quinlan et al., 1999a; Erisir and Harris, 2003; Philpot et al., 2007; Cho et al., 2009; Smith et al., 2009; Durand et al., 2012). The dominance of GluN2B suggests that the synaptic modification threshold favors LTP (Philpot et al., 2007; Yashiro and Philpot, 2008) and V1 neurons are more receptive to potentiation of an open eye's inputs (Cho et al., 2009). This may explain why just 1 hour of visual experience in an infant is enough to improve acuity of an eye treated for congenital cataracts (Maurer et al., 1999). Thus, this stage reflects the establishment of nascent excitatory synapses and initiation of plasticity in V1 circuits.

Stage 2: young children (1-4 years) -- visually driven plasticity

During the second stage of V1 development, we found progressive increases in GluA2, PSD-95, and GluN2A but the dominant feature was the wave of inter-individual variability. The variability was similar to our previous findings for pre- (Synapsin, Synaptophysin), post-synaptic (Gephyrin, PSD-95), and a non-neuronal protein (Golli myelin basic protein, MBP) (Pinto et al., 2015; Siu et al., 2015). Variability peaking with GluN1 and GluN2B at ~1 year, GluN2A at ~1.5 years, GluA2 at ~2 years, and ending with PSD-95 at ~2.5 years. Those waves may reflect true inter-individual variability in young children with cortical development taking off at different ages. The waves may also represent high levels of intra-individual variability driven by the dynamics of network states where expression of each synaptic protein could be high one day and low the next. Since the data here are cross-sectional, we cannot differentiate between these 2 ideas, but the implications for them on cortical development are different. For example, if the waves reflect on-going dynamics then they could function similar to how feedback about the network state shifts processing of olfactory circuits in *C. elegans* (Gordus et al., 2015). In that model, environmental or other factors could modulate the state of synaptic plasticity. Rather than thinking about the waves as random or unpredictable, they may reveal a feature of visually driven plasticity needed to develop adaptive circuits that support visual processing.

Stage 3: older children (5-11 years) -- closure of the critical period

Expression of GluN2B, PSD-95, GluA2 and the AMPA:NMDA balance peaked in the third stage. These changes could end the CP for ocular dominance plasticity (Erisir and Harris, 2003; Huang et al., 2015). For example, in mouse V1 PSD-95 peaks at the end of the CP and consolidates AMPA-containing synapses (Huang et al., 2015). This stage also coincides with the end of susceptibility for children developing amblyopia (Epelbaum et al., 1993; Keech and Kutschke, 1995; Lewis and Maurer, 2005).

By the end of stage 3, the 2A:2B balance was roughly equal. A shift to more GluN2A in V1 is driven by visual experience (Quinlan et al., 1999b) and the findings here show that the 2A:2B shift begins in young children, but is still not complete by the end of the CP for developing amblyopia. In contrast, the 2A:2B shift in animal models is complete by the end of the CP (Sheng et al., 1994; Quinlan et al., 1999a; Beston et al., 2010). Perhaps the slow 2A:2B shift in combination with peak expression of GluA2 allows for strong engagement of both Hebbian and homeostatic forms of experience-dependent plasticity (Turrigiano, 2017).

Stage 4: teens and young adults (12-55 years) -- synaptic stability

Through teens and young adults there was continued development as the 2A:2B balance switched to favor GluN2A and peak expression of GluN2A did not occur until ~40 years. This may seem like surprisingly slow development for human V1, but it was comparable to the development of some GABAergic proteins (GAD65 and GABA_Aα1) (Pinto et al., 2010) as well as cortical myelin (classic-MBP) (Siu et al., 2015).

In mouse V1, the developmental shift to more GluN2A is slower for parvalbumin-positive (PV+) inhibitory interneurons than pyramidal neurons (Mierau et al., 2016). Perhaps the slow 2A:2B shift in human V1 reflects late maturation of PV+ cells. Fast-spiking PV+ cells also have GluA2-containing AMPARs (Kooijmans et al., 2014), so they are a site where changes in visual experience could activate inhibitory and excitatory aspects of short-term plasticity in human V1 (Lunghi 2011) (Lunghi et al., 2015a; 2015b). Interestingly, blocking NMDARs prevents surround-suppression in monkey V1 (Self et al., 2012) and even a low dose of the non-competitive NMDAR antagonist, ketamine, impairs the performance of human observers on a spatial integration task (Meuwese et al., 2013).

The late 2A:2B shift is likely to adjust the synaptic modification threshold making it more difficult for visual experience to engage LTP (Yashiro and Philpot, 2008). More GluN2A will also shorten the decay time of NMDARs (Stocca and Vicini, 1998; Vicini et al., 1998) even for triheteromeric receptors (Hansen et al., 2014). In addition, GluN2A-containing NMDARs are more stable in the synapse (Groc et al., 2006) and their activation promotes cell survival (Liu et al., 2007). These features of GluN2A-containing receptors suggests that this stage reflects a time of synaptic stability in human V1.

Stage 5: aging (>55 years) -- degeneration

The last stage saw a dramatic ~75% loss of GluN2A expression, bringing it back to levels found in infants (<1 year of age). In contrast, there was no change in GluN2B expression so the 2A:2B balance switched back to GluN2B in aging.

Age-related changes in human vision (Bennett et al., 2007; Betts et al., 2007) and monkey receptive field properties (Leventhal et al., 2003; Wang et al., 2005; Zhang et al., 2008) have been described as resulting from poor signal-to-noise caused by a loss of inhibition. Our previous study of GABAergic proteins in human V1 found a modest loss of GAD65 (Pinto et al., 2010), but that was much less than the loss of GluN2A found here. Since GluN2A-containing NMDARs are dense on PV+ inhibitory interneurons in young mice (Mierau et al., 2016), the loss of GluN2A in aging human V1 may involve PV+ cells.

The age-related 2A:2B shift to more GluN2B is likely to cause slower decay times and weaker conductances at NMDARs (Cull-Candy et al., 1998; Vicini et al., 1998; Hansen et al., 2014). It could also slide the synaptic modification threshold so that visual experience can more readily engage LTP. That plasticity, however, may come at the cost of higher metabolic stress, GluN2B-activated excitotoxicity (Liu et al., 2007) and other vulnerabilities linked with NMDARs changes in aging (Magnusson et al., 2010). It is clear that the aging cortex does not simply become

juvenile-like (Williams et al., 2010) and the specific loss of GluN2A found here could be a harbinger of degeneration in human V1.

Summary

The current results and our other investigations of human V1 show that synaptic and non-synaptic proteins develop through a series of orchestrated stages that extend across the lifespan (Murphy et al., 2005; Pinto et al., 2010; Williams et al., 2010; Pinto et al., 2015; Siu et al., 2015). The glutamatergic proteins studied here are central players in visually-driven plasticity, receptive field properties, and visual function. We found a late shift in the 2A:2B balance and a gradual maturation of GluA2. These findings will enable researchers to test the efficacy of specific neuroplasticity-based therapies at different stages of the lifespan.

4.5 References

- Banerjee A, Larsen RS, Philpot BD, Paulsen O (2016) Roles of Presynaptic NMDA Receptors in Neurotransmission and Plasticity. *Trends in Neurosciences* 39:26–39.
- Beaulieu C, Kisvarday Z, Somogyi P, Cynader M, Cowey A (1992) Quantitative distribution of GABA-immunopositive and-immunonegative neurons and synapses in the monkey striate cortex (area 17). *Cereb Cortex* 2:295–309.
- Bennett PJ, Sekuler R, Sekuler AB (2007) The effects of aging on motion detection and direction identification. *VISION RESEARCH* 47:799–809.
- Beston BR, Jones DG, Murphy KM (2010) Experience-dependent changes in excitatory and inhibitory receptor subunit expression in visual cortex. *Front Synaptic Neurosci* 2:138.
- Betts LR, Sekuler AB, Bennett PJ (2007) The effects of aging on orientation discrimination. *VISION RESEARCH* 47:1769–1780.
- Braddick O, Birtles D, Wattam-Bell J, Atkinson J (2005) Motion- and orientation-specific cortical responses in infancy. *VISION RESEARCH* 45:3169–3179.
- Burkhalter A (1993) Development of Forward and Feedback Connections between Areas V1 and V2 of Human Visual Cortex. *Cereb Cortex* 3:476–487.
- Burkhalter A, Bernardo KL, Charles V (1993) Development of local circuits in human visual cortex. *J Neurosci* 13:1916–1931.
- Chen WS, Bear MF (2007) Activity-dependent regulation of NR2B translation contributes to metaplasticity in mouse visual cortex. *Neuropharmacology* 52:200–214.
- Cho KKA, Khibnik L, Philpot BD, Bear MF (2009) The ratio of NR2A/B NMDA receptor subunits determines the qualities of ocular dominance plasticity in visual cortex. *Proceedings of the National Academy of Sciences* 106:5377–5382.
- Christopoulos A, Lew MJ (2000) Beyond eyeballing: fitting models to experimental data. *Crit Rev Biochem Mol Biol* 35:359–391.
- Cooke SF, Bear MF (2014) How the mechanisms of long-term synaptic potentiation and depression serve experience-dependent plasticity in primary visual cortex. *Philosophical Transactions of the Royal Society B: Biological Sciences* 369:20130284–20130284.
- Cooper LN, Bear MF (2012) The BCM theory of synapse modification at 30: interaction of theory with experiment. *Nat Rev Neurosci* 13:798–810.

- Cull-Candy SG, Brickley SG, Misra C, Feldmeyer D, Momiyama A, Farrant M (1998) NMDA receptor diversity in the cerebellum: identification of subunits contributing to functional receptors. *Neuropharmacology* 37:1369–1380.
- Dahlhaus M, Li KW, van der Schors RC, Saiepour MH, van Nierop P, Heimel JA, Hermans JM, Loos M, Smit AB, Levelt CN (2011) The synaptic proteome during development and plasticity of the mouse visual cortex. *Mol Cell Proteomics* 10:M110.005413–M110.005413.
- Daw NW, Fox K, Sato H, Czepita D (1992) Critical period for monocular deprivation in the cat visual cortex. *Journal of Neurophysiology* 67:197–202.
- Durand S, Patrizi A, Quast KB, Hachigian L, Pavlyuk R, Saxena A, Carninci P, Hensch TK, Fagiolini M (2012) NMDA receptor regulation prevents regression of visual cortical function in the absence of Mecp2. *Neuron* 76:1078–1090.
- Elleberg D, Lewis TL, Liu CH, Maurer D (1999) Development of spatial and temporal vision during childhood. *VISION RESEARCH* 39:2325–2333.
- Epelbaum M, Milleret C, Buisseret P, Dufier JL (1993) The sensitive period for strabismic amblyopia in humans. *Ophthalmology* 100:323–327.
- Erisir A, Harris JL (2003) Decline of the critical period of visual plasticity is concurrent with the reduction of NR2B subunit of the synaptic NMDA receptor in layer 4. *Journal of Neuroscience* 23:5208–5218.
- Fagiolini M, Fritschy J-M, Löw K, Möhler H, Rudolph U, Hensch TK (2004) Specific GABAA circuits for visual cortical plasticity. *Science* 303:1681–1683.
- Fagiolini M, Katagiri H, Miyamoto H, Mori H, Grant SGN, Mishina M, Hensch TK (2003) Separable features of visual cortical plasticity revealed by N-methyl-D-aspartate receptor 2A signaling. *Proc Natl Acad Sci U S A* 100:2854–2859.
- Germine LT, Duchaine B, Nakayama K (2011) Where cognitive development and aging meet: face learning ability peaks after age 30. *Cognition* 118:201–210.
- Gordus A, Pokala N, Levy S, Flavell SW, Bargmann CI (2015) Feedback from network states generates variability in a probabilistic olfactory circuit. *Cell* 161:215–227.
- Groc L, Heine M, Cousins SL, Stephenson FA, Lounis B, Cognet L, Choquet D (2006) NMDA receptor surface mobility depends on NR2A-2B subunits. *Proc Natl Acad Sci U S A* 103:18769–18774.

- Hansen KB, Ogden KK, Yuan H, Traynelis SF (2014) Distinct functional and pharmacological properties of Triheteromeric GluN1/GluN2A/GluN2B NMDA receptors. *Neuron* 81:1084–1096.
- Harkany T, Mackie K, Doherty P (2008) Wiring and firing neuronal networks: endocannabinoids take center stage. *Current Opinion in Neurobiology* 18:338–345.
- Hartshorne JK, Germine LT (2015) When does cognitive functioning peak? The asynchronous rise and fall of different cognitive abilities across the life span. *Psychol Sci* 26:433–443.
- Hensch TK (2004) Critical period regulation. *Annu Rev Neurosci* 27:549–579.
- Heynen AJ, Yoon B-J, Liu C-H, Chung HJ, Hugarir RL, Bear MF (2003) Molecular mechanism for loss of visual cortical responsiveness following brief monocular deprivation. *Nat Neurosci* 6:854–862.
- Huang X, Stodieck SK, Goetze B, Cui L, Wong MH, Wenzel C, Hosang L, Dong Y, Löwel S, Schlüter OM (2015) Progressive maturation of silent synapses governs the duration of a critical period. *Proceedings of the National Academy of Sciences* 112:E3131–E3140.
- Huntley GW, Vickers JC, Janssen W, Brose N, Heinemann SF, Morrison JH (1994) Distribution and synaptic localization of immunocytochemically identified NMDA receptor subunit proteins in sensory-motor and visual cortices of monkey and human. *J Neurosci* 14:3603–3619.
- Huttenlocher PR, de Courten C, Garey LJ, Van der Loos H (1982) Synaptogenesis in human visual cortex--evidence for synapse elimination during normal development. *Neuroscience Letters* 33:247–252.
- Isaac JT, Crair MC, Nicoll RA, Malenka RC (1997) Silent synapses during development of thalamocortical inputs. *Neuron* 18:269–280.
- Keech RV, Kutschke PJ (1995) Upper age limit for the development of amblyopia. *J Pediatr Ophthalmol Strabismus* 32:89–93.
- Kim E, Sheng M (2004) PDZ domain proteins of synapses. *Nat Rev Neurosci* 5:771–781.
- Kleinschmidt A, Bear MF, Singer W (1987) Blockade of “NMDA” receptors disrupts experience-dependent plasticity of kitten striate cortex. *Science* 238:355–358.
- Kooijmans RN, Self MW, Wouterlood FG, Beliën JAM, Roelfsema PR (2014) Inhibitory interneuron classes express complementary AMPA-receptor patterns in macaque primary visual cortex. *Journal of Neuroscience* 34:6303–6315.

- Kovács I, Kozma P, Fehér A, Benedek G (1999) Late maturation of visual spatial integration in humans. *Proc Natl Acad Sci U S A* 96:12204–12209.
- Lambo ME, Turrigiano GG (2013) Synaptic and intrinsic homeostatic mechanisms cooperate to increase L2/3 pyramidal neuron excitability during a late phase of critical period plasticity. *Journal of Neuroscience* 33:8810–8819.
- Lee H-G, Jo J, Hong H-H, Kim KK, Park J-K, Cho S-J, Park C (2016) State-of-the-art housekeeping proteins for quantitative western blotting: Revisiting the first draft of the human proteome. *Proteomics* 16:1863–1867.
- Levelt CN, Hübener M (2012) Critical-period plasticity in the visual cortex. *Annu Rev Neurosci* 35:309–330.
- Leventhal AG, Wang Y, Pu M, Zhou Y, Ma Y (2003) GABA and its agonists improved visual cortical function in senescent monkeys. *Science Signalling* 300:812.
- Lewis TL, Maurer D (2005) Multiple sensitive periods in human visual development: Evidence from visually deprived children. *Dev Psychobiol* 46:163–183.
- Liu Y, Wong TP, Aarts M, Rooyackers A, Liu L, Lai TW, Wu DC, Lu J, Tymianski M, Craig AM, Wang YT (2007) NMDA receptor subunits have differential roles in mediating excitotoxic neuronal death both in vitro and in vivo. *Journal of Neuroscience* 27:2846–2857.
- Lunghi C, Berchicci M, Morrone MC, Di Russo F (2015a) Short-term monocular deprivation alters early components of visual evoked potentials. *The Journal of Physiology* 593:4361–4372.
- Lunghi C, Emir UE, Morrone MC, Bridge H (2015b) Short-term monocular deprivation alters GABA in the adult human visual cortex. *Curr Biol* 25:1496–1501.
- Magnusson KR, Brim BL, Das SR (2010) Selective Vulnerabilities of N-methyl-D-aspartate (NMDA) Receptors During Brain Aging. *Front Aging Neurosci* 2:11.
- Maurer D, Lewis TL, Brent HP, Levin AV (1999) Rapid improvement in the acuity of infants after visual input. *Science* 286:108–110.
- Meuwese JDI, van Loon AM, Scholte HS, Lirk PB, Vulink NCC, Hollmann MW, Lamme VAF (2013) NMDA receptor antagonist ketamine impairs feature integration in visual perception. Herzog MH, ed. *PLoS ONE* 8:e79326.
- Mierau SB, Patrizi A, Hensch TK, Fagiolini M (2016) Cell-Specific Regulation of N-Methyl-D-Aspartate Receptor Maturation by Mecp2 in Cortical Circuits. *Biol Psychiatry* 79:746–754.

- Murphy KM, Balsor J, Beshara S, Siu C, Pinto JGA (2014) A high-throughput semi-automated preparation for filtered synaptoneurosomes. *Journal of Neuroscience Methods* 235:35–40.
- Murphy KM, Beston BR, Boley PM, Jones DG (2005) Development of human visual cortex: a balance between excitatory and inhibitory plasticity mechanisms. *Dev Psychobiol* 46:209–221.
- Owsley C (2011) Aging and vision. *VISION RESEARCH* 51:1610–1622.
- Philpot BD, Cho KKA, Bear MF (2007) Obligatory role of NR2A for metaplasticity in visual cortex. *Neuron* 53:495–502.
- Philpot BD, Espinosa JS, Bear MF (2003) Evidence for altered NMDA receptor function as a basis for metaplasticity in visual cortex. *Journal of Neuroscience* 23:5583–5588.
- Philpot BD, Sekhar AK, Shouval HZ, Bear MF (2001) Visual experience and deprivation bidirectionally modify the composition and function of NMDA receptors in visual cortex. *Neuron* 29:157–169.
- Pinto JGA, Hornby KR, Jones DG, Murphy KM (2010) Developmental changes in GABAergic mechanisms in human visual cortex across the lifespan. *Front Cell Neurosci* 4:16
Available at: http://www.frontiersin.org/Journal/Abstract.aspx?s=156&name=cellular_neuroscience&ART_DOI=10.3389/fncel.2010.00016.
- Pinto JGA, Jones DG, Williams CK, Murphy KM (2015) Characterizing synaptic protein development in human visual cortex enables alignment of synaptic age with rat visual cortex. *Front Neural Circuits* 9:3.
- Quinlan EM, Olstein DH, Bear MF (1999a) Bidirectional, experience-dependent regulation of N-methyl-D-aspartate receptor subunit composition in the rat visual cortex during postnatal development. *Proc Natl Acad Sci U S A* 96:12876–12880.
- Quinlan EM, Philpot BD, Hugarir RL, Bear MF (1999b) Rapid, experience-dependent expression of synaptic NMDA receptors in visual cortex in vivo. *Nat Neurosci* 2:352–357.
- Ramoas AS, Mower AF, Liao D, Jafri SI (2001) Suppression of cortical NMDA receptor function prevents development of orientation selectivity in the primary visual cortex. *Journal of Neuroscience* 21:4299–4309.
- Rivadulla CC, Sharma JJ, Sur MM (2001) Specific roles of NMDA and AMPA receptors in direction-selective and spatial phase-selective responses in visual cortex. *J Neurosci* 21:1710–1719.

- Rumpel S, Hatt H, Gottmann K (1998) Silent synapses in the developing rat visual cortex: evidence for postsynaptic expression of synaptic plasticity. *J Neurosci* 18:8863–8874.
- Scherzer CR, Landwehrmeyer GB, Kerner JA, Counihan TJ, Kosinski CM, Standaert DG, Daggett LP, Veliçelebi G, Penney JB, Young AB (1998) Expression of N-methyl-D-aspartate receptor subunit mRNAs in the human brain: hippocampus and cortex. *J Comp Neurol* 390:75–90.
- Self MW, Kooijmans RN, Supèr H, Lamme VA, Roelfsema PR (2012) Different glutamate receptors convey feedforward and recurrent processing in macaque V1. *Proc Natl Acad Sci U S A* 109:11031–11036.
- Sheng M, Cummings J, Roldan LA, Jan YN, Jan LY (1994) Changing subunit composition of heteromeric NMDA receptors during development of rat cortex. *Nature* 368:144–147.
- Siu CR, Balsor JL, Jones DG, Murphy KM (2015) Classic and Golli Myelin Basic Protein have distinct developmental trajectories in human visual cortex. *Front Neurosci* 9:138.
- Smith GB, Heynen AJ, Bear MF (2009) Bidirectional synaptic mechanisms of ocular dominance plasticity in visual cortex. *Philosophical Transactions of the Royal Society B: Biological Sciences* 364:357–367.
- Stocca G, Vicini S (1998) Increased contribution of NR2A subunit to synaptic NMDA receptors in developing rat cortical neurons. *The Journal of Physiology* 507 (Pt 1):13–24.
- Taylor G, Hipp D, Moser A, Dickerson K, Gerhardstein P (2014) The development of contour processing: evidence from physiology and psychophysics. *Front Psychol* 5:719.
- Turrigiano GG (2008) The self-tuning neuron: synaptic scaling of excitatory synapses. *Cell* 135:422–435.
- Turrigiano GG (2017) The dialectic of Hebb and homeostasis. *Philosophical Transactions of the Royal Society B: Biological Sciences* 372:20160258.
- Turrigiano GG, Nelson SB (2004) Homeostatic plasticity in the developing nervous system. *Nat Rev Neurosci* 5:97–107.
- Vicini S, Wang JF, Li JH, Zhu WJ, Wang YH, Luo JH, Wolfe BB, Grayson DR (1998) Functional and pharmacological differences between recombinant N-methyl-D-aspartate receptors. *Journal of Neurophysiology* 79:555–566.
- Wang Y, Zhou Y, Ma Y, Leventhal AG (2005) Degradation of signal timing in cortical areas V1 and V2 of senescent monkeys. *Cereb Cortex* 15:403–408.

Williams K, Irwin DA, Jones DG, Murphy KM (2010) Dramatic Loss of Ube3A Expression during Aging of the Mammalian Cortex. *Front Aging Neurosci* 2:18.

Yashiro K, Philpot BD (2008) Regulation of NMDA receptor subunit expression and its implications for LTD, LTP, and metaplasticity. *Neuropharmacology* 55:1081–1094.

Yoshii A, Sheng MH, Constantine-Paton M (2003) Eye opening induces a rapid dendritic localization of PSD-95 in central visual neurons. *Proc Natl Acad Sci U S A* 100:1334–1339.

Zhang J, Wang X, Wang Y, Fu Y, Liang Z, Ma Y, Leventhal AG (2008) Spatial and temporal sensitivity degradation of primary visual cortical cells in senescent rhesus monkeys. *Eur J Neurosci* 28:201–207.

Zilles K, Werners R, Büsching U, Schleicher A (1986) Ontogenesis of the laminar structure in areas 17 and 18 of the human visual cortex. A quantitative study. *Anat Embryol* 174:339–353.

Chapter 5. Development of the tetrapartite synapse in human primary visual cortex (V1)

Abstract

Recently, I have shown evidence for prolonged development of glutamatergic synaptic proteins in human V1 that suggest excitatory synapses are plastic to experience-dependent modification across the lifespan. In addition to pre- and post-synaptic elements, glutamatergic synapses also contain astrocytes and extracellular matrix (ECM) that together comprise the 'tetrapartite' synapse. Many studies have shown astrocytes and ECM have integral roles in development of neural circuits and function. In human brain, astrocytes and ECM are uniquely complex in structure and function, yet little is known about how the tetrapartite synapse develops in the human visual cortex that could support changes in plasticity and perception across the lifespan. I used Western blotting to study the expression of the astrocyte marker glial fibrillary acidic protein (GFAP), ECM receptor subunit $\beta 3$ -Integrin, and dendritic spine protein Drebrin (Developmentally Regulated Brain protein) in postmortem samples of human V1 that ranged in age from 20 days to 79 years. I found that development of Drebrin expression increases into adulthood. There was a loss of Drebrin and $\beta 3$ -integrin in aging that may contribute to aberrant spines in this stage. GFAP expression peaked early in infancy, a period well characterized by synapse production and elimination that suggests the participation of astrocytes in synaptic refinement in human V1. This study is the first to identify the lifelong development of mechanisms in the tetrapartite synapse that regulates glutamatergic dendritic spine plasticity in human V1.

5.1 Introduction

Recently, I showed that a set of glutamatergic synaptic proteins in human primary visual cortex (V1) develops over 5 stages that suggests V1 participates in plasticity and visual development across the lifespan (Siu et al., 2017). Dendritic spines are the main sites of glutamatergic synapses, and rapidly change in shape, size, and number in response to changes in activity (Fischer et al., 1998; Rocha and Sur, 1995; Trachtenberg et al., 2002). This structural-plasticity in dendritic spines is dependent on Drebrin, a protein that regulates actin-based spine morphology (Hayashi and Shirao, 1999; Hayashi et al., 1996). In addition to pre- and post-synaptic elements, however, glutamatergic synapses are closely regulated by astrocytes and the extracellular matrix (ECM) that led to the terms ‘tripartite’ (Araque et al., 1999) and ‘tetrapartite’ synapses (Dityatev and Rusakov, 2011; Park and Goda, 2016). Since the expression of glutamatergic proteins in human V1 continue to develop and change across the lifespan, I sought to examine the expression of other tetrapartite synapse markers to determine their developmental trajectories (Figure 1).

The insertion of AMPAR activates silent synapses (Huang et al., 2015), stabilizes spine strength by decreasing actin-based motility and rounding the shape of the synapse (Fischer et al., 2000), and increases Drebrin clustering in spines (Takahashi et al., 2009). This clustering of Drebrin is necessary for clustering of PSD-95 to the synapse (Takahashi et al., 2003) that terminates the critical period (CP) for ocular dominance plasticity (ODP) in V1 (Huang et al., 2015). In cat V1, the expression of Drebrin dramatically decreased at the end of the CP, indicating it may play a role in experience-dependent modification of synapses in the visual cortex (Imamura et al., 1992). In my study of glutamate proteins in human V1, I found that both PSD-95 and GluA2

increase in expression until 8-10 years of age, roughly the end of the period for susceptibility of developing amblyopia (Siu et al., 2017).

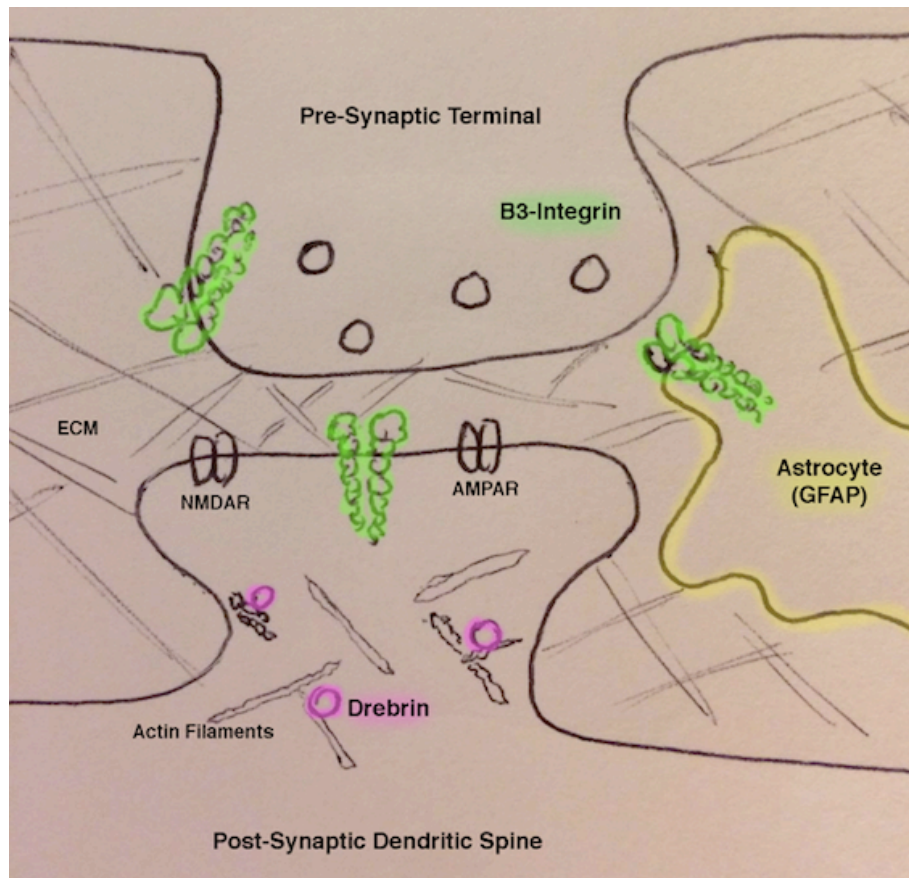


Figure 1 - The tetrapartite synapse. I studied expression levels of GFAP (yellow), a marker for Astrocyte expression; β 3-integrin (green), receptors for extracellular matrix ligands found on pre-synaptic, post-synaptic and astrocytic membranes; and Drebrin (pink), a dendritic spine plasticity protein bound to actin filaments. Together these molecules regulate different aspects of synaptic plasticity.

The ECM is composed mainly of chondroitin sulfate proteoglycan proteins (CSPGs) that develop around synapses to restrain motility in the adult visual cortex (Berardi et al., 2004; de Vivo et al., 2013). Integrin receptors are synaptic receptors for ECM ligands and have a unique role of regulating synaptic strength by ECM and glia signalling (Park and Goda, 2016). For example,

β 3-integrin activity-dependent trafficking of GluA2-containing AMPA is necessary for homeostatic synaptic scaling (Cingolani et al., 2008; Pozo et al., 2012). Expression of β 3-integrin receptors are necessary for the coordinated pre- and post-synaptic activity required for the development of the NMDA receptor GluN2A:GluN2B (2A:2B) subunit switch (Chavis and Westbrook, 2001). In my study of human V1, I found that the 2A:2B switch developed until 40 years of age, providing evidence for prolonged development of synaptic strength in human visual cortex.

Astrocytes closely monitor glutamatergic synapses and regulate synaptic strength by releasing glutamate to both pre- and post-synaptic receptors (Bezzi et al., 1998; Lehre and Rusakov, 2002; Min and Nevian, 2012; Montana, 2004). In the visual cortex, astrocytes regulate receptive field (RF) properties of pyramidal neurons (Perea et al., 2014), meanwhile are themselves selective to visual stimuli that map onto RF properties of V1 neurons (Schummers et al., 2008), and undergo experience-dependent plasticity to monocular deprivation (Hawrylak and Greenough, 1995).

Astrocytes secrete many neuronal factors including hevin, that is required for developmental refinement of thalamic input to V1 (Risher et al., 2014) and ECM molecules (Wiese et al., 2012) like SPARC that inhibits β 3-integrin and causing changes in AMPAR surface levels (Jones et al., 2011). The expression of glial fibrillary acidic protein (GFAP) is strongly associated with size and complexity of astrocytic processes, and has been used as a marker to show that a single human astrocyte can cover up to 2 million synapses (Oberheim et al., 2009).

I chose to study those tetrapartite synaptic proteins that contribute to dendritic spine plasticity: Drebrin -- actin-binding dendritic spine protein, β 3-integrin -- ECM receptor, and astrocyte marker (GFAP) (Eng, 1985) in postmortem human V1 samples from cases aged 20 days to 79

years. These results support my previous finding of 5 stages of glutamatergic synaptic development in human V1 (Siu et al., 2017). These results show the complex development of different components of the tetrapartite glutamatergic synapse.

5.2 Materials and Methods

Samples

The samples used in this study were all collected from a set of postmortem human cases obtained from the Brain and Tissue Bank for Developmental Disorders at the University of Maryland (Baltimore, MD, USA). The use of postmortem human tissue in our study was approved by the McMaster University Research Ethics Board. The samples were collected within 23 hours post-mortem, were from individuals without any history of brain disorders who died with little or no trauma. Primary visual cortex (V1) samples were collected from the posterior pole of the left hemisphere and included both superior and inferior areas of the calcarine fissure. Samples were flash frozen in isopentane and dry ice at the Brain and Tissue Bank, then stored at -80°C . A total of 31 human cases were used that ranged in age from 20 days to 79 years (Table 1).

Age	Sex	Post Mortem Interval (Hrs)	Cause of Death
20 days	M	9	Asphyxia
20 days	F	14	Pneumonia
86 days	F	23	Unknown
96 days	M	12	Bronchopneumonia
98 days	M	16	Tetralogy of Fallot
119 days	M	22	Bronchopneumonia
120 days	M	23	Pneumonia
133 days	M	16	Accident
136 days	F	11	Pneumonia
273 days	M	10	SIDS
1 year 123 days	M	21	Dehydration
2 years 57 days	F	21	Acute Myocarditis
2 years 75 days	F	11	Meningitis

Age	Sex	Post Mortem Interval (Hrs)	Cause of Death
3 years 123 days	F	11	Drowning
4 years 203 days	M	15	Accident, drowning
4 years 258 days	M	17	Drowning
5 years 144 days	M	17	Accident, drowning
8 years 50 days	F	20	Compressional Asphyxia
8 years 214 days	F	20	Rejection of Cardiac Allograft Transplantation
9 years 46 days	F	20	Asthma
12 years 164 days	M	22	Cardiac Arrhythmia
13 years 99 days	M	5	Asphyxia by Hanging
15 years 81 days	M	16	Multiple Injuries
19 years 76 days	F	16	Multiple Injuries
22 years 359 days	M	4	Multiple Injuries
32 years 223 days	M	13	Ruptured aortic aneurysm
50 years 156 days	M	8	Cardiovascular Disease
53 years 330 days	F	5	Pulmonary Thromboembolus
69 years 110 days	M	12	Coronary Artery Disease
71 years 333 days	F	9	Multiple medical disorders
79 years 181 days	F	14	Drug Overdose

Table 1 -- List of human cases used in this study. For each human case listed age, sex, postmortem interval (in hours), and cause of death.

Sample Preparation

To study expression of all elements of the tetrapartite synapse, I prepared postmortem human V1 tissue samples using a homogenate tissue preparation.

First, a piece of tissue (50 - 100mg) was cut from the frozen section of human V1. Frozen tissue pieces were suspended in the appropriate amount of cold homogenization buffer (1ml buffer: 50mg tissue, 0.5mM DTT, 2mM EDTA, 2mM EGTA, 10mM HEPES, 10mg/L leupeptin, 100nM microcystin, 0.1mM PMSF, 50mg/L soybean trypsin inhibitor) before being homogenized by hand in a glass-glass Dounce homogenizer (Kones, Vineland, NJ, USA). I measured total protein concentration of each sample using Bicinchoninic Acid (BCA) Assay (Pierce, Rockford, IL, USA) and equated each sample to the same protein concentration (1µg protein/ml) by diluting each sample with appropriate amounts of sample loading buffer (M260 Next Gel® Sample loading buffer 4x, Amresco LLC, Solon, OH, USA), and Laemmli buffer (Cayman Chemical Company, Ann Arbor, MI, USA). This step is necessary for quantitative Western blotting to ensure equal amounts of protein are loaded into each of the wells. This step helps normalize the samples before measuring relative levels of protein expression, especially in a developmental study where many of the proteins measured are developmentally regulated. A control sample was made by taking a small amount of each of the 31 homogenized human V1 samples and combining them into one, then 11 lane of each blot was loaded with this control sample.

Immunoblotting

I loaded equal amounts (20 µg) of each of the homogenate samples on 4-20% SDS polyacrylamide gels (SDS-PAGE), and separated the samples by molecular weight using gel electrophoresis and transferred the gels to polyvinylidene difluoride (PVDF-FL) blot membranes (EMD Millipore, Billerica, MA, USA). Each human sample was run multiple times on different blots. I pre-incubated blots in blocking buffer for 1 hour (Odyssey Blocking Buffer 1:1 with

phosphate blocking buffer (PBS)) (Li-Cor Biosciences, Lincoln, NE, USA), then incubated in primary antibody overnight at 4°C under agitation. I used the following primary antibodies: Anti-Drebrin (1:1000, [10R-D117A], Fitzgerald Industries International, Acton, MA, USA), Anti-Integrin β 3 (1:1000 [AB2984], Millipore, Billerica, MA, USA), and Anti-GFAP (1:2000 [MAB360], Millipore, Billerica, MA, USA). I washed the blots with PBS-Tween (0.05% PBS-T) (Sigma, St. Louis, MO, USA) (3x10min), followed by 1 hour incubation in the appropriate IRDye labeled secondary antibody (Anti-Mouse, 1:8000; Anti-Rabbit, 1:10,000) (Li-Cor Biosciences, Lincoln, NE, USA), and washed again in PBS-T (3x10min). The blots were stripped using Blot Restore Membrane Rejuvenation kit (EMD Millipore, Billerica, MA, USA) to re-probe with each primary antibody.

Band analysis & image manipulation

I visualized the blots on an Odyssey Infrared scanner (Li-Cor Biosciences, Lincoln, NE, USA) and quantified the bands using densitometry (Li-Cor Odyssey Software Version 3.0) (Li-Cor Biosciences, Lincoln, NE, USA). The density of each band was calculated by dividing the integrated intensity of the area of the band by the width and subtracting the background. The density of each sample was divided by the control sample that was run on the same blot in order to compare expression across blots while controlling for inter-blot variability.

Curve fitting and statistical analysis

I plotted the results using scatter plots to visualize the developmental trajectories of each run (grey dots) and the average of all the runs (black dots) for each protein across the lifespan.

Developmental trajectories were fit to all the data points using model-fitting (Christopoulos and Lew, 2000) by evaluating curve-fits with the goodness of fit (R^2), statistical significance ($p < 0.05$) and the least sum of squares using Matlab (The Mathworks, Inc, Natick, MA). In scatter plots, Drebrin data were well-fit using a quadratic function ($Y = a + bx + cx^2$), $\beta 3$ -integrin data were fit using a linear function ($Y = mx + b$), and GFAP data was described using a weighted average. I also binned the results into developmental age groups to compare among different stages across the lifespan: < 0.3 , Neonates; 0.3-1 years, Infants; 1-4 years, Young Children; 5-11 years, Older Children; 12-20 years, Teens; 21-55 years, Young Adults; > 55 years, Older Adults. I plotted the histograms using the mean and standard error of the mean (SEM) of protein expression in each age group, and compared statistical significance between the groups using bootstrapping to randomly sample from a simulated data set using the mean and standard deviation from the group being compared. Bootstrapping was done using R statistical software package (R Core Team, 2014, R: A language and environment for statistical computing. R Foundation for Statistical Computing, <http://www.R-project.org>, RRID: SCR_001905), by simulating a normally distributed data set (with 1,000,000 points) of the comparison age group using the standard error and the mean. I compared the mean from all other age groups to this simulated data set, using a Monte Carlo simulation -- randomly sampling N number of cases, where N is the number of cases in the other age groups. This simulation was run 10,000 times to populate an expected distribution for N cases. I calculated the confidence intervals (95%, 99%, 99.9%) for the simulated data set and compared the observed group means. Age groups were considered to be statistically significantly different when the mean was outside the 95% confidence interval. Significances are represented on histograms by $p < 0.05^*$, $p < 0.01^{**}$, and $p < 0.001^{***}$.

Analysis of inter-individual variability

In previous studies of human V1 development, waves of inter-individual variability have been found across development of synaptic and non-synaptic proteins that suggests a unique phase of variability in early childhood (Pinto et al., 2015; Siu et al., 2017; Siu et al., 2015). I analyzed the inter-individual variability for the proteins used in this study by calculating the Fano Factor (Variance-to-Mean Ratio, VMR) for each protein by dividing the variance by the mean for a moving window of 3 age-adjacent human samples. I presented the VMR data using scatter plots. I presented the data using model-fitting approach to show the trend of variability in the data when possible, and when no fit was appropriate the data was described using a weighted average.

5.3 Results

Postmortem interval

First, I tested the correlation of protein expression with postmortem interval (PMI) of the collected human V1 samples. I did not find a significant correlation between PMI and protein expression for any of the proteins used in this study (β 3-Integrin, $R^2=0.04$, n.s.; GFAP, $R^2=0.05$, n.s.; Drebrin, $R^2=0.11$, n.s.), therefore I did not exclude any human cases from the study.

Prolonged development of dendritic spine plasticity in human V1

I analyzed the prolonged development of the tetrapartite synapse in human V1 by identifying the expression of markers for dendritic spine morphology, ECM-synapse signalling, and astrocyte development in human V1. Drebrin is an actin-binding protein localized to the post-synaptic excitatory dendritic spines (reviewed in (Sekino et al., 2007)) that governs spine morphogenesis (Hayashi and Shirao, 1999) and clustering of PSD-95 to the synapse (Takahashi et al., 2003). Interestingly, the activity of GluA2-containing AMPAR specifically promote clustering and stabilization of Drebrin in spines (Takahashi et al., 2009). Furthermore, Drebrin expression has been found to span the CP in cat V1, and is reduced at the end of the CP (Imamura et al., 1992). I identified expression of Drebrin in the human V1 across the lifespan, and found it has prolonged development well into adulthood (Fig 2A, B). Drebrin development was well-fit by a quadratic function that peaked around 44 years of age, then declined in older adulthood ($R^2=0.34$, $p<0.01$) (Fig 2A). I binned the data into age groups and used bootstrapping statistics to compare group means and found Drebrin expression was significantly higher in young adults (21-55 years) compared to all other age groups across the lifespan ($p<0.05$) (Fig 2B). This prolonged development of Drebrin in human V1 matches similar prolonged development of

other synaptic plasticity regulating mechanisms like myelin basic protein (Siu et al., 2015) and the 2A:2B balance (Siu et al., 2017) that each develop well into adulthood, and suggests prolonged plasticity of excitatory synapses that reaches peak maturation in the 4th decade, followed by a significant loss in aging ($p < 0.05$).

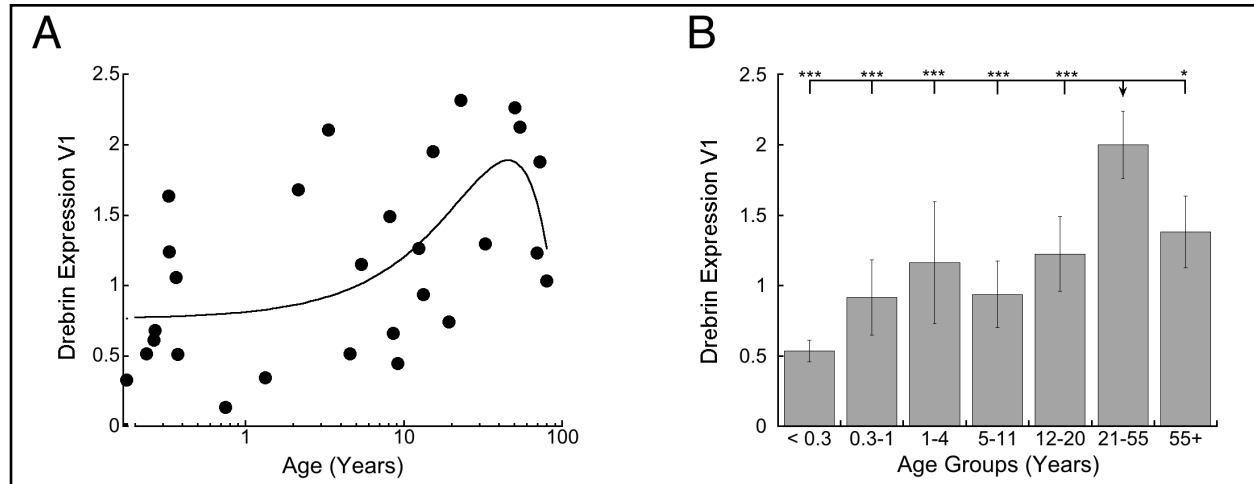


Figure 2 -- Development of Drebrin expression in human V1 across the lifespan. **(A)** A scatterplot of Drebrin expression across the lifespan fit with a quadratic function ($R^2=0.34$, $p < 0.01$) with peak expression ~ 44 years. **(B)** Age-binned results for Drebrin expression. For the scatterplots, grey dots represent each run, black dots represent the average for each case and age was plotted on a logarithmic scale. For the histograms, protein expression was binned into age groups (<0.3 years, Neonates; 0.3-1 years, Infants; 1-4 years, Young children; 5-11 years, Older children; 12-20 years, Adolescence; 21-55 years, Young adults; 55+ years, Older adults) with bars that show the mean and standard error of the mean (SEM). (* $p < 0.05$, ** $p < 0.01$, *** $p < 0.001$).

Loss of $\beta 3$ -Integrin in aging human V1

$\beta 3$ -Integrin is an ECM-ligand receptor found on pre- and post-synaptic excitatory (Chavis and Westbrook, 2001; Cingolani et al., 2008) and inhibitory (Charrier et al., 2010) synapses, as well as on astrocytic membranes (Jones et al., 2011). The activation of $\beta 3$ -Integrin receptors is dependent on intracellular and extracellular signalling from ligands excreted by both ECM (Jalali

et al., 2001) and glial cells such as TNF- α (Gao et al., 2002). β 3-Integrin regulates synaptic strength through both GluA2-containing AMPAR (Cingolani et al., 2008), is necessary for the developmental switch from GluN2B to GluN2A (Chavis and Westbrook, 2001), and mediates dendritic spine plasticity through NMDA receptors (Shi and Ethell, 2006). I quantified the expression of β 3-Integrin receptor subunit across the lifespan in human V1 and found high expression in infancy, that was reduced in childhood remaining steady until adulthood, then declined in aging (55+ years) (Fig 3A, B). The scatterplot of β 3-Integrin human V1 development was best fit by a linear function that decreased into aging ($R^2=0.29$, $p<0.0001$) (Fig 3A). Bootstrap comparison across age groups showed a peak of β 3-Integrin expression in neonates (<0.3 years) that declines in infancy (0.3-1 years, $p<0.01$), older children (5-11 years, $p<0.01$), adolescence (12-20 years, $p<0.001$), young adults (21-55 years, $p<0.001$), and has a 4-fold loss in older adults (55+ years, $p<0.001$) (Fig 3B).

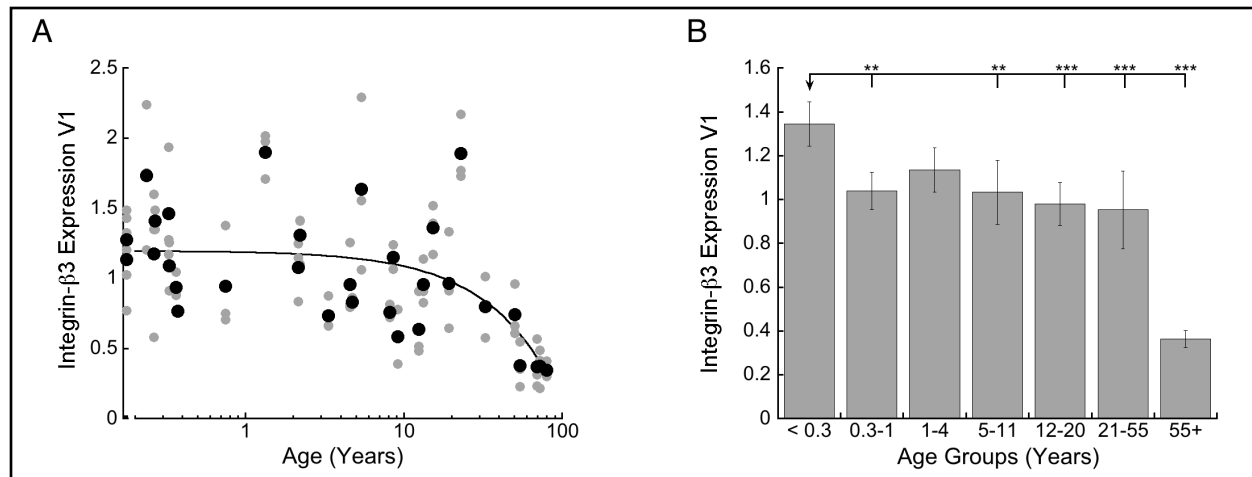


Figure 3 -- Development of β 3-Integrin expression in human V1 across the lifespan. **(A)** A scatterplot of β 3-Integrin expression across the lifespan fit with a linear function ($R^2=0.29$, $p<0.0001$). **(B)** Age-binned results for β 3-Integrin expression. Scatterplot, histogram, and significance levels are plotted using the conventions described in Figure 1.

Astrocyte-marker GFAP multiple changes in human V1

Astrocytes are a major component of synaptic formation, and maturation (Chung et al., 2015), and release proteins that are necessary for development of synaptic connectivity and refining dendritic spines (Risher et al., 2014). Human astrocytes are especially complex compared to other species, as a single astrocyte can cover up to 2 million synapses compared to a rodent astrocyte covering to 120,000 (Oberheim et al., 2009). Glial fibrillary protein (GFAP) is the major protein marker for intermediate filaments in astrocytes (Eng, 1985) and expression of GFAP is proportional to the size and complexity of the astrocytic processes (Oberheim et al., 2009). I quantified the expression of GFAP across the lifespan in human V1 and found variable GFAP expression that was not well-fit by a model, so I described the trend using a weighted average (Fig 4A). I compared GFAP data in age groups and found a significant 2.5x increase in expression within the first year of development ($p < 0.001$), a significant decrease in young childhood (1-4 years, $p < 0.001$) and back to neonate levels in late childhood (5-11 years, $p < 0.001$). GFAP expression in infants was higher than adolescents (12-20 years, $p < 0.001$), and young adults ($p < 0.05$), but was not significantly different from older adults (> 55 years) (Fig 4B). The notable increase in astrocyte expression in infancy coincides with a time of rapid synaptogenesis in human V1 (Huttenlocher et al., 1982).

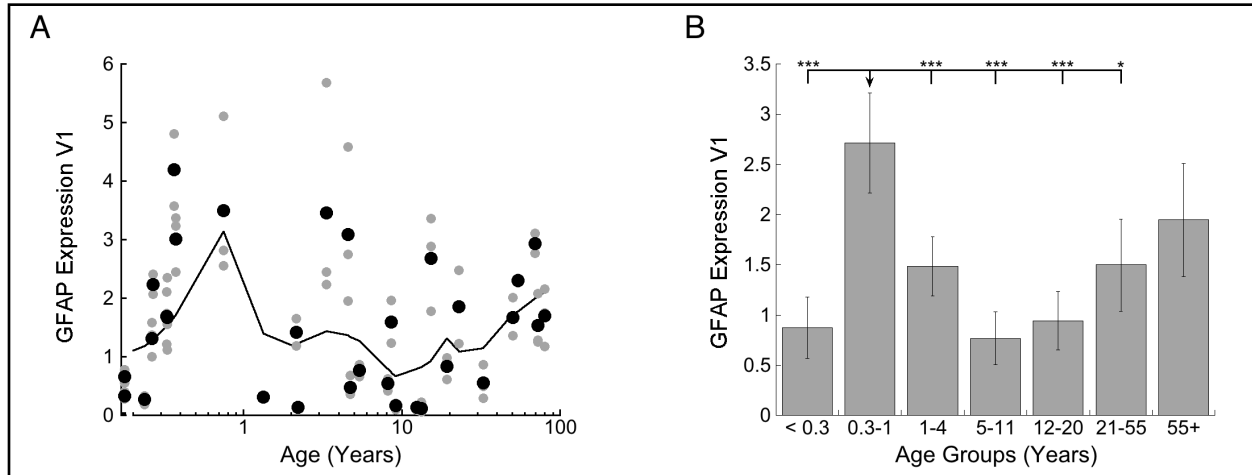


Figure 4 -- Development of GFAP expression in human V1 across the lifespan. **(A)** A scatterplot of GFAP expression across the lifespan was described using a weighted average. **(B)** Age-binned results for GFAP expression. Scatterplot, histogram, and significance levels are plotted using the conventions described in Figure 1.

Interindividual Variability

I measured the interindividual variability for β 3-Integrin, Drebrin, and GFAP by calculating the variance-to-mean ratio (VMR) for a sliding window of 3 adjacent ages. There was a wave of inter-individual variability in GFAP protein expression, that well-fit by a gaussian curve that peaked around 2.3 years of age before declining across the rest of the lifespan ($R^2=0.38$, $p<0.001$) (Fig 5C). The VMR for Drebrin showed a trend toward high interindividual variability in childhood, with 4 points that are have high VMR, but are balanced by an equal amount of points that have low VMR within the same age range. This trend was described using a weighted average that showed this period of VMR variability around 2 years of age (Fig 5B). There was no change in VMR for β 3-Integrin expression in human V1, that was described using a weighted average (Fig 5A). Interestingly, the wave of interindividual variability for GFAP expression overlaps with VMR waves found in glutamatergic receptors (Siu et al., 2017), pre- and post-

synaptic proteins (Pinto et al., 2015) and oligodendrocyte protein golli-MBP (Siu et al., 2015), providing further evidence for this variable stage of development in V1.

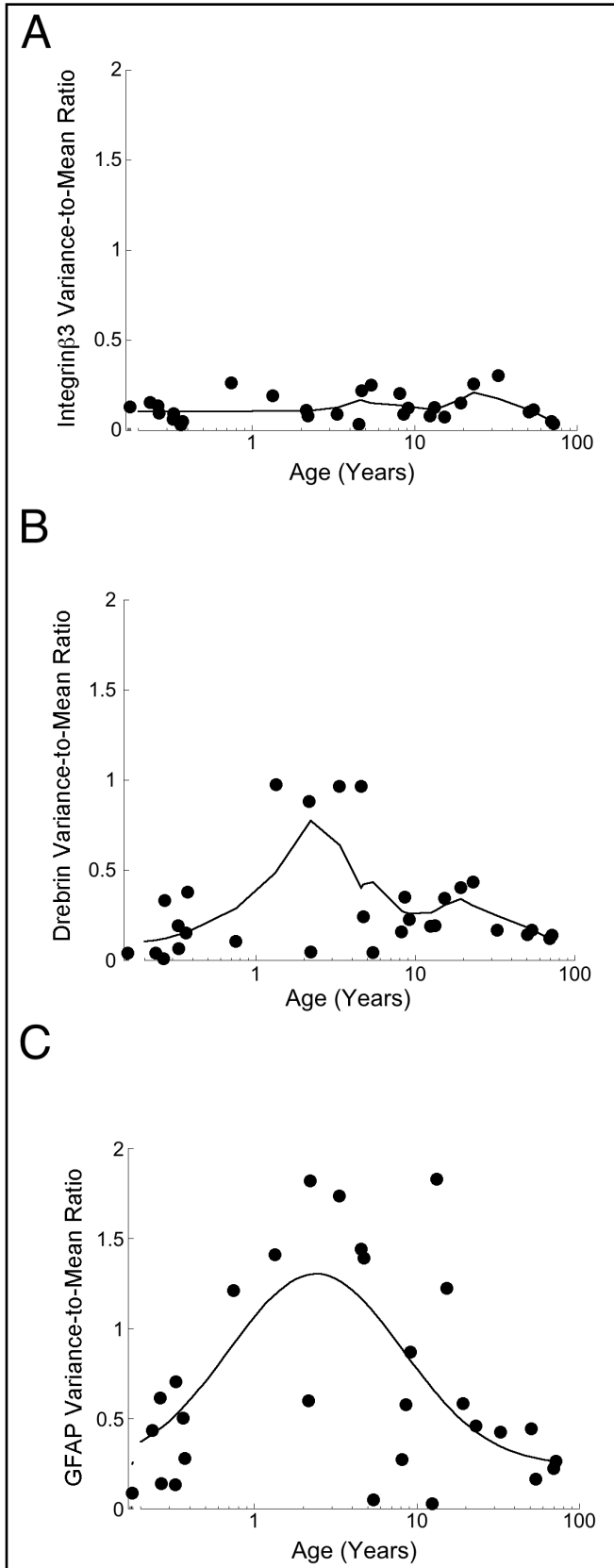


Figure 5 -- Development of the VMR for β 3-Integrin (A), Drebrin (B), and GFAP (C) in human V1 across the lifespan. (A) β 3-Integrin VMR expression showed no peak, described with a weighted average (B) Drebrin VMR expression described using a weighted average (B) GFAP VMR expression fit with a Gaussian curve that peaks \sim 2.3 years of age ($R^2=0.38$, $p<0.001$). Black dots are the VMR for a moving window of 3 cases adjacent in age.

5.4 Discussion

This study provides evidence for how elements of the tetrapartite synapse: extracellular matrix and astrocytes, develop in human V1 across the lifespan. I found changes in infancy, early childhood, young adulthood, and aging that support previously characterized stages of prolonged synaptic and cortical myelin development in human V1 (Pinto et al., 2015; Siu et al., 2015; 2017). Together these studies provide evidence for a system of structural and functional molecular mechanisms in human V1 that develop across the lifespan to support experience-dependent plasticity and visual perception across the lifespan.

Quantification of markers for dendritic spines, astrocytes, and ECM development using Western blotting in postmortem cortical tissue must be evaluated with caution considering the nature of rapid structural changes associated with each of these components. For example, GFAP is a marker for astrocytic processes and quantification of global GFAP expression is a good measure to quantify relative changes in size or number of astrocytic processes. Human astrocytes are uniquely complex compared to other species (Oberheim et al., 2009), however, in this study I cannot assume morphological classes of astrocytes despite the likelihood that these changes contribute to changes in global GFAP expression. In addition, Drebrin is a marker for activity-dependent spine development, but spines undergo rapid activity-dependent change (Kasai et al., 2003), therefore our measurements of Drebrin expression across development are only snapshots of a transient structure. Although our technique for evaluating protein expression in postmortem human cortex provides invaluable information about expression of specific molecular mechanisms linked to plasticity and visual perception in human brain, finer details such as morphology, laminar distribution, or physiological response properties cannot be inferred from

this study alone. Furthermore, in this study I used whole homogenate tissue in order to fully capture developmental changes in these proteins in V1, including GFAP which can be expressed in large astrocytic processes. Due to this, it is highly likely that the developmental changes I captured for these proteins are expressed in non-synaptic structures, and are not only reflective of ‘tetrapartite synapse’ development. Therefore, in order to be characterize the tetrapartite synapse development more specifically, it will be important in future studies to use a specialized tissue preparation for human tissue, such as synaptoneurosomes, or anatomical studies to identify where these developmental changes occur in human V1.

Peak astrocyte expression corresponds with period of rapid synapse formation in human V1

The first year of human visual cortex development is well-characterized by the peak number of dendritic spines around 5 months of age (Michel and Garey, 1984) and rapid synapse production that peaks around 8 months of age (Huttenlocher et al., 1982), that is followed by a longer period of synaptic pruning that reaches adult-levels within a few years. I found a rapid increase in astrocyte marker GFAP expression that increased 3-fold by 4 months of age (Fig 4). Astrocytes are active participants in the formation of developing synapses (Chung et al., 2015), and also key mediators of elimination and pruning of weaker synapses by continuously engulfing and phagocytosing both excitatory and inhibitory synapses across development and adult cortex (Chung et al., 2013). Previously, I found a significant loss of GluN1 in the first year of human V1 development (Siu et al., 2017) that points to a significant transition period for excitatory synapses possibly due to synaptic pruning. This significant increase of GFAP in the first year of

V1 development points to astrocyte-mediated pruning of synapses that contributes to period of synapse elimination found in anatomical studies of human V1.

Astrocytes make up the ‘tripartite synapse’ (Araque et al., 1999) by bidirectionally communicating with both pre-synaptic membranes (Lehre and Rusakov, 2002) and post-synaptic spines (Haber et al., 2006) by releasing glutamate to presynaptic NMDAR (Min and Nevian, 2012) and enhances the selectivity of V1 neurons by increasing glutamate transmission to both excitatory and inhibitory neurons (Perea et al., 2014). Infancy marks the onset of binocular acuity (Braddick et al., 1980; Held et al., 1980), orientation and direction selectivity (Braddick, 1993; Braddick and Atkinson, 2011; Hood et al., 1992), and the peak of GFAP at this stage may contribute to a volley of excitatory and inhibitory transmission that influences the development of selectivity for those receptive field properties.

Interindividual variability in astrocytic expression in childhood

I calculated the interindividual variability for protein expression relative to the mean of 3 adjacent ages, and found a wave of interindividual variability in GFAP expression in early childhood, that peaked around 2.3 years of age (Fig 5C). This wave of high variability in GFAP expression may be a feature rapid change in size and complexity of human astrocytic processes that at any given moment in this stage rapidly change, or a feature of differences in astrocyte size and complexity between individuals. The timing of this wave of variability in GFAP expression is coincident with the timing of high interindividual variability in synaptic proteins (Pinto et al., 2015; Siu et al., 2015; 2017).

Drebrin expression in dendritic spines showed a trend for high variability also in this early stage of development, could not be distinguished from many points of low interindividual variability also in early childhood (Fig 5B). Development of β 3-Integrin expression showed low interindividual variability across the entire lifespan. In this study alone it is impossible to infer if the variance-to-mean ratio shows true inter- or intra-individual variability. These change in VMR across the lifespan, however, is a good way to isolate specific developmental periods where the composition of human V1 synapses is different between individuals.

Prolonged increase of Drebrin expression into adulthood

I found a prolonged increase of Drebrin expression that peaks well into adulthood around 40 years of age. This prolonged development of drebrin in human V1 matches similar prolonged development of other synaptic plasticity regulating mechanisms like the classic isoform of myelin basic protein (MBP) (Siu et al., 2015) and the GluN2A:GluN2B (2A:2B) balance (Siu et al., 2017) that each develop well into adulthood.

Drebrin has 2 isoforms, the early developing isoform ‘Drebrin E’ that is ubiquitous throughout neurons, and the adult form ‘Drebrin A’ that is localized to spines (Hayashi and Shirao, 1999; Shirao and Obata, 1986). In this study, I have quantified the isoform Drebrin A, that indirectly shows a prolonged trajectory of dendritic spine maturation into adulthood in human V1.

Interestingly, stabilization and accumulation of Drebrin is dependent on upregulation of AMPAR (Takahashi et al., 2009), that I previously shown peak GluA2 AMPAR subunit in late childhood in human V1. Furthermore, the increase in Drebrin expression is directly related to the increase of dendritic spine head size (Kobayashi et al., 2007), spine stability, and synaptic strength

through promotion of PSD-95 clustering (Takahashi et al., 2003). Drebrin accumulation has been linked to the end of CP plasticity in cat V1 (Imamura et al., 1992). Myelin accumulation is also linked with the end of the CP (McGee et al., 2005), and both Drebrin and classic-MBP mature in human V1 until 40 years of age (Siu et al., 2015). Although the end of susceptibility to amblyopia in humans is 6-10 years (Lewis and Maurer, 2005), the late development of these CP regulators indicate V1 retains at least some plasticity into adulthood.

Age-related losses of β 3-integrin and Drebrin expression human V1

There was a significant loss β 3-integrin and Drebrin expression in older adults (>55 years) in human V1. This characteristic of cortical aging has been found in human V1 before, with losses of the classic isoform of myelin basic protein (MBP) (Siu et al., 2015), GABA synthesizing protein GAD65 (Pinto et al., 2010), ubiquitin ligase protein Ube3a (Williams et al., 2010), and NMDA receptor subunit GluN2A (Siu et al., 2017). Together, with the loss of β 3-integrin and Drebrin in human V1, those age-related losses in human V1 suggests multiple mechanisms that could contribute to reduced synaptic plasticity and visual perception in older adults.

Although Integrins are ECM receptors, they are actually associated with every element of the tetrapartite synapse (Park & Goda, 2016), making this loss of β 3-Integrin in aging human V1 impactful for total synaptic function. β 3-integrin regulates both AMPAR and NMDAR function. -TNF- α is a pro-inflammatory cytokine released by astrocytes that depends on β 3-integrin binding to GluA2 for synaptic scaling (Cingolani et al., 2008). TNF- α increases in very elderly and Alzheimer's disease (AD) populations compared to younger adults (Bruunsgaard et al., 2001; Michaud et al., 2013; Sarkar and Fisher, 2006). The loss of β 3-integrin may have a role in

the disruption of TNF- α mediated synaptic scaling of AMPAR trafficking to the synapse in aging (Henley and Wilkinson, 2013; 2016).

The loss of GluN2A in human v1 switches the 2A:2B balance to favour GluN2B in aging human V1 (Siu et al., 2017). β 3-Integrin-mediated signalling is necessary for the maturation of the 2A:2B balance (Chavis & Westbrook, 2001) Our finding points to the loss of β 3-integrin in aging human V1 as a possible mechanism that contributes to the shift of the 2A:2B balance back towards an immature state (Siu et al., 2017), and a mechanism for the loss of synaptic stability in aging (McGeachie et al., 2011). Interestingly, β 3-Integrins also regulate glycine receptor trafficking and stabilization in inhibitory synapses (Charrier et al., 2010), indicating that the loss of β 3-Integrin in aging may contribute to the loss of inhibition in V1 that underlies age-related loss of visual receptive field properties in the visual cortex (Leventhal, 2003).

Integrin receptors, however, are made up of multiple dimers including at least 24 different combinations of 18 alpha (α) and 8 beta (β) subunits (Hynes, 2002) that are each tied to unique functions. Therefore, my report of β 3-integrin loss in human V1 is not a reflection of loss for total integrin receptor function. In addition, much of what is known about Integrin receptors comes from studies in the hippocampus (Chavis and Westbrook, 2001; Cingolani et al., 2008; Pozo et al., 2012; Shi and Ethell, 2006), and more animal models about Integrin function in the visual cortex may be necessary to better elucidate the developmental expression in human V1.

Loss of Drebrin in the cortex has previously been found in human diseases associated with abnormal spine morphology such as Alzheimer's Disease (AD) and Down's Syndrome (DS) (Shim and Lubec, 2002). The age-related loss of Drebrin expression has been previously

characterized by 32-42% loss in normal aging human brain, and up to 81% in Alzheimer's disease (AD) (Hatanpaa et al., 1999), and is considered a major molecular bases for cognitive impairment associated with normal aging and AD. Loss of Drebrin is associated loss of dendritic spines in aging (Dickstein et al., 2013), and with a decrease in both mEPSC and mIPSC (Ivanov et al., 2009), and that loss contributes to impaired maintenance of dendritic spines in the visual cortex (Kim et al., 2016). This study provides new information about how elements of the tetrapartite synapse develop in human V1 across the lifespan. These data can help animal and human studies to target more relevant developmental time points in the human lifespan for efficacy in harnessing neuroplasticity for therapeutic use.

5.5 References

- Araque, A., Parpura, V., Sanzgiri, R. P., & Haydon, P. G. (1999). Tripartite synapses: glia, the unacknowledged partner. *Trends in Neurosciences*, 22(5), 208–215.
- Berardi, N., Pizzorusso, T., & Maffei, L. (2004). Extracellular matrix and visual cortical plasticity: freeing the synapse. *Neuron*, 44(6), 905–908. <http://doi.org/10.1016/j.neuron.2004.12.008>
- Bezzi, P., Carmignoto, G., Pasti, L., Vesce, S., Rossi, D., Rizzini, B. L., et al. (1998). Prostaglandins stimulate calcium-dependent glutamate release in astrocytes. *Nature*, 391(6664), 281–285. <http://doi.org/10.1038/34651>
- Braddick, O. (1993). Segmentation versus integration in visual motion processing. *Trends in Neurosciences*, 16(7), 263–268.
- Braddick, O., & Atkinson, J. (2011). Development of human visual function. *Vision Research*, 51(13), 1588–1609. <http://doi.org/10.1016/j.visres.2011.02.018>
- Braddick, O., Atkinson, J., Julesz, B., Kropfl, W., Bodis-Wollner, I., & Raab, E. (1980). Cortical binocularity in infants. *Nature*, 288(5789), 363–365.
- Brunnsgaard, H., Pedersen, M., & Pedersen, B. K. (2001). Aging and proinflammatory cytokines. *Current Opinion in Hematology*, 8(3), 131–136.
- Charrier, C., Machado, P., Tweedie-Cullen, R. Y., Rutishauser, D., Mansuy, I. M., & Triller, A. (2010). A crosstalk between $\beta 1$ and $\beta 3$ integrins controls glycine receptor and gephyrin trafficking at synapses. *Nature Neuroscience*, 13(11), 1388–1395. <http://doi.org/10.1038/nn.2645>
- Chavis, P., & Westbrook, G. (2001). Integrins mediate functional pre- and postsynaptic maturation at a hippocampal synapse. *Nature*, 411(6835), 317–321. <http://doi.org/10.1038/35077101>
- Christopoulos, A., & Lew, M. J. (2000). Beyond eyeballing: fitting models to experimental data. *Critical Reviews in Biochemistry and Molecular Biology*, 35(5), 359–391. <http://doi.org/10.1080/10409230091169212>
- Chung, W.-S., Allen, N. J., & Eroglu, C. (2015). Astrocytes Control Synapse Formation, Function, and Elimination. *Cold Spring Harbor Perspectives in Biology*, 7(9), a020370–26. <http://doi.org/10.1101/cshperspect.a020370>

- Chung, W.-S., Clarke, L. E., Wang, G. X., Stafford, B. K., Sher, A., Chakraborty, C., et al. (2013). Astrocytes mediate synapse elimination through MEGF10 and MERTK pathways. *Nature*, 504(7480), 394–400. <http://doi.org/10.1038/nature12776>
- Cingolani, L. A., Thalhammer, A., Yu, L. M. Y., Catalano, M., Ramos, T., Colicos, M. A., & Goda, Y. (2008). Activity-dependent regulation of synaptic AMPA receptor composition and abundance by beta3 integrins. *Neuron*, 58(5), 749–762. <http://doi.org/10.1016/j.neuron.2008.04.011>
- de Vivo, L., Landi, S., Panniello, M., Baroncelli, L., Chierzi, S., Mariotti, L., et al. (2013). Extracellular matrix inhibits structural and functional plasticity of dendritic spines in the adult visual cortex. *Nature Communications*, 4, 1484. <http://doi.org/10.1038/ncomms2491>
- Dickstein, D. L., Weaver, C. M., Luebke, J. I., & Hof, P. R. (2013). Dendritic spine changes associated with normal aging. *Neuroscience*, 251, 21–32. <http://doi.org/10.1016/j.neuroscience.2012.09.077>
- Dityatev, A., & Rusakov, D. A. (2011). Molecular signals of plasticity at the tetrapartite synapse. *Current Opinion in Neurobiology*, 21(2), 353–359. <http://doi.org/10.1016/j.conb.2010.12.006>
- Eng, L. F. (1985). Glial fibrillary acidic protein (GFAP): the major protein of glial intermediate filaments in differentiated astrocytes. *Journal of Neuroimmunology*, 8(4-6), 203–214. [http://doi.org/10.1016/s0165-5728\(85\)80063-1](http://doi.org/10.1016/s0165-5728(85)80063-1)
- Fischer, M., Kaech, S., Knutti, D., & Matus, A. (1998). Rapid actin-based plasticity in dendritic spines. *Neuron*, 20(5), 847–854.
- Fischer, M., Kaech, S., Wagner, U., Brinkhaus, H., & Matus, A. (2000). Glutamate receptors regulate actin-based plasticity in dendritic spines. *Nature Neuroscience*, 3(9), 887–894. <http://doi.org/10.1038/78791>
- Gao, B., Saba, T. M., & Tsan, M.-F. (2002). Role of alpha(v)beta(3)-integrin in TNF-alpha-induced endothelial cell migration. *American Journal of Physiology. Cell Physiology*, 283(4), C1196–205. <http://doi.org/10.1152/ajpcell.00064.2002>
- Haber, M., Zhou, L., & Murai, K. K. (2006). Cooperative astrocyte and dendritic spine dynamics at hippocampal excitatory synapses. *The Journal of Neuroscience : the Official Journal of the Society for Neuroscience*, 26(35), 8881–8891. <http://doi.org/10.1523/JNEUROSCI.1302-06.2006>

- Hatanpaa, K., Isaacs, K. R., Shirao, T., Brady, D. R., & Rapoport, S. I. (1999). Loss of proteins regulating synaptic plasticity in normal aging of the human brain and in Alzheimer disease. *Journal of Neuropathology and Experimental Neurology*, *58*(6), 637–643.
- Hawrylak, N., & Greenough, W. T. (1995). Monocular deprivation alters the morphology of glial fibrillary acidic protein-immunoreactive astrocytes in the rat visual cortex. *Brain Research*, *683*(2), 187–199.
- Hayashi, K., & Shirao, T. (1999). Change in the shape of dendritic spines caused by overexpression of drebrin in cultured cortical neurons. *The Journal of Neuroscience : the Official Journal of the Society for Neuroscience*, *19*(10), 3918–3925.
- Hayashi, K., Ishikawa, R., Ye, L. H., He, X. L., Takata, K., Kohama, K., & Shirao, T. (1996). Modulatory role of drebrin on the cytoskeleton within dendritic spines in the rat cerebral cortex. *Journal of Neuroscience*, *16*(22), 7161–7170.
- Held, R., Birch, E., & Gwiazda, J. (1980). Stereoacuity of human infants. *Proceedings of the National Academy of Sciences*, *77*(9), 5572–5574.
- Henley, J. M., & Wilkinson, K. A. (2013). AMPA receptor trafficking and the mechanisms underlying synaptic plasticity and cognitive aging. *Dialogues in Clinical Neuroscience*, *15*(1), 11–27.
- Henley, J. M., & Wilkinson, K. A. (2016). Synaptic AMPA receptor composition in development, plasticity and disease. *Nature Reviews Neuroscience*, *17*(6), 337–350. <http://doi.org/10.1038/nrn.2016.37>
- Hood, B., Atkinson, J., Braddick, O., & Wattam-Bell, J. (1992). Orientation selectivity in infancy: behavioural evidence for temporal sensitivity. *Perception*, *21*(3), 351–354. <http://doi.org/10.1068/p210351>
- Huang, X., Stodieck, S. K., Goetze, B., Cui, L., Wong, M. H., Wenzel, C., et al. (2015). Progressive maturation of silent synapses governs the duration of a critical period. *Proceedings of the National Academy of Sciences*, *112*(24), E3131–E3140. <http://doi.org/10.1073/pnas.1506488112>
- Huttenlocher, P. R., de Courten, C., Garey, L. J., & Van der Loos, H. (1982). Synaptogenesis in human visual cortex--evidence for synapse elimination during normal development. *Neuroscience Letters*, *33*(3), 247–252.
- Hynes, R. O. (2002). Integrins: bidirectional, allosteric signaling machines. *Cell*, *110*(6), 673–687.

- Imamura, K., Shirao, T., Mori, K., & Obata, K. (1992). Changes of drebrin expression in the visual cortex of the cat during development. *Neuroscience Research*, 13(1), 33–41.
- Ivanov, A., Esclapez, M., & Ferhat, L. (2009). Role of drebrin A in dendritic spine plasticity and synaptic function: Implications in neurological disorders. *Communicative & Integrative Biology*, 2(3), 268–270.
- Jalali, S., del Pozo, M. A., Chen, K., Miao, H., Li, Y., Schwartz, M. A., et al. (2001). Integrin-mediated mechanotransduction requires its dynamic interaction with specific extracellular matrix (ECM) ligands. *Proceedings of the National Academy of Sciences*, 98(3), 1042–1046. <http://doi.org/10.1073/pnas.031562998>
- Jones, E. V., Bernardinelli, Y., Tse, Y. C., Chierzi, S., Wong, T. P., & Murai, K. K. (2011). Astrocytes control glutamate receptor levels at developing synapses through SPARC-beta-integrin interactions. *The Journal of Neuroscience : the Official Journal of the Society for Neuroscience*, 31(11), 4154–4165. <http://doi.org/10.1523/JNEUROSCI.4757-10.2011>
- Kasai, H., Matsuzaki, M., Noguchi, J., Yasumatsu, N., & Nakahara, H. (2003). Structure-stability-function relationships of dendritic spines. *Trends in Neurosciences*, 26(7), 360–368. [http://doi.org/10.1016/S0166-2236\(03\)00162-0](http://doi.org/10.1016/S0166-2236(03)00162-0)
- Kim, H., Kunz, P. A., Mooney, R., Philpot, B. D., & Smith, S. L. (2016). Maternal Loss of Ube3a Impairs Experience-Driven Dendritic Spine Maintenance in the Developing Visual Cortex. *The Journal of Neuroscience : the Official Journal of the Society for Neuroscience*, 36(17), 4888–4894. <http://doi.org/10.1523/JNEUROSCI.4204-15.2016>
- Kobayashi, C., Aoki, C., Kojima, N., Yamazaki, H., & Shirao, T. (2007). Drebrin a content correlates with spine head size in the adult mouse cerebral cortex. *The Journal of Comparative Neurology*, 503(5), 618–626. <http://doi.org/10.1002/cne.21408>
- Lehre, K. P., & Rusakov, D. A. (2002). Asymmetry of Glia near Central Synapses Favors Presynaptically Directed Glutamate Escape. *Biophysical Journal*, 83(1), 125–134. [http://doi.org/10.1016/S0006-3495\(02\)75154-0](http://doi.org/10.1016/S0006-3495(02)75154-0)
- Leventhal, A. G. (2003). GABA and Its Agonists Improved Visual Cortical Function in Senescent Monkeys. *Science*, 300(5620), 812–815. <http://doi.org/10.1126/science.1082874>
- Lewis, T. L., & Maurer, D. (2005). Multiple sensitive periods in human visual development: Evidence from visually deprived children. *Developmental Psychobiology*, 46(3), 163–183. <http://doi.org/10.1002/dev.20055>

- McGeachie, A. B., Cingolani, L. A., & Goda, Y. (2011). Stabilising influence: integrins in regulation of synaptic plasticity. *Neuroscience Research*, 70(1), 24–29. <http://doi.org/10.1016/j.neures.2011.02.006>
- McGee, A. W., Yang, Y., Fischer, Q. S., Daw, N. W., & Strittmatter, S. M. (2005). Experience-driven plasticity of visual cortex limited by myelin and Nogo receptor. *Science*, 309(5744), 2222–2226. <http://doi.org/10.1126/science.1114362>
- Michaud, M., Balardy, L., Moulis, G., Gaudin, C., Peyrot, C., Vellas, B., ... & Nourhashemi, F. (2013). Proinflammatory cytokines, aging, and age-related diseases. *Journal of the American Medical Directors Association*, 14(12), 877-882.
- Michel, A. E., & Garey, L. J. (1984). The development of dendritic spines in the human visual cortex. *Human Neurobiology*, 3(4), 223–227.
- Min, R., & Nevian, T. (2012). Astrocyte signaling controls spike timing-dependent depression at neocortical synapses. *Nature Neuroscience*, 15(5), 746–753. <http://doi.org/10.1038/nn.3075>
- Montana, V. (2004). Vesicular Glutamate Transporter-Dependent Glutamate Release from Astrocytes. *Journal of Neuroscience*, 24(11), 2633–2642. <http://doi.org/10.1523/JNEUROSCI.3770-03.2004>
- Oberheim, N. A., Takano, T., Han, X., He, W., Lin, J. H. C., Wang, F., et al. (2009). Uniquely hominid features of adult human astrocytes. *The Journal of Neuroscience : the Official Journal of the Society for Neuroscience*, 29(10), 3276–3287. <http://doi.org/10.1523/JNEUROSCI.4707-08.2009>
- Park, Y. K., & Goda, Y. (2016). Integrins in synapse regulation. *Nature Publishing Group*, 17(12), 745–756. <http://doi.org/10.1038/nrn.2016.138>
- Perea, G., Yang, A., Boyden, E. S., & Sur, M. (2014). Optogenetic astrocyte activation modulates response selectivity of visual cortex neurons in vivo. *Nature Communications*, 5, 3262. <http://doi.org/10.1038/ncomms4262>
- Pinto, J. G. A., Hornby, K. R., Jones, D. G., & Murphy, K. M. (2010). Developmental changes in GABAergic mechanisms in human visual cortex across the lifespan. *Frontiers in Cellular Neuroscience*, 4, 16. <http://doi.org/10.3389/fncel.2010.00016>
- Pinto, J. G. A., Jones, D. G., Williams, C. K., & Murphy, K. M. (2015). Characterizing synaptic protein development in human visual cortex enables alignment of synaptic age with rat visual cortex. *Frontiers in Neural Circuits*, 9, 3. <http://doi.org/10.3389/fncir.2015.00003>

- Pozo, K., Cingolani, L. A., Bassani, S., Laurent, F., Passafaro, M., & Goda, Y. (2012). β 3 integrin interacts directly with GluA2 AMPA receptor subunit and regulates AMPA receptor expression in hippocampal neurons. *Proceedings of the National Academy of Sciences of the United States of America*, 109(4), 1323–1328. <http://doi.org/10.1073/pnas.1113736109>
- Risher, W. C., Patel, S., Kim, I. H., Uezu, A., Bhagat, S., Wilton, D. K., et al. (2014). Astrocytes refine cortical connectivity at dendritic spines. *eLife*, 3. <http://doi.org/10.7554/eLife.04047>
- Rocha, M., & Sur, M. (1995). Rapid acquisition of dendritic spines by visual thalamic neurons after blockade of N-methyl-D-aspartate receptors. *Proceedings of the National Academy of Sciences*, 92(17), 8026–8030.
- Sarkar, D., & Fisher, P. B. (2006). Molecular mechanisms of aging-associated inflammation. *Cancer Letters*, 236(1), 13–23. <http://doi.org/10.1016/j.canlet.2005.04.009>
- Schummers, J., Yu, H., & Sur, M. (2008). Tuned responses of astrocytes and their influence on hemodynamic signals in the visual cortex. *Science*, 320(5883), 1638–1643. <http://doi.org/10.1126/science.1156120>
- Sekino, Y., Kojima, N., & Shirao, T. (2007). Role of actin cytoskeleton in dendritic spine morphogenesis. *Neurochemistry International*, 51(2-4), 92–104. <http://doi.org/10.1016/j.neuint.2007.04.029>
- Shi, Y., & Ethell, I. M. (2006). Integrins control dendritic spine plasticity in hippocampal neurons through NMDA receptor and Ca²⁺/calmodulin-dependent protein kinase II-mediated actin reorganization. *The Journal of Neuroscience : the Official Journal of the Society for Neuroscience*, 26(6), 1813–1822. <http://doi.org/10.1523/JNEUROSCI.4091-05.2006>
- Shim, K. S., & Lubec, G. (2002). Drebrin, a dendritic spine protein, is manifold decreased in brains of patients with Alzheimer's disease and Down syndrome. *Neuroscience Letters*, 324(3), 209–212.
- Shirao, T., & Obata, K. (1986). Immunochemical homology of 3 developmentally regulated brain proteins and their developmental change in neuronal distribution. *Brain Research*, 394(2), 233–244.
- Siu, C. R., Balsor, J. L., Jones, D. G., & Murphy, K. M. (2015). Classic and Golli Myelin Basic Protein have distinct developmental trajectories in human visual cortex. *Frontiers in Neuroscience*, 9, 138–10. <http://doi.org/10.3389/fnins.2015.00138>

- Siu, C. R., Beshara, S. P., Jones, D. G., & Murphy, K. M. (2017). Development of Glutamatergic Proteins in Human Visual Cortex across the Lifespan. *The Journal of Neuroscience : the Official Journal of the Society for Neuroscience*, 37(25), 6031–6042. <http://doi.org/10.1523/JNEUROSCI.2304-16.2017>
- Takahashi, H., Sekino, Y., Tanaka, S., Mizui, T., Kishi, S., & Shirao, T. (2003). Drebrin-dependent actin clustering in dendritic filopodia governs synaptic targeting of postsynaptic density-95 and dendritic spine morphogenesis. *The Journal of Neuroscience : the Official Journal of the Society for Neuroscience*, 23(16), 6586–6595.
- Takahashi, H., Yamazaki, H., Hanamura, K., Sekino, Y., & Shirao, T. (2009). Activity of the AMPA receptor regulates drebrin stabilization in dendritic spine morphogenesis. *Journal of Cell Science*, 122(Pt 8), 1211–1219. <http://doi.org/10.1242/jcs.043729>
- Trachtenberg, J. T., Chen, B. E., Knott, G. W., Feng, G., Sanes, J. R., Welker, E., & Svoboda, K. (2002). Long-term in vivo imaging of experience-dependent synaptic plasticity in adult cortex. *Nature*, 420(6917), 788–794. <http://doi.org/10.1038/nature01273>
- Wiese, S., Karus, M., & Faissner, A. (2012). Astrocytes as a source for extracellular matrix molecules and cytokines. *Frontiers in Pharmacology*, 3, 120. <http://doi.org/10.3389/fphar.2012.00120>
- Williams, K., Irwin, D. A., Jones, D. G., & Murphy, K. M. (2010). Dramatic Loss of Ube3A Expression during Aging of the Mammalian Cortex. *Frontiers in Aging Neuroscience*, 2, 18. <http://doi.org/10.3389/fnagi.2010.00018>

Chapter 6. Development of synaptic mechanisms in human extrastriate cortex

Abstract

A new study of late development of face perception suggests that human visual areas mature by cortical proliferation rather than synaptic pruning (Gomez et al., 2017). Those methods to detect cortical pruning and proliferation can be insensitive, however, to fine-scale mechanisms that regulate synaptic plasticity and perception. Recently, I studied the development of synaptic proteins in human V1 and found prolonged developmental trajectories of myelin (Siu et al., 2015), GABAergic (Pinto et al., 2010), and glutamatergic expression (Siu et al., 2017) that increase into adulthood. Although cortical areas are thought to develop sequentially, it seems unlikely those proteins will develop even later in extrastriate areas. Thus, some other mechanisms in human extrastriate exist to support plasticity of specialized visual perception. It is time to revisit the model for sequential development in the human visual cortex at the synaptic level, especially during the later stages when higher order visual percepts emerge. I studied the neurobiological basis of synaptic plasticity and visual perception in human extrastriate cortex to help simplify the complex results found in perceptual learning and imaging studies. I quantified synaptic protein expression in postmortem human cortical tissue samples. I measured glutamatergic (GluN1, GluA2, GluN2A, GluN2B, PSD-95), GABAergic (GABA_Aα1, GABA_Aα2, GABA_Aα3, Gephyrin) and pre-synaptic vesicle proteins (Synapsin, Synaptophysin) in postmortem human extrastriate areas V2d and V4 from cases ranging in ages from 8 to 79 years. I characterized multiple trajectories of development across the lifespan that show extrastriate development is not just a sequential transformation of V1 development. In particular, NMDAR development in human V2d and V4 suggests extrastriate has different plasticity than V1 in adulthood.

6.1 Introduction

Human extrastriate development is largely characterized by prolonged maturation of higher-order visual abilities (Bogfjellmo et al., 2014; Germine et al., 2011; Golarai et al., 2010; Hadad et al., 2011; Meier and Giaschi, 2017; Scherf et al., 2011; Segalowitz et al., 2017; Susilo et al., 2013), rapid perceptual learning (Du et al., 2016; Hussain et al., 2009; McMahon and Leopold, 2012; Su et al., 2012), and sequential maturation of cortical areas as highlighted by brain imaging and anatomical studies (Huttenlocher, 1990; Rakic et al., 1986). Activity-dependent synaptic plasticity can also differ between visual cortical areas, for example, an identical stimulation in primate extra striate that elicits long-term potentiation (LTP) produces long-term depression (LTD) in V1 (Murayama et al., 1997). It can be difficult to interpret the development of extrastriate, however, without understanding underlying synaptic mechanisms that enable synaptic plasticity.

Many animal models have shown that glutamatergic and GABAergic synaptic proteins regulate specific receptive field properties, and are labile to experience-dependent plasticity and developmental changes in the visual cortex (Berardi et al., 2003; Beston et al., 2010; Fox and Daw, 1993; Tropea et al., 2009; Yashiro and Philpot, 2008). Some studies have characterized synaptic proteins in human extrastriate cortex (Caspers et al., 2015; Eickhoff et al., 2007; Eickhoff et al., 2008; Williams et al., 2010), yet the question remains, how do molecular mechanisms that support synaptic plasticity in human extrastriate change across development? A large number of synaptic proteins regulate excitatory and inhibitory neurotransmission involved in mediating neuroplasticity. Glutamatergic and GABAergic receptor proteins both play essential roles in the development and plasticity of the visual cortex. The developmental

increase of glutamate receptors AMPAR into NMDAR- dominated silent synapses activates the critical period for plasticity in V1 (Rumpel et al., 1998), and changes the AMPAR: NMDAR ratio that participates in the generation of direction and phase-selective responses of V1 neurons (Rivadulla et al., 2001). AMPAR and NMDAR trafficking require an increase of PSD-95 excitatory scaffolding protein to the post-synaptic membrane (Yoshii et al., 2003) resulting in increased synaptic strength (Chen et al., 2015).

The increase in PSD-95 consolidates silent synapses that end the critical period (CP) for ocular dominance plasticity (ODP) (Huang et al., 2015). Both PSD-95 and GluA2-containing AMPAR are necessary for homeostatic synaptic scaling (Gainey et al., 2009; Sun & Turrigiano, 2011). Furthermore, the insertion of GluA2-containing AMPA receptors is suppressed by the GluN2B subunit of NMDA receptors (NMDAR) (Hall et al., 2007). Immature NMDAR contain GluN2B (2B) and switch to contain GluN2A with visual experience (Monyer et al., 1994; Sheng et al., 1994), that accelerates EPSC kinetics (Flint et al., 1997; Quinlan et al., 1999b), and decreases the probability for LTP (Yoshimura et al., 2003). GluN2A subunit is necessary for the development of orientation selectivity in V1 (Fagiolini et al., 2003), and the developmental GluN2A:GluN2B (2A:2B) switch has been found to regulate the beginning (Roberts and Ramoa, 1999) and the peak (Chen et al., 2000) the critical period for ocular dominance plasticity in animal models. In human V1, the peak of the 2A:2B switch developed until 40 years of age (Siu et al., 2017), suggesting these receptors may also regulate adult plasticity in human.

Development of inhibitory synapses is necessary for establishing the excitatory-inhibitory balance in the visual cortex that initiates the critical period plasticity (Fagiolini and Hensch, 2000), and sharpens receptive field selectivity in V1 (Sato et al., 1995) and extrastriate areas (Yi

et al., 2002). Inhibitory scaffolding protein Gephyrin stabilizes GABA receptors to the postsynaptic membrane (Yu et al., 2007), by binding to GABA_Aα1 (α1), GABA_Aα2 (α2), GABA_Aα3 (α3) subunits directly (Mukherjee et al., 2011; Studer et al., 2006; Tretter et al., 2008). Immature subunits α3 and α2 regulate GABAergic firing in V1, while mature subunit α1 drives cortical plasticity in visual neurons (Fagiolini et al., 2004) and accelerates the decay of the post-synaptic inhibitory current (iPSC) (Heinen et al., 2004). Interestingly, in cat V1 the developmental maturation of GABA_A receptor subunits coincides with the developmental maturation of 2A:2B switch (Chen et al., 2001) both of which are required for experience-dependent plasticity in the visual cortex (Kleinschmidt et al., 1987).

Previously, I have shown the developmental expression of those glutamatergic and GABAergic synaptic proteins across the lifespan in human V1 and found prolonged trajectories that support multiple stages of plasticity in V1 (Pinto et al., 2010; Siu et al., 2017). In addition, I have quantified the pace of human V1 development using a tool for total synaptic maturation -- the sum of 4 highly conserved pre-synaptic vesicle proteins (Synapsin, Synaptophysin) and postsynaptic scaffolding proteins (PSD-95, Gephyrin) that together represent efficient synaptic transmission and synaptic strength. In human V1 this synaptic maturation peaks as a monotonic arc that peaks around 10 years of age (Pinto et al., 2015). According to theories of successive cortical development (Huttenlocher, 1990; Rakic et al., 1986), extrastriate areas mature after primary sensory areas. Thus, I hypothesized the total synaptic maturation in dorsal and ventral extrastriate areas develops later than V1 (Fig 1). The delay in synaptic development may align with the development of higher-order visual perception like global motion and face perception

(Bogfjellmo et al., 2014; Germine et al., 2011; Golarai et al., 2010; Hadad et al., 2011; Meier & Giaschi, 2017; Scherf et al., 2011; Segalowitz et al., 2017; Sur et al., 2013).

To study mechanisms of plasticity in human extrastriate across development, I investigated the expression of a set of pre-synaptic vesicle proteins (Synapsin, Synaptophysin), GABAergic (GABA_Aα1, GABA_Aα2, GABA_Aα3, Gephyrin) and glutamatergic receptor proteins (GluN1, GluA2, GluN2A, GluN2B, PSD-95) in postmortem human extrastriate areas V2d and V4 from cases ranging in age from 8 to 79 years of age. I found neurobiological changes in human V2d and V4 that could support plasticity of higher-order visual perception late into adulthood.

6.2 Materials and Methods

Samples

To study the development of human extrastriate cortex, I used human postmortem cases ranging from 8 to 80 years old obtained from the University of Maryland Brain and Tissue Bank for Developmental Disorders (Baltimore, MD, USA). A total of 14 human cases were chosen with no history of psychological disorder or brain trauma upon death, included 7 males and 7 females, and ranged in ages between 8 and 79 years (Table 1). To control for cortical tissue quality and protein degradation, samples from each case were collected within 24 hours postmortem, 1-cm coronal slices were sectioned and immediately frozen in isopentane and dry ice, then stored at -80°C. Visual cortex samples were taken from the posterior pole of the left hemisphere including both superior and inferior portions of the calcarine fissure. I used gyral and sulcal patterns to dissect cortical samples from presumptive areas for V2d and V4, that represent respective components of the dorsal and ventral visual streams (Desimone and Schein, 1987; Felleman and Van Essen, 1987).

Age (Years)	Age Group	Sex	Post Mortem Interval (Hours)
8.14	Older Children	F	20
8.59	Older Children	F	20
9.13	Older Children	F	20
12.45	Adolescence	M	22
13.27	Adolescence	M	5
15.22	Adolescence	M	16
19.21	Adolescence	F	16
22.98	Young Adults	M	4

Age (Years)	Age Group	Sex	Post Mortem Interval (Hours)
32.61	Young Adults	M	13
50.43	Young Adults	M	8
53.90	Young Adults	F	5
69.30	Older Adults	M	12
71.91	Older Adults	F	9
79.50	Older Adults	F	14

Table 1. Human cases used in this study. For each case showing Age (Years), Age Group, Sex, and Postmortem Interval (hours)

Sample preparation

V2d and V4 tissue pieces (50-100mg) were cut from the dorsal and ventral regions anterior to presumptive V1 of the frozen piece of human visual cortex. Each piece was collected in cold homogenization buffer (1ml buffer: 50 mg tissue, 0.5mM DTT, 2mM EDTA, 2mM EGTA, 10mM HEPES, 10mg/L leupeptin, 100nM microcystin, 0.1mM PMSF, 50mg/L soybean trypsin inhibitor), and homogenized in a glass-glass Dounce hand homogenizer (Kontes, Vineland, NJ, USA). To enrich tissue for quantification of synaptic proteins, I prepared V2d and V4 homogenate samples into synaptosomes that isolate pre- and post-synaptic membrane compartments for more precise measurements of synaptic protein expression (Hollingsworth et al., 1985; Murphy et al., 2014; Quinlan et al., 1999a). To do this I filtered the homogenate sample through a coarse (100 μ g), then fine (5 μ g) pore hydrophilic mesh filter (Millipore, Bedford, MA, USA), centrifuged the sample at 1000 x g for 10 minutes, resuspended in boiling 1% sodium-dodecyl-sulfate (SDS), heated for 10 minutes, and stored at -80°C. To control for

variability of total protein concentration across samples, I used a bicinchoninic acid (BCA) assay (Pierce, ThermoFisher Scientific, Rockford, IL, USA) to measure total protein concentration of each sample in triplicate, and compared these data to a set of protein standards (0.25, 0.5, 1.0, 2.0 mg/ml) (Bovine Serum Albumin (BSA) protein standards, Bio-Rad Laboratories, Hercules, CA, USA). A small amount (3 μ l) of each sample and protein standard was combined into a 1:100 solution with BCA assay solution, pipetted in triplicate into a 96-well microplate, and incubated for 45 minutes in a biological incubator warmed to 45°C to activate the colorimetric reaction. Incubated samples were scanned in a microplate absorbance reader (iMark, Bio-Rad Laboratories, Hercules, CA, USA) to quantify the colorimetric reaction for each sample. Absorbance values for each of the triplications were calculated and averaged for each sample, and compared to a linear equation fit to the protein standards to determine the amount of Laemmli buffer (Cayman Chemical Company, Ann Arbor, MI, USA) and sample buffer (M260 Next Gel Sample loading buffer 4x, Amresco, LLC, Solon, OH, USA) to add to each sample for a final protein concentration of 1 μ g/ μ l. A control sample was made by combining small amounts from each case of V2d and V4 and was run in lane 1 on each blot to normalize across blots. Each antibody was run on each human case multiple times.

Immunoblotting

I used Western blotting to quantify expression of synaptic proteins across different ages of postmortem human cases. Western blotting with human postmortem synaptosome tissue is a valuable method that combines the precision of molecular labeling with the broad interest in human cortical development. I separated synaptosome samples (20 μ g) on 4-20% SDS-

polyacrylamide gels (SDS-PAGE) and then transferred to polyvinylidene difluoride (PVDF-FL) membrane blots (EMD Millipore, Billerica, MA, USA). V2d and V4 samples were randomly assigned across blots within each run. Blots were pre-incubated in blocking buffer (Odyssey Blocking Buffer 1:1 with phosphate buffer saline (PBS)) (Li-Cor Biosciences, Lincoln, NE, USA) for 1 hour, incubated in primary antibody overnight at 4°C using the following primary antibodies: Anti-NMDAR1, 1:4000 (BD Pharmingen, San Jose, CA); Anti-NR2A, 1:1000 (EMD Millipore, Billerica, MA, USA); Anti-NMDAR2B, 1:1000 (EMD Millipore, Billerica, MA, USA); Anti-GluA2, 1:1000 (Invitrogen, Waltham, MA, USA); Anti-PSD95, 1:16000 (EMD Millipore, Billerica, MA, USA); Anti-Gephyrin, Anti-GABA_Aα1; Anti-GABA_Aα2; Anti-GABA_Aα3; Anti-Synapsin; Anti-Synaptophysin. Next, the blots were washed with PBS-Tween (0.05% PBS-T, Sigma, St. Louis, MO, USA) (3x10min), incubated for 2 hours at room temperature with the corresponding IRDye labeled secondary antibody (Anti-Mouse, 1:8000; Anti-Rabbit, 1:10,000; Li-Cor Biosciences, Lincoln, NE, USA), then washed again in PBS-T (3x10min) in preparation for scanning. Blots were re-probed with each antibody after scanning and stripped between antibody incubations with Blot Restore Membrane Rejuvenation kit (EMD Millipore, Billerica, MA, USA).

Imaging & Band Analysis

Blots were scanned using an Odyssey infrared scanner (Li-Cor Biosciences; Lincoln, NE, USA), and bands were visualized by scanning with either red (700nm channel) or green (800nm channel) lasers at optimal intensities. The bands were quantified using densitometry, in which a density profile for each band was calculated by integrating pixel intensity across the area of the

band and subtracting the background. The intensity of each band was divided by the width to control for variations in lane width. Finally, the density of each sample was divided by the density of the control sample run on each blot to normalize for individual blot differences (sample density/control density).

Receptor subunit index

To quantify maturation of synaptic function, I calculated a contrast index for developmentally-regulated pairs of proteins that represent: excitatory-inhibitory (E-I) post-synaptic balance (PSD-95:Gephyrin), pre-synaptic transmission efficiency (Synapsin:Synaptophysin), NMDA:AMPA receptor balance (GluN1:GluA2), GABA_A receptor function (GABA_Aα1:GABA_Aα3, GABA_Aα1:GABA_Aα2) and NMDA subunit development (GluN2A:GluN2B). Index values for each of the pairs range between +1 and -1, where 0 represents equal amounts of both proteins or balanced expression.

Curve fitting and statistical analysis

These results were plotted in 2 ways to analyze changes in expression in human V2d and V4 across the lifespan. First, to describe lifelong trajectories of protein expression, scatter plots were made showing the expression from each run (grey dots) and the expression of the average of the runs (black dots). I used a model-fitting approach (Christopoulos and Lew, 2000) when possible to find the curve of best-fit to describe the trajectory of changes using all of the data across the lifespan, and plotted using KaleidaGraph (Synergy Software, Reading, PA, USA). Many trajectories of development were found best-fit to different proteins and in the 2 different

regions. A quadratic function was fit to the data for Synaptophysin, GluN1, the pre-synaptic index, the GABA_Aα1:GABA_Aα3 index, the GluA2-GluN1 index, and the 2A:2B index in V2d, and to Synaptophysin, GABA_Aα2, GluN2A, Synapsin:Synaptophysin index, GABA_Aα1:GABA_Aα2 index, GABA_Aα1:GABA_Aα3 index, GluA2:GluN1 index and 2A:2B index in V4 ($Y=A+B*\log(x)+C*\log(x)^2$). A Gaussian function was fit to data for PSD-95, Gephyrin, and GABA_Aα1 in V2d, and to GABA_Aα1 in V4 ($Y=A*\exp(-((\log(x/\mu))^2)/(2*(\sigma^2)))+B$). A single-exponential decay function was fit to the data for GABA_Aα3, GluN1, GluA2 in V4 ($Y=A*\exp(-(x/\tau))+B$). A linear function was fit to data for GABA_Aα3 and GluA2 in V2d ($Y=A*x+B$). Finally, a weighted average was used to describe the data for synapsin, GABA_Aα2, GluN2B, GluN2A, PSD-95:Gephyrin index, and GABA_Aα1:GABA_Aα2 index in V2d, and for synapsin, PSD-95, Gephyrin, GluN2B, and the PSD-95:Gephyrin index for V4.

Second, to compare across stages of V2d and V4 development, I binned the cases into four developmental age groups, that have been previously quantified in human V1: childhood (5-11 years), adolescence (12-20 years), young adults (21-55 years), older adults (55+ years) with the mean expression and standard deviation for protein expression in each group plotted using histograms. I used bootstrapping to make statistical comparisons between the age groups for each protein that helped provide robust comparisons of the standard error and confidence intervals for each group. To do this, I used statistical software R (R Core Team (2014), R: A language and environment for statistical computing. R Foundation for Statistical Computing, Vienna, Austria, URL <http://www.R-project.org/>) to calculate the bootstrap population by using the mean and standard deviation of the group being compared to simulate a normally distributed population of 1,000,000 data points. I used this population, distributed around to mean of the

comparison group, to see if observed means of other groups were significantly different. I used a Monte Carlo simulation to randomly sample from the simulated population N (N=the number of cases in the other age groups) times. I ran this simulation 10,000 times to generate an expected distribution for the N number of cases. I calculated confidence intervals for the simulated distribution (95%, 99%, 99.9%) and compared with the observed group means. The groups were considered significantly different when the observed mean was outside the 95% confidence interval ($p < 0.05$, $p < 0.01$, $p < 0.001$). I used bootstrapping to compare protein expression between age groups within an area, and to make pairwise comparisons of protein expression between areas (V2d, V4 and previous results of V1). In addition, I used bootstrapping to compare the mean and standard deviation of each the age groups of indexed proteins to see if the group is significantly different from 0.

All of the V1 data in this paper has been previously published (Pinto et al., 2010; 2015; Siu et al., 2017). In order to compare V1 development to extrastriate development shown in this paper, I adapted the figures of V1 expression for each protein as an inset graph in the upper right corner for each histogram. The black bars in the V1 inset graph are the groups being compared to the V2d and V4 data, whereas the white bars are younger age groups that have been characterized in V1, but are not characterized for V2d and V4.

Sum of total synaptic protein

I calculated the sum of 4 synaptic proteins in V2d and V4 samples: Synapsin, Synaptophysin, PSD-95, and Gephyrin, that together represent all functional synapses in the cortex, and have previously been used as a tool for calculating and translating synaptic age from humans to

rodents (Pinto et al., 2015). I plotted these data against a Gaussian curve fit to the development of this sum of proteins previously reported in human V1 (Pinto et al., 2015). Using this tool for studying synaptic development I predicted the development of dorsal stream area V2d and ventral stream area V4 based on perceptual studies that show dorsal stream visual processing such as global motion perception peaks around mid-adolescence (Bogfjellmo et al., 2014; Bucher et al., 2006; Hadad et al., 2011; Schrauf et al., 1999), while face processing peaks in young adulthood (Golarai et al., 2010; Gomez et al., 2017; Hartshorne and Germine, 2015; Scherf et al., 2011; Segalowitz et al., 2017; Susilo et al., 2013) (Fig 1A). In order to compare development of extrastriate total protein expression to V1, Matlab was used to calculate the 95% confidence interval around the V1 data by calculating 95% confidence interval for future observations (Fig 1B). I also calculated the Chi-square statistic (χ^2) to test if V2d and V4 data points were significantly different from V1 data.

6.3 Results

Postmortem interval

I quantified the effect of postmortem interval (PMI) on total synaptic protein concentration as measured by the BCA assay for synaptosomes of each human sample taken from cortical areas V2d (n=14) and V4a (n=14). There was no significant correlation between PMI and total protein concentration in V2d ($R^2=0.16$, n.s.) or V4 ($R^2=0.05$, n.s.). I binned cases into PMI groups (0-5 hours, 6-12 hours, 13-19 hours, >20 hours), and found no significant difference in total protein concentration between groups in V2d (Kruskal-Wallis=4.65, n.s.) or V4 (Kruskal-Wallis=1.26, n.s.). Since no effect of PMI was found on protein expression, all of samples were included in the following analyses.

Total synaptic development in V2d and V4 follows common trajectory from V1

To test if dorsal (V2d) and ventral (V4) streams of extrastriate follow a common trajectory to V1 synaptic development, I quantified the development of a sum of 4 pre- and post-synaptic proteins (Synapsin, Synaptophysin, PSD-95, Gephyrin). Those proteins maintain basic functional properties of mature excitatory and inhibitory synapses and have been used previously to characterize the pace of human V1 development (Pinto et al., 2015)). Synapsin and synaptophysin regulate pre-synaptic vesicle exo- and endocytosis, respectively (Bahler et al., 1990; Kwon and Chapman, 2011). PSD-95 and Gephyrin are scaffolding proteins for glutamatergic and GABAergic post-synaptic receptors, and regulate synaptic strength in excitatory and inhibitory synapses respectively (Chen et al., 2015; Yu et al., 2007). Together, these proteins account for most of the variance in the development of human V1 homogenate,

and their sum was used as a tool for translating synaptic development between rat and human (Pinto et al., 2015). I plotted the data from V2d and V4 against a Gaussian function previously fit to V1 data (Fig 1), along with predictive models for V2d and V4 synaptic development. I predicted V2d and V4 synaptic development based on perceptual evidence for late development global motion processing and face recognition, respectively (Bogfjellmo et al., 2014; Golarai et al., 2010; Gomez et al., 2017; Hadad et al., 2011; Hartshorne & Germine, 2015; K. Meier & Giaschi, 2017; Scherf et al., 2011; Segalowitz et al., 2017; Susilo et al., 2013) (Fig 1A). I compared the data points for total synaptic proteins in V2d and V4 to the V1 95% confidence interval (CI) for total synaptic data points, and found that 100% of the V2d and V4 points were within the 95% CI of V1 expression (Fig 1B). The development of total synaptic protein in V2d was not significantly different from V1 (Chi-square $X^2 = 5.08$, $p=0.92$), nor was the total synaptic protein development of V4 (Chi-Square $X^2=2.36$, $p=0.99$). These results suggest the trajectory of basic synaptic development in V2d and V4 mature at approximately the same rate, and follow the same developmental profile as V1 (Fig 1).

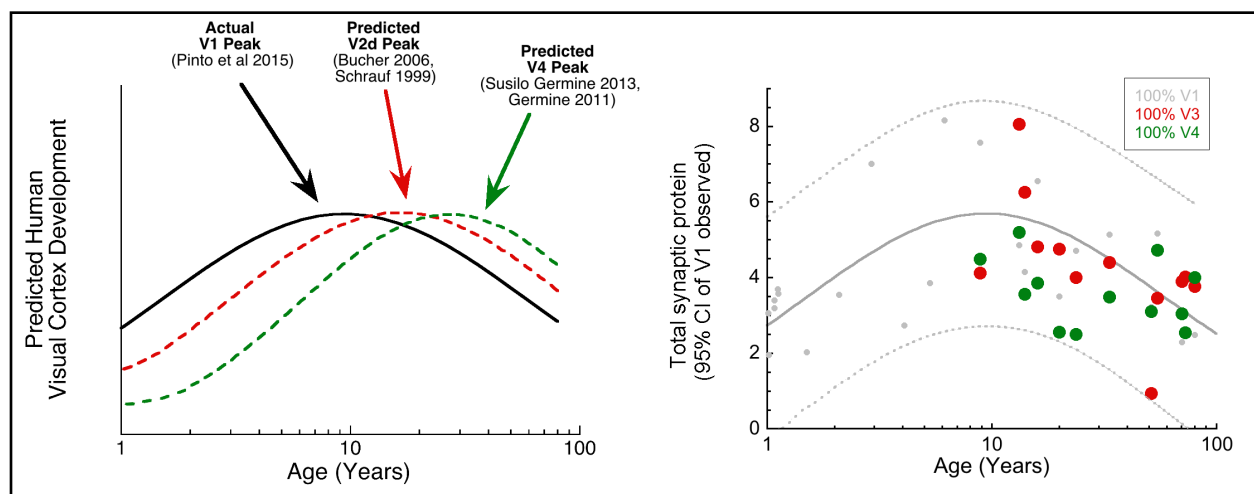


Figure 1 -- The sum of four synaptic proteins (total synaptic protein expression) for V1 (Pinto et al., 2015), V2d, and V4. **A)** Total synaptic protein function for human V1 (Pinto et al., 2015) and

predicted development of human visual extrastriate for V2d (dorsal stream) and V4 (ventral stream). The dorsal stream (V2d) is predicted to develop later than V1 because of evidence for visual perception for biological motion peaking around mid-adolescence. The ventral stream (V4) is predicted to develop later than V1 because of evidence for visual perception for face recognition peaking in early adulthood. **B)** Actual V2d and V4 total synaptic protein data plotted within the 95% confidence interval around the V1 observations. 100% of V2d and V4 points lay within this confidence interval.

Trajectories of individual proteins development differently in extrastriate

To identify the contribution of each protein to the total synaptic protein trajectory, I characterized the individual development of synapsin, synaptophysin, PSD-95 and gephyrin, and analyzed the results using three types of analysis. First, using a scatterplot to show all data points with either a model of best fit to the data or described using a weighted average. Second, I compared protein expression across developmental age groups (childhood (5-11 years), adolescence (12-20 years), young adults (21-55 years), older adults (>55 years)). Third, protein expression in extrastriate areas V2d and V4 were compared against protein expression in the same age group in previously published human V1 (Pinto et al., 2015). I also quantified the relative balance between pre-synaptic (Synapsin:Synaptophysin) and post-synaptic (PSD-95:Gephyrin) pairs.

Synapsin does not change across development in V2d or V4

Synapsin clusters and traffics pre-synaptic vesicles for exocytosis of readily releasable pools of neurotransmitter (Bahler et al., 1990). Synapsin expression did not change across development in either V2d or V4, described using a weighted average (Fig 2a, 3a). There was no significant difference in synapsin expression across age groups (Fig 2b, 3b) that is similar to the same age groups in V1 (Upper inset, Fig 2b, 3b). Synapsin expression in V2d is significantly lower in childhood, adolescence, and young adults compared to V1 expression ($p < 0.001$) (Upper inset,

Fig 2b) and higher than young adults and older adults in V4 ($p < 0.01$). Synapsin expression in V4 was significantly lower than V1 expression across all age groups ($p < 0.001$) (Fig 3b).

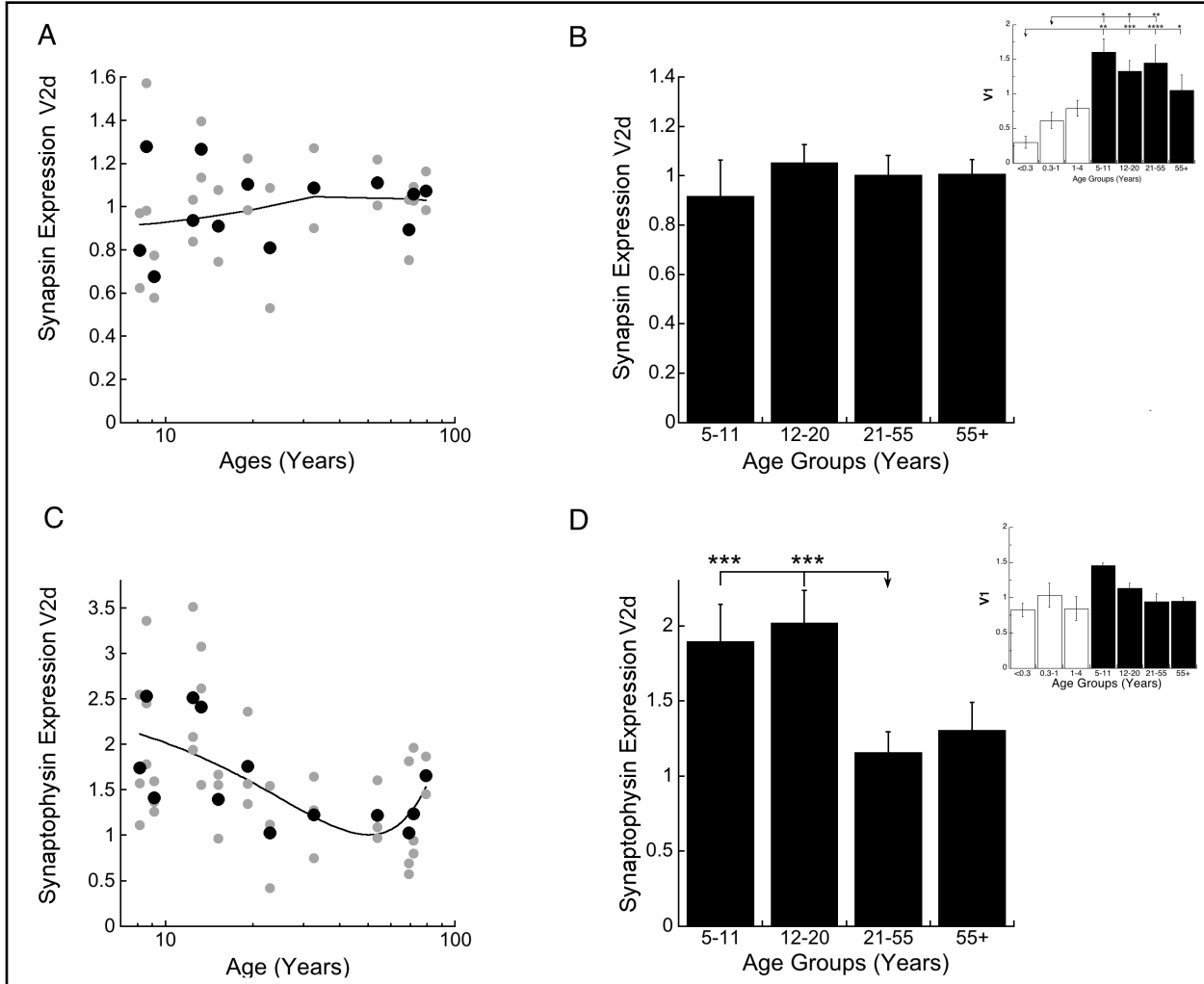


Figure 2 -- Development of Synapsin and Synaptophysin expression in human V2d. **A)** Scatterplot of Synapsin across the lifespan fit with a weighted function. **B)** Age-binned results for Synapsin expression in V2d. Upper inset, V1 Synapsin age group data from (Pinto et al., 2015) **C)** Scatterplot of synaptophysin across the lifespan fit with an inverted quadratic function ($R^2=0.25$, $p < 0.05$) that reached a local minima around 50 years. **D)** Age-binned results for synaptophysin expression in V2d. Upper inset, V1 Synaptophysin data from (Pinto et al., 2015). For the scatterplots, grey dots represent each run and black dots represent the average across the runs for each case. Age is plotted on a logarithmic scale. For histograms, protein expression was binned into age groups (5-11 years, older children; 12-20 years, adolescence; 21-55 years, young adulthood; 55+, older adults), showing the mean and SEM. * $p < 0.05$, ** $p < 0.01$, *** $p < 0.001$.

Synaptophysin shows loss of expression in adulthood in both V2d and V4

Synaptophysin regulates rapid kinetics of endocytosis and vesicle recycling during and after synaptic activity (Kwon and Chapman, 2011). Development of synaptophysin expression was similar in V2d and V4 (Pearson's Correlation, $R^2=0.31$, $p<0.05$). In V2d and V4, there was high synaptophysin expression in childhood that decreased significantly to minimum expression at 50 years of age, well-fit by an inverted quadratic function in V2d ($R^2=0.25$, $p<0.05$) (Fig 2c) and V4 ($R^2=0.16$, $p<0.05$) (Fig 3c). Across age groups, synaptophysin expression in V2d was decreased significantly lower in young adults from childhood ($p<0.001$) and adolescence ($p<0.001$) and remained unchanged in older adults (Fig 2d). Across age groups in V4 showed a similar pattern, where synaptophysin expression was higher in adolescence ($p<0.05$) and childhood ($p<0.01$) compared to young adults and remained low in older adults (Fig 3d). Synaptophysin developmental expression across these age groups in V2d was similar to V1, but V2d synaptophysin expression in adolescence was nearly double that expression in V1 adolescence ($p<0.001$) (Upper inset, Fig 2d). The age groups of synaptophysin expression in V4 were not significantly different than expression in V1 (Upper inset, Fig 3d). Synaptophysin expression in V2d, however, was nearly double the expression of synaptophysin in V4 across all age groups ($p<0.001$).

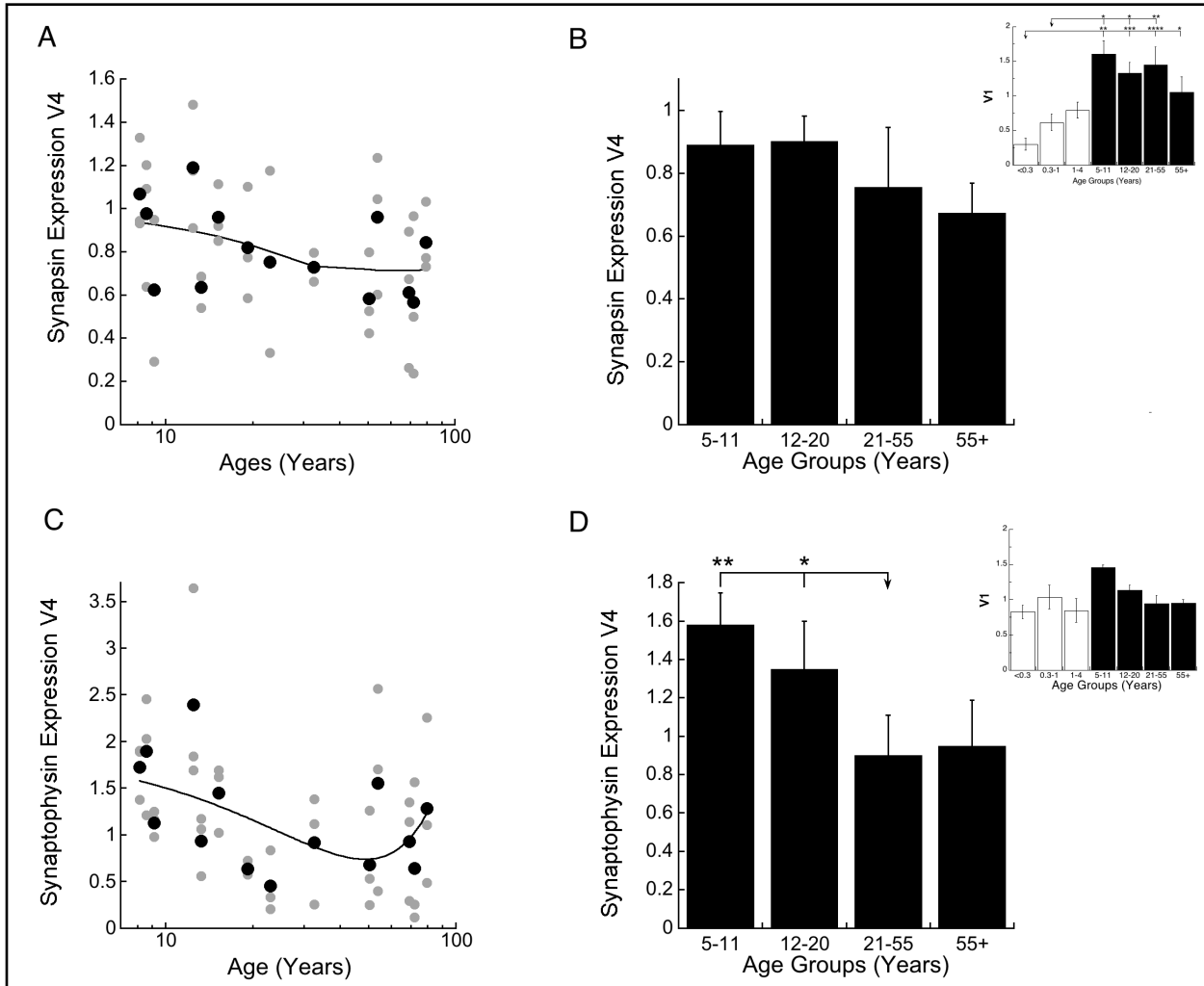


Figure 3 -- Development of Synapsin and Synaptophysin expression in human V4. **A)** Scatterplot of Synapsin across the lifespan fit with a weighted function. **B)** Age-binned results for Synapsin expression in V4. Upper inset, V1 Synapsin age group data from (Pinto et al., 2015). **C)** Scatterplot of synaptophysin across the lifespan fit with an inverted quadratic function ($R^2=0.16$, $p<0.05$) that reached a local minima around 50 years. **D)** Age-binned results for synaptophysin expression in V4. Upper inset, V1 Synaptophysin age group data from (Pinto et al., 2015). Scatterplot, histogram and significance levels plotted using the conventions described in Figure 2.

Pre-synaptic transmission balance delayed in V2d and V4

To capture the maturation of pre-synaptic function across development, I calculated the relative index between synapsin and synaptophysin in V2d and V4 (Fig 4). In V2d, there was more

synaptophysin in childhood that shifts to balanced expression around 33 years of age, completely favored synapsin by 45 years, then shifted back toward more synaptophysin in older adults, a trajectory well-fit by a quadratic function ($R^2=0.26$, $p<0.01$) (Fig 4a). Compared across age groups, there was a significant shift in expression from children ($p<0.001$) and adolescence ($p<0.01$) compared to balanced expression in young and older adults (Fig 4b). Synapsin-synaptophysin index in V2d follows a similar profile previously found in V1 that shifts from more synaptophysin to balanced expression across development (Pinto et al., 2015), but the shift to balanced expression is delayed in V2d by about 32 years (Upper inset, Fig 4b). There was significantly more synaptophysin in these 4 age groups of V2d development (childhood ($p<0.001$), adolescence ($p<0.001$), young adults ($p<0.01$), older adults ($p<0.001$)) compared to V1 that already shifted to balanced expression by childhood (Fig 4b).

Development of the pre-synaptic index in V4 was not significantly different than V2d (Pearson's Correlation, $R^2=0.62$, $p<0.01$). In V4, there was more synaptophysin in childhood that shifted to balanced expression around 26 years, peaks around 45 years, and remains balanced in older adults, well-fit by a quadratic function ($R^2=0.13$, $p<0.05$) (Fig 4c). Across age groups there was significantly more synaptophysin in childhood ($p<0.001$) compared to balanced expression in young adults ($p<0.01$), adolescence and older adults (Fig 4d). The pre-synaptic index in V4 follows a similar profile to V1 that shifts from more synaptophysin to synapsin across development (Pinto 2015), but the shift is delayed in V4 by about 25 years (Upper inset, Fig 4d). There was significantly more synaptophysin across all age groups in V4 (childhood ($p<0.001$), adolescence ($p<0.001$), young adults ($p<0.01$), older adults ($p<0.05$)) compared to V1, that already shifted to balanced expression by childhood (Upper inset, Fig 4d).

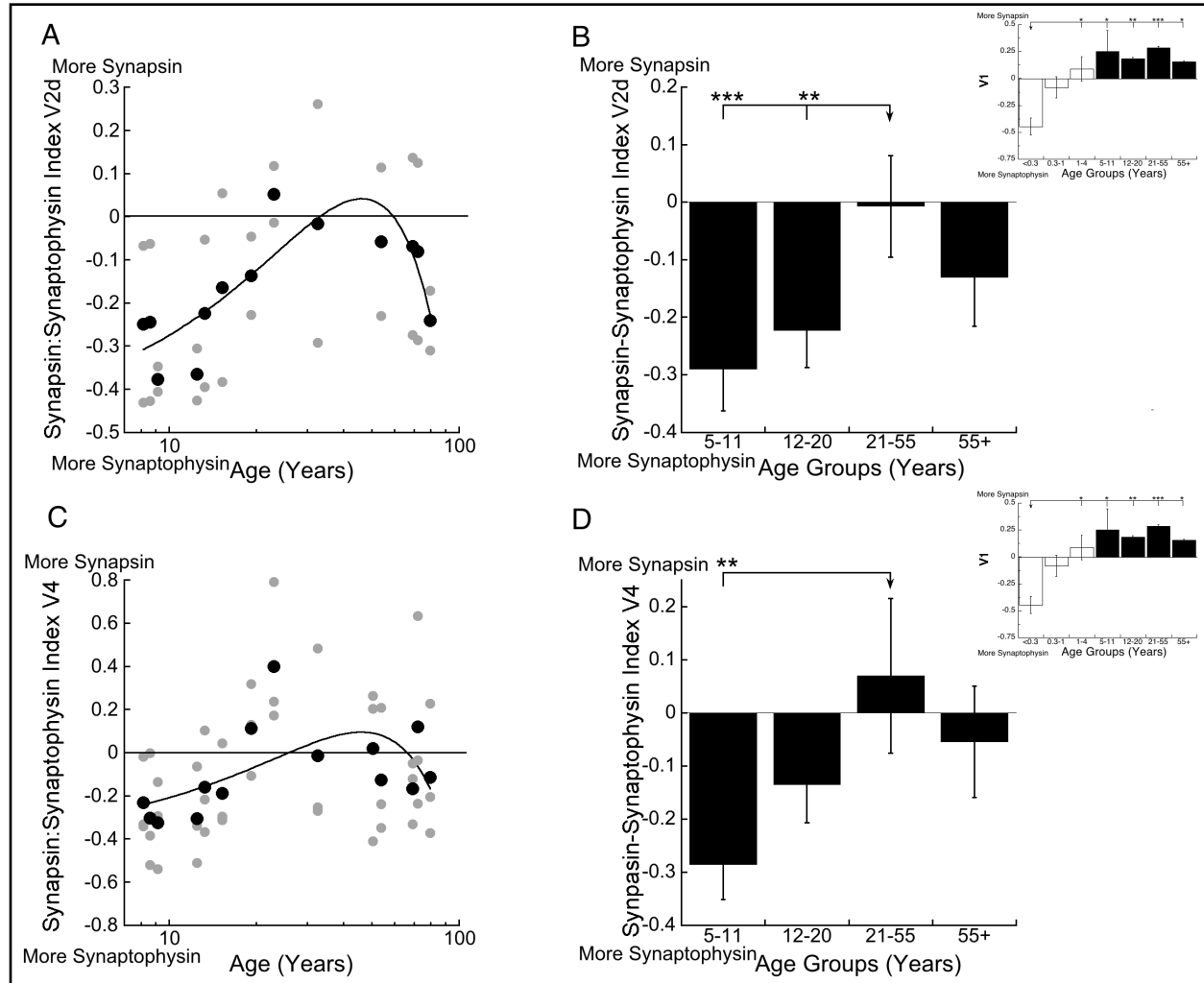


Figure 4 -- Development of Synapsin:Synaptophysin balance (Synapsin-Synaptophysin)/(Synapsin+Synaptophysin) in human V2d and V4 **A)** Scatterplot of Synapsin:Synaptophysin balance across the lifespan in V2d, well-fit by a quadratic equation ($R^2=0.26$, $p<0.01$) that peaked around 45 years. **B)** Age-binned results for Synapsin:Synaptophysin balance expression in V2d. Upper inset, V1 age group data from (Pinto et al., 2015). **C)** Scatterplot of Synapsin:Synaptophysin balance across the lifespan in V4, well-fit by a quadratic equation ($R^2=0.13$, $p<0.05$) that peaked around 45 years. **D)** Age-binned results for Synapsin:Synaptophysin balance expression in V4. Upper inset, V1 age group data from (Pinto et al., 2015) Scatterplot, histogram and significance levels plotted using the conventions described in Figure 2.

Peak of PSD-95 expression is delayed, Gephyrin in V2d is similar to V1

PSD-95 is the excitatory scaffolding protein that binds NMDA and AMPA receptors to the postsynaptic membrane and is necessary for synaptic scaling (Sun and Turrigiano, 2011). Peak expression of PSD-95 is linked with maturation of silent synapses that ends the critical period in V1 (Huang et al., 2015) and is correlated with synaptic maturation and strength (Chen et al., 2015). In V2d, PSD-95 expression had a bump in expression in adolescence that peaks around 14 years, then declines into adulthood, and was well-fit by a Gaussian function ($R^2=0.22$, $p<0.01$) (Fig 5a). Across age groups, expression was high in adolescence that decreased by about 20% in young adults ($p<0.01$) and remained low in older adults (Fig 5b). This trajectory is similar to PSD-95 expression in human V1 synaptosome (Upper inset, Fig 5b) and homogenate (Pinto et al., 2015) samples. The peak in V2d, however, is delayed relative to V1 by about 5 years. There is significantly more PSD-95 in adolescence in V2d compared to V1 ($p<0.001$). In addition, PSD-95 expression is higher in V2d than V4 in young children ($p<0.01$) and adolescence ($p<0.001$), and similar expression between the areas in later years.

Gephyrin is a post-synaptic inhibitory scaffolding protein that binds GABA_A receptors, is required for stability of GABAergic synapses (Yu et al., 2007), and regulates homeostatic changes in inhibitory transmission (Tyagarajan and Fritschy, 2014). In V2d, Gephyrin expression was high in childhood and decreased across the lifespan, a trajectory well-fit by a Gaussian function ($R^2=0.10$, $p<0.05$) (Fig 5c). Across age groups, gephyrin expression was high in childhood and decreased significantly in young adults ($p<0.01$) (Fig 5d). The trajectory and timing of gephyrin expression in V2d are similar to that found in V1 (Upper inset, Fig 5d), but magnitude of gephyrin expression in V2d is half the expression found in V1 in childhood

($p < 0.001$), adolescence ($p < 0.001$), and young adults ($p < 0.001$) (Upper inset, Fig 5d). Gephyrin expression was significantly higher in V2d in adolescence compared to V4 ($p < 0.001$), but similar expression in all other age groups.

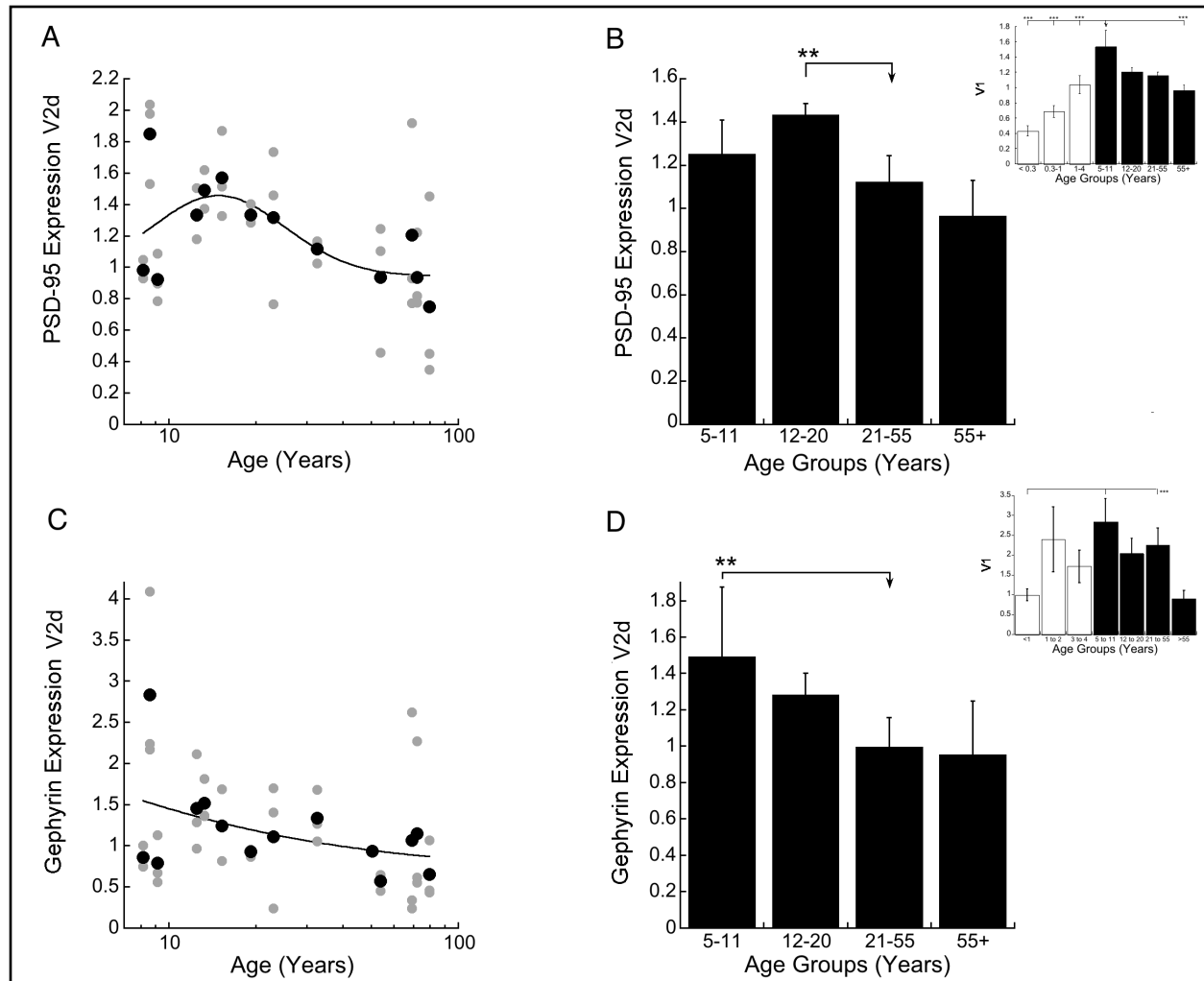


Figure 5 -- Development of PSD-95 and Gephyrin expression in human V2d. **A)** Scatterplot of PSD-95 across the lifespan fit with a Gaussian function ($R^2=0.22$, $p < 0.01$) that peaked around 14 years of age. **B)** Age-binned results for PSD-95 expression in V2d. Upper inset, V1 age group data from (Siu et al., 2017). **C)** Scatterplot of Gephyrin across the lifespan fit with a Gaussian function ($R^2=0.10$, $p < 0.05$). **D)** Age-binned results for Gephyrin expression in V2d. Upper inset, V1 age group data from (Pinto et al., 2010). Scatterplot, histogram and significance levels plotted using the conventions described in Figure 2.

PSD-95 no peak in V4, Gephyrin in V4 similar to V1

In V4, PSD-95 expression did not show significant change across the lifespan. Those results are described by a weighted function that is relatively flat across development (Fig 6a). Comparison across age groups showed no significant change across the lifespan (Fig 6b). Due to the absence of a peak in PSD-95 expression in V4, this trajectory is different from PSD-95 expression across the same ages in V1 (Upper inset, Fig 6b). For example, there is significantly lower PSD-95 expression in V4 and V2d in childhood ($p < 0.001$) and adolescence ($p < 0.001$) compared to V1 expression (Upper inset, Fig 6b). Gephyrin expression in V4 decreased across the lifespan, like in V2d, but the high amounts of variability across the lifespan reduced the goodness-of-fit, so I described this data with a weighted function (Fig 6c). Across age groups, there was slightly higher gephyrin expression in childhood compared to other age groups, though this peak was not significant (Fig 6d). This trajectory is similar to previously identified gephyrin expression in the same age span in V1 samples, but with significantly lower expression by over half in V4 compared to V1 childhood, adolescence, and young adults ($p < 0.001$) (Upper inset, Fig 6d).

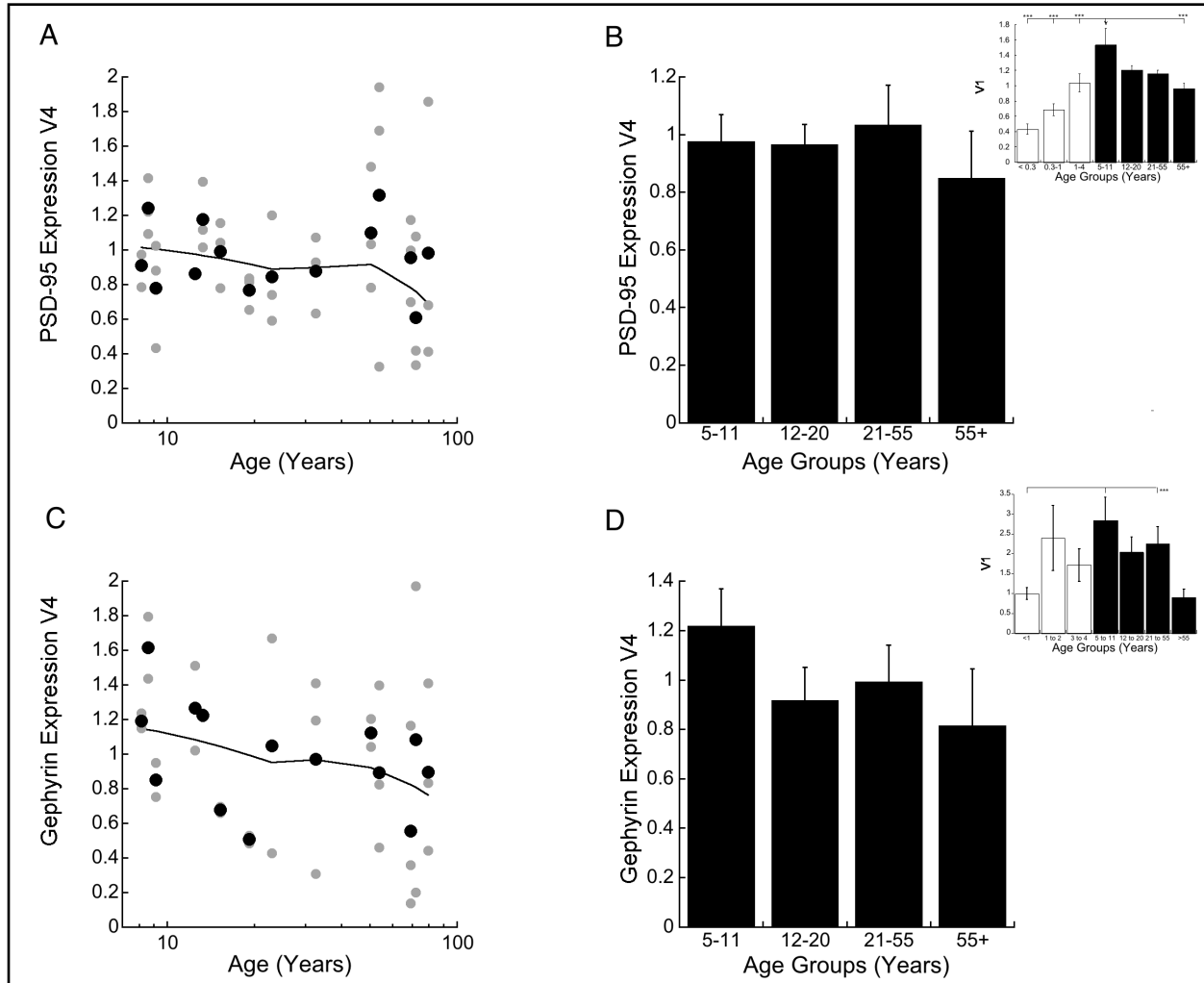


Figure 6 -- Development of PSD-95 and Gephyrin expression in human V4. **A)** Scatterplot of PSD-95 across the lifespan fit with a weighted function. **B)** Age-binned results for PSD-95 expression in V4. Upper inset, V1 age group data from (Siu et al., 2017). **C)** Scatterplot of Gephyrin across the lifespan fit with a weighted function. **D)** Age-binned results for Gephyrin expression in V4. Upper inset, V1 age group data from (Pinto et al., 2010). Scatterplot, histogram and significance levels plotted using the conventions described in Figure 2.

Excitatory-Inhibitory balance in V2d and V4

To capture the maturation of post-synaptic excitatory-inhibitory (E-I) balance across development, I calculated the relative index between PSD-95 and Gephyrin (Fig 7). In V2d, PSD-95:Gephyrin relative expression was balanced across the lifespan that was described by a

weighted average (Fig 7a). Across age groups, there were no significant differences in expression (Fig 7b). The profile of PSD-95:Gephyrin development in V2d is similar to that found in V1 (Upper inset, Fig 7b) that shifts rapidly by 5 months of age, then remains balanced across the lifespan, however there is significantly more PSD-95 in V2d in adolescence ($p < 0.001$) and young adulthood ($p < 0.001$) compared to V1.

The relative balance of PSD-95:Gephyrin in V4 showed a trend to shift from balanced expression to more PSD-95 around adolescence but was not well-fit to a function, so I described the data using a weighted average (Fig 7c). Across age groups, there was a significant shift from balanced expression in children to more PSD-95 in adolescence ($p < 0.001$) then returned to balanced expression in adulthood (Fig 7d). Although significant, the magnitude of this shift is very small compared to V1 where expression is considered balanced at this age (Upper inset, Fig 7d). Compared to V1, there is significantly more Gephyrin in childhood ($p < 0.05$), that shifts to significantly more PSD-95 in adolescence ($p < 0.001$) and young adults ($p < 0.05$) in V4 (Upper inset, Fig 7d). There is significantly more PSD-95 in V4 in adolescence and adulthood compared to V1, however, there is no significant difference between PSD-95:Gephyrin development between V2d and V4.

Together, the sum of those pre- and post-synaptic proteins in V2d and V4 share a common trajectory with V1 (Fig 1b), but individually those proteins provide some evidence for slight delays in dorsal and ventral stream development (as predicted in Fig 1a). This suggests that other synaptic proteins in extrastriate contribute to a developmental delay of higher-order visual areas. I tested this idea by quantifying the development of a subset of GABAergic and glutamatergic

synaptic proteins linked to regulation of synaptic plasticity and function in the visual cortex, and that have been previously quantified in human V1 to compare across regions.

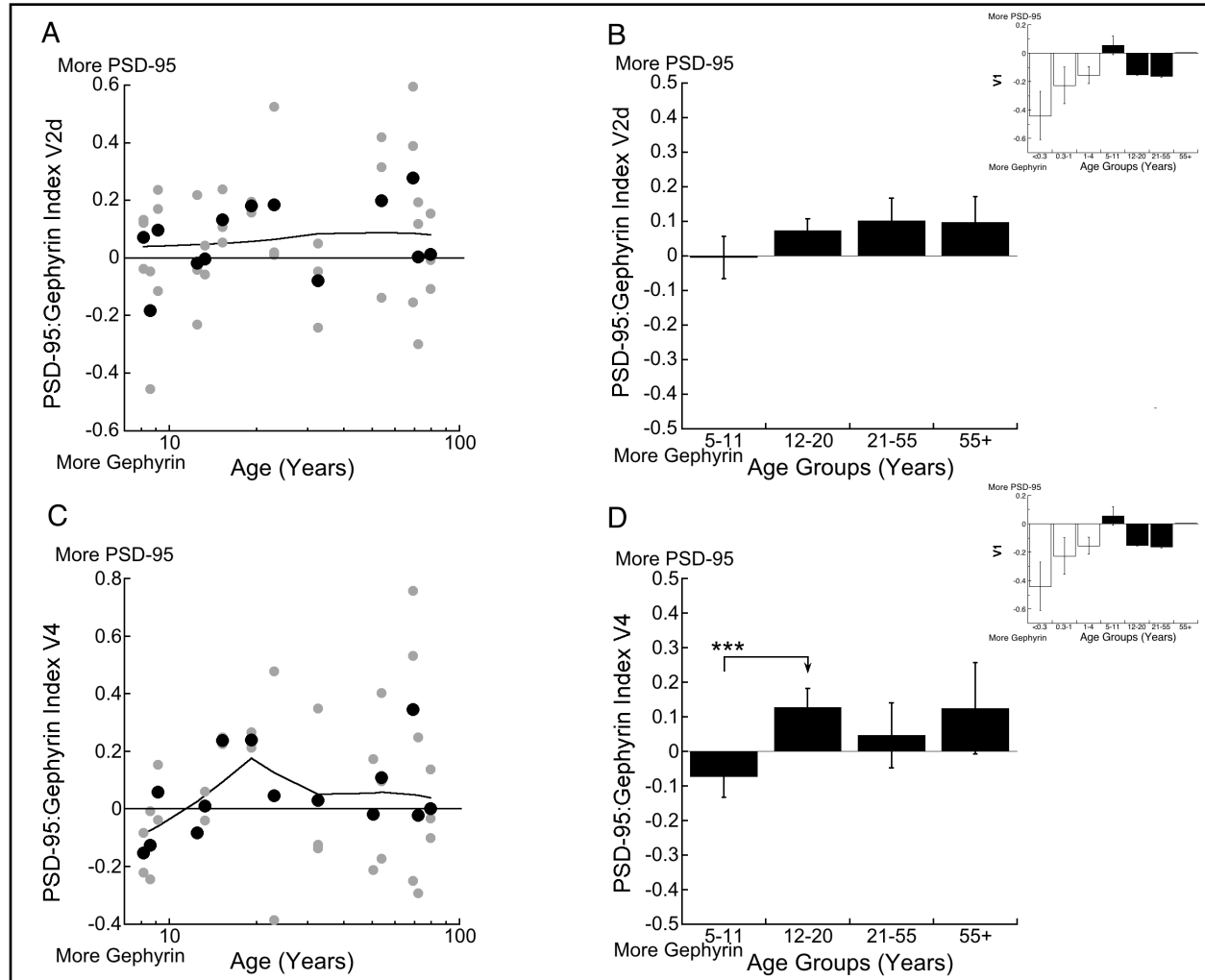


Figure 7 -- Development of PSD-95:Gephyrin balance (PSD-95-Gephyrin)/(PSD-95+Gephyrin) in human V2d and V4 **A)** Scatterplot of PSD-95:Gephyrin balance across the lifespan in V2d fit by a weighted function **B)** Age-binned results for PSD-95:Gephyrin balance expression in V2d. Upper inset, V1 age group data from (Pinto et al., 2015). **C)** Scatterplot of PSD-95:Gephyrin balance across the lifespan in V4 fit by a weighted function **D)** Age-binned results for PSD-95:Gephyrin balance expression in V4. Upper inset, V1 age group data from (Pinto et al., 2015). Scatterplot, histogram and significance levels plotted using the conventions described in Figure 2.

GABA_A receptor subunit development in V2d and V4

To characterize development of inhibitory synapses in extrastriate cortex, I studied expression of 3 GABA_A receptor subunits, GABA_Aα1 (α1), GABA_Aα2 (α2), GABA_Aα3 (α3) in V2d and V4 across the lifespan. Visual experience shifts the GABA_A subunit composition from α3 to α1, that increases the kinetics of the receptor, increases the magnitude of IPSCs (Heinen et al., 2004), drives cortical plasticity (Fagiolini et al., 2004), and increases binding affinity to GABA (Pritchett et al., 1989), while α2 regulates GABAergic cell firing (Fagiolini et al., 2004).

GABA_Aα1 peak delayed significantly in V2d

In V2d, GABA_Aα1 expression was low in childhood, increased to peak expression around 50 years, then decreased again, a profile well-fit by a quadratic function ($R^2=0.21$, $p<0.05$) (Fig 8a). Across age groups, GABA_Aα1 expression was high in young adults compared to expression in childhood ($p<0.001$), adolescence (12-20 years) ($p<0.01$) and older adults ($p<0.01$) (Fig 8b). This profile is similar expression in V1 (Upper inset, Fig 8b), but the timing of the peak is delayed by about 36 years in V2d. Interestingly, the magnitude of GABA_Aα1 expression was significantly lower in all age groups in V2d compared to V1 ($p<0.001$) (Upper inset, Fig 8b), and higher in expression in adolescence compared to V4 ($p<0.001$).

GABA_Aα2 no change across V2d development

In V2d, GABA_Aα2 showed no significant changes across the lifespan, described by a weighted average (Fig 8c). Across age groups, GABA_Aα2 showed a trend to increase in expression from adolescence to older adults but there was no significant differences between groups (Fig 8d). These results were similar to the same age groups in human V1 (Upper inset, Fig 8d), where

there was no change in expression of GABA_Aα2 after 10 years of age (Pinto et al., 2010). The magnitude of GABA_Aα2 expression over twice as high in V2d compared to V1 across all age groups. ($p < 0.01$) (Upper inset, Fig 8d), and compared to V4 in adolescence ($p < 0.001$), young adulthood ($p < 0.001$) and older adulthood ($p < 0.001$).

GABA_Aα3 declines across V2d development, unlike V1

In V2d, GABA_Aα3 expression declined from childhood to older adults, that was well-fit by a linear function ($R^2 = 0.32$, $p < 0.001$) (Fig 8e). Across age groups, GABA_Aα3 expression was not different across children, teens, or young adults, but there was a significant decrease by nearly 50% in older adults ($p < 0.001$) (Fig 8f). This profile is different from the GABA_Aα3 trajectory in V1 (Upper inset, Fig 8f), where there is no change in GABA_Aα3 expression across the lifespan (Pinto et al., 2010). GABA_Aα3 expression in V2d is greater than in V1 in young adults ($p < 0.01$), but significantly lower than in V1 in older adults ($p < 0.001$) by about 50% compared to V1 (Upper inset, Fig 8f). There is significantly more GABA_Aα3 in V2d than in V4 in adolescence ($p < 0.001$), but all other age groups have similar expression.

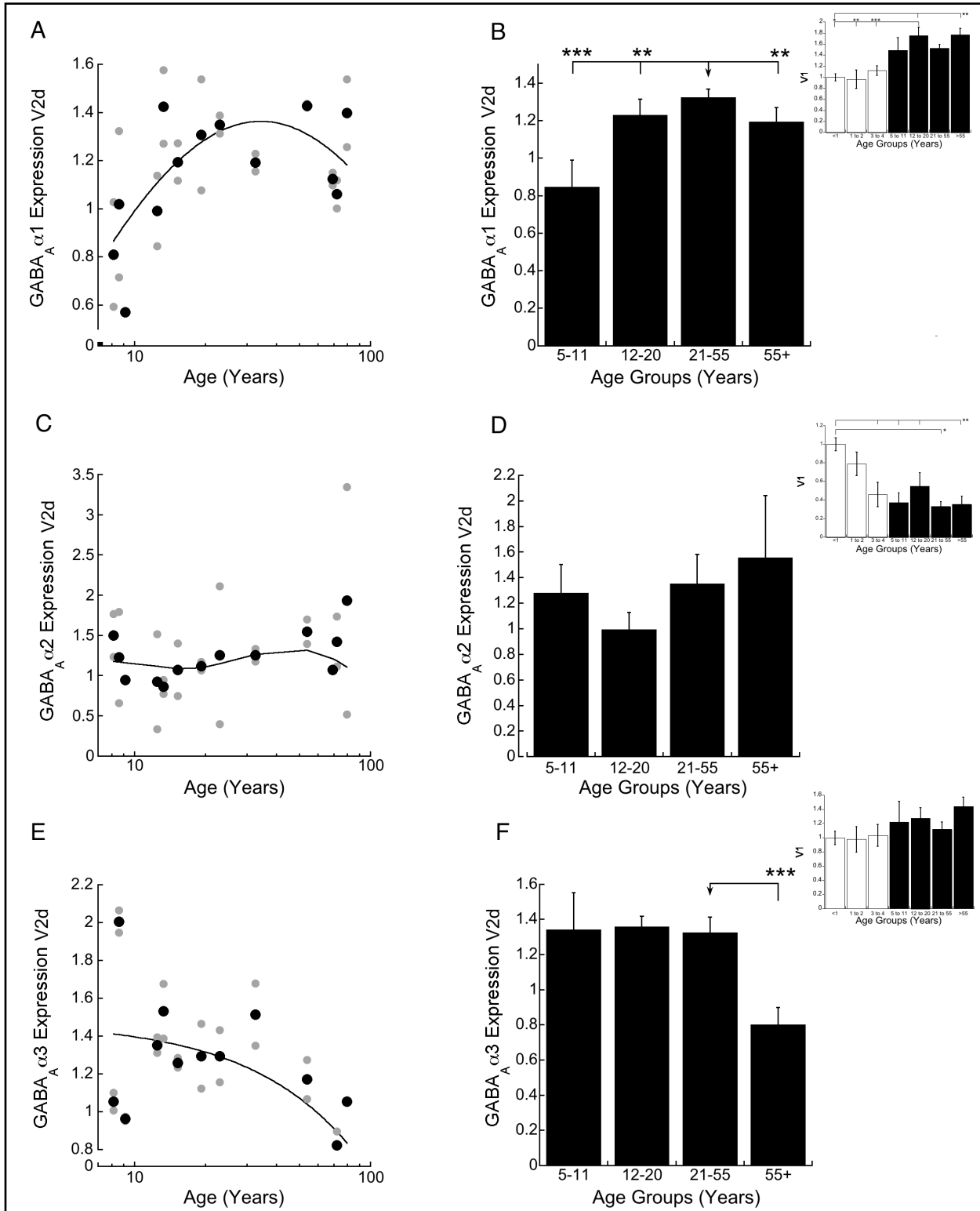


Figure 8 -- Development of GABA_Aα1, GABA_Aα2, and GABA_Aα3 expression in human V2d. **A)** Scatterplot of GABA_Aα1 across the lifespan fit with a gaussian function ($R^2=0.18$, $p<0.05$) that peaked around 45 years **B)** Age-binned results for GABA_Aα1 expression in V4. **C)** Scatterplot of GABA_Aα2 across the lifespan fit with a weighted function **D)** Age-binned results

for GABA_Aα2 expression in V2d. **E)** Scatterplot of GABA_Aα3 across the lifespan fit with a linear function ($R^2=0.32$, $p<0.001$) **(F)** Age-binned results for GABA_Aα3 in V2d. Scatterplot, histogram and significance levels plotted using the conventions described in Figure 2. Histograms in upper right inset show V1 GABA data previously published in (Pinto et al., 2010).

GABA_Aα1 peak delayed significantly in V4

In V4, GABA_Aα1 expression slowly increased into adulthood that was described by a weighted average (Fig 9a). Across age groups, GABA_Aα1 expression was significantly higher in young adults ($p<0.001$) and older adults ($p<0.05$) compared to children (5-11 years) (Fig 9b). Compared to V1, there is a similar increase in development of GABA_Aα1 expression, but the peak of GABA_Aα1 in V4 is delayed by about 30 years (Upper inset, Fig 9b). GABA_Aα1 expression is significantly lower in V4 compared to V1 in childhood ($p<0.001$), adolescence ($p<0.001$), and older adults ($p<0.001$) (Upper inset, Fig 9b).

GABA_Aα2 delayed loss in V4

In V4, GABA_Aα2 expression was high in childhood then decreased until about 45 years of age, well-fit by an inverted quadratic function ($R^2=0.27$, $p<0.01$) (Fig 9c). Across age groups, GABA_Aα2 expression was significantly lower in young adults than in childhood ($p<0.001$) (Fig 9d). This profile is similar to that of GABA_Aα2 expression previously found in V1 (Upper inset, Fig 9d), but the timing of the loss in expression is delayed by about 35 years in V4. In addition, the magnitude of GABA_Aα2 expression is higher in V4 compared to V1 across all age groups ($p<0.05$) (Upper inset, Fig 9d).

GABA_A α 3 declines across V4 development, unlike V1

In V4, GABA_A α 3 expression was high in childhood and decreased rapidly to adult-like levels in adolescence, well-fit by an exponential decay function ($R^2=0.25$, $p<0.01$) (Fig 9e). Across age groups, GABA_A α 3 expression was significantly decreased in older adults from children by half ($p<0.001$) and from adolescence and young adults by about a third ($p<0.001$) (Fig 9f). This profile is different to that found in V1 (Upper inset, Fig 9f), as there is no loss in expression after childhood in V1. There is significantly lower expression of GABA_A α 3 in V4 in adolescence (12-20 years) ($p<0.001$) and older adults ($p<0.001$) compared to V1 (Upper inset, Fig 9f).

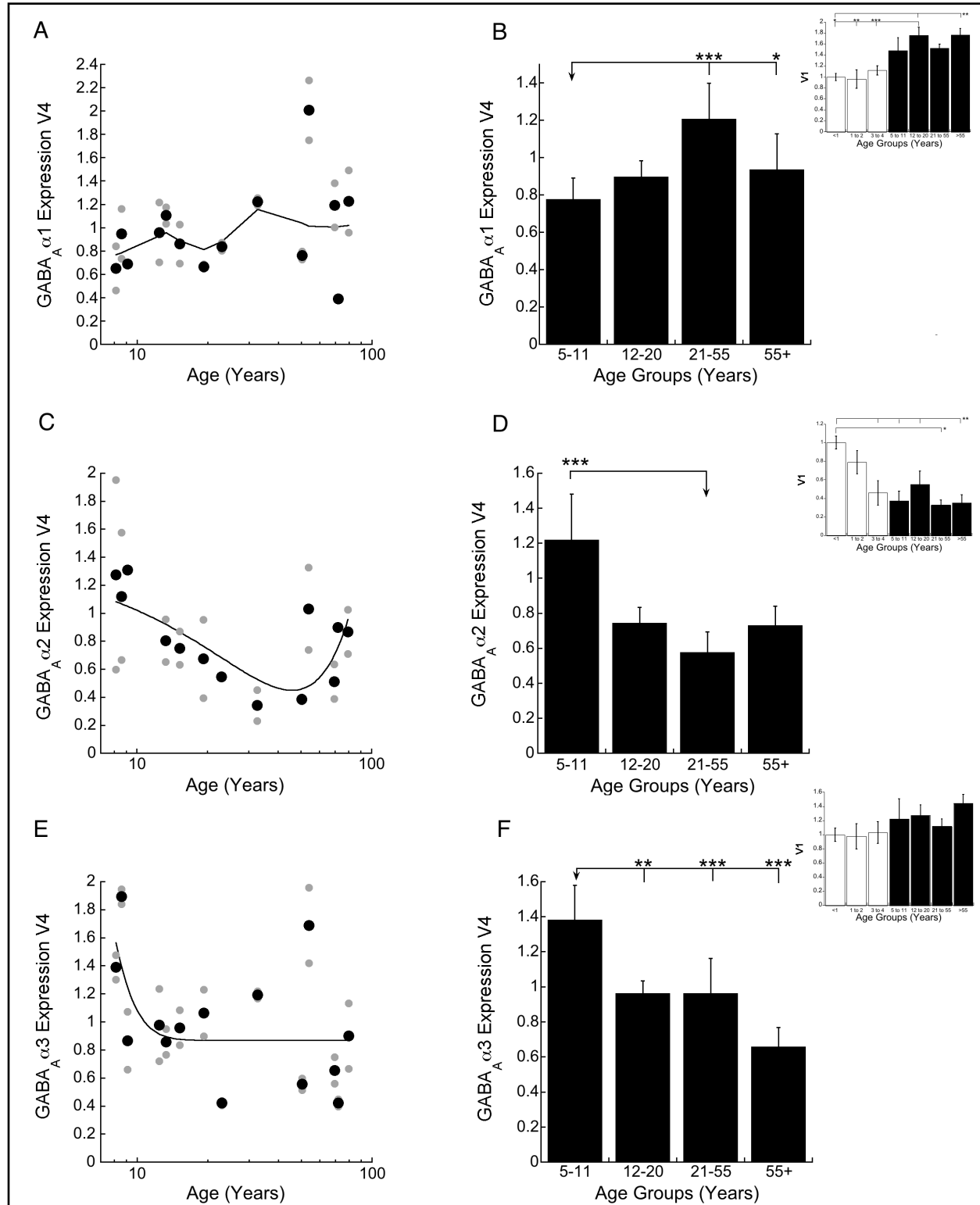


Figure 9 -- Development of GABA_Aα1, GABA_Aα2, and GABA_Aα3 expression in human V4. **A**) Scatterplot of GABA_Aα1 across the lifespan described using a weighted average. **B**) Age-binned results for GABA_Aα1 expression in V2d. **C**) Scatterplot of GABA_Aα2 across the lifespan fit with an inverted quadratic function ($R^2=0.27$, $p<0.01$) that reached minima around 35 years **D**) Age-

binned results for GABA_Aα₂ expression in V4. **E)** Scatterplot of GABA_Aα₃ across the lifespan fit with an exponential decay function ($R^2=0.25$, $p<0.01$) **(F)** Age-binned results for GABA_Aα₃ in V4. Scatterplot, histogram and significance levels plotted using the conventions described in Figure 2. Histograms in upper right inset show V1 GABA data previously published in (Pinto et al., 2010).

To capture the developmentally-regulated balance of the GABA_A receptor, I calculated 2 indices between these subunits, GABA_Aα₂-GABA_Aα₁ ($\alpha_2:\alpha_1$) index, and GABA_Aα₃-GABA_Aα₁ ($\alpha_3:\alpha_1$) index in both areas V2d and V4.

Delayed development of 2 indices in V2d and V4: GABA_Aα₂-GABA_Aα₁ and GABA_Aα₃-GABA_Aα₁

The balance of GABA_Aα₂-GABA_Aα₁ in V2d showed a trend to shift from balanced expression in childhood toward more GABA_Aα₁ in adolescence, that returned to balanced expression through adulthood. These data showed significant variability across and within cases that reduced the goodness-of-fit for a model, so I used a weighted average to describe the data (Fig 10a). Across age groups, there was a significant shift from balanced expression in childhood to relatively more GABA_Aα₁ in adolescence ($p<0.01$) (Fig 10b). This trajectory is similar to V1 development that shifts from more GABA_Aα₂ to more GABA_Aα₁ across the lifespan, but the degree of the shift is slighter and delayed by about a decade in V2d (Upper inset, Fig 10b). There is significantly more α₃ in V2d in childhood ($p<0.01$), young adulthood ($p<0.05$), and older adulthood ($p<0.001$) compared to V1 (Upper inset, Fig 10b).

The balance of GABA_Aα₃-GABA_Aα₁ in V2d had significantly more GABA_Aα₃ in childhood that shifted around 30 years of age to more GABA_Aα₁ in adulthood that peaks at 74 years, well-

fit by a quadratic function ($R^2=0.58$, $p<0.0001$) (Fig 10c). Within age groups, there was significantly more GABA_Aα₃ in childhood (5-11 years) ($p<0.001$), balanced expression in teens and young adults, and significantly more GABA_Aα₁ in older adults ($p<0.001$) (Fig 10d). The developmental shift was significant with significantly higher expression of GABA_Aα₁ in older adults compared to all other groups ($p<0.001$) (Fig 10d). This profile is similar to that previously found in V1 that shifts from GABA_Aα₃ to GABA_Aα₁ across the lifespan, but the shift from more GABA_Aα₃ to more GABA_Aα₁ in V2d is delayed by about 30 years (Upper inset, Fig 10d). There is significantly more GABA_Aα₃ in childhood (5-11 years) V2d compared to V1 ($p<0.01$) (Upper inset, Fig 10d). Development of GABA_Aα₃-GABA_Aα₁ index expression was not different between V2d and V4.

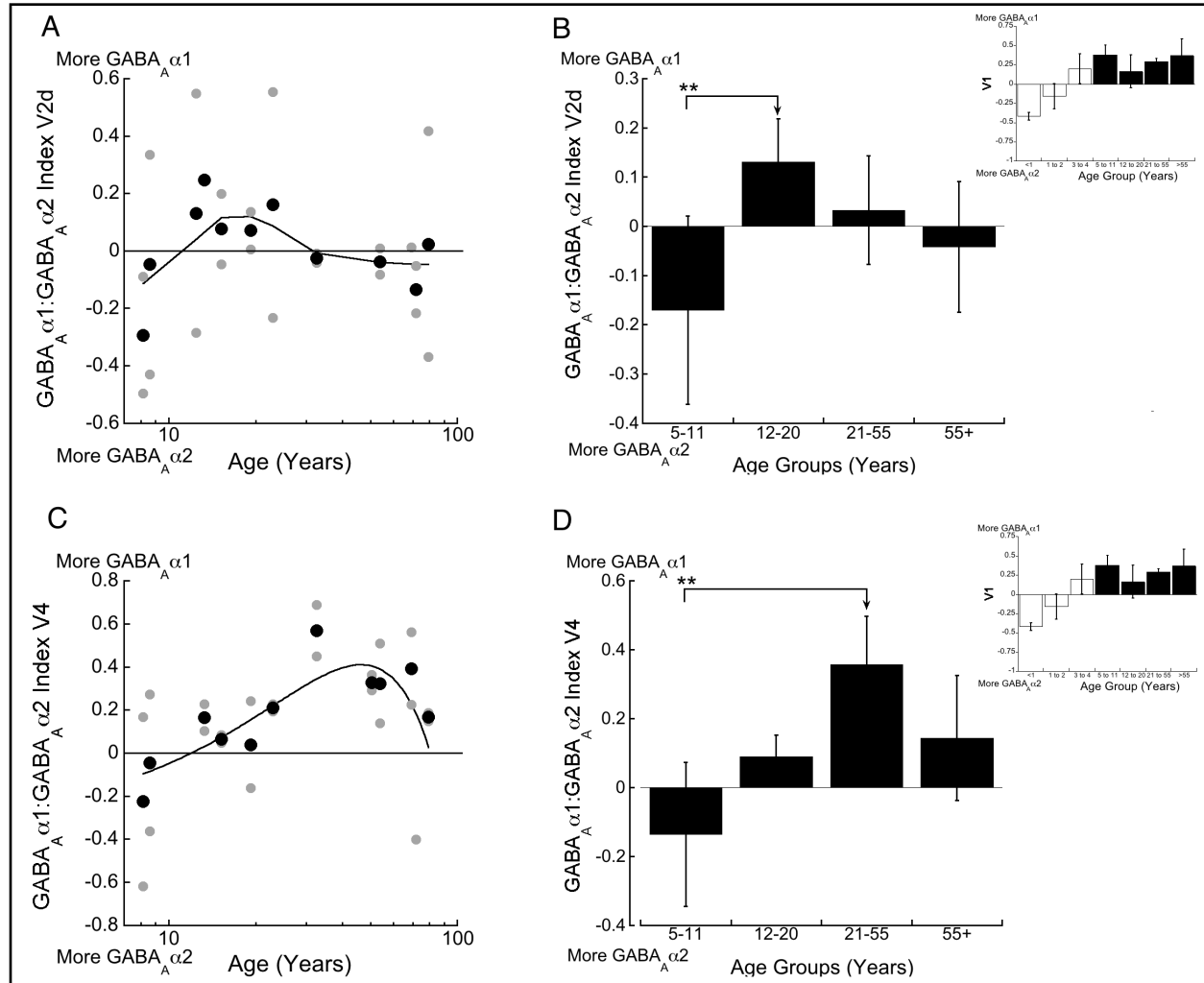


Figure 10 -- Development of GABA_Aα1:GABA_Aα2 balance ($\alpha1-\alpha2/\alpha1+\alpha2$) in human V2d and V4 **A**) Scatterplot of GABA_Aα1:GABA_Aα2 balance across the lifespan in V2d fit by a weighted function **B**) Age-binned results for GABA_Aα1:GABA_Aα2 balance expression in V2d **C**) Scatterplot of GABA_Aα1:GABA_Aα2 balance across the lifespan in V4 fit by a quadratic function ($R^2=0.31$, $p<0.01$) **D**) Age-binned results for GABA_Aα1:GABA_Aα2 balance expression in V4. Scatterplot, histogram and significance levels plotted using the conventions described in Figure 2. Histograms in upper right inset show V1 GABA data previously published in (Pinto et al., 2010).

In V4, the balance of GABA_Aα2-GABA_Aα1 showed a shift from balanced expression in childhood to more GABA_Aα1 by 12 years of age, peaks around 45 years, then shifts back toward balanced, well-fit by a quadratic function ($R^2=0.31$, $p<0.01$) (Fig 11a). Across age groups, there

was balanced expression of GABA_Aα2-GABA_Aα1 in childhood and adolescence, significantly more GABA_Aα1 in young adults ($p < 0.01$), and returned to balanced expression in older adults (Fig 11b). There was significantly more GABA_Aα1 expression in young adults compared to expression in childhood ($p < 0.01$) (Fig 11b). This profile is similar to that previously found in V1 across the lifespan, but the shift from more GABA_Aα2 to more GABA_Aα1 is delayed by about 8 years in V4 (Upper inset, Fig 11b). There is significantly more GABA_Aα3 in childhood in V4 compared to V1 ($p < 0.01$) (Upper inset, Fig 11b).

The GABA_Aα3-GABA_Aα1 balance in V4 showed significantly more GABA_Aα3 in young ages that shifted to more GABA_Aα1 around 20 years, peaking around 53 years, that was well-fit by a quadratic function ($R^2 = 0.31$, $p < 0.01$) (Fig 11c). There was significantly more GABA_Aα3 in childhood, balanced expression in adolescence, and significantly more GABA_Aα1 in young and older adults ($p < 0.05$) (Fig 11d). There was a significant shift in relative expression of GABA_Aα3-GABA_Aα1 from childhood ($p < 0.001$) and adolescence ($p < 0.01$) to young adults (Fig 11d). This profile is similar to the shift found previously in human V1, but the shift in V4 of more GABA_Aα3 to more GABA_Aα1 is delayed by about 20 years (Upper inset, Fig 11d). There is significantly more GABA_Aα3 in childhood ($p < 0.01$) in V4 compared to V1.

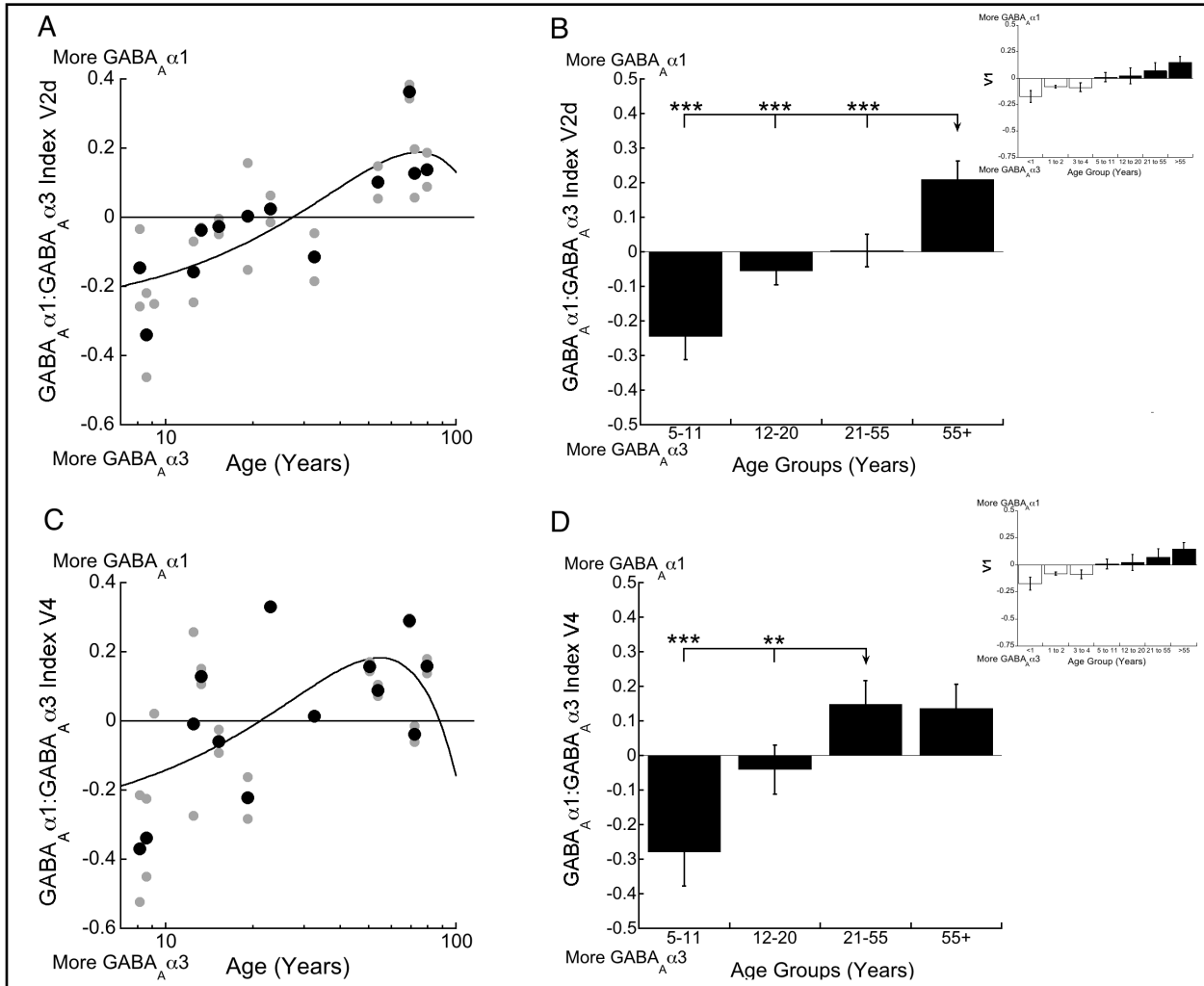


Figure 11 -- Development of GABA_Aα1:GABA_Aα3 balance (α1-α2/α1+α2) in human V2d and V4 **A**) Scatterplot of GABA_Aα1:GABA_Aα2 balance across the lifespan in V2d fit by a quadratic function ($R^2=0.58$, $p<0.0001$) **B**) Age-binned results for GABA_Aα1:GABA_Aα3 balance expression in V2d **C**) Scatterplot of GABA_Aα1:GABA_Aα3 balance across the lifespan in V4 fit by a quadratic function ($R^2=0.31$, $p<0.01$) **D**) Age-binned results for GABA_Aα1:GABA_Aα3 balance expression in V4. Scatterplot, histogram and significance levels plotted using the conventions described in Figure 2. Histograms in upper right inset show V1 GABA data previously published in (Pinto et al., 2010).

Glutamatergic receptor development in V2d and V4

To characterize the development of excitatory transmission in extrastriate areas, I quantified changes in NMDA receptor subunit - GluN1, and AMPA receptor subunit - GluA2 in human V2d and V4. GluN1 is the obligatory subunit for NMDA receptors, that are necessary for ocular dominance plasticity (ODP) (Kleinschmidt et al., 1987), metaplasticity (Kirkwood, Rioult, & Bear, 1996), orientation selectivity (Ramoia et al., 2001), and feedback visual processing (Self et al., 2012; van Loon et al., 2016). GluA2 is a calcium-impermeable AMPAR subunit mediating fast excitatory transmission into post-synaptic terminals and is necessary for synaptic scaling that drives homeostatic plasticity (Gainey et al., 2009).

GluN1 expression delayed in V2d & V4, while GluA2 expression follows V1 development

In V2d, GluN1 was high in childhood, decreased slowly until 46 years, then increased in older adults, well-fit by a quadratic function ($R^2=0.42$, $p<0.0001$) (Fig 12a). Across age groups, GluN1 expression in V2d was significantly higher in childhood ($p<0.001$), adolescence ($p<0.001$) than young adults, then increased again in older adults ($p<0.001$) (Fig 12b). This rapid decrease in expression follows a profile found previously in V1 early in development. Interestingly, the loss to maturity is delayed in V2d by about 40 years compared to the loss in V1 (Upper inset, Fig 12b). GluN1 expression is significantly higher in V2d across all age groups compared to V1 ($p<0.001$) (Upper inset, Fig 12b), and higher than in V4 in adolescence ($p<0.001$) and young adults ($p<0.05$).

In V2d, GluA2 expression declines linearly with age ($R^2=0.46$, $p<0.001$) (Fig 12c). GluA2 expression was high in children and adolescence ($p<0.001$) and decreased significantly in young

adults, then decreased further in older adults ($p < 0.001$) (Fig 12d). The GluA2 peak expression in V2d matches the V1 peak in childhood and both decrease across the lifespan (Upper inset, Fig 12d). GluA2 expression is significantly higher in V2d in young adults compared to V1 ($p < 0.001$) (Upper inset, Fig 12d).

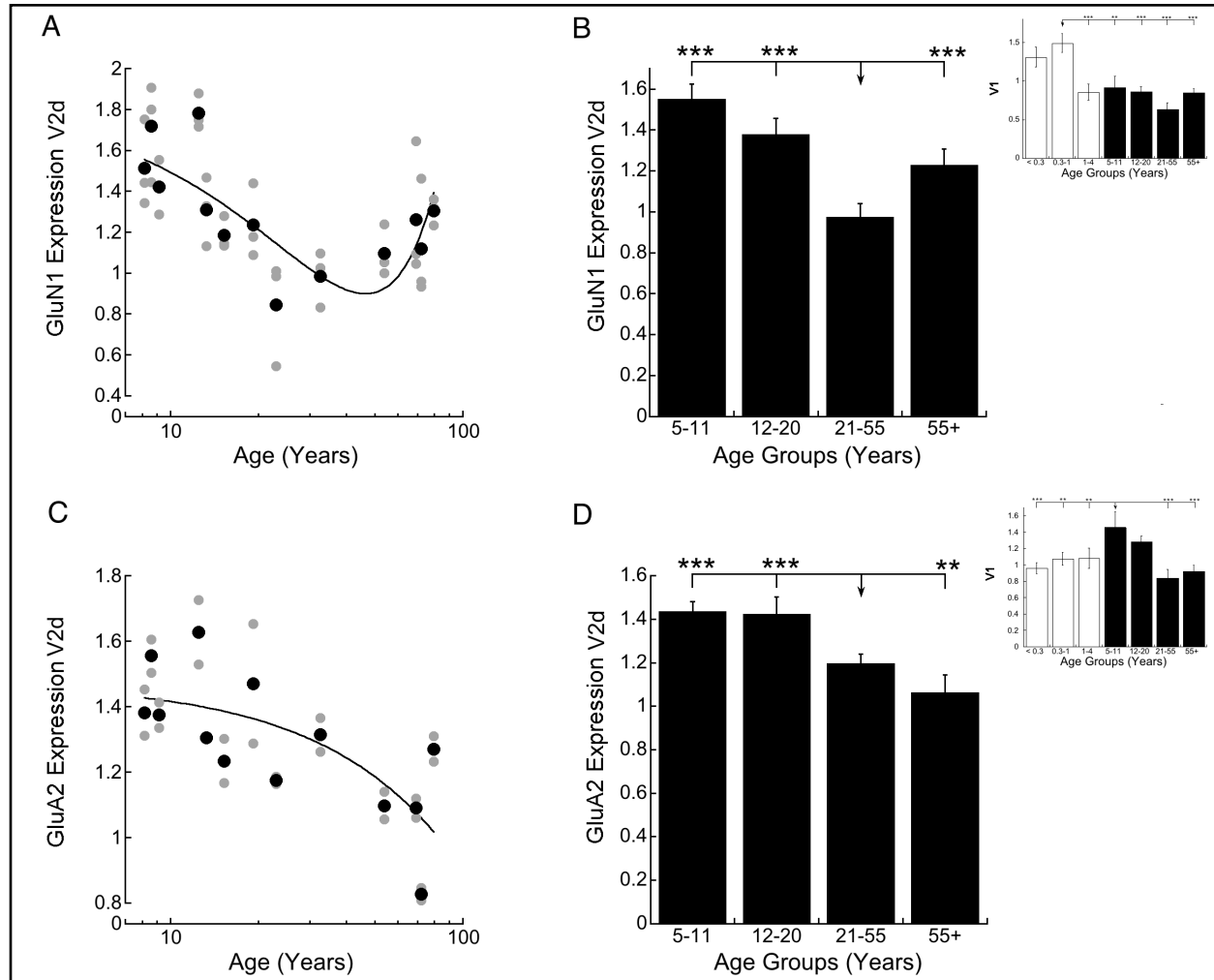


Figure 12 -- Development of GluN1 and GluA2 expression in human V2d. **A)** Scatterplot of GluN1 across the lifespan fit with a quadratic function ($R^2=0.42$, $p < 0.0001$). **B)** Age-binned results for GluN1 expression in V2d. **C)** Scatterplot of GluA2 across the lifespan fit with a linear function ($R^2=0.46$, $p < 0.001$). **D)** Age-binned results for GluA2 expression in V2d. Scatterplot, histogram and significance levels plotted using the conventions described in Figure 2. Histograms in upper right inset show V1 data previously published in (Siu et al., 2017).

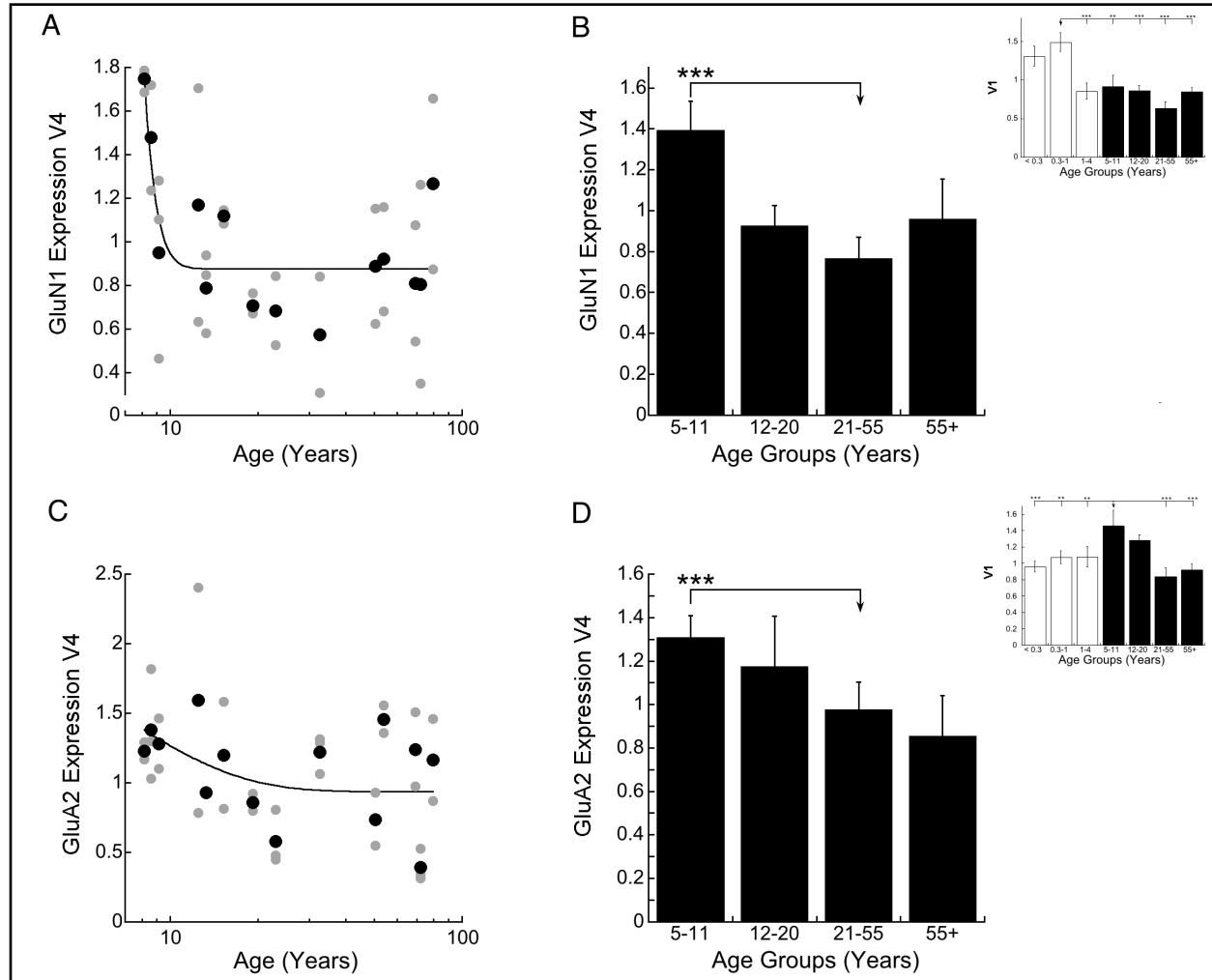


Figure 13 -- Development of GluN1 and GluA2 expression in human V4. **A)** Scatterplot of GluN1 across the lifespan fit with an exponential decay function ($R^2=0.41$, $p<0.001$) **B)** Age-binned results for GluN1 expression in V4. **C)** Scatterplot of GluA2 across the lifespan fit with an exponential decay function ($R^2=0.13$, $p<0.05$). **D)** Age-binned results for GluA2 expression in V4. Scatterplot, histogram and significance levels plotted using the conventions described in Figure 2. Histograms in upper right inset show V1 data previously published in (Siu et al., 2017).

In V4, GluN1 was similar to that in V2d (Pearson’s Correlation, $R^2=0.23$, $p<0.05$), with high expression in childhood then rapidly declined, well-fit by an exponential decay function ($R^2=0.41$, $p<0.001$) (Fig 13a). Across groups, GluN1 was significantly higher in childhood ($p<0.001$) compared to young adults (Fig 13b). This profile of development is similar to that previously found in V1, but the dramatic loss of GluN1 is shifted in V4 into adolescence, a delay

of at least 10 years (Upper inset, Fig 13b). There is significantly more GluN1 in childhood in V4 compared to V1 ($p < 0.001$) (Upper inset, Fig 13b).

In V4, GluA2 expression is high in childhood then decreases across the lifespan, fit by an exponential decay function ($R^2 = 0.13$, $p < 0.05$) (Fig 13c). Across age groups, GluA2 expression was high in childhood, and decreased significantly in young adults ($p < 0.001$) (Fig 13d). The trajectory, timing, and expression levels of GluA2 development was not significantly different between V2d, V4 or V1 (Upper inset, Fig 13d).

Delayed development of AMPA:NMDA receptor balance in V2d and V4

To quantify the relative balance between AMPAR and NMDAR in extrastriate development, I calculated the relative balance between GluA2:GluN1 in V2d and V4 (Fig 14). In V2d, balanced expression of GluA2:GluN1 index shifted to relatively more GluA2 around 12 years of age to peak GluA2 expression at around 45 years, then shifted back toward balanced expression, well-fit by a quadratic function ($R^2 = 0.36$, $p < 0.05$) (Fig 14a). There was balanced expression of GluA2 and GluN1 in childhood and adolescence, that shifted to significantly more GluA2 in young adults ($p < 0.001$), then shifted back to balanced expression in older adults (Fig 14b). This profile of development is similar to that previously found in V1 early in development, but the shift of more GluN1 to more GluA2 is delayed by about 35 years in V2d (Upper inset, Fig 14b). There is significantly more GluN1 in V2d in childhood, adolescence, and older adults compared to V1 ($p < 0.001$) (Upper inset, Fig 14b), but no significant difference in GluN1:GluA2 development between V2d and V4 across age groups.

The balance of GluA2:GluN1 in V4 showed a similar trend (Pearson's Correlation, $R^2=0.24$, $p<0.05$) to V2d. Balanced GluA2-GluN1 expression in childhood shifts to relatively more GluA2 around 10 years of age that peaks around 35 years, then shifts back toward balance, well-fit by a quadratic function ($R^2=0.16$, $p<0.05$) (Fig 14c). There was a developmental shift from balanced expression in childhood to more GluA2 in adolescence ($p<0.001$), that shifts back toward balanced expression in older adults ($p<0.001$) (Fig 14c). This developmental profile is similar to that previously found in V1 early in development, however, the shift from more GluN1 to more GluA2 is delayed by 10 years and the peak is delayed by about 25 years in V4 (Upper inset, Fig 14c). In childhood, there is significantly more GluN1 in V4 compared to V1 ($p<0.001$) (Upper inset, Fig 14c).

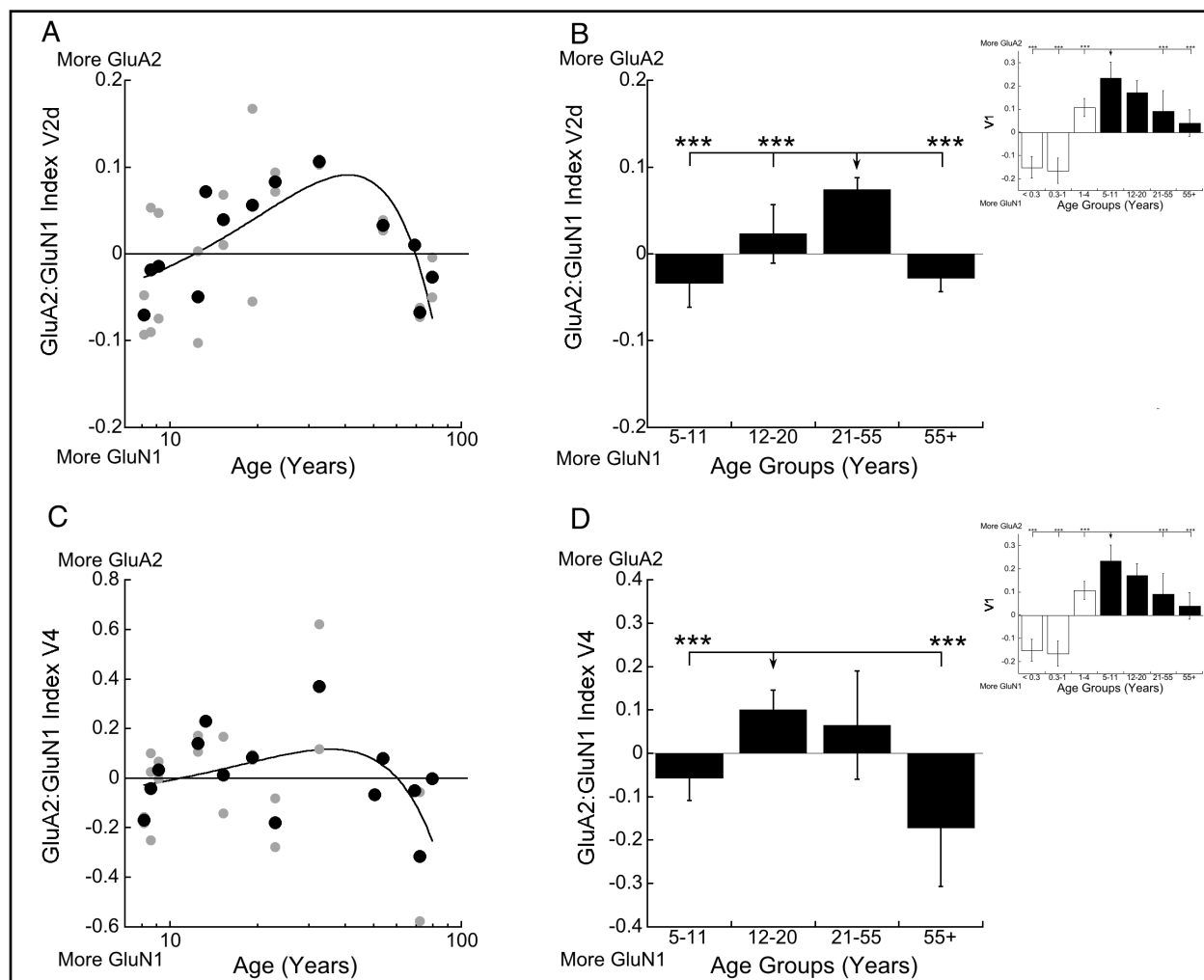


Figure 14 -- Development of GluA2:GluN1 balance (GluA2-GluN1/GluA2+GluN1) in human V2d and V4. **A)** Scatterplot of GluA2:GluN1 balance across the lifespan fit with a quadratic function ($R^2=0.36$, $p<0.05$) that peaked around 45 years **B)** Age-binned results for GluA2:GluN1 balance expression in V2d. **C)** Scatterplot of GluA2:GluN1 across the lifespan fit with a quadratic function ($R^2=0.16$, $p<0.05$) that peaked around 35 years. **D)** Age-binned results for GluA2:GluN1 balance expression in V4. Scatterplot, histogram and significance levels plotted using the conventions described in Figure 2. Histograms in upper right inset show V1 data previously published in (Siu et al., 2017).

NMDAR receptor subunit development: GluN2A and GluN2B

GluN1, the obligatory NMDAR subunit has a significant developmental delay in both extrastriate areas, which underlies the delay of the NMDAR:AMPA shift by about 30 years in both areas. To see if NMDAR subunit development can account for functional delays in

development of extrastriate, I chose to investigate development of functional subunits of the NMDA receptor, GluN2A and GluN2B, across development in V2d (Fig 15) and V4 (Fig 16). To reduce any variability of the data I normalized GluN2A and GluN2B expression to GluN1, as GluN1 is a component of all NMDA receptors. GluN2A and GluN2B are developmentally regulated (Monyer et al., 1994) and are necessary for unique aspects of plasticity and visual perception. The relative balance between the two proteins is a key regulator for synaptic LTP and LTD (Philpot et al., 2003). GluN2B is an immature NMDAR subunit that is necessary for synapse formation and maturation early in development (Tovar and Westbrook, 1999) and regulates excitatory transmission by suppressing the surface expression of AMPAR at the synapse (Hall et al., 2007). Increases in GluN2B decreases the sliding modification threshold for a synapse, meaning greater expression of GluN2B increases the likelihood of inducing LTP (Philpot et al., 2007). GluN2A is a mature NMDAR subunit that is necessary for orientation selectivity (Fagiolini et al., 2003) and increases the modification threshold for inducing LTD (Philpot et al., 2007).

GluN2B expression does not change with development in extrastriate, GluN2A significant changes with development

In V2d, there was no significant change in GluN2B expression across the lifespan, described by a weighted average (Fig 15a). Across age groups GluN2B expression showed no significant difference due to large variability within each group (Fig 15b). This developmental profile is different from GluN2B in V1, where there is a significant peak of GluN2B in childhood in V1 ($p < 0.001$) that is not found in V2d (Upper inset, Fig 15b).

GluN2A expression in V2d showed a trend of higher expression in adolescence that decreased in adulthood, but with high amounts of variability across the lifespan reduced the goodness-of-fit for a function, so the data was described using a weighted average (Fig 15c). Across age groups, GluN2A expression was high in childhood ($p < 0.05$) and adolescence ($p < 0.001$) then decreased by over 50% in young adults, then increased significantly in older adults ($p < 0.001$) (Fig 15d). This developmental profile in V2d is different from the profile previously studied in V1 across the same age span, where GluN2A expression increases to a dramatic peak in young adulthood in V1, nearly 5x the expression of young adults in V2d (Upper inset, Fig 15d). There is significantly lower GluN2A expression in V2d in childhood ($p < 0.001$) and young adults ($p < 0.001$) compared to V1 (Upper inset, Fig 15d).

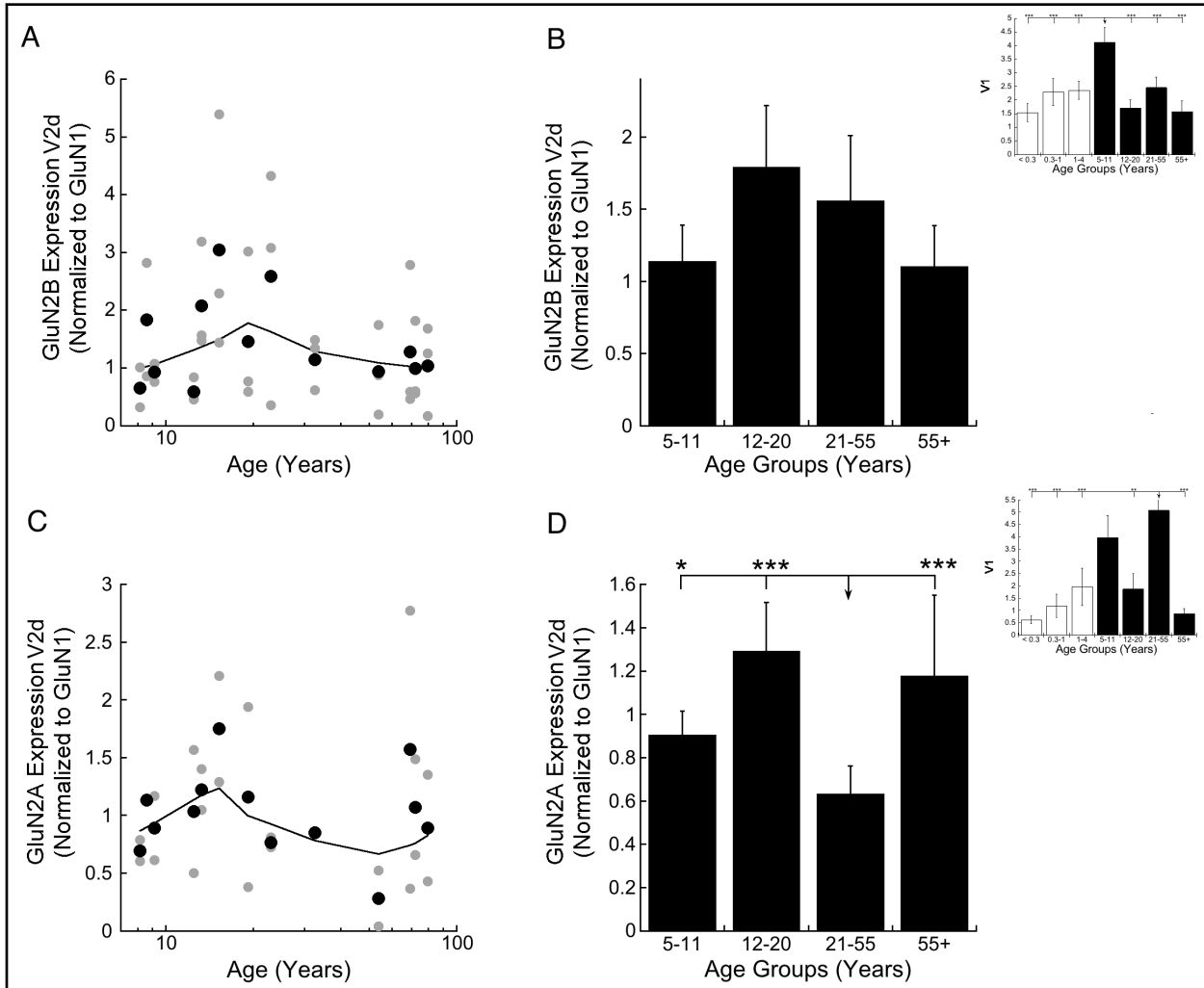


Figure 15 -- Development of GluN2A (2A) and GluN2B (2B) expression in human V2d. **A)** Scatterplot of 2B across the lifespan fit with a weighted average. **B)** Age-binned results for 2B expression in V2d. **C)** Scatterplot of 2A across the lifespan fit with a weighted average. **D)** Age-binned results for 2A expression in V2d. Scatterplot, histogram and significance levels plotted using the conventions described in Figure 2. Histograms in upper right inset show V1 data previously published in (Siu et al., 2017).

In V4, GluN2B showed no significant change across the lifespan, and was described using a weighted average (Fig 16a), and there was no significant difference between the groups (Fig 16b). This pattern of GluN2B development is different from that previously found in V1, where there is a significant peak of expression in childhood that is nearly double the expression found

here in V4 ($p < 0.001$) (Upper inset, Fig 16b). GluN2B development is not significantly different between V2d and V4.

GluN2A expression in V4 showed a decrease in expression from childhood through adolescence until 36 years of age, then an increase into older adult years, well-fit by a quadratic function ($R^2 = 0.32$, $p < 0.01$) (Fig 16c). Across age groups there was a significant decrease in adolescence ($p < 0.001$) that increased into young adults ($p < 0.001$) and older adults ($p < 0.001$) (Fig 16d). The developmental profile of GluN2A in V4 is different from the profile from V1, where there is a rapid loss of GluN2A in older adults, but in V4 GluN2A peaks in this age group (Upper inset, Fig 16d). GluN2A expression in V4 is significantly lower in childhood ($p < 0.001$), adolescence ($p < 0.001$), and young adults ($p < 0.001$) compared to V1. Alternatively, GluN2A expression is significantly higher in older adults in V4 compared to V1 ($p < 0.05$) (Upper inset, Fig 16b), and but is slower in V4 in adolescence than in V2d ($p < 0.001$).

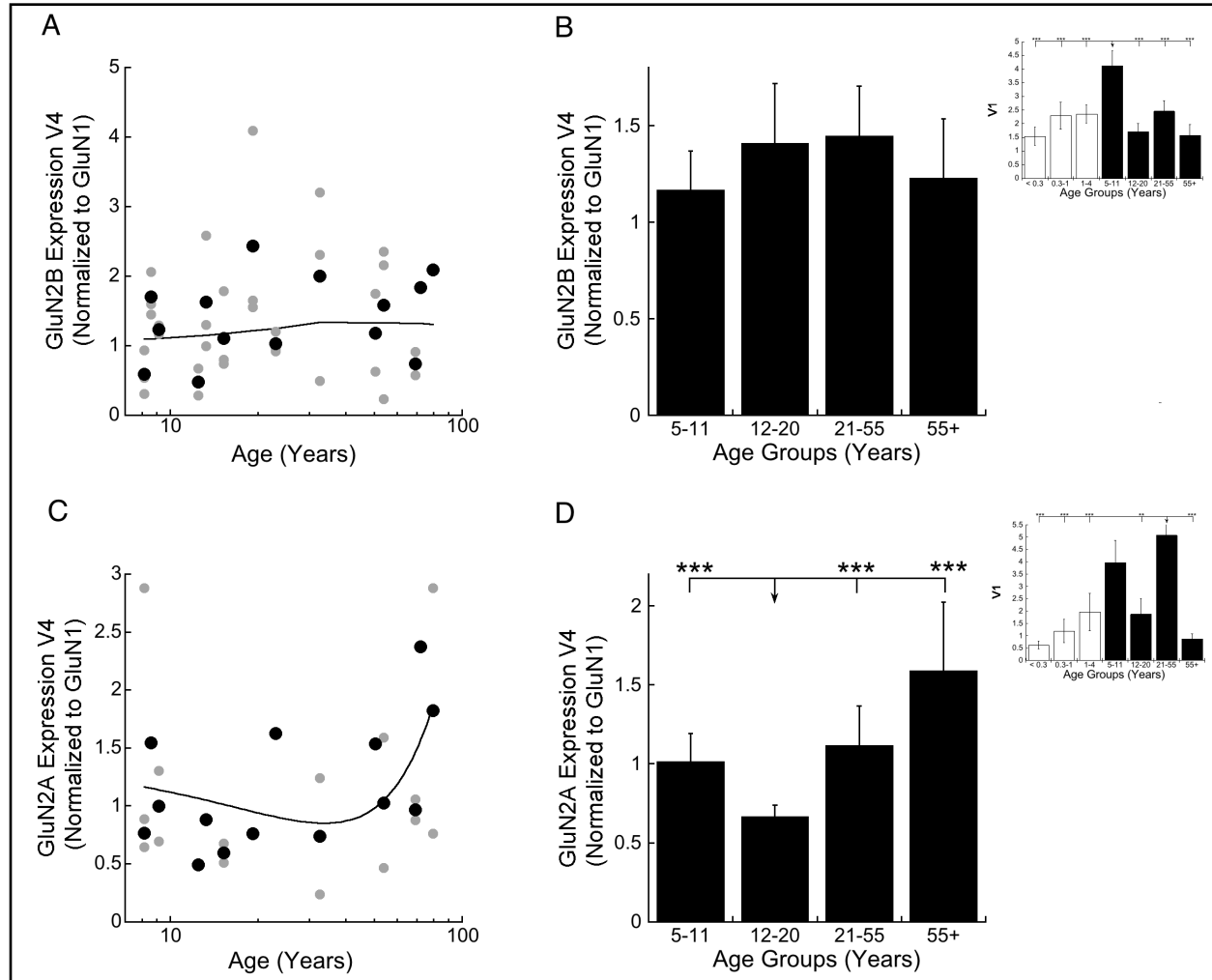


Figure 16 -- Development of GluN2A (2A) and GluN2B (2B) expression in human V4. **A)** Scatterplot of 2B across the lifespan fit with a weighted average. **B)** Age-binned results for 2B expression in V2d. **C)** Scatterplot of 2A across the lifespan fit with an inverted quadratic function ($R^2=0.32$, $p<0.01$) that reaches a minima around 36 years **D)** Age-binned results for 2A expression in V2d. Scatterplot, histogram and significance levels plotted using the conventions described in Figure 2. Histograms in upper right inset show V1 data previously published in (Siu et al., 2017).

2A:2B balance develops differently in extrastriate compared to V1

I measured the 2A:2B index to show the relative balance of expression between GluN2A and GluN2B across development of V2d and V4, and found surprising trajectories compared to previous reports of 2A:2B in V1 development.

In V2d, there is balanced 2A:2B expression in childhood that shifts toward more GluN2B expression into adulthood to peak GluN2B expression by 40 years of age, then shifts back toward more GluN2A in older adults; a trajectory well-fit by a quadratic function ($R^2=0.24$, $p<0.05$) (Fig 17a). Across age groups, expression is balanced in childhood and adolescence, shifts to significantly more GluN2B in young adults ($p<0.001$) then shifts back to balanced expression in older adults (Fig 17b). The developmental profile of 2A:2B in V2d is contrasted sharply against the development trajectory of 2A:2B in V1, as expression is significantly different between the two areas in childhood ($p<0.01$), young adults ($p<0.001$), and older adults ($p<0.01$). 2A:2B expression shows significantly more 2A in V2d in childhood ($p<0.01$) and older adults ($p<0.01$), and significantly more 2B in V2d in young adults ($p<0.001$) compared to V1.

In V4, the initially balanced expression of 2A:2B shifted to significantly more GluN2B until around 31 years, then shifted back toward more GluN2A around 60 years of age, a trajectory well-fit by a quadratic function ($R^2=0.20$, $p<0.05$) (Fig 17c). Across age groups, 2A:2B expression was balanced in childhood, shifted to significantly more GluN2B in adolescence ($p<0.001$), then back to balanced expression in young adults and older adults (Fig 17d). The developmental shift to more GluN2B in adolescence was significantly different from all other age groups ($p<0.001$) (Fig 17d). Like the developmental profile of 2A:2B in V2d, development in V4 is contrasted sharply with 2A:2B in human V1 (Upper inset, Fig 17d), as there was significantly more 2B in V4 in adolescence ($p<0.001$) and young adults ($p<0.001$), and significantly more 2A in V4 in older adults ($p<0.01$) compared to V1. There is significantly more 2B in V4 in adolescence compared to V2d ($p<0.001$), and significantly more 2B in V2d in young adulthood compared to V4 ($p<0.001$). This is the first report of the 2A:2B balance in

human extrastriate development across the lifespan. Our results provide the first neurobiological evidence for contrasting forms of plasticity in human extrastriate areas compared to V1 in adulthood (Murayama et al., 1997).

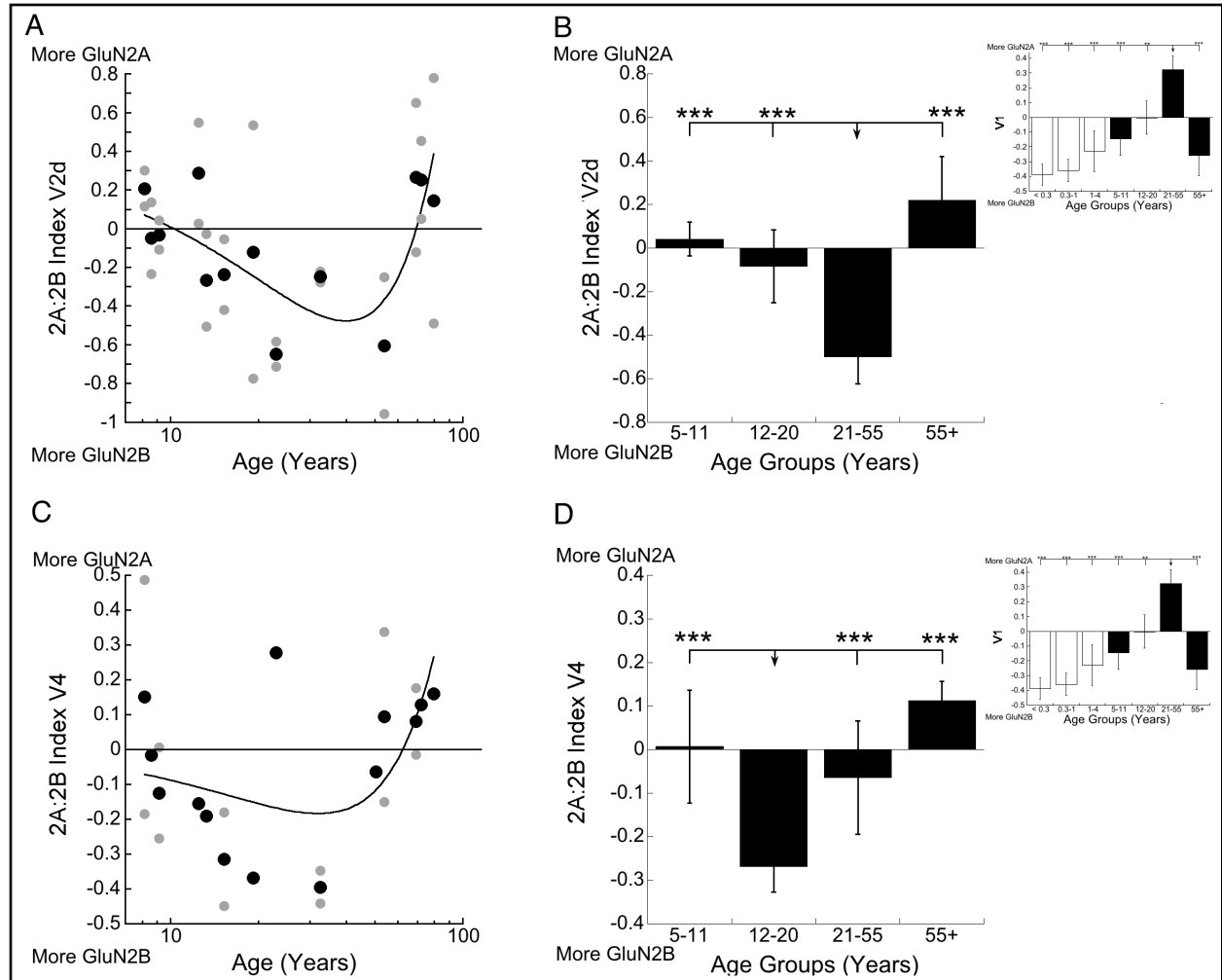


Figure 17 -- Development of 2A:2B balance (2A-2B)/(2A+2B) in human V2d and V4. **A)** Scatterplot of 2A:2B balance across the lifespan fit with a quadratic function ($R^2=0.24$, $p<0.05$) that peaks around 40 years of age **B)** Age-binned results for 2A:2B balance expression in V2d. **C)** Scatterplot of 2A:2B across the lifespan fit with an inverted quadratic function ($R^2=0.20$, $p<0.05$) and peaked toward 2B around 31 years. **D)** Age-binned results for 2A:2B balance expression in V4. Scatterplot, histogram and significance levels plotted using the conventions described in Figure 2. Histograms in upper right inset show V1 data previously published in (Siu et al., 2017).

6.4 Discussion

This study presents the expression of neurobiological mechanisms across development of human extrastriate areas V2d and V4. My results can help simplify the field by providing a neurobiological basis for the development of higher-order visual perception and plasticity in the human extrastriate cortex. Furthermore, this study provides neurobiological evidence for contrasting forms of plasticity in human extrastriate compared to V1.

Western blotting with human synaptosomes from cases across different ages provided reliable measurements of synaptic protein expression changes across the lifespan. This approach, however, does not provide information on cell type, circuit or layer localization, or synaptic function. Some proteins, like NMDAR are components of both pre- and post-synaptic membranes (Bouvier et al., 2015; Buchanan et al., 2012; Corlew et al., 2007), or extra-synaptic and their specific localization cannot be detected through Western blotting alone. These data are nonetheless necessary for identifying neurobiological mechanisms of human extrastriate visual processing and for creating more links between structure and function across cortical regions in human brain.

Some synaptic proteins develop at the same rate in V1 and extrastriate

The sum of proteins for basic synaptic function (synapsin, synaptophysin, PSD-95, gephyrin) in human V2d and V4 followed a significantly similar profile to V1 (Pinto et al., 2015) that peaks around 10 years of age that decreased into adulthood (Fig 1). Our samples do not include younger ages (>8 years) to compare to V1, but I did not find evidence for delayed development of V2d and V4 in this component of synaptic stabilization. 3 out of 4 synaptic proteins

(synapsin, synaptophysin, and gephyrin) that make up this common trajectory in V2d and V4 follow the same profile individually as in V1 (Pinto et al., 2010; 2015). Synapsin is a reliable marker for identifying pre-synaptic terminals in all synapses (Micheva et al., 2010). Synapsin expression in human V1 increases in development to reach adult levels by 8.7 years (Pinto et al., 2015). Synapsin expression in V2d or V4 also did not change after 8 years of age, indicating that stability of the neurotransmitter release system is reached by childhood across all of these visual areas. Similarities in synapsin expression measured in synaptosome in V2d and V4, and in homogenate samples in V1 suggests that all changes in synapsin expression is driven by expression in synaptic terminals.

Synaptophysin, Gephyrin, and GluA2 showed peaks of expression in childhood (5-11) that decreased with age in all 3 visual areas V2d, V4 and V1. Interestingly, each of these proteins are necessary for synaptic plasticity (Gainey et al., 2009; Janz et al., 1999; Tyagarajan and Fritschy, 2014). This stage of development in humans is characterized by the end of the period of susceptibility to amblyopia (Lewis and Maurer, 2005), and in V1 some markers for the end of critical period plasticity also peak in this stage like PSD-95 and GluN2B (Siu et al., 2017).

Synaptophysin is involved in regulation of vesicle endocytosis through Synaptobrevin retrieval (Gordon et al., 2011; Kwon and Chapman, 2011). Loss of synaptophysin does not impact vesicle recycling but does impact synaptic plasticity (Janz et al., 1999). Gephyrin clusters and binds GABA_A receptors, especially subunits $\alpha 1$ (Mukherjee et al., 2011), $\alpha 2$ (Tretter et al., 2008), and $\alpha 3$ (Tretter et al., 2011), to the post-synaptic membrane and is necessary for the stability of inhibitory synapses (Yu et al., 2007) and inhibitory LTP (Petrini et al., 2014). The peak of Gephyrin expression in V1 was nearly double the peak found in V2d and V4 that could indicate

greater inhibitory synaptic stabilization, or more inhibitory synapses in V1. GluA2, the Ca²⁺-impermeable AMPA receptor subunit is required for trafficking of AMPAR necessary for homeostatic synaptic scaling (Gainey et al., 2009), that is regulated by visual activity (Bai and Wong-Riley, 2003; Wong-Riley, 2002). GluA2 couples neuronal activity with energy metabolism of cytochrome oxidase in the visual cortex (Dhar et al., 2009). In monkey visual cortex, GluA2 is highly expressed on fast-spiking parvalbumin-positive (PV+) inhibitory interneurons (Kooijmans et al., 2014) that likely regulates calcium influx into PV+ cells. The peak of GluA2 expression in V2d and V4 parallels V1 development, and suggests a peak in metabolic function, possibly in PV+ cells, across the those visual areas at this same stage of development.

PSD-95:Gephyrin index is relatively balanced across the lifespan in V2d and V4, suggesting that the total E-I balance is maintained across the lifespan in extrastriate as well as in V1 across these ages. The E-I balance is maintained through homeostatic synaptic scaling (Barral and Reyes, 2016), and is crucial for optimal circuit function across development, while E-I imbalance is associated with disease and delayed development (D'Souza et al., 2016). The development of E-I balance extends beyond visual cortex, as mRNA expression of VGlut and VGAT, pre-synaptic glutamate and GABA vesicle transporter, is balanced by school age (5-12 years) in human prefrontal cortex and is maintained across the lifespan (Fung et al., 2011). Human prefrontal cortex also shows a peak of synaptophysin protein expression around 10 years of age that decreases to reach adult-levels in adolescence (Glantz et al., 2007), similar to synaptophysin expression that we found in V1 (Pinto et al., 2015), and in V2d and V4. Interestingly, this study used prefrontal cortex samples from the same postmortem cases as used in this study, and in our previous studies of human V1 (Murphy et al., 2005; Pinto et al., 2010; 2015; Siu et al., 2015;

2017; Williams et al., 2010). In addition, my lab previously found that Ube3a, a ubiquitin ligase protein that is necessary for experience-dependent plasticity, also develops similarly across V3, V4, and V1 and has a significant loss in aging in all 3 areas (Williams et al., 2010).

Pre-synaptic vesicle proteins, glutamatergic and GABA_A maturation delayed in V2d and V4

Four proteins showed significant delay in maturation in V2d, V4, or both extrastriate areas compared to development in V1. GABA_A α 1 in V2d and V4, and PSD-95 in V2d showed delayed increase in expression. GluN1 in V2d and V4, and GABA_A α 2 in V4 showed delayed loss of expression. Additionally, there were profound delays in maturation of 4 indices that span pre-synaptic, GABAergic, and glutamatergic development in V2d and V4. The pre-synaptic index, GABA_A α 2:GABA_A α 1 index, GABA_A α 3-GABA_A α 1 index, and GluN1-GluA2 index each showed significant delays in development in both extrastriate areas compared to previously studied developmental profiles of V1 (Pinto et al., 2010; 2015; Siu et al., 2017).

The delay in maturation after V1 development of some individual proteins and some developmentally-regulated balances between protein pairs are slightly longer in V2d than V4. These results provides evidence in humans for a dorsal stream delay in development that has been suggested previously in mice (Smith et al., 2017) and in humans (Atkinson, 2017; Taylor et al., 2009). For example, the peak of PSD-95 expression in V2d was delayed about 5 years after the peak in childhood V1 (Siu et al., 2017), while there was no peak in V4. The peak of PSD-95 is considered to consolidate silent synapses the end of critical period (Huang et al., 2015). Peak expression of GABA_A α 1, the fast-kinetic mature GABA_A receptor, is delayed by over 36 years

in V2d and by 31 years in V4. GABA_A α 1 subunit drives cortical plasticity in rodent V1 (Fagiolini et al., 2004), but may be responsible for different functions across different regions, as inhibition in cats regulates temporal receptive field properties in area 18, but spatial properties in area 17 (Jirrmann et al., 2008). GluN1, the obligatory subunit of NMDAR receptors, declines slowly across V2d development that reaches lowest expression by 46 years (Fig 12b), while GluN1 in V4 declined rapidly in adolescence, and remained low across the lifespan (Fig 13a). GluN1 in V1 is high in infants and declines rapidly by 1 year of age (Siu et al., 2017), suggesting that rate and profile that GluN1 matures is very prolonged in V2d compared to both V4 and V1. These delays in individual protein development contributed to the delay of maturation of relative protein balances. For example, the late loss of GluN1 caused the developmental AMPA:NMDA shift from more GluN1 to more GluA2 in V2d to peak about 35 years after V1 (Siu et al., 2017) and 10 years after V4. The shift toward more GluA2 in the synapse suggests insertion of AMPA receptors that stabilize silent synapses, that increases probability for depolarization, and therefore strengthens excitatory connections (Huang et al., 2015). The late increase of GABA_A α 1 in combination with the late loss of GABA_A α 3 and GABA_A α 2 in V4 caused delays in the developmentally regulated balances between α 3: α 1 and α 2: α 1 that drive the kinetics and binding affinity of GABA_A receptors. The shift in V2d from more α 3 to more α 1 was delayed 30 years beyond the V1 shift (Pinto et al., 2010), and 10 years beyond the V4 shift. Meanwhile, the shift in V4 from α 2 to α 1 in development was delayed by 40 years after the V1 shift (Pinto et al., 2010), and delayed 30 years after V2d development. Although both indices of GABA_A maturation in extrastriate areas are delayed to V1, there is some discrepancy for the composition of GABA_A receptors in V2d and V4 areas across development. The balance between

Synapsin: Synaptophysin also showed a delayed in V2d that matured nearly 30 years later than V1, and 7 years later than V4. The balance of these pre-synaptic receptors increases the probability for efficient neurotransmitter release and synaptic vesicle recycling.

Together, these synaptic protein balances encompass the basic components for experience-dependent plasticity in excitatory and inhibitory circuits. The maturation of these balances allow for fast, efficient neurotransmission and post-synaptic kinetics for strengthening connections. Interestingly, compared to V1, where most of these balances develop within the first few years of life, the development in V2d is delayed by an average of 30 years, while maturation in V4 is delayed by an average of 20 years. Furthermore, these protein balances regulate synaptic plasticity and their delayed development extended the potential for plasticity in extrastriate into adulthood that could support the late development of higher-order visual perception including face recognition (Golarai et al., 2010; Mondloch et al., 2002; Susilo et al., 2013), face memory (Germine et al., 2011), motion-defined form (Bucher et al., 2006), and contour integration (Kovacs et al., 1999). Interestingly, perceptual learning for those higher-order visual stimuli require surprisingly few trials in adulthood (Doshier and Lu, 2006; Hussain et al., 2009), compared to lower-order stimuli that can be resistant to improvement even after thousands of trials (Levi and Li, 2009). Our findings suggest delayed development of neurobiological mechanisms for plasticity in extrastriate compared to V1 supports the plasticity for learning complex visual stimuli in adulthood (Karni and Bertini, 1997; Fang Wang et al., 2016). In addition, the dorsal stream areas require visual experience for proper functional development, whereas ventral stream is more resilient experience-dependent development (Smith et al., 2017).

The delay in maturation of many functional synaptic units in area V2d may reflect some dependency on specific types of visual experience such as dorsal stream visual abilities.

Contrasting 2A:2B development in V2d and V4 compared to V1

There were some proteins that had profiles of development in V2d or V4 that were totally different from their development in V1. On the GABAergic side, there was a rapid loss of GABA_Aα3 expression in V2d and V4 in aging that is not lost in V1 (Pinto et al., 2010), and may contribute to the larger effects of aging on higher-order visual perception (Habak and Faubert, 2000) and receptive field properties (Yu et al., 2006) in extrastriate areas.

On the glutamatergic side, there was a profound difference in patterns of GluN2A and GluN2B development in V2d and V4 that shifted the 2A:2B balance off course from V1 development (Siu et al., 2017). GluN2B expression did not show a peak in childhood in V2d and V4, unlike V1 development where the peak in childhood was 4x higher than the rest of the age groups (Siu et al., 2017). Alternatively, GluN2A expression changed significantly across the lifespan in both areas V2d and V4 that were both different to V1 development. In V2d, there was a significant loss of GluN2A expression in young adults, followed by a significant increase in older adults (Fig 15d). In V4, the loss of GluN2A was earlier, in adolescence with increased by over 200% in older adults. GluN2B is the immature NMDA receptor subunit that regulates slow decay kinetics of the NMDAR, and expression of GluN2B suppresses the insertion of GluA2-containing AMPA receptors (Hall et al., 2007). In V1, the loss of GluN2B in development is associated with end of the critical period (Erisir and Harris, 2003). There is a developmental shift in V1 from more GluN2B-containing NMDA receptors in young brains to an activity-dependent

insertion of GluN2A-containing NMDAR (Monyer et al., 1994; Quinlan et al., 1999b; Sheng et al., 1994). The inclusion of GluN2A subunit immediately alters the kinetics of the receptor for fast glutamatergic transmission (Flint et al., 1997).

The 2A:2B index revealed a developmental trajectory in extrastriate that directly contrasts the development of 2A:2B in V1 (Siu et al., 2017). In V2d and V4 there is a significant shift toward more GluN2B with development, that shifts to significantly more GluN2B in adolescence in V4 (Fig 17d) and in young adults in V2d (Fig 17b), then a shift back to balanced 2A:2B expression in aging in both areas. The relative amounts of 2A:2B bidirectionally regulates metaplasticity in the visual cortex (Philpot et al., 2001; Quinlan et al., 1999a), where more GluN2B expression shifts the sliding modification threshold towards higher probability to elicit LTP, and more GluN2A expression shifts towards higher probability of LTD (Philpot et al., 2001). In human V1, I previously found a prolonged developmental 2A:2B shift across the lifespan that showed more GluN2B early in childhood that shifted towards more GluN2A around 12 years of age, and showed peak GluN2A expression ~40 years before returning to balance in older adults (Siu et al., 2017). Our findings in V2d and V4 show the 2A:2B balance shift in the opposite direction compared to V1. In addition, the magnitude of the shift in adulthood toward more GluN2B in V2d and V4 is similar to the magnitude of the shift toward GluN2A in V1. The timing of this shift suggests that this developmental shift toward more GluN2B occurs slightly later in V2d than in V4. The development in both areas suggest contrasting forms of plasticity in extrastriate compared to V1 in adulthood. This contrast has been shown previously in monkey visual cortex, where high-frequency electrical stimulation elicits LTP in the inferotemporal extrastriate cortex and identical stimulation in V1 elicits LTD (Murayama et al., 1997). In addition to plasticity

differences, these neurobiological differences between extrastriate and V1 may underlie unique receptive field properties in these areas.

Summary

This study provides a simple neurobiological basis for understanding complex development of higher-order visual perception and plasticity in the human extrastriate cortex. Results from this study can be used to target neurobiological mechanisms that aid in therapy or training for visual disorders. The development of glutamatergic, GABAergic and synaptic vesicle proteins across V2d, V4 have shown 3 patterns compared to trajectories of V1 development: same, delayed, or different. These trajectories together help narrow the gap between structure and function in the development of human visual areas.

Previously, my lab and I have characterized 5 stages of human synaptic development in V1 by quantifying patterns of glutamatergic and GABAergic synaptic protein expression (Pinto et al., 2010; Siu et al., 2017). I used those stages of synaptic development to compare with protein trajectories I found in development of V2d and V4 for glutamatergic (Fig 18), GABAergic (Fig 19) and pre-synaptic (Fig 20) proteins. These summary figures help emphasize that those synaptic proteins do not follow one trajectory of development across cortical areas. In addition, the synaptic development of V2d and V4 highlight a unique phase during the 4th stage of development (12-55 years) when many synaptic proteins peak in adolescence (12-20 years), separating this long stage into 2 phases of extrastriate development. Adolescence appears to develop as a unique stage of synaptic maturation in extrastriate areas in especially in V2d, where GluN2B, PSD-95, GluN2A, GABA_Aα3, Synapsin, and Synaptophysin peak during this stage.

This stage of development for V2d aligns with the perceptual improvements in adolescence of visual functions like global motion perception that stem from the dorsal stream of visual processing. In V4, young adulthood is a prominent stage for development where GluN2B, PSD-95, and GABA_A $\alpha 1$ peak. This stage aligns with development of face perception that matures in young adulthood that stems from ventral stream processing. Although these visual areas are early along the dorsal and ventral visual pathways, this evidence for neurobiological development across the human lifespan helps simplify new imaging studies on specialized visual processing from extrastriate and for harnessing potential for plasticity that is sustained into adulthood in these areas.

Relative to V1			Stage 1	Stage 2	Stage 3	Stage 4		Stage 5	
			<1 year	1-4 years	5-11 years	12-20 years	21-55 years	>55 years	
Individual Glutamate Protein Development	GluN1	V1	GluN1						
		V2d			GluN1				
		V4			GluN1				
	GluN2B	V1			GluN2B				
		V2d				GluN2B			
		V4					GluN2B		
	GluA2	V1				GluA2			
		V2d				GluA2			
		V4				GluA2			
	PSD-95	V1				PSD-95			
		V2d					PSD-95		
		V4						PSD-95	
	GluN2A	V1					GluN2A		
		V2d					GluN2A		
		V4							GluN2A
	Index Development	GluA2: GluN1	V1	GluN1		GluA2			
			V2d			GluN1		GluA2	
			V4				GluA2		GluN1
Index Development	2A:2B	V1				GluN2A		GluN2B	
		V2d					GluN2B	GluN2A	
		V4				GluN2B		GluN2A	

Figure 18 -- Summary of the five stages of development for glutamatergic proteins in V1 (Siu et al., 2017), V2d and V4. Changes for individual proteins are shown in grey levels with darker shades representing higher expression and lighter shades representing lower expression. The stage labelled with the protein name is the peak of expression. All V2d and V4 expression was calculated relative to the V1 to show differences in magnitude compared to V1 development. GluN1, GluN2B, and PSD-95 peak later in V2d and V4 than in V1, peak expression of GluN2B in V2d or V4 is not as high as the peak in V1 (shown in dark black). GluN2A expression in V2d and V4 is very light in comparison to V1 expression. Changes for the indices are colour coded, red for more GluN1 and GluN2B, green for GluA2 and GluN2A. The developmental switch to more GluA2 in V2d and V4 occurs later than in V1, however the developmental 2A:2B switch is totally opposite to that found in V1, where 2B dominates in adolescence and young adulthood in V4 and V2d, respectively.

Relative to V1			Stage 1 <1 year	Stage 2 1-4 years	Stage 3 5-11 years	Stage 4 12-20 years	Stage 4 21-55 years	Stage 5 >55 years
Individual GABA Protein Development	GABA _A α2	V1	GABA _A α2					
		V2d						GABA _A α2
		V4			GABA _A α2			
	Gephyrin	V1			Gephyrin			
		V2d			Gephyrin			
		V4			Gephyrin			
	GABA _A α3	V1						GABA _A α3
		V2d				GABA _A α3		
		V4			GABA _A α3			
	GABA _A α1	V1						GABA _A α1
		V2d					GABA _A α1	
		V4					GABA _A α1	
Index Development	α1:α2	V1	GABA _A α2		GABA _A α1			
		V2d			GABA _A α2	GABA _A α1		
		V4			GABA _A α2		GABA _A α1	
Index Development	α1:α3	V1	GABA _A α3					GABA _A α1
		V2d			GABA _A α3			GABA _A α1
		V4			GABA _A α3		GABA _A α1	

Figure 19 -- Summary of the five stages of development for GABAergic proteins in V1 (Pinto et al., 2010), V2d and V4. Changes for individual proteins are shown in grey levels with darker shades representing higher expression and lighter shades representing lower expression. The stage labelled with the protein name is the peak of expression. All V2d and V4 expression was calculated relative to the V1 to show differences in magnitude compared to V1 development. GABA_Aα2 peaks later in V2d and V4 than in V1, whereas GABA_Aα3 and GABA_Aα1 peak earlier in V2d and V4 compared to V1. Gephyrin expression peaks at the same time in all 3 areas, however is reduced in expression in both V2d and V4. Changes for the indices are colour coded, red for more GABA_Aα2 and GABA_Aα3, green for GABA_Aα1. The developmental switch from more GABA_Aα2 and GABA_Aα3 to more GABA_Aα1 in V2d and V4 occurs later than in V1.

Relative to V1		Stage 1	Stage 2	Stage 3	Stage 4		Stage 5
		<1 year	1-4 years	5-11 years	12-20 years	21-55 years	>55 years
Individual Pre-Synaptic Protein Development	Synapsin	V1			Synapsin		
		V2d				Synapsin	
		V4				Synapsin	
	Synaptophysin	V1			Synaptophysin		
		V2d				Synaptophysin	
		V4			Synaptophysin		
Index Development	Synapsin:	V1	Synaptophysin			Synapsin	
	Synaptophysin	V2d		Synaptophysin			
		V4			Synaptophysin		Synapsin

Figure 20 -- Summary of the five stages of development for pre-synaptic vesicle proteins in V1 (Pinto et al., 2015), V2d and V4. Changes for individual proteins are shown in grey levels with darker shades representing higher expression and lighter shades representing lower expression. The stage labelled with the protein name is the peak of expression. All V2d and V4 expression was calculated relative to the V1 to show differences in magnitude compared to V1 development. Synapsin peaks later in V2d and V4 compared to V1, but peak expression levels are significantly lower. Synaptophysin in V2d and V4 peaks around the same stage, and with same magnitude as V1. Changes for the index is colour coded, red for more Synaptophysin, green for more Synapsin. The developmental switch from more synaptophysin to more synapsin occurs later in both V2d and V4 compared to V1.

6.5 References

- Atkinson, J. (2017, March 1). The Davida Teller Award Lecture, 2016: Visual Brain Development: A review of “Dorsal Stream Vulnerability-”motion, mathematics, amblyopia, actions, and attention. *Journal of Vision*. <http://doi.org/10.1167/17.3.26>
- BAHLER, M., Benfenati, F., VALTORTA, F., & GREENGARD, P. (1990). The Synapsins and the Regulation of Synaptic Function. *Bioessays*, *12*(6), 259–263. <http://doi.org/10.1002/bies.950120603>
- Bai, X., & Wong-Riley, M. T. T. (2003). Neuronal activity regulates protein and gene expressions of GluR2 in postnatal rat visual cortical neurons in culture. *Journal of Neurocytology*, *32*(1), 71–78.
- Barral, J., & D Reyes, A. (2016). Synaptic scaling rule preserves excitatory–inhibitory balance and salient neuronal network dynamics. *Nature Neuroscience*, *19*(12), 1690–1696. <http://doi.org/10.1038/nn.4415>
- Berardi, N., Pizzorusso, T., Ratto, G. M., & Maffei, L. (2003). Molecular basis of plasticity in the visual cortex. *Trends in Neurosciences*, *26*(7), 369–378. [http://doi.org/10.1016/S0166-2236\(03\)00168-1](http://doi.org/10.1016/S0166-2236(03)00168-1)
- Beston, B. R., Jones, D. G., & Murphy, K. M. (2010). Experience-Dependent Changes in Excitatory and Inhibitory Receptor Subunit Expression in Visual Cortex. *Frontiers in Synaptic Neuroscience*, *2*. <http://doi.org/10.3389/fnsyn.2010.00138>
- Bogfjellmo, L. G., Bex, P. J., & Falkenberg, H. K. (2014). The development of global motion discrimination in school aged children. *Journal of Vision*, *14*(2), 19–19. <http://doi.org/10.1167/14.2.19>
- Bouvier, G., Bidoret, C., Casado, M., & Paoletti, P. (2015). Presynaptic NMDA receptors: Roles and rules. *Neuroscience*, *311*, 322–340. <http://doi.org/10.1016/j.neuroscience.2015.10.033>
- Buchanan, K. A., Blackman, A. V., Moreau, A. W., Elgar, D., Costa, R. P., Lalanne, T., et al. (2012). Target-specific expression of presynaptic NMDA receptors in neocortical microcircuits. *Neuron*, *75*(3), 451–466. <http://doi.org/10.1016/j.neuron.2012.06.017>
- Bucher, K., Dietrich, T., Marcar, V. L., Brem, S., Halder, P., Boujraf, S., et al. (2006). Maturation of luminance- and motion-defined form perception beyond adolescence: A combined ERP and fMRI study. *NeuroImage*, *31*(4), 1625–1636. <http://doi.org/10.1016/j.neuroimage.2006.02.032>

- Caspers, J., Palomero-Gallagher, N., Caspers, S., Schleicher, A., Amunts, K., & Zilles, K. (2015). Receptor architecture of visual areas in the face and word-form recognition region of the posterior fusiform gyrus., *220*(1), 205–219. <http://doi.org/10.1007/s00429-013-0646-z>
- Chen, L., Cooper, N. G., & Mower, G. D. (2000). Developmental changes in the expression of NMDA receptor subunits (NR1, NR2A, NR2B) in the cat visual cortex and the effects of dark rearing. *Brain Research. Molecular Brain Research*, *78*(1-2), 196–200.
- Chen, L., Yang, C., & Mower, G. D. (2001). Developmental changes in the expression of GABA(A) receptor subunits (alpha(1), alpha(2), alpha(3)) in the cat visual cortex and the effects of dark rearing. *Brain Research. Molecular Brain Research*, *88*(1-2), 135–143.
- Chen, X., Levy, J. M., Hou, A., Winters, C., Azzam, R., Sousa, A. A., et al. (2015). PSD-95 family MAGUKs are essential for anchoring AMPA and NMDA receptor complexes at the postsynaptic density. *Proceedings of the National Academy of Sciences of the United States of America*, *112*(50), E6983–92. <http://doi.org/10.1073/pnas.1517045112>
- Christopoulos, A., & Lew, M. J. (2000). Beyond eyeballing: fitting models to experimental data. *Critical Reviews in Biochemistry and Molecular Biology*, *35*(5), 359–391. <http://doi.org/10.1080/10409230091169212>
- Corlew, R., Wang, Y., Ghermazien, H., Erisir, A., & Philpot, B. D. (2007). Developmental switch in the contribution of presynaptic and postsynaptic NMDA receptors to long-term depression. *The Journal of Neuroscience : the Official Journal of the Society for Neuroscience*, *27*(37), 9835–9845. <http://doi.org/10.1523/JNEUROSCI.5494-06.2007>
- D'Souza, R. D., Meier, A. M., Bista, P., Wang, Q., & Burkhalter, A. (2016). Recruitment of inhibition and excitation across mouse visual cortex depends on the hierarchy of interconnecting areas. *eLife*, *5*, 1025. <http://doi.org/10.7554/eLife.19332>
- Desimone, R., & Schein, S. J. (1987). Visual properties of neurons in area V4 of the macaque: sensitivity to stimulus form. *Journal of Neurophysiology*, *57*(3), 835–868.
- Dhar, S. S., Liang, H. L., & Wong-Riley, M. T. T. (2009). Nuclear respiratory factor 1 co-regulates AMPA glutamate receptor subunit 2 and cytochrome oxidase: tight coupling of glutamatergic transmission and energy metabolism in neurons. *Journal of Neurochemistry*, *108*(6), 1595–1606. <http://doi.org/10.1111/j.1471-4159.2009.05929.x>
- Dosher, B. A., & Lu, Z.-L. (2006). Level and mechanisms of perceptual learning: Learning first-order luminance and second-order texture objects. *Vision Research*, *46*(12), 1996–2007. <http://doi.org/10.1016/j.visres.2005.11.025>
- Du, Y., Zhang, F., Wang, Y., Bi, T., & Qiu, J. (2016). Perceptual Learning of Facial Expressions. *Vision Research*, *128*(C), 19–29. <http://doi.org/10.1016/j.visres.2016.08.005>

- Eickhoff, S. B., Rottschy, C., & Zilles, K. (2007). Laminar distribution and co-distribution of neurotransmitter receptors in early human visual cortex., *212*(3-4), 255–267. <http://doi.org/10.1007/s00429-007-0156-y>
- Eickhoff, S. B., Rottschy, C., Kujovic, M., Palomero-Gallagher, N., & Zilles, K. (2008). Organizational principles of human visual cortex revealed by receptor mapping. *Cerebral Cortex (New York, N.Y. : 1991)*, *18*(11), 2637–2645. <http://doi.org/10.1093/cercor/bhn024>
- Erisir, A., & Harris, J. L. (2003). Decline of the critical period of visual plasticity is concurrent with the reduction of NR2B subunit of the synaptic NMDA receptor in layer 4. *The Journal of Neuroscience : the Official Journal of the Society for Neuroscience*, *23*(12), 5208–5218.
- Fagiolini, M., & Hensch, T. K. (2000). Inhibitory threshold for critical-period activation in primary visual cortex. *Nature*, *404*(6774), 183–186. <http://doi.org/10.1038/35004582>
- Fagiolini, M., Fritschy, J.-M., Löw, K., Möhler, H., Rudolph, U., & Hensch, T. K. (2004). Specific GABAA circuits for visual cortical plasticity. *Science*, *303*(5664), 1681–1683. <http://doi.org/10.1126/science.1091032>
- Fagiolini, M., Katagiri, H., Miyamoto, H., Mori, H., Grant, S. G. N., Mishina, M., & Hensch, T. K. (2003). Separable features of visual cortical plasticity revealed by N-methyl-D-aspartate receptor 2A signaling. *Proceedings of the National Academy of Sciences*, *100*(5), 2854–2859. <http://doi.org/10.1073/pnas.0536089100>
- Felleman, D. J., & Van Essen, D. C. (1987). Receptive field properties of neurons in area V3 of macaque monkey extrastriate cortex. *Journal of Neurophysiology*, *57*(4), 889–920. Retrieved from <http://eutils.ncbi.nlm.nih.gov/entrez/eutils/elink.fcgi?dbfrom=pubmed&id=3585463&retmode=ref&cmd=prlinks>
- Flint, A. C., Maisch, U. S., Weishaupt, J. H., Kriegstein, A. R., & Monyer, H. (1997). NR2A subunit expression shortens NMDA receptor synaptic currents in developing neocortex. *Journal of Neuroscience*, *17*(7), 2469–2476.
- Fox, K., & Daw, N. W. (1993). Do Nmda Receptors Have a Critical Function in Visual Cortical Plasticity. *Trends in Neurosciences*, *16*(3), 116–122.
- Fung, S. J., Webster, M. J., & Weicker, C. S. (2011). Expression of VGluT1 and VGAT mRNAs in human dorsolateral prefrontal cortex during development and in schizophrenia. *Brain Research*, *1388*(C), 22–31. <http://doi.org/10.1016/j.brainres.2011.03.004>

- Gainey, M. A., Hurvitz-Wolff, J. R., Lambo, M. E., & Turrigiano, G. G. (2009). Synaptic Scaling Requires the GluR2 Subunit of the AMPA Receptor. *Journal of Neuroscience*, 29(20), 6479–6489. <http://doi.org/10.1523/JNEUROSCI.3753-08.2009>
- Germine, L. T., Duchaine, B., & Nakayama, K. (2011). Where cognitive development and aging meet: Face learning ability peaks after age 30. *Cognition*, 118(2), 201–210. <http://doi.org/10.1016/j.cognition.2010.11.002>
- Glantz, L. A., Gilmore, J. H., Hamer, R. M., Lieberman, J. A., & Jarskog, L. F. (2007). Synaptophysin and postsynaptic density protein 95 in the human prefrontal cortex from mid-gestation into early adulthood. *Neuroscience*, 149(3), 582–591. <http://doi.org/10.1016/j.neuroscience.2007.06.036>
- Golarai, G., Liberman, A., Yoon, J. M. D., & Grill-Spector, K. (2010). Differential development of the ventral visual cortex extends through adolescence. *Frontiers in Human Neuroscience*, 3, 80. <http://doi.org/10.3389/neuro.09.080.2009>
- Gomez, J., Barnett, M. A., Natu, V., Mezer, A., Palomero-Gallagher, N., Weiner, K. S., et al. (2017). Microstructural proliferation in human cortex is coupled with the development of face processing. *Science*, 355(6320), 68–71. <http://doi.org/10.1126/science.aag0311>
- Gordon, S. L., Leube, R. E., & Cousin, M. A. (2011). Synaptophysin is required for synaptobrevin retrieval during synaptic vesicle endocytosis. *The Journal of Neuroscience : the Official Journal of the Society for Neuroscience*, 31(39), 14032–14036. <http://doi.org/10.1523/JNEUROSCI.3162-11.2011>
- Habak, C., & Faubert, J. (2000). Larger effect of aging on the perception of higher-order stimuli. *Vision Research*, 40(8), 943–950.
- Hadad, B.-S., Maurer, D., & Lewis, T. L. (2011). Long trajectory for the development of sensitivity to global and biological motion. *Developmental Science*, 14(6), 1330–1339. <http://doi.org/10.1111/j.1467-7687.2011.01078.x>
- Hall, B. J., Ripley, B., & Ghosh, A. (2007). NR2B signaling regulates the development of synaptic AMPA receptor current. *The Journal of Neuroscience : the Official Journal of the Society for Neuroscience*, 27(49), 13446–13456. <http://doi.org/10.1523/JNEUROSCI.3793-07.2007>
- Hartshorne, J. K., & Germine, L. T. (2015). When does cognitive functioning peak? The asynchronous rise and fall of different cognitive abilities across the life span. *Psychological Science*, 26(4), 433–443. <http://doi.org/10.1177/0956797614567339>

- Heinen, K., Bosman, L. W. J., Spijker, S., van Pelt, J., Smit, A. B., Voorn, P., et al. (2004). Gaba_A receptor maturation in relation to eye opening in the rat visual cortex. *Neuroscience*, *124*(1), 161–171. <http://doi.org/10.1016/j.neuroscience.2003.11.004>
- Hollingsworth, E. B., McNeal, E. T., Burton, J. L., Williams, R. J., Daly, J. W., & Creveling, C. R. (1985). Biochemical characterization of a filtered synaptoneurosome preparation from guinea pig cerebral cortex: cyclic adenosine 3′:5′-monophosphate-generating systems, receptors, and enzymes. *Journal of Neuroscience*, *5*(8), 2240–2253.
- Huang, X., Stodieck, S. K., Goetze, B., Cui, L., Wong, M. H., Wenzel, C., et al. (2015). Progressive maturation of silent synapses governs the duration of a critical period. *Proceedings of the National Academy of Sciences*, *112*(24), E3131–E3140. <http://doi.org/10.1073/pnas.1506488112>
- Hussain, Z., Sekuler, A. B., & Bennett, P. J. (2009). How much practice is needed to produce perceptual learning? *Vision Research*, *49*(21), 2624–2634. <http://doi.org/10.1016/j.visres.2009.08.022>
- Huttenlocher, P. R. (1990). Morphometric Study of Human Cerebral-Cortex Development. *Neuropsychologia*, *28*(6), 517–527.
- Janz, R., Südhof, T. C., Hammer, R. E., Unni, V., Siegelbaum, S. A., & Bolshakov, V. Y. (1999). Essential roles in synaptic plasticity for synaptogyrin I and synaptophysin I. *Neuron*, *24*(3), 687–700.
- Jirrmann, K.-U., Pernberg, J., & Eysel, U. T. (2008). Region-specificity of GABA_A receptor mediated effects on orientation and direction selectivity in cat visual cortical area 18. *Experimental Brain Research*, *192*(3), 369–378. <http://doi.org/10.1007/s00221-008-1583-6>
- Karni, A., & Bertini, G. (1997). Learning perceptual skills: behavioral probes into adult cortical plasticity. *Current Opinion in Neurobiology*, *7*(4), 530–535.
- Kirkwood, A., Rioult, M. G., & Bear, M. F. (1996). Experience-dependent modification of synaptic plasticity in visual cortex. *Nature*, *381*(6582), 526–528. <http://doi.org/10.1038/381526a0>
- Kleinschmidt, A., Bear, M. F., & Singer, W. (1987). Blockade of Nmda Receptors Disrupts Experience-Dependent Plasticity of Kitten Striate Cortex. *Science*, *238*(4825), 355–358. <http://doi.org/10.1126/science.2443978>
- Kooijmans, R. N., Self, M. W., Wouterlood, F. G., Belien, J. A. M., & Roelfsema, P. R. (2014). Inhibitory Interneuron Classes Express Complementary AMPA-Receptor Patterns in

- Macaque Primary Visual Cortex. *Journal of Neuroscience*, 34(18), 6303–6315. <http://doi.org/10.1523/JNEUROSCI.3188-13.2014>
- Kovacs, I., Kozma, P., Fehér, A., & Benedek, G. (1999). Late maturation of visual spatial integration in humans. *Proceedings of the National Academy of Sciences*, 96(21), 12204–12209.
- Kwon, S. E., & Chapman, E. R. (2011). Synaptophysin Regulates the Kinetics of Synaptic Vesicle Endocytosis in Central Neurons. *Neuron*, 70(5), 847–854. <http://doi.org/10.1016/j.neuron.2011.04.001>
- Levi, D. M., & Li, R. W. (2009). Perceptual learning as a potential treatment for amblyopia: a mini-review. *Vision Research*, 49(21), 2535–2549. <http://doi.org/10.1016/j.visres.2009.02.010>
- Lewis, T. L., & Maurer, D. (2005). Multiple sensitive periods in human visual development: Evidence from visually deprived children. *Developmental Psychobiology*, 46(3), 163–183. <http://doi.org/10.1002/dev.20055>
- MARGARET T T WONG-RILEY, P. J. (2002). AMPA glutamate receptor subunit 2 in normal and visually deprived macaque visual cortex. *Doi.org*, 1–11. <http://doi.org/10.1017/S0952523802195022>
- McMahon, D. B. T., & Leopold, D. A. (2012). Stimulus Timing-Dependent Plasticity in High-Level Vision. *Current Biology*, 22(4), 332–337. <http://doi.org/10.1016/j.cub.2012.01.003>
- Meier, K., & Giaschi, D. (2017). Effect of spatial and temporal stimulus parameters on the maturation of global motion perception. *Vision Research*, 135, 1–9. <http://doi.org/10.1016/j.visres.2017.04.004>
- Micheva, K. D., Busse, B., Weiler, N. C., O'Rourke, N., & Smith, S. J. (2010). Single-Synapse Analysis of a Diverse Synapse Population: Proteomic Imaging Methods and Markers. *Neuron*, 68(4), 639–653. <http://doi.org/10.1016/j.neuron.2010.09.024>
- Mondloch, C. J., Le Grand, R., & Maurer, D. (2002). Configural Face Processing Develops more Slowly than Featural Face Processing. *Perception*, 31(5), 553–566. <http://doi.org/10.1068/p3339>
- Monyer, H., Burnashev, N., Laurie, D. J., Sakmann, B., & Seeburg, P. H. (1994). Developmental and regional expression in the rat brain and functional properties of four NMDA receptors. *Neuron*, 12(3), 529–540.

- Mukherjee, J., Kretschmannova, K., Gouzer, G., Maric, H.-M., Ramsden, S., Tretter, V., et al. (2011). The residence time of GABA(A)Rs at inhibitory synapses is determined by direct binding of the receptor $\alpha 1$ subunit to gephyrin. *The Journal of Neuroscience : the Official Journal of the Society for Neuroscience*, 31(41), 14677–14687. <http://doi.org/10.1523/JNEUROSCI.2001-11.2011>
- Murayama, Y., Fujita, I., & Kato, M. (1997). Contrasting forms of synaptic plasticity in monkey inferotemporal and primary visual cortices. *NeuroReport*, 8(6), 1503–1508.
- Murphy, K. M., Balsor, J., Beshara, S., Siu, C., & Pinto, J. G. A. (2014). A high-throughput semi-automated preparation for filtered synaptoneurosomes. *Journal of Neuroscience Methods*, 235, 35–40. <http://doi.org/10.1016/j.jneumeth.2014.05.036>
- Murphy, K. M., Beston, B. R., Boley, P. M., & Jones, D. G. (2005). Development of human visual cortex: a balance between excitatory and inhibitory plasticity mechanisms. *Developmental Psychobiology*, 46(3), 209–221. <http://doi.org/10.1002/dev.20053>
- Petrini, E. M., Ravasenga, T., Hausrat, T. J., Iurilli, G., Olcese, U., Racine, V., et al. (2014). Synaptic recruitment of gephyrin regulates surface GABAA receptor dynamics for the expression of inhibitory LTP. *Nature Communications*, 5, 3921. <http://doi.org/10.1038/ncomms4921>
- Philpot, B. D., Cho, K. K. A., & Bear, M. F. (2007). Obligatory role of NR2A for metaplasticity in visual cortex. *Neuron*, 53(4), 495–502. <http://doi.org/10.1016/j.neuron.2007.01.027>
- Philpot, B. D., Espinosa, J. S., & Bear, M. F. (2003). Evidence for altered NMDA receptor function as a basis for metaplasticity in visual cortex. *Journal of Neuroscience*, 23(13), 5583–5588.
- Philpot, B. D., Sekhar, A. K., Shouval, H. Z., & Bear, M. F. (2001). Visual experience and deprivation bidirectionally modify the composition and function of NMDA receptors in visual cortex. *Neuron*, 29(1), 157–169.
- Pinto, J. G. A., Hornby, K. R., Jones, D. G., & Murphy, K. M. (2010). Developmental changes in GABAergic mechanisms in human visual cortex across the lifespan. *Frontiers in Cellular Neuroscience*, 4, 16. <http://doi.org/10.3389/fncel.2010.00016>
- Pinto, J. G. A., Jones, D. G., Williams, C. K., & Murphy, K. M. (2015). Characterizing synaptic protein development in human visual cortex enables alignment of synaptic age with rat visual cortex. *Frontiers in Neural Circuits*, 9, 3. <http://doi.org/10.3389/fncir.2015.00003>
- PRITCHETT, D. B., SONTHEIMER, H., SHIVERS, B. D., YMER, S., KETTENMANN, H., SCHOFIELD, P. R., & Seeburg, P. H. (1989). Importance of a Novel Gabaa Receptor

Subunit for Benzodiazepine Pharmacology. *Nature*, 338(6216), 582–585. <http://doi.org/10.1038/338582a0>

- Quinlan, E. M., Olstein, D. H., & Bear, M. F. (1999a). Bidirectional, experience-dependent regulation of N-methyl-D-aspartate receptor subunit composition in the rat visual cortex during postnatal development. *Proceedings of the National Academy of Sciences*, 96(22), 12876–12880.
- Quinlan, E. M., Philpot, B. D., Huganir, R. L., & Bear, M. F. (1999b). Rapid, experience-dependent expression of synaptic NMDA receptors in visual cortex in vivo. *Nature Neuroscience*, 2(4), 352–357. <http://doi.org/10.1038/7263>
- RAKIC, P., BOURGEOIS, J. P., ECKENHOFF, M. F., Zecevic, N., & GOLDMANRAKIC, P. S. (1986). Concurrent Overproduction of Synapses in Diverse Regions of the Primate Cerebral-Cortex. *Science*, 232(4747), 232–235.
- Ramoia, A. S., Mower, A. F., Liao, D., & Jafri, S. (2001). Suppression of cortical NMDA receptor function prevents development of orientation selectivity in the primary visual cortex. *Journal of Neuroscience*, 21(12), 4299–4309.
- Rivadulla, C., Sharma, J., & Sur, M. (2001). Specific roles of NMDA and AMPA receptors in direction-selective and spatial phase-selective responses in visual cortex. *The Journal of Neuroscience : the Official Journal of the Society for Neuroscience*, 21(5), 1710–1719.
- Roberts, E. B., & Ramoa, A. S. (1999). Enhanced NR2A subunit expression and decreased NMDA receptor decay time at the onset of ocular dominance plasticity in the ferret. *Journal of Neurophysiology*, 81(5), 2587–2591.
- Rumpel, S., Hatt, H., & Gottmann, K. (1998). Silent synapses in the developing rat visual cortex: evidence for postsynaptic expression of synaptic plasticity. *Journal of Neuroscience*, 18(21), 8863–8874.
- Sato, H., Katsuyama, N., Tamura, H., Hata, Y., & Tsumoto, T. (1995). Mechanisms underlying direction selectivity of neurons in the primary visual cortex of the macaque. *Journal of Neurophysiology*, 74(4), 1382–1394.
- Scherf, K. S., Luna, B., Avidan, G., & Behrmann, M. (2011). "What" Precedes "Which": Developmental Neural Tuning in Face- and Place-Related Cortex. *Cerebral Cortex*, 21(9), 1963–1980. <http://doi.org/10.1093/cercor/bhq269>
- Schrauf, M., Wist, E. R., & Ehrenstein, W. H. (1999). Development of dynamic vision based on motion contrast. *Experimental Brain Research*, 124(4), 469–473.

- Segalowitz, S. J., Sternin, A., Lewis, T. L., Dywan, J., & Maurer, D. (2017). Electrophysiological evidence of altered visual processing in adults who experienced visual deprivation during infancy. *Developmental Psychobiology*, *59*(3), 375–389. <http://doi.org/10.1002/dev.21502>
- Self, M. W., Kooijmans, R. N., Supèr, H., Lamme, V. A., & Roelfsema, P. R. (2012). Different glutamate receptors convey feedforward and recurrent processing in macaque V1. *Proceedings of the National Academy of Sciences of the United States of America*, *109*(27), 11031–11036. <http://doi.org/10.1073/pnas.1119527109>
- Sheng, M., Cummings, J., Roldan, L. A., Jan, Y. N., & Jan, L. Y. (1994). Changing subunit composition of heteromeric NMDA receptors during development of rat cortex. *Nature*, *368*(6467), 144–147. <http://doi.org/10.1038/368144a0>
- Siu, C. R., Balsor, J. L., Jones, D. G., & Murphy, K. M. (2015). Classic and Golgi Myelin Basic Protein have distinct developmental trajectories in human visual cortex. *Frontiers in Neuroscience*, *9*, 138–10. <http://doi.org/10.3389/fnins.2015.00138>
- Siu, C. R., Beshara, S. P., Jones, D. G., & Murphy, K. M. (2017). Development of Glutamatergic Proteins in Human Visual Cortex across the Lifespan. *The Journal of Neuroscience : the Official Journal of the Society for Neuroscience*, *37*(25), 6031–6042. <http://doi.org/10.1523/JNEUROSCI.2304-16.2017>
- Smith, I. T., Townsend, L. B., Huh, R., Zhu, H., & Smith, S. L. (2017). Stream-dependent development of higher visual cortical areas. *Nature Neuroscience*, *20*(2), 200–208. <http://doi.org/10.1038/nn.4469>
- Studer, R., Boehmer, von, L., Haenggi, T., Schweizer, C., Benke, D., Rudolph, U., & Fritschy, J.-M. (2006). Alteration of GABAergic synapses and gephyrin clusters in the thalamic reticular nucleus of GABA A receptor $\alpha 3$ subunit-null mice. *European Journal of Neuroscience*, *24*(5), 1307–1315. <http://doi.org/10.1111/j.1460-9568.2006.05006.x>
- Su, J., Chen, C., He, D., & Fang, F. (2012). Effects of face view discrimination learning on N170 latency and amplitude. *Vision Research*, *61*(C), 125–131. <http://doi.org/10.1016/j.visres.2011.08.024>
- Sun, Q., & Turrigiano, G. G. (2011). PSD-95 and PSD-93 Play Critical But Distinct Roles in Synaptic Scaling Up and Down. *Journal of Neuroscience*, *31*(18), 6800–6808. <http://doi.org/10.1523/JNEUROSCI.5616-10.2011>
- Susilo, M., Germine, L., & Duchaine, B. (2013). Face recognition ability matures late: evidence from individual differences in young adults. *Journal of Experimental Psychology. Human Perception and Performance*, *39*(5), 1212–1217. <http://doi.org/10.1037/a0033469>

- Taylor, N. M., Jakobson, L. S., Maurer, D., & Lewis, T. L. (2009). Differential vulnerability of global motion, global form, and biological motion processing in full-term and preterm children. *Neuropsychologia*, 47(13), 2766–2778. <http://doi.org/10.1016/j.neuropsychologia.2009.06.001>
- Tovar, K. R., & Westbrook, G. L. (1999). The incorporation of NMDA receptors with a distinct subunit composition at nascent hippocampal synapses in vitro. *The Journal of Neuroscience : the Official Journal of the Society for Neuroscience*, 19(10), 4180–4188.
- Tretter, V., Jacob, T. C., Mukherjee, J., Fritschy, J.-M., Pangalos, M. N., & Moss, S. J. (2008). The clustering of GABA(A) receptor subtypes at inhibitory synapses is facilitated via the direct binding of receptor alpha 2 subunits to gephyrin. *The Journal of Neuroscience : the Official Journal of the Society for Neuroscience*, 28(6), 1356–1365. <http://doi.org/10.1523/JNEUROSCI.5050-07.2008>
- Tretter, V., Kerschner, B., Milenkovic, I., Ramsden, S. L., Ramerstorfer, J., Saiepour, L., et al. (2011). Molecular basis of the γ -aminobutyric acid A receptor $\alpha 3$ subunit interaction with the clustering protein gephyrin. *The Journal of Biological Chemistry*, 286(43), 37702–37711. <http://doi.org/10.1074/jbc.M111.291336>
- Tropea, D., Van Wart, A., & Sur, M. (2009). Molecular mechanisms of experience-dependent plasticity in visual cortex. *Philosophical Transactions of the Royal Society of London. Series B, Biological Sciences*, 364(1515), 341–355. <http://doi.org/10.1098/rstb.2008.0269>
- Tyagarajan, S. K., & Fritschy, J.-M. (2014). Gephyrin: a master regulator of neuronal function? *Nature Publishing Group*, 15(3), 141–156. <http://doi.org/10.1038/nrn3670>
- van Loon, A. M., Fahrenfort, J. J., van der Velde, B., Lirk, P. B., Vulink, N. C. C., Hollmann, M. W., et al. (2016). NMDA Receptor Antagonist Ketamine Distorts Object Recognition by Reducing Feedback to Early Visual Cortex. *Cerebral Cortex (New York, N.Y. : 1991)*, 26(5), 1986–1996. <http://doi.org/10.1093/cercor/bhv018>
- Wang, Fang, Huang, J., Lv, Y., Ma, X., Bin Yang, Wang, E., et al. (2016). Predicting perceptual learning from higher-order cortical processing. *NeuroImage*, 124(Part A), 682–692. <http://doi.org/10.1016/j.neuroimage.2015.09.024>
- Wang, Yi, Fujita, I., Tamura, H., & Murayama, Y. (2002). Contribution of GABAergic inhibition to receptive field structures of monkey inferior temporal neurons. *Cerebral Cortex*, 12(1), 62–74.
- Williams, K., Irwin, D. A., Jones, D. G., & Murphy, K. M. (2010). Dramatic Loss of Ube3A Expression during Aging of the Mammalian Cortex. *Frontiers in Aging Neuroscience*, 2, 18. <http://doi.org/10.3389/fnagi.2010.00018>

- Yashiro, K., & Philpot, B. D. (2008). Regulation of NMDA receptor subunit expression and its implications for LTD, LTP, and metaplasticity. *Neuropharmacology*, *55*(7), 1081–1094. <http://doi.org/10.1016/j.neuropharm.2008.07.046>
- Yoshii, A., Sheng, M. H., & Constantine-Paton, M. (2003). Eye opening induces a rapid dendritic localization of PSD-95 in central visual neurons. *Proceedings of the National Academy of Sciences*, *100*(3), 1334–1339. <http://doi.org/10.1073/pnas.0335785100>
- Yoshimura, Y., Ohmura, T., & Komatsu, Y. (2003). Two forms of synaptic plasticity with distinct dependence on age, experience, and NMDA receptor subtype in rat visual cortex. *Journal of Neuroscience*, *23*(16), 6557–6566.
- Yu, S., Wang, Y., Li, X., Zhou, Y., & Leventhal, A. G. (2006). Functional degradation of extrastriate visual cortex in senescent rhesus monkeys. *Neuroscience*, *140*(3), 1023–1029. <http://doi.org/10.1016/j.neuroscience.2006.01.015>
- Yu, W., Jiang, M., Miralles, C. P., Li, R.-W., Chen, G., & de Blas, A. L. (2007). Gephyrin clustering is required for the stability of GABAergic synapses. *Molecular and Cellular Neuroscience*, *36*(4), 484–500. <http://doi.org/10.1016/j.mcn.2007.08.008>

Chapter 7. General Discussion

7.1 Summary of Main Findings

This thesis advances the study of human visual cortex development by addressing three main gaps in the literature. The first gap concerns translating neurobiological mechanisms for use in human tissue. The second gap is our lack of understanding the neurobiological mechanisms that support lifelong changes in human visual perception and plasticity. The third gap is our poor understanding of the pace and trajectory of sequential development across human visual cortical areas.

In Chapter 2, I addressed the first gap by establishing a protocol for studying synaptic proteins in the human brain. Chapter 2 described detailed protocols for a synaptoneurosome preparation using human cortical tissues. This technique was refined for the purpose of studying synaptic proteins in human cortical tissue, and this chapter outlines specific considerations for using fresh frozen postmortem human tissue. This chapter presents an important method for translating between synaptic neurobiological mechanisms studied in animal models to useful studies in human brain development. Synaptoneurosome's were prepared for use in human visual cortex tissue when I studied glutamatergic proteins in human V1 (Chapter 4), and human extrastriate development (Chapter 6) across the lifespan.

In Chapter 3, I addressed the second gap by investigating the developmental trajectory of myelin proteins in human V1. Myelin is considered a structural brake on the critical period (McGee et al., 2005), so I hypothesized that classic-MBP, the mature compaction myelin protein, would be

upregulated near the end of susceptibility to amblyopia in humans, 6-10 years of age (Lewis & Maurer, 2005). In addition, we mapped the expression of golli-MBP, immature oligodendrocyte protein, and found a complementary trajectory that is highly expressed early in human V1 development, switches to more classic-MBP around 12 years of age then switches back to more golli-MBP in older adults. This study provides evidence for a prolonged period of plasticity in human V1 as classic-MBP continued to increase until the 4th decade of life, before a significant loss of classic-MBP expression in aging.

In Chapter 4, I further addressed the second gap by expanding on the idea of prolonged plasticity in human V1 from Chapter 3 by examining the development of glutamatergic synaptic proteins that are known from animal models to play integral parts in visual plasticity and perception. I provided further evidence of prolonged plasticity in human V1, as the prolonged development of NMDAR subunit GluN2A extended the 2A:2B balance to mature until 40 years of age. In addition, I found evidence for five stages of development in human V1 that are each characterized by a distinct pattern of glutamatergic synaptic expression.

Chapter 5 extends my work in Chapter 4 by addressing questions that arose from studying glutamatergic proteins in human V1. Chapter 5 explored glutamatergic synapses by quantifying the developmental expression of components of the tetrapartite synapse, including astrocyte expression, ECM receptor expression and dendritic spine protein expression. This study gives rise to new questions about prolonged glutamatergic development in human V1.

In Chapter 6, I addressed the third gap by studying developmental expression of excitatory and inhibitory proteins in human extrastriate areas V2d and V4. I studied proteins that have all been previously characterized in development of human V1, which allowed me to compare the developmental trajectories across visual cortical areas. The identified neurobiological mechanisms of plasticity in human extrastriate areas matured in later stages of development when higher-order visual perceptions emerge (Germine et al., 2011; Hadad et al., 2011; Kovacs et al., 1999). In particular, I found evidence for glutamatergic mechanisms, 2A:2B, that underlie contrasting forms of plasticity in V2d and V4 compared to V1 in adulthood.

My results suggest there are five stages of development in the human visual cortex, each characterized by different types of synaptic plasticity. Quantifying the expression of neurobiological mechanisms in each stage of development in the human visual cortex is an important step in assessing plasticity in humans that will help predict the usefulness of therapies and treatments for visual disorders. In this discussion, I will summarize the main findings from each chapter in my thesis by describing how these results fit in with previous neurobiological studies in human visual cortex. These findings are a step toward improving our understanding of mechanisms of neuroplasticity in humans, that could help translation of effective clinical therapies across the lifespan.

7.2 Stages of Human Visual Cortex Development and Clinical Implications

Expression profiles for the development of neurobiological mechanisms studied in this thesis show multiple changes across the lifespan (Figure 1). These findings can be described by five stages of development that exhibit unique patterns of plasticity and visual perception in animal and perceptual studies. These findings help to clarify the neurobiological underpinnings of these stages of plasticity in human brain, and may help to identify new therapeutic targets for recovery of visual disorders.

Protein	Stage 1 <1 Year	Stage 2 1-4 Years	Stage 3 5-11 Years	Stage 4 12-20 Years 21-55 Years		Stage 5 >55 Years	Reference
GluN1	GluN1						Chapter 4
GABA _A α2	GABA _A α2						Pinto et al., 2010
Golli MBP	Golli-MBP						Chapter 3
β-tubulin	β-Tubulin						Chapter 3
CB1	CB1		CB1				Pinto et al., 2010
GFAP	GFAP					GFAP	Chapter 5
VGAT	VGAT						Pinto et al., 2010
β3-Integrin	β3-Integrin						Chapter 5
Ube3a	Ube3a						Williams et al., 2010
GluN2B			GluN2B				Chapter 4
GluA2			GluA2				Chapter 4
PSD-95			PSD-95				Chapter 4
Gephyrin			Gephyrin				Pinto et al., 2010
Synaptophysin			Synaptophysin				Pinto et al., 2015
GAD67			GAD67				Pinto et al., 2010
Synapsin			Synapsin				Pinto et al., 2015
GAD65				GAD65			Pinto et al., 2010
GluN2A					GluN2A		Chapter 4
Classic MBP					Classic-MBP		Chapter 3
Drebrin					Drebrin		Chapter 5
GABA _A α3						GABA _A α3	Pinto et al., 2010
GABA _A α1						GABA _A α1	Pinto et al., 2010

Figure 1 - Individual protein development for Human primary visual cortex (V1). Columns in order from left to right: Protein studied, Stage 1 expression - Infancy (<1 Year), Stage 2 expression - Young Childhood (<1-4 years), Stage 3 - Older childhood (5-11 years); Stage 4 - Adolescence (12-20 Years) and Young Adulthood (21-55 years); Stage 5 - Older Adulthood (>55 Years). Protein expression relative to the peak represented by gradations in grey levels, where black is the high expression, and white is low expression. These data are from a collection of studies on the human visual cortex including Chapter 3, Chapter 4, and Chapter 5 of this thesis,

as well as 3 previously published studies (Pinto et al., 2010; Pinto et al., 2015; Williams et al., 2010), the corresponding source study for each protein is the last column.

Infancy (0-1 year): The onset of mechanisms for binocularity and CP in human V1

Infant visual development is characterized by significant changes in many visual functions including binocularity (Braddick et al., 1980; Held et al., 1980; Thorn et al., 1994, Birch and Held, 1985), orientation selectivity (Morrone and Burr, 1986, Hood, 1992), contrast sensitivity (Allen et al., 1996, Pirchio et al., 1978), visual acuity (Gwiazda et al., 1980, Maurer et al., 1999), global motion sensitivity (Blumenthal et al., 2013), and face perception (Deen et al., 2017).

Activation of inhibitory interneurons is required for development of orientation selectivity in V1 (Lee et al., 2014a; Lee et al., 2014b), and the increase in GABAergic inhibition initiates the onset of the CP for ODP in mice (Fagiolini et al., 2004; Hensch et al., 1998). The onset of binocular vision is dependent on visual experience, as binocularity is absent at birth and comes after about 4 months visual experience in both preterm and term babies (Jando et al., 2012).

This stage of human visual cortex development is characterized by synaptogenesis peaking around 8 months of age, followed by a slower period of synaptic pruning (Huttenlocher et al., 1982).

Neurobiological studies from my lab have further characterized this stage with the initial maturation of GABA transmission (Pinto et al., 2010), and evidence for the onset of excitatory-inhibitory (E-I) balance in human V1. For example, endocannabinoid receptor, CB1, is high in infancy (Pinto et al., 2010), and is necessary for maturation of GABA release in visual cortex (Jiang et al., 2010). GABA_A receptors are immature at this stage (high $\alpha 2$ and $\alpha 3$), but quickly show signs of maturation as $\alpha 1$ expression starts to increase and eventually shifts the balance of

$\alpha 3$ to $\alpha 1$ at around 1 year of age (Pinto et al., 2010). That maturation of the GABA_A receptor has been shown to be necessary for ODP in mice (Fagiolini et al., 2004). In Chapter 4, I found that NMDAR obligatory subunit GluN1 expression in human V1 was also high in infants, then rapidly decreases after 1 year (Siu et al., 2017). This rapid shift in NMDAR and GABA_A receptor subunit expression could contribute to the E-I balance around 1 year of age. Further evidence for the E-I balance in human V1 in infancy is also shown by the relative expression of PSD-95 and Gephyrin, post-synaptic scaffolding proteins for excitatory and inhibitory receptors, respectively that reach a balance by 5 months of age (Pinto et al., 2015) (Figure 2).

Protein Index	Stage 1 <1 Year	Stage 2 1-4 Years	Stage 3 5-11 Years	Stage 4 12-20 Years	Stage 4 21-55 Years	Stage 5 >55 Years	Reference
GABA _A α 1: GABA _A α 2	GABA _A α 2		GABA _A α 1				Pinto et al., 2010
AMPA:NMDA	GluN1		GluA2				Chapter 4
PSD-95:Gephyrin	Gephyrin		PSD-95				Pinto et al., 2015
Classic MBP:Golli MBP	Golli MBP			Classic MBP			Chapter 3
2A:2B				GluN2A		GluN2B	Chapter 4
VGAT:GAD65	VGAT				GAD65		Pinto et al., 2010
Synapsin:Synaptophysin	Synaptophysin				Synapsin		Pinto et al., 2015
Gephyrin:GAD65			Gephyrin			GAD65	Pinto et al., 2010
GABA _A α 1: GABA _A α 3	GABA _A α 3					GABA _A α 1	Pinto et al., 2010

Figure 2 -- The development of index protein expression in human V1. Columns in order from left to right: Protein index studied, Stage 1 expression - Infancy (<1 Year), Stage 2 expression - Young Childhood (<1-4 years), Stage 3 - Older childhood (5-11 years); Stage 4 - Adolescence (12-20 Years) and Young Adulthood (21-55 years); Stage 5 - Older Adulthood (>55 Years). Relative levels of protein expression are represented as graded shades of green or red. Bright colours indicates peak levels of that protein, while lighter colours represent less relative expression. White cells indicate there is balanced expression between the two proteins. Proteins are labelled when there was peak relative expression across the lifespan.

This stage of E-I balance in humans provides neurobiological evidence for the initiation of the CP in humans, as the onset of E-I balance in mice initiates ODP (Fagiolini and Hensch, 2000).

This stage marks the onset of the sensitive period for developing amblyopia, where the average age of diagnosis is about 1.2 years (Birch and Holmes, 2010). Early treatment of cataracts in

infancy shows rapid improvement in visual acuity even within 1 hour of removal (Maurer et al., 1999), and the earlier the treatment in infancy the better chance of developing normal acuity (Birch et al., 1993). Despite this, even adults who were treated for dense bilateral cataracts in infancy show signs of abnormalities in V1 event-related potentials to glass patterns (Segalowitz et al., 2017). Thus, patterned visual input is necessary at this early age for normal lifelong vision (Lewis and Maurer, 2009). Furthermore, I found expression of GFAP, astrocyte marker, increase by 3 months of age in V1 (Chapter 5). Astrocytes are large glial cells with processes that can extend to cover millions of synapses in human cortex (Oberheim et al., 2009). Furthermore, astrocytes participate in bidirectional glutamatergic and GABAergic signalling to both excitatory and inhibitory synapses that result in active participation in regulating the E-I balance (Fellin et al., 2006; Papouin et al., 2017; Perea et al., 2014). The pattern of neurobiological mechanisms expressed at this stage of human V1 development contribute toward balancing excitatory and inhibitory transmission, and is dependent on matched patterned binocular vision. Monocular deprivation in the CP causes reorganization of layer IV circuits that results in an imbalance of excitatory and inhibitory transmission, that is reversed with normal binocular visual experience (Maffei et al., 2006; Maffei et al., 2004; Nahmani and Turrigiano, 2014). The imbalance of excitatory and inhibitory transmission results in imbalanced ocular dominance in the visual cortex, resulting in depression of the weak and potentiation of the strong eye (Kuhlman et al., 2013). Thus, therapeutic targets in infancy include matching visual activity processed through each eye in order to regain E-I balance in the visual cortex.

Young Childhood (1-4 years): Neuronal variability for optimal circuits

Young childhood is characterized by a period of interindividual variability captured in oligodendrocyte protein Golli-MBP (Siu et al., 2015), in a set of glutamatergic proteins (Siu et al., 2017), and in dendritic spine protein Drebrin (Chapter 5). My lab has previously identified waves of interindividual variability in pre-synaptic proteins Synapsin and Synaptophysin, post-synaptic proteins PSD-95 and Gephyrin (Pinto et al., 2015), as well as in Ube3a expression early in childhood (Williams et al., 2010). Interestingly, not all developmentally regulated proteins in human V1 show a interindividual variability, like classic-MBP, β -tubulin, β 3-integrin, GFAP, or GAPDH.

During this developmental stage (~1-3 years), children most susceptible to abnormal binocular experience (Banks et al., 1975). My studies point to this period of inter - or intra- individual variability, especially in the glutamatergic proteins as be a key indication for plasticity in developing visual circuits. Inter-individual variability suggests that different people develop at different rates, and therefore have varying levels of protein expression compared to their cohort members. Intra-variability, however, suggests that all children in this stage have variable amounts of protein expression from one moment to the next. Clearly this is a period for change where there is a greater dynamic range of protein expression that could contribute to increased plasticity, learning for optimal behavioural performance (Garrett et al., 2013). Interestingly, this stage of interindividual variability comes just after the E-I balance has been reached in human V1 (Figure 2). Balanced excitation and inhibition in the cortex establishes criticality in the cortex, a dynamic range of spontaneous activity that maximizes the range of inputs that can be processed (Shew et al., 2009). Thus, this stage of variability we see in childhood, may be a result of the E-I balance achieved in infancy.

Interindividual variability is not uncommon in human studies. High interindividual variability in PET imaging across human visual cortex areas can be attributed to variances in borders and shape of visual areas between individuals and within individuals between hemispheres (Hasnain et al., 2011), as well as physiological variability where different visual areas may process the same visual stimuli across individuals (Hasnain et al., 1998).

As discussed in Chapter 4, this stage of variability may be a prominent feature of visual development when visual circuits ‘learn’ complex processing and create variability in responses to fine-tune efficient behaviour (Gordus et al., 2015; Siu et al., 2017). The functional result of neuronal variability has yet to be fully understood as either adaptive or maladaptive in developing circuits (Dinstein et al., 2015). These studies are the first steps toward characterizing neural variability across the lifespan in human visual cortex, as further studies will be necessary to test these the benefits or costs of variability in visual perception.

Older Childhood (5-11 Years): End of susceptibility of CP in human V1

This stage of development is considered the end of period of susceptibility to amblyopia in humans (Assaf, 1982; Lewis and Maurer, 2005; Epelbaum et al., 1993). Thus, I hypothesized an upregulation of molecular mechanisms that reflect the brakes on CP plasticity in this stage (Bavelier et al., 2010). PSD-95 and GluA2 peaked between 5-11 years in human V1 (Siu et al., 2017), two glutamatergic proteins that have been correlated with the end of CP in mice, and the peak maturation of silent synapses (Chen et al., 2015; Huang et al., 2015). Potentiated synaptic activity increases the trafficking of PSD-95 to the post-synaptic membrane that creates “slots” for AMPAR insertion (Chen et al., 2015). GluA2-containing AMPARS are recruited to the

synapse following high-frequency stimulation resulting in LTP, that contributes to stabilizing synapses (Liu and Cull-Candy, 2000). Furthermore, GluA2 is necessary for synaptic scaling, that is a homeostatic mechanism to maintain synaptic strength over fluctuations in synaptic activity (Gainey et al., 2009). The homeostatic scaling up (or down) of AMPAR is dependent on firing rates of synaptic activity, and may cooperate with competitive Hebbian plasticity during the CP to refine cortical connectivity and promote synaptic stability based on visual input (Desai et al., 2002; Mrsic-Flogel et al., 2007; Turrigiano and Nelson, 2004).

GluA2-containing AMPAR are highly expressed on PV+ cells in primate (Kooijmans et al., 2014), indicating the excitatory input onto PV+ is upregulated at this time in human V1. Increased excitability of PV+ cells constrains plasticity (Gu et al., 2016). Gephyrin expression peaks at this stage of V1 development (Pinto et al., 2010; 2015), that is directly related to strength and stability of inhibitory synapses (Tyagarajan and Fritschy, 2014). To fully classify the mechanisms for the end of CP plasticity in humans, it will be important to characterize the development of PV+ inhibitory interneurons across development of human V1.

There is significant visual plasticity for recovery from amblyopia at this stage in human vision as both amblyopes and children with normal vision experience perceptual improvement with training (Li et al., 2005; Liao et al., 2016; Mintz-Hittner and Fernandez, 2000). Although this stage sees the end of susceptibility for developing amblyopia, there is perceptual and neurobiological evidence for multiple sensitive periods across development (Lewis and Maurer, 2005), as recovery from abnormal vision can continue to be achieved through perceptual learning.

Young Adults (21-55 years): Prolonged adult plasticity

Many specialized visual abilities continue to improve well into adulthood including face and motion perception (Germiné et al., 2011; Hadad et al., 2015; Susilo et al., 2013). Although many visual neuroscientists attribute this later developing vision solely to the late maturation of extrastriate areas, I found significant evidence for prolonged maturation of plasticity mechanisms in human V1. Those mechanisms include Classic MBP -- mature myelin protein, GluN2A -- mature NMDAR subunit, and Drebrin -- actin-binding dendritic spine protein, that each develop until late 30s or early 40s in human V1 (Figure 1). These results align with previous findings of maturation for GABAergic transmission by the prolonged development of GABA producing protein GAD65, and GABA_Aα1 receptor subunit in human V1 that influences efficient GABA transmission in this stage (Pinto et al., 2010) (Figure 1).

Interestingly, a very important finding in this thesis is evidence for mechanisms underlying contrasting forms of plasticity in human V1 and extrastriate areas in adulthood. In V1, the 2A:2B balance shifts towards more GluN2A in adulthood. This developmental profile has been characterized before in many species (Chen et al., 2000; Flint et al., 1997; Monyer et al., 1994; Sheng et al., 1994; Zhang and Sun, 2011), and the function of this subunit balance regulates metaplasticity in the visual cortex and other areas (Abraham and Bear, 1996; Philpot et al., 2001; 2003; 2007; Yashiro and Philpot, 2008). Metaplasticity is the probability that synaptic activity will elicit potentiation or depression of a synapse, dependent on the synapses previous history of synaptic activity, that is dependent on NMDAR receptor subunits GluN2A and GluN2B (Philpot et al., 2003; 2007; Yashiro and Philpot, 2008), where more GluN2A in a synapse can decrease the probability of eliciting LTP, and GluN2B in a synapse can increase the probability of eliciting

LTP. Metaplasticity has been well characterized in animal models, but in human V1, the protracted development of the 2A:2B balance into adulthood was unprecedented. Furthermore, the development of 2A:2B ratio in human extrastriate suggests that different plasticity mechanisms are present in adulthood, that could support adult LTP plasticity in extrastriate while supporting adult LTD in V1 that has previously been found in monkeys (Murayama et al., 1997). The 2A:2B balance is associated with limiting CP plasticity in animal models (Chen et al., 2000; Erisir and Harris, 2003; Roberts and Ramoa, 1999), as is the increase in intracortical myelination (McGee et al., 2005), and the rise in Drebrin (Imamura et al., 1992). Although it does not appear that juvenile-like CP plasticity extends past 6-10 years of age, that marks the end of susceptibility to developing amblyopia, the prolonged development of these mechanisms in human V1 suggest there is adult-like plasticity well into the 5th decade of life. Perceptual studies show there is plasticity in adulthood that allows recovery from amblyopia (Levi and Polat, 1996). Adults with amblyopia can improve visual acuity with extensive perceptual training (Levi, 2005), and have success in refining contrast sensitivity (Liao et al., 2016), orientation selectivity (Jehee et al., 2012), stereopsis (Ding and Levi, 2011), spatial discrimination (Li and Levi, 2004) and face learning (Du et al., 2016; McMahan and Leopold, 2012). Thus, the prolonged development of neurobiological mechanisms for plasticity in human V1 and extrastriate provide evidence for the potential for synaptic plasticity in adulthood that can be harnessed through visual perceptual learning.

Older Adults (>55 years): Maintaining function

Aging visual cortex is characterized largely by changes in contrast sensitivity (Allard et al., 2013b), orientation selectivity (Betts et al., 2007), face perception (Konar et al., 2013; Wilson et al., 2011), increases in receptive field size (Brewer and Barton, 2014), and changes in motion perception (Bennett et al., 2007; Hutchinson et al., 2012; Owsley, 2011). Some of those age-related changes in visual perception have been attributed to the loss of inhibitory transmission in the cortex, that has been rescued by increasing GABA levels (Leventhal, 2003). Even in the human V1, levels of GAD65 decrease (Pinto et al., 2010), along with Ube3a plasticity protein (Williams et al., 2010). Here, I showed there are significant losses in synaptic proteins in human V1, such as β -tubulin and β 3-integrin that may contribute to maladaptive changes in vision. Interestingly, some of the losses in protein expression in human V1 (Figure 1) switch the balance of their functional pair toward a juvenile-like state (Figure 2). For example, the loss of GluN2A in aging shifts the 2A:2B balance toward more GluN2B, that regulates juvenile, LTP-dominated plasticity. In addition, the loss of mature myelin protein classic-MBP in aging shifts the Classic MBP:Golli MBP balance back toward immature myelin protein Golli MBP. These shifts toward a more juvenile state suggest a shift toward a more plastic environment in adulthood that may be needed in order to maintain visual function in a degenerating optical system (Artal et al., 2003; Glasser and Campbell, 1999). The shift toward more juvenile-like plasticity in NMDAR subunits suggests it is possible that visual perceptual learning in this stage may have significant improvements, like in early childhood. Despite this, not all of the synaptic mechanisms for plasticity shift back toward an immature state, like the GABA_A proteins that remain with mature subunits dominating could suggest an imbalance in the system at this time. Interestingly, none of the synaptic proteins studied in extrastriate areas V2d or V4 showed the a significant loss in

aging as found for many proteins in V1, even though vision studies have suggested that later developing high-order visual perceptions, like face recognition and motion perception, are the first to be lost in aging (Habak and Faubert, 2000; Wilson et al., 2011; Yu et al., 2006).

7.3 Future Directions

The work in this thesis contributes to the field by identifying expression of synaptic and non-synaptic proteins in the human visual cortex that contribute to neuroplasticity and visual perception at all stages across the lifespan. These findings will help the future of vision research in both animal models looking to translate mechanistic findings to human application, and for human researchers who are looking to identify neurobiological mechanisms that underlie perceptual behaviour in development and aging. The next step for this research is to identify where and how these synaptic mechanisms develop in a neural circuit, and different cell types across the lifespan. These results will help fine-tune the of resolution of functional imaging studies in humans by pinpointing neurobiological targets, and help broaden the impact of animal knock-out studies in humans across the lifespan.

References

- Abraham, W. C., & Bear, M. F. (1996). Metaplasticity: The plasticity of synaptic plasticity. *Trends in Neurosciences*, 19(4), 126–130. [http://doi.org/10.1016/S0166-2236\(96\)80018-X](http://doi.org/10.1016/S0166-2236(96)80018-X)
- Agervi, P., Nilsson, M., & Martin, L. (2010). Foveal function in children treated for amblyopia. *Acta Ophthalmologica*, 88(2), 222–226. <http://doi.org/10.1111/j.1755-3768.2008.01432.x>
- Aggarwal, S., Yurlova, L., & Simons, M. (2011). Central nervous system myelin: structure, synthesis and assembly. *Trends in Cell Biology*, 21(10), 585–593. <http://doi.org/10.1016/j.tcb.2011.06.004>
- Albright, T. D., Desimone, R., & Gross, C. G. (1984). Columnar Organization of Directionally Selective Cells in Visual Area Mt of the Macaque. *Journal of Neurophysiology*, 51(1), 16–31.
- Allard, R., Lagacé-Nadon, S., & Faubert, J. (2013a). Feature tracking and aging. *Frontiers in Psychology*, 4, 427. <http://doi.org/10.3389/fpsyg.2013.00427>
- Allard, R., Renaud, J., Molinatti, S., & Faubert, J. (2013b). Contrast sensitivity, healthy aging and noise. *Vision Research*, 92(C), 47–52. <http://doi.org/10.1016/j.visres.2013.09.004>
- Allen, D., Tyler, C. W., & Norcia, A. M. (1996). Development of Grating Acuity and Contrast Sensitivity in the Central and Peripheral Visual Field of the Human Infant. *Vision Research*, 36(13), 1945–1953. [http://doi.org/10.1016/0042-6989\(95\)00257-X](http://doi.org/10.1016/0042-6989(95)00257-X)
- Ang, L. C., Munoz, D. G., Shul, D., & George, D. H. (1991). Smi-32 Immunoreactivity in Human Striate Cortex During Postnatal-Development. *Brain Research. Developmental Brain Research*, 61(1), 103–109.
- Araque, A., Parpura, V., Sanzgiri, R. P., & Haydon, P. G. (1999). Tripartite synapses: glia, the unacknowledged partner. *Trends in Neurosciences*, 22(5), 208–215.
- Arden, G. B., Barnard, W. M., & Mushin, A. S. (1974). Visually Evoked-Responses in Amblyopia. *British Journal of Ophthalmology*, 58(3), 183–192.
- Artal, P., Guirao, A., Berrio, E., Piers, P., & Norrby, S. (2003). Optical aberrations and the aging eye. *International Ophthalmology Clinics*, 43(2), 63–77.
- Assaf, A. A. (1982). The Sensitive Period - Transfer of Fixation After Occlusion for Strabismic Amblyopia. *British Journal of Ophthalmology*, 66(1), 64–70.

- Bai, X., & Wong-Riley, M. T. T. (2003). Neuronal activity regulates protein and gene expressions of GluR2 in postnatal rat visual cortical neurons in culture. *Journal of Neurocytology*, 32(1), 71–78.
- Banerjee, A., Larsen, R. S., Philpot, B. D., & Paulsen, O. (2016). Roles of Presynaptic NMDA Receptors in Neurotransmission and Plasticity. *Trends in Neurosciences*, 39(1), 26–39. <http://doi.org/10.1016/j.tins.2015.11.001>
- Banks, M. S., Aslin, R. N., & Letson, R. D. (1975). Sensitive period for the development of human binocular vision. *Science*, 190(4215), 675–677.
- Barnes, C. A., Rao, G., & Shen, J. (1997). Age-related decrease in the N-methyl-D-aspartateR-mediated excitatory postsynaptic potential in hippocampal region CA1. *Nba*, 18(4), 445–452.
- Barria, A., & Malinow, R. (2002). Subunit-Specific NMDA Receptor Trafficking to Synapses. *Neuron*, 35(2), 1–9. [http://doi.org/10.1016/s0896-6273\(02\)00776-6](http://doi.org/10.1016/s0896-6273(02)00776-6)
- Baumann, N., & Pham-Dinh, D. (2001). Biology of oligodendrocyte and myelin in the mammalian central nervous system. *Physiological Reviews*, 81(2), 871–927.
- Bavelier, D., Levi, D. M., Li, R. W., Dan, Y., & Hensch, T. K. (2010). Removing Brakes on Adult Brain Plasticity: From Molecular to Behavioral Interventions. *Journal of Neuroscience*, 30(45), 14964–14971. <http://doi.org/10.1523/JNEUROSCI.4812-10.2010>
- Becker, L. E., Armstrong, D. L., Chan, F., & Wood, M. M. (1984). Dendritic development in human occipital cortical neurons. *Brain Research*, 315(1), 117–124.
- Bennett, P. J., Sekuler, R., & Sekuler, A. B. (2007). The effects of aging on motion detection and direction identification. *Vision Research*, 47(6), 799–809. <http://doi.org/10.1016/j.visres.2007.01.001>
- Beston, B. R., Jones, D. G., & Murphy, K. M. (2010). Experience-Dependent Changes in Excitatory and Inhibitory Receptor Subunit Expression in Visual Cortex. *Frontiers in Synaptic Neuroscience*, 2. <http://doi.org/10.3389/fnsyn.2010.00138>
- Betts, L. R., Sekuler, A. B., & Bennett, P. J. (2007). The effects of aging on orientation discrimination. *Vision Research*, 47(13), 1769–1780. <http://doi.org/10.1016/j.visres.2007.02.016>
- Betts, L. R., Taylor, C. P., Sekuler, A. B., & Bennett, P. J. (2005). Aging Reduces Center-Surround Antagonism in Visual Motion Processing. *Neuron*, 45(3), 361–366. <http://doi.org/10.1016/j.neuron.2004.12.041>

- Birch, E. E., Swanson, W. H., STAGER, D. R., WOODY, M., & EVERETT, M. (1993). Outcome After Very Early Treatment of Dense Congenital Unilateral Cataract. *Investigative Ophthalmology & Visual Science*, 34(13), 3687–3699.
- Birch, E. E., Shimojo, S., & Held, R. (1985). Preferential-looking assessment of fusion and stereopsis in infants aged 1-6 months. *Investigative ophthalmology & visual science*, 26(3), 366-370.
- Birch, E. E., & Holmes, J. M. (2010). The clinical profile of amblyopia in children younger than 3 years of age. *Journal of American Association for Pediatric Ophthalmology and Strabismus*, 14(6), 494-497.
- Blazquez-Llorca, L., García-Marín, V., & DeFelipe, J. (2010). GABAergic complex basket formations in the human neocortex. *The Journal of Comparative Neurology*, 518(24), 4917–4937. <http://doi.org/10.1002/cne.22496>
- Blumenthal, E. J., Bosworth, R. G., & Dobkins, K. R. (2013). Fast development of global motion processing in human infants. *Journal of Vision*, 13(13), 8–8. <http://doi.org/10.1167/13.13.8>
- Bogfjellmo, L. G., Bex, P. J., & Falkenberg, H. K. (2014). The development of global motion discrimination in school aged children. *Journal of Vision*, 14(2), 19–19. <http://doi.org/10.1167/14.2.19>
- Bouvier, G., Bidoret, C., Casado, M., & Paoletti, P. (2015). Presynaptic NMDA receptors: Roles and rules. *Neuroscience*, 311, 322–340. <http://doi.org/10.1016/j.neuroscience.2015.10.033>
- Braddick, O., Atkinson, J., Julesz, B., Kropfl, W., Bodis-Wollner, I., & Raab, E. (1980). Cortical binocularity in infants. *Nature*, 288(5789), 363–365.
- Brewer, A. A., & Barton, B. (2014). Visual cortex in aging and Alzheimer's disease: changes in visual field maps and population receptive fields. *Frontiers in Psychology*, 5, 74. <http://doi.org/10.3389/fpsyg.2014.00074>
- Bucher, K., Dietrich, T., Marcar, V. L., Brem, S., Halder, P., Boujraf, S., et al. (2006). Maturation of luminance- and motion-defined form perception beyond adolescence: A combined ERP and fMRI study. *NeuroImage*, 31(4), 1625–1636. <http://doi.org/10.1016/j.neuroimage.2006.02.032>
- Burkhalter, A. (1993). Development of forward and feedback connections between areas V1 and V2 of human visual cortex. *Cerebral Cortex*, 3(5), 476–487.
- Burkhalter, A., & Bernardo, K. L. (1989). Organization of corticocortical connections in human visual cortex. *Proceedings of the National Academy of Sciences*, 86(3), 1071–1075.

- Burkhalter, A., Bernardo, K. L., & Charles, V. (1993). Development of local circuits in human visual cortex. *Journal of Neuroscience*, *13*(5), 1916–1931.
- Cabungcal, J.-H., Steullet, P., Morishita, H., Kraftsik, R., Cuenod, M., Hensch, T. K., & Do, K. Q. (2013). Perineuronal nets protect fast-spiking interneurons against oxidative stress. *Proceedings of the National Academy of Sciences of the United States of America*, *110*(22), 9130–9135. <http://doi.org/10.1073/pnas.1300454110>
- Campbell, F. W., & Kulikowski, J. J. (1966). Orientational selectivity of the human visual system. *The Journal of Physiology*, *187*(2), 437–445. [http://doi.org/10.1111/\(ISSN\)1469-7793](http://doi.org/10.1111/(ISSN)1469-7793)
- Campbell, F. W., & Maffei, L. (1970). Electrophysiological evidence for the existence of orientation and size detectors in the human visual system. *The Journal of Physiology*, *207*(3), 635–652.
- Cantlon, J. F., Pineda, P., Dehaene, S., & Pelphrey, K. A. (2010). Cortical Representations of Symbols, Objects, and Faces Are Pruned Back during Early Childhood. *Cerebral Cortex*, *21*(1), 191–199. <http://doi.org/10.1093/cercor/bhq078>
- Carter, B. C., & Jahr, C. E. (2016). Postsynaptic, not presynaptic NMDA receptors are required for spike-timing-dependent LTD induction. *Nature Neuroscience*, *19*(9), 1218–1224. <http://doi.org/10.1038/nn.4343>
- Carulli, D., Pizzorusso, T., Kwok, J. C. F., Putignano, E., Poli, A., Forostyak, S., et al. (2010). Animals lacking link protein have attenuated perineuronal nets and persistent plasticity. *Brain*, *133*(8), 2331–2347. <http://doi.org/10.1093/brain/awq145>
- Chen, L., Cooper, N. G., & Mower, G. D. (2000). Developmental changes in the expression of NMDA receptor subunits (NR1, NR2A, NR2B) in the cat visual cortex and the effects of dark rearing. *Brain Research. Molecular Brain Research*, *78*(1-2), 196–200.
- Chen, L., Yang, C., & Mower, G. D. (2001). Developmental changes in the expression of GABA(A) receptor subunits (alpha(1), alpha(2), alpha(3)) in the cat visual cortex and the effects of dark rearing. *Brain Research. Molecular Brain Research*, *88*(1-2), 135–143.
- Chen, X., Levy, J. M., Hou, A., Winters, C., Azzam, R., Sousa, A. A., et al. (2015). PSD-95 family MAGUKs are essential for anchoring AMPA and NMDA receptor complexes at the postsynaptic density. *Proceedings of the National Academy of Sciences of the United States of America*, *112*(50), E6983–92. <http://doi.org/10.1073/pnas.1517045112>
- Cho, K. K. A., Khibnik, L., Philpot, B. D., & Bear, M. F. (2009). The ratio of NR2A/B NMDA receptor subunits determines the qualities of ocular dominance plasticity in visual cortex. *Proceedings of the National Academy of Sciences of the United States of America*, *106*(13), 5377–5382. <http://doi.org/10.1073/pnas.0808104106>

- Cingolani, L. A., Thalhammer, A., Yu, L. M. Y., Catalano, M., Ramos, T., Colicos, M. A., & Goda, Y. (2008). Activity-dependent regulation of synaptic AMPA receptor composition and abundance by beta3 integrins. *Neuron*, 58(5), 749–762. <http://doi.org/10.1016/j.neuron.2008.04.011>
- Conel, J. L. R. (1939). The postnatal development of the human cerebral cortex. Vol. 1. The cortex of the newborn.
- Conel, J. L. (1940). THE POST-NATAL DEVELOPMENT OF THE HUMAN CEREBRAL CORTEX. VOL. I. THE CORTEX OF THE NEWBORN. *The Journal of Nervous and Mental Disease*, 92(5), 689.
- Conel, J. L. (1941). The postnatal development of the human cerebral cortex: The cortex of the one-month infant.
- Conel, J. L. (1959). The Postnatal Development of the Human Cerebral Cortex: The Cortex of the Twenty-four-month Infant.
- Conel, J. L. (1963). The Postnatal Development of the Human Cerebral Cortex, V. 7: The Cortex of the Four-year Child. Harvard University Press.
- Conel, J. L. (1967). The postnatal development of the human cerebral cortex. Vol. 8: The cortex of the six-year child.
- Corlew, R., Wang, Y., Ghermazien, H., Erisir, A., & Philpot, B. D. (2007). Developmental switch in the contribution of presynaptic and postsynaptic NMDA receptors to long-term depression. *The Journal of Neuroscience : the Official Journal of the Society for Neuroscience*, 27(37), 9835–9845. <http://doi.org/10.1523/JNEUROSCI.5494-06.2007>
- Deen, B., Richardson, H., Dilks, D. D., Takahashi, A., Keil, B., Wald, L. L., et al. (2017). Organization of high-level visual cortex in human infants. *Nature Communications*, 8, 13995. <http://doi.org/10.1038/ncomms13995>
- Denison, R. N., Vu, A. T., Yacoub, E., Feinberg, D. A., & Silver, M. A. (2014). Functional mapping of the magnocellular and parvocellular subdivisions of human LGN. *NeuroImage*, 102, 358–369. <http://doi.org/10.1016/j.neuroimage.2014.07.019>
- Desai, N. S., Cudmore, R. H., Nelson, S. B., & Turrigiano, G. G. (2002). Critical periods for experience-dependent synaptic scaling in visual cortex. *Nature Neuroscience*, 1–8. <http://doi.org/10.1038/nn878>
- Desimone, R., & Schein, S. J. (1987). Visual properties of neurons in area V4 of the macaque: sensitivity to stimulus form. *Journal of Neurophysiology*, 57(3), 835–868.

- Dhar, S. S., Liang, H. L., & Wong-Riley, M. T. T. (2009). Nuclear respiratory factor 1 co-regulates AMPA glutamate receptor subunit 2 and cytochrome oxidase: tight coupling of glutamatergic transmission and energy metabolism in neurons. *Journal of Neurochemistry*, *108*(6), 1595–1606. <http://doi.org/10.1111/j.1471-4159.2009.05929.x>
- Di Cristo, G., Chattopadhyaya, B., Kuhlman, S. J., Fu, Y., Bélanger, M.-C., Wu, C. Z., et al. (2007). Activity-dependent PSA expression regulates inhibitory maturation and onset of critical period plasticity. *Nature Neuroscience*, *10*(12), 1569–1577. <http://doi.org/10.1038/nn2008>
- Ding, J., & Levi, D. M. (2011). Recovery of stereopsis through perceptual learning in human adults with abnormal binocular vision. *Proceedings of the National Academy of Sciences of the United States of America*, *108*(37), E733–41. <http://doi.org/10.1073/pnas.1105183108>
- Dinstein, I., Heeger, D. J., & Behrmann, M. (2015). Neural variability: friend or foe? *Trends in Cognitive Sciences*, *19*(6), 322–328. <http://doi.org/10.1016/j.tics.2015.04.005>
- Distler, C., Bachevalier, J., Kennedy, C., Mishkin, M., & Ungerleider, L. G. (1996). Functional development of the corticocortical pathway for motion analysis in the macaque monkey: a 14C-2-deoxyglucose study. *Cerebral Cortex*, *6*(2), 184–195.
- Dityatev, A., & Rusakov, D. A. (2011). Molecular signals of plasticity at the tetrapartite synapse. *Current Opinion in Neurobiology*, *21*(2), 353–359. <http://doi.org/10.1016/j.conb.2010.12.006>
- Dityatev, A., & Schachner, M. (2003). Extracellular matrix molecules and synaptic plasticity. *Nature Reviews Neuroscience*, *4*(6), 456–468. <http://doi.org/10.1038/nrn1115>
- Dityatev, A., & Schachner, M. (2006). The extracellular matrix and synapses. *Cell and Tissue Research*, *326*(2), 647–654. <http://doi.org/10.1007/s00441-006-0217-1>
- Dosher, B. A., & Lu, Z.-L. (2006). Level and mechanisms of perceptual learning: Learning first-order luminance and second-order texture objects. *Vision Research*, *46*(12), 1996–2007. <http://doi.org/10.1016/j.visres.2005.11.025>
- Du, Y., Zhang, F., Wang, Y., Bi, T., & Qiu, J. (2016). Perceptual Learning of Facial Expressions. *Vision Research*, *128*(C), 19–29. <http://doi.org/10.1016/j.visres.2016.08.005>
- Duffy, K. R., Murphy, K. M., Frosch, M. P., & Livingstone, M. S. (2007). Cytochrome Oxidase and Neurofilament Reactivity in Monocularly Deprived Human Primary Visual Cortex. *Cerebral Cortex*, *17*(6), 1283–1291. <http://doi.org/10.1093/cercor/bhl038>
- Duncan, C. E., Webster, M. J., Rothmond, D. A., Bahn, S., Elashoff, M., & Weickert, C. S. (2010). Prefrontal GABAA receptor $\alpha 1$ -subunit expression in normal postnatal human

- development and schizophrenia. *Journal of Psychiatric Research*, 44(10), 673–681. <http://doi.org/10.1016/j.jpsychires.2009.12.007>
- Dunning, D. D., Hoover, C. L., Soltesz, I., Smith, M. A., & O'Dowd, D. K. (1999). GABA(A) receptor-mediated miniature postsynaptic currents and alpha-subunit expression in developing cortical neurons. *Journal of Neurophysiology*, 82(6), 3286–3297.
- Ellemberg, D., Lewis, T. L., Liu, C. H., & Maurer, D. (1999). Development of spatial and temporal vision during childhood. *Vision Research*, 39(14), 2325–2333.
- Engel, S. A. (1994). Fmri of Human Visual-Cortex (Vol 369, Pg 525, 1994). *Nature*, 370(6485), 106–106.
- Engel, S., Zhang, X. M., & Wandell, B. (1997). Colour tuning in human visual cortex measured with functional magnetic resonance imaging. *Nature*, 388(6637), 68–71. <http://doi.org/10.1038/40398>
- Epelbaum, M., Milleret, C., Buisseret, P., & Duffer, J. L. (1993). The sensitive period for strabismic amblyopia in humans. *Ophthalmology*, 100(3), 323–327.
- Erchova, I., Vasalauskaite, A., Longo, V., & Sengpiel, F. (2017). Enhancement of visual cortex plasticity by dark exposure. *Philosophical Transactions of the Royal Society of London. Series B, Biological Sciences*, 372(1715), 20160159–9. <http://doi.org/10.1098/rstb.2016.0159>
- Erisir, A., & Harris, J. L. (2003). Decline of the critical period of visual plasticity is concurrent with the reduction of NR2B subunit of the synaptic NMDA receptor in layer 4. *The Journal of Neuroscience : the Official Journal of the Society for Neuroscience*, 23(12), 5208–5218.
- Fagiolini, M., & Hensch, T. K. (2000). Inhibitory threshold for critical-period activation in primary visual cortex. *Nature*, 404(6774), 183–186. <http://doi.org/10.1038/35004582>
- Fagiolini, M., Fritschy, J.-M., Löw, K., Möhler, H., Rudolph, U., & Hensch, T. K. (2004). Specific GABAA circuits for visual cortical plasticity. *Science*, 303(5664), 1681–1683. <http://doi.org/10.1126/science.1091032>
- Fagiolini, M., Katagiri, H., Miyamoto, H., Mori, H., Grant, S. G. N., Mishina, M., & Hensch, T. K. (2003). Separable features of visual cortical plasticity revealed by N-methyl-D-aspartate receptor 2A signaling. *Proceedings of the National Academy of Sciences*, 100(5), 2854–2859. <http://doi.org/10.1073/pnas.0536089100>
- Fellin, T., Pascual, O., & Haydon, P. G. (2006). Astrocytes coordinate synaptic networks: balanced excitation and inhibition. *Physiology (Bethesda, Md.)*, 21, 208–215. <http://doi.org/10.1152/physiol.00161.2005>

- Fernandez, R., Monacelli, A., & Duffy, C. J. (2013). Visual motion event related potentials distinguish aging and Alzheimer's disease. *Journal of Alzheimer's Disease : JAD*, 36(1), 177–183. <http://doi.org/10.3233/JAD-122053>
- Flint, A. C., Maisch, U. S., Weishaupt, J. H., Kriegstein, A. R., & Monyer, H. (1997). NR2A subunit expression shortens NMDA receptor synaptic currents in developing neocortex. *Journal of Neuroscience*, 17(7), 2469–2476.
- Fox, P. T., MINTUN, M. A., RAICHLE, M. E., MIEZIN, F. M., ALLMAN, J. M., & VANESSEN, D. C. (1986). Mapping Human Visual-Cortex with Positron Emission Tomography. *Nature*, 323(6091), 806–809. <http://doi.org/10.1038/323806a0>
- Gainey, M. A., Hurvitz-Wolff, J. R., Lambo, M. E., & Turrigiano, G. G. (2009). Synaptic Scaling Requires the GluR2 Subunit of the AMPA Receptor. *Journal of Neuroscience*, 29(20), 6479–6489. <http://doi.org/10.1523/JNEUROSCI.3753-08.2009>
- Gan, Q., Salussolia, C. L., & Wollmuth, L. P. (2014). Assembly of AMPA receptors: mechanisms and regulation. *The Journal of Physiology*, 593(1), 39–48. <http://doi.org/10.1113/jphysiol.2014.273755>
- Gao, X., Maurer, D., & Nishimura, M. (2010). Similarities and differences in the perceptual structure of facial expressions of children and adults. *Journal of Experimental Child Psychology*, 105(1-2), 98–115. <http://doi.org/10.1016/j.jecp.2009.09.001>
- Garrett, D. D., Samanez-Larkin, G. R., MacDonald, S. W. S., Lindenberger, U., McIntosh, A. R., & Grady, C. L. (2013). Moment-to-moment brain signal variability: A next frontier in human brain mapping? *Neuroscience and Biobehavioral Reviews*, 37(4), 610–624. <http://doi.org/10.1016/j.neubiorev.2013.02.015>
- Germine, L. T., Duchaine, B., & Nakayama, K. (2011). Where cognitive development and aging meet: Face learning ability peaks after age 30. *Cognition*, 118(2), 201–210. <http://doi.org/10.1016/j.cognition.2010.11.002>
- Glasser, A., & Campbell, M. C. (1999). Biometric, optical and physical changes in the isolated human crystalline lens with age in relation to presbyopia. *Vision Research*, 39(11), 1991–2015.
- Gogtay, N., Giedd, J. N., Lusk, L., Hayashi, K. M., Greenstein, D., Vaituzis, A. C., et al. (2004). Dynamic mapping of human cortical development during childhood through early adulthood. *Proceedings of the National Academy of Sciences*, 101(21), 8174–8179. <http://doi.org/10.1073/pnas.0402680101>
- Golarai, G., Liberman, A., Yoon, J. M. D., & Grill-Spector, K. (2010). Differential development of the ventral visual cortex extends through adolescence. *Frontiers in Human Neuroscience*, 3, 80. <http://doi.org/10.3389/neuro.09.080.2009>

- Gomez, J., Barnett, M. A., Natu, V., Mezer, A., Palomero-Gallagher, N., Weiner, K. S., et al. (2017). Microstructural proliferation in human cortex is coupled with the development of face processing. *Science*, 355(6320), 68–71. <http://doi.org/10.1126/science.aag0311>
- GOODALE, M. A., & MILNER, A. D. (1992). Separate Visual Pathways for Perception and Action. *Trends in Neurosciences*, 15(1), 20–25.
- Gordus, A., Pokala, N., Levy, S., Flavell, S. W., & Bargmann, C. I. (2015). Feedback from Network States Generates Variability in a Probabilistic Olfactory Circuit. *Cell*, 161(2), 215–227. <http://doi.org/10.1016/j.cell.2015.02.018>
- Grady, C. L., Haxby, J. V., Horwitz, B., Schapiro, M. B., Rapoport, S. I., Ungerleider, L. G., et al. (1992). Dissociation of Object and Spatial Vision in Human Extrastriate Cortex - Age-Related-Changes in Activation of Regional Cerebral Blood-Flow Measured with [O-15]Water and Positron Emission Tomography. *Journal of Cognitive Neuroscience*, 4(1), 23–34. <http://doi.org/10.1162/jocn.1992.4.1.23>
- Groc, L., Heine, M., Cousins, S. L., Stephenson, F. A., Lounis, B., Cognet, L., & Choquet, D. (2006). NMDA receptor surface mobility depends on NR2A-2B subunits. *Proceedings of the National Academy of Sciences*, 103(49), 18769–18774. <http://doi.org/10.1073/pnas.0605238103>
- Gu, Y., Tran, T., Murase, S., Borrell, A., Kirkwood, A., & Quinlan, E. M. (2016). Neuregulin-Dependent Regulation of Fast-Spiking Interneuron Excitability Controls the Timing of the Critical Period. *The Journal of Neuroscience : the Official Journal of the Society for Neuroscience*, 36(40), 10285–10295. <http://doi.org/10.1523/JNEUROSCI.4242-15.2016>
- Gutierrez-Igarza, K., Fogarty, D. J., Perez-Cerda, F., Donate-Oliver, F., Albus, K., & Matute, C. (1996). Localization of AMPA-selective glutamate receptor subunits in the adult cat visual cortex. *Visual neuroscience*, 13(1), 61-72.
- Gwiazda, J., Brill, S., Mohindra, I., & Held, R. (1980). Preferential looking acuity in infants from two to fifty-eight weeks of age. *American Journal of Optometry and Physiological Optics*, 57(7), 428–432.
- Habak, C., & Faubert, J. (2000). Larger effect of aging on the perception of higher-order stimuli. *Vision Research*, 40(8), 943–950.
- Hadad, B., Schwartz, S., Maurer, D., & Lewis, T. L. (2015). Motion perception: a review of developmental changes and the role of early visual experience. *Frontiers in Integrative Neuroscience*, 9(583), 5532–18. <http://doi.org/10.3389/fnint.2015.00049>
- Hadad, B.-S., Maurer, D., & Lewis, T. L. (2011). Long trajectory for the development of sensitivity to global and biological motion. *Developmental Science*, 14(6), 1330–1339. <http://doi.org/10.1111/j.1467-7687.2011.01078.x>

- Hall, B. J., Ripley, B., & Ghosh, A. (2007). NR2B signaling regulates the development of synaptic AMPA receptor current. *The Journal of Neuroscience : the Official Journal of the Society for Neuroscience*, 27(49), 13446–13456. <http://doi.org/10.1523/JNEUROSCI.3793-07.2007>
- Hartshorne, J. K., & Germine, L. T. (2015). When does cognitive functioning peak? The asynchronous rise and fall of different cognitive abilities across the life span. *Psychological Science*, 26(4), 433–443. <http://doi.org/10.1177/0956797614567339>
- Hasnain, M. K., Fox, P. T., & Woldorff, M. G. (1998). Intersubject variability of functional areas in the human visual cortex. *Human Brain Mapping*, 6(4), 301–315.
- Haxby, J. V., Grady, C. L., Horwitz, B., Ungerleider, L. G., Mishkin, M., Carson, R. E., et al. (1991a). Dissociation of object and spatial visual processing pathways in human extrastriate cortex. *Proceedings of the National Academy of Sciences*, 88(5), 1621–1625.
- Haxby, J. V., Grady, C. L., Ungerleider, L. G., & Horwitz, B. (1991b). Mapping the Functional Neuroanatomy of the Intact Human Brain with Brain Work Imaging. *Neuropsychologia*, 29(6), 539–555.
- Haxby, J. V., Horwitz, B., Ungerleider, L. G., Maisog, J. M., Pietrini, P., & Grady, C. L. (1994). The functional organization of human extrastriate cortex: a PET-rCBF study of selective attention to faces and locations. *Journal of Neuroscience*, 14(11 Pt 1), 6336–6353.
- He, Y., Hof, P. R., Janssen, W. G., Vissavajjhala, P., & Morrison, J. H. (2001). AMPA GluR2 subunit is differentially distributed on GABAergic neurons and pyramidal cells in the macaque monkey visual cortex. *Brain Research*, 921(1-2), 60–67.
- Heinen, K., Baker, R. E., Spijker, S., Rosahl, T., van Pelt, J., & Brussaard, A. B. (2003). Impaired dendritic spine maturation in GABAA receptor $\alpha 1$ subunit knock out mice. *Neuroscience*, 122(3), 699–705. [http://doi.org/10.1016/S0306-4522\(03\)00477-9](http://doi.org/10.1016/S0306-4522(03)00477-9)
- Heinen, K., Bosman, L. W. J., Spijker, S., van Pelt, J., Smit, A. B., Voorn, P., et al. (2004). Gabaa receptor maturation in relation to eye opening in the rat visual cortex. *Neuroscience*, 124(1), 161–171. <http://doi.org/10.1016/j.neuroscience.2003.11.004>
- Held, R., Birch, E., & Gwiazda, J. (1980). Stereoacuity of human infants. *Proceedings of the National Academy of Sciences*, 77(9), 5572–5574.
- Hendry, S. H., Huntsman, M. M., Viñuela, A., Möhler, H., de Blas, A. L., & Jones, E. G. (1994). GABAA receptor subunit immunoreactivity in primate visual cortex: distribution in macaques and humans and regulation by visual input in adulthood. *Journal of Neuroscience*, 14(4), 2383–2401.

- Henley, J. M., & Wilkinson, K. A. (2016). Synaptic AMPA receptor composition in development, plasticity and disease. *Nature Reviews Neuroscience*, *17*(6), 337–350. <http://doi.org/10.1038/nrn.2016.37>
- Hensch, T. K., Fagiolini, M., Mataga, N., Stryker, M. P., Baekkeskov, S., & Kash, S. F. (1998). Local GABA circuit control of experience-dependent plasticity in developing visual cortex. *Science*, *282*(5393), 1504–1508. <http://doi.org/10.1126/science.282.5393.1504>
- Herguedas, B., Garcia-Nafria, J., Cais, O., Fernandez-Leiro, R., Krieger, J., Ho, H., & Greger, I. H. (2016). Structure and organization of heteromeric AMPA-type glutamate receptors. *Science*, *352*(6285), aad3873–aad3873. <http://doi.org/10.1126/science.aad3873>
- Hohmann, A., & Creutzfeldt, O. D. (1975). Squint and the development of binocularity in humans. *Nature*, *254*(5501), 613–614.
- Holmes, J. M. (2011). Effect of Age on Response to Amblyopia Treatment in Children. *Archives of Ophthalmology*, *129*(11), 1451–7. <http://doi.org/10.1001/archophthalmol.2011.179>
- Hood, B., Atkinson, J., Braddick, O., & Wattam-Bell, J. (1992). Orientation selectivity in infancy: behavioural evidence for temporal sensitivity. *Perception*, *21*(3), 351–354. <http://doi.org/10.1068/p210351>
- Horton, J. C., & Hedley-Whyte, E. T. (1984). Mapping of cytochrome oxidase patches and ocular dominance columns in human visual cortex. *Philosophical Transactions of the Royal Society B: Biological Sciences*, *304*(1119), 255–272.
- Horton, J. C., & HUBEL, D. H. (1981). Regular patchy distribution of cytochrome oxidase staining in primary visual cortex of macaque monkey. *Nature*, *292*(5825), 762–764.
- Huang, X., Stodieck, S. K., Goetze, B., Cui, L., Wong, M. H., Wenzel, C., et al. (2015). Progressive maturation of silent synapses governs the duration of a critical period. *Proceedings of the National Academy of Sciences*, *112*(24), E3131–E3140. <http://doi.org/10.1073/pnas.1506488112>
- Huang, Z. J., Kirkwood, A., Pizzorusso, T., Porciatti, V., Morales, B., Bear, M. F., et al. (1999). BDNF regulates the maturation of inhibition and the critical period of plasticity in mouse visual cortex. *Cell*, *98*(6), 739–755.
- HUBEL, D. H., & WIESEL, T. N. (1959). Receptive fields of single neurones in the cat's striate cortex. *The Journal of Physiology*, *148*(3), 574–591.
- HUBEL, D. H., & WIESEL, T. N. (1962). Receptive fields, binocular interaction and functional architecture in the cat's visual cortex. *The Journal of Physiology*, *160*(1), 106–154. [http://doi.org/10.1111/\(ISSN\)1469-7793](http://doi.org/10.1111/(ISSN)1469-7793)

- HUBEL, D. H., & WIESEL, T. N. (1970). The period of susceptibility to the physiological effects of unilateral eye closure in kittens. *The Journal of Physiology*, 206(2), 419–436.
- Huntley, G. W., Vickers, J. C., Janssen, W., Brose, N., Heinemann, S. F., & Morrison, J. H. (1994). Distribution and synaptic localization of immunocytochemically identified NMDA receptor subunit proteins in sensory-motor and visual cortices of monkey and human. *Journal of Neuroscience*, 14(6), 3603–3619.
- Hussain, Z., Sekuler, A. B., & Bennett, P. J. (2009). How much practice is needed to produce perceptual learning? *Vision Research*, 49(21), 2624–2634. <http://doi.org/10.1016/j.visres.2009.08.022>
- Hutchinson, C. V., Arena, A., Allen, H. A., & Ledgeway, T. (2012). Psychophysical correlates of global motion processing in the aging visual system: A critical review. *Neuroscience and Biobehavioral Reviews*, 36(4), 1266–1272. <http://doi.org/10.1016/j.neubiorev.2012.02.009>
- Huttenlocher, P. R. (1990). Morphometric Study of Human Cerebral-Cortex Development. *Neuropsychologia*, 28(6), 517–527.
- Huttenlocher, P. R., de Courten, C., Garey, L. J., & Van der Loos, H. (1982). Synaptogenesis in human visual cortex--evidence for synapse elimination during normal development. *Neuroscience Letters*, 33(3), 247–252.
- Imamura, K., Shirao, T., Mori, K., & Obata, K. (1992). Changes of drebrin expression in the visual cortex of the cat during development. *Neuroscience Research*, 13(1), 33–41.
- Jando, G., Miko-Barath, E., Marko, K., Hollody, K., Toeroek, B., & Kovacs, I. (2012). Early-onset binocularity in preterm infants reveals experience-dependent visual development in humans. *Proceedings of the National Academy of Sciences*, 109(27), 11049–11052. <http://doi.org/10.1073/pnas.1203096109>
- Jehee, J. F. M., Ling, S., Swisher, J. D., van Bergen, R. S., & Tong, F. (2012). Perceptual learning selectively refines orientation representations in early visual cortex. *The Journal of Neuroscience : the Official Journal of the Society for Neuroscience*, 32(47), 16747–53a. <http://doi.org/10.1523/JNEUROSCI.6112-11.2012>
- Jiang, B., Huang, S., de Pasquale, R., Millman, D., Song, L., Lee, H.-K., et al. (2010). The maturation of GABAergic transmission in visual cortex requires endocannabinoid-mediated LTD of inhibitory inputs during a critical period. *Neuron*, 66(2), 248–259. <http://doi.org/10.1016/j.neuron.2010.03.021>
- Karni, A., & Bertini, G. (1997). Learning perceptual skills: behavioral probes into adult cortical plasticity. *Current Opinion in Neurobiology*, 7(4), 530–535.

- Kavcic, V., Martin, T., & Zalar, B. (2013). Aging effects on visual evoked potentials (VEPs) for motion direction discrimination. *International Journal of Psychophysiology*, *89*(1), 78–87. <http://doi.org/10.1016/j.ijpsycho.2013.05.012>
- Kinney, J. W., Davis, C. N., Tabarean, I., Conti, B., Bartfai, T., & Behrens, M. M. (2006). A specific role for NR2A-containing NMDA receptors in the maintenance of parvalbumin and GAD67 immunoreactivity in cultured interneurons. *The Journal of Neuroscience : the Official Journal of the Society for Neuroscience*, *26*(5), 1604–1615. <http://doi.org/10.1523/JNEUROSCI.4722-05.2006>
- Kirkwood, A., & Bear, M. F. (1994). Hebbian Synapses in Visual-Cortex. *Journal of Neuroscience*, *14*(3), 1634–1645.
- Klausberger, T., Roberts, J. D. B., & Somogyi, P. (2002). Cell type- and input-specific differences in the number and subtypes of synaptic GABA(A) receptors in the hippocampus. *The Journal of Neuroscience : the Official Journal of the Society for Neuroscience*, *22*(7), 2513–2521.
- Kleinschmidt, A., Bear, M. F., & Singer, W. (1987). Blockade of Nmda Receptors Disrupts Experience-Dependent Plasticity of Kitten Striate Cortex. *Science*, *238*(4825), 355–358. <http://doi.org/10.1126/science.2443978>
- KLEKAMP, J., RIEDEL, A., HARPER, C., & KRETSCHMANN, H. J. (1991). Quantitative Changes During the Postnatal Maturation of the Human Visual-Cortex. *Journal of the Neurological Sciences*, *103*(2), 136–143.
- Konar, Y., Bennett, P. J., & Sekuler, A. B. (2013). Effects of aging on face identification and holistic face processing. *Vision Research*, *88*(C), 38–46. <http://doi.org/10.1016/j.visres.2013.06.003>
- Kooijmans, R. N., Self, M. W., Wouterlood, F. G., Belien, J. A. M., & Roelfsema, P. R. (2014). Inhibitory Interneuron Classes Express Complementary AMPA-Receptor Patterns in Macaque Primary Visual Cortex. *Journal of Neuroscience*, *34*(18), 6303–6315. <http://doi.org/10.1523/JNEUROSCI.3188-13.2014>
- Kougioumtzidou, E., Shimizu, T., Hamilton, N. B., Tohyama, K., Sprengel, R., Monyer, H., et al. (2017). Signalling through AMPA receptors on oligodendrocyte precursors promotes myelination by enhancing oligodendrocyte survival. *eLife*, *6*, 31. <http://doi.org/10.7554/eLife.28080>
- Kovacs, I., Kozma, P., Fehér, A., & Benedek, G. (1999). Late maturation of visual spatial integration in humans. *Proceedings of the National Academy of Sciences*, *96*(21), 12204–12209.

- Kuhlman, S. J., Olivas, N. D., Tring, E., Ikrar, T., Xu, X., & Trachtenberg, J. T. (2013). A disinhibitory microcircuit initiates critical-period plasticity in the visual cortex. *Nature*, *501*(7468), 543–546. <http://doi.org/10.1038/nature12485>
- Kumar, S. S., Bacci, A., Kharazia, V., & Huguenard, J. R. (2002). A developmental switch of AMPA receptor subunits in neocortical pyramidal neurons. *The Journal of Neuroscience : the Official Journal of the Society for Neuroscience*, *22*(8), 3005–3015.
- Leat, S. J., Yadav, N. K., & Irving, E. L. (2010). Development of Visual Acuity and Contrast Sensitivity in Children. *Journal of Optometry*, *2*(1), 19–26. <http://doi.org/10.3921/joptom.2009.19>
- Lee, F. H. F., Su, P., Xie, Y.-F., Wang, K. E., Wan, Q., & Liu, F. (2016). Disrupting GluA2-GAPDH Interaction Affects Axon and Dendrite Development. *Scientific Reports*, 1–15. <http://doi.org/10.1038/srep30458>
- Lee, S.-H., Kwan, A. C., & Dan, Y. (2014a). Interneuron subtypes and orientation tuning. *Nature*, *508*(7494), E1–E2. <http://doi.org/10.1038/nature13128>
- Lee, S.-H., Kwan, A. C., Zhang, S., Phoumthippavong, V., Flannery, J. G., Masmanidis, S. C., et al. (2014b). Activation of specific interneurons improves V1 feature selectivity and visual perception. *Nature*, *488*(7411), 379–383. <http://doi.org/10.1038/nature11312>
- LEINFELDER, P. J. (1962). Amblyopia associated with congenital cataract. *Transactions of the American Ophthalmological Society*, *60*, 236–242.
- Leuba, G., & Garey, L. J. (1987). Evolution of neuronal numerical density in the developing and aging human visual cortex. *Human Neurobiology*, *6*(1), 11–18.
- Leventhal, A. G. (2003). GABA and Its Agonists Improved Visual Cortical Function in Senescent Monkeys. *Science*, *300*(5620), 812–815. <http://doi.org/10.1126/science.1082874>
- Levi, D. M. (1975). Patterned and Unpatterned Visual Evoked-Responses in Strabismic and Anisometric Amblyopia. *American Journal of Optometry and Physiological Optics*, *52*(7), 455–464.
- Levi, D. M. (2005). Perceptual learning in adults with amblyopia: a reevaluation of critical periods in human vision. *Developmental Psychobiology*, *46*(3), 222–232. <http://doi.org/10.1002/dev.20050>
- Levi, D. M., & Klein, S. (1982). Hyperacuity and amblyopia. *Nature*, *298*(5871), 268–270.
- Levi, D. M., & Li, R. W. (2009). Perceptual learning as a potential treatment for amblyopia: a mini-review. *Vision Research*, *49*(21), 2535–2549. <http://doi.org/10.1016/j.visres.2009.02.010>

- Levi, D. M., & Polat, U. (1996). Neural plasticity in adults with amblyopia. *Proceedings of the National Academy of Sciences*, *93*(13), 6830–6834.
- Levi, D. M., McKee, S. P., & Movshon, J. A. (2011). Visual deficits in anisometropia. *Vision Research*, *51*(1), 48–57. <http://doi.org/10.1016/j.visres.2010.09.029>
- Levi, D. M., Yu, C., Kuai, S.-G., & Rislove, E. (2007). Global contour processing in amblyopia. *Vision Research*, *47*(4), 512–524. <http://doi.org/10.1016/j.visres.2006.10.014>
- Lewis, T. L., & Maurer, D. (2005). Multiple sensitive periods in human visual development: Evidence from visually deprived children. *Developmental Psychobiology*, *46*(3), 163–183. <http://doi.org/10.1002/dev.20055>
- Lewis, T. L., & Maurer, D. (2009). Effects of Early Pattern Deprivation on Visual Development. *Optometry and Vision Science : Official Publication of the American Academy of Optometry*, *86*(6), 640–646. <http://doi.org/10.1097/OPX.0b013e3181a7296b>
- Li, C., Xiao, L., Liu, X., Yang, W., Shen, W., Hu, C., et al. (2013). A functional role of NMDA receptor in regulating the differentiation of oligodendrocyte precursor cells and remyelination. *Glia*, *61*(5), 732–749. <http://doi.org/10.1002/glia.22469>
- Li, R. W., & Levi, D. M. (2004). Characterizing the mechanisms of improvement for position discrimination in adult amblyopia. *Journal of Vision*, *4*(6), 7–7. <http://doi.org/10.1167/4.6.7>
- Li, R. W., Young, K. G., Hoenig, P., & Levi, D. M. (2005). Perceptual learning improves visual performance in juvenile amblyopia. *Investigative Ophthalmology & Visual Science*, *46*(9), 3161–3168. <http://doi.org/10.1167/iovs.05-0286>
- Liao, D., Scannevin, R. H., & Huganir, R. (2001). Activation of silent synapses by rapid activity-dependent synaptic recruitment of AMPA receptors. *The Journal of Neuroscience : the Official Journal of the Society for Neuroscience*, *21*(16), 6008–6017.
- Liao, M., Zhao, H., Liu, L., Li, Q., Dai, Y., Zhang, Y., & Zhou, Y. (2016). Training to improve contrast sensitivity in amblyopia: correction of high-order aberrations. *Scientific Reports*, 1–8. <http://doi.org/10.1038/srep35702>
- Liu, S., & Cull-Candy, S. G. (2000). Synaptic activity at calcium-permeable AMPA receptors induces a switch in receptor subtype. *Nature*, *405*(6785), 454–458. <http://doi.org/10.1038/35013064>
- Livingstone, M. S., & HUBEL, D. H. (1987). Psychophysical Evidence for Separate Channels for the Perception of Form, Color, Movement, and Depth. *Journal of Neuroscience*, *7*(11), 3416–3468.

- LIVINGSTONE, M., & HUBEL, D. (1988). Segregation of Form, Color, Movement, and Depth - Anatomy, Physiology, and Perception. *Science*, 240(4853), 740–749.
- Lu, H. D., & Roe, A. W. (2008). Functional Organization of Color Domains in V1 and V2 of Macaque Monkey Revealed by Optical Imaging. *Cerebral Cortex*, 18(3), 516–533. <http://doi.org/10.1093/cercor/bhm081>
- Lundgaard, I., Luzhynskaya, A., Stockley, J. H., Wang, Z., Evans, K. A., Swire, M., et al. (2013). Neuregulin and BDNF Induce a Switch to NMDA Receptor-Dependent Myelination by Oligodendrocytes. *PLoS Biology*, 11(12), e1001743. <http://doi.org/10.1371/journal.pbio.1001743>
- Luu, J. Y., & Levi, D. M. (2013). Sensitivity to synchronicity of biological motion in normal and amblyopic vision. *Vision Research*, 83(C), 9–18. <http://doi.org/10.1016/j.visres.2013.02.012>
- Maffei, A., Nataraj, K., Nelson, S. B., & Turrigiano, G. G. (2006). Potentiation of cortical inhibition by visual deprivation. *Nature*, 443(7107), 81–84. <http://doi.org/10.1038/nature05079>
- Maffei, A., Nelson, S. B., & Turrigiano, G. G. (2004). Selective reconfiguration of layer 4 visual cortical circuitry by visual deprivation. *Nature Neuroscience*, 7(12), 1353–1359. <http://doi.org/10.1038/nn1351>
- Malikovic, A., Vucetic, B., Milisavljevic, M., Tosevski, J., Sazdanovic, P., Milojevic, B., & Malobabic, S. (2011). Occipital sulci of the human brain: variability and morphometry. *Anatomical Science International*, 87(2), 61–70. <http://doi.org/10.1007/s12565-011-0118-6>
- MARGARET T T WONG-RILEY, P. J. (2002). AMPA glutamate receptor subunit 2 in normal and visually deprived macaque visual cortex. *Doi.org*, 1–11. <http://doi.org/10.1017/S0952523802195022>
- Maurer, D., Lewis, T. L., Brent, H. P., & Levin, A. V. (1999). Rapid Improvement in the Acuity of Infants After Visual Input. *Science*, 286(5437), 108–110. <http://doi.org/10.1126/science.286.5437.108>
- Mavroudis, I. A., Manani, M. G., Petrides, F., Dados, D., Ciobica, A., Padurariu, M., et al. (2015). Age-related dendritic and spinal alterations of pyramidal cells of the human visual cortex. *Folia Neuropathologica*, 53(2), 100–110. <http://doi.org/10.5114/fn.2015.52406>
- McGee, A. W., Yang, Y., Fischer, Q. S., Daw, N. W., & Strittmatter, S. M. (2005). Experience-driven plasticity of visual cortex limited by myelin and Nogo receptor. *Science*, 309(5744), 2222–2226. <http://doi.org/10.1126/science.1114362>

- McKee, S. P., Levi, D. M., & Movshon, J. A. (2003). The pattern of visual deficits in amblyopia. *Journal of Vision*, 3(5), 380–405. <http://doi.org/10.1167/3.5.5>
- McMahon, D. B. T., & Leopold, D. A. (2012). Stimulus Timing-Dependent Plasticity in High-Level Vision. *Current Biology*, 22(4), 332–337. <http://doi.org/10.1016/j.cub.2012.01.003>
- Meier, K., & Giaschi, D. (2017). Effect of spatial and temporal stimulus parameters on the maturation of global motion perception. *Vision Research*, 135, 1–9. <http://doi.org/10.1016/j.visres.2017.04.004>
- Mele, M., Leal, G., & Duarte, C. B. (2016). Role of GABA AR trafficking in the plasticity of inhibitory synapses. *Journal of Neurochemistry*, 139(6), 997–1018. <http://doi.org/10.1111/jnc.13742>
- Michel, A. E., & Garey, L. J. (1984). The development of dendritic spines in the human visual cortex. *Human Neurobiology*, 3(4), 223–227.
- Micheva, K. D., Wolman, D., Mensh, B. D., Pax, E., Buchanan, J., Smith, S. J., & Bock, D. D. (2016). A large fraction of neocortical myelin ensheathes axons of local inhibitory neurons. *eLife*, 5, 3347. <http://doi.org/10.7554/eLife.15784>
- Micu, I., Jiang, Q., Coderre, E., Ridsdale, A., Zhang, L., Woulfe, J., et al. (2005). NMDA receptors mediate calcium accumulation in myelin during chemical ischaemia. *Nature*, 1–5. <http://doi.org/10.1038/nature04474>
- Miller, D. J., Duka, T., Stimpson, C. D., Schapiro, S. J., Baze, W. B., McArthur, M. J., et al. (2012). Prolonged myelination in human neocortical evolution. *Proceedings of the National Academy of Sciences of the United States of America*, 109(41), 16480–16485. <http://doi.org/10.1073/pnas.1117943109>
- Mintz-Hittner, H. A., & Fernandez, K. M. (2000). Successful amblyopia therapy initiated after age 7 years: compliance cures. *Archives of Ophthalmology*, 118(11), 1535–1541.
- Mishkin, M., Ungerleider, L. G., & MACKO, K. A. (1983). Object Vision and Spatial Vision - 2 Cortical Pathways. *Trends in Neurosciences*, 6(10), 414–417. [http://doi.org/10.1016/0166-2236\(83\)90190-X](http://doi.org/10.1016/0166-2236(83)90190-X)
- Mitchell, D. E., Freeman, R. D., Millodot, M., & HAEGERSTROM, G. (1973). Meridional Amblyopia - Evidence for Modification of Human Visual System by Early Visual Experience. *Vision Research*, 13(3), 535–

- Mondloch, C. J., Le Grand, R., & Maurer, D. (2002). Configural Face Processing Develops more Slowly than Featural Face Processing. *Perception*, 31(5), 553–566. <http://doi.org/10.1068/p3339>
- Monyer, H., Burnashev, N., Laurie, D. J., Sakmann, B., & Seeburg, P. H. (1994). Developmental and regional expression in the rat brain and functional properties of four NMDA receptors. *Neuron*, 12(3), 529–540.
- Monyer, H., Sprengel, R., Schoepfer, R., Herb, A., Higuchi, M., Lomeli, H., et al. (1992). Heteromeric NMDA receptors: molecular and functional distinction of subtypes. *Science*, 256(5060), 1217–1221.
- MORRONE, M. C., & BURR, D. C. (1986). Evidence for the Existence and Development of Visual Inhibition in Humans. *Nature*, 321(6067), 235–237. <http://doi.org/10.1038/321235a0>
- Mrsic-Flogel, T. D., Hofer, S. B., Ohki, K., Reid, R. C., Bonhoeffer, T., & Hübener, M. (2007). Homeostatic Regulation of Eye-Specific Responses in Visual Cortex during Ocular Dominance Plasticity. *Neuron*, 54(6), 961–972. <http://doi.org/10.1016/j.neuron.2007.05.028>
- Mukherjee, J., Kretschmannova, K., Gouzer, G., Maric, H.-M., Ramsden, S., Tretter, V., et al. (2011). The residence time of GABA(A)Rs at inhibitory synapses is determined by direct binding of the receptor $\alpha 1$ subunit to gephyrin. *The Journal of Neuroscience : the Official Journal of the Society for Neuroscience*, 31(41), 14677–14687. <http://doi.org/10.1523/JNEUROSCI.2001-11.2011>
- Murayama, Y., Fujita, I., & Kato, M. (1997). Contrasting forms of synaptic plasticity in monkey inferotemporal and primary visual cortices. *NeuroReport*, 8(6), 1503–1508.
- Nahmani, M., & Turrigiano, G. G. (2014). Deprivation-induced strengthening of presynaptic and postsynaptic inhibitory transmission in layer 4 of visual cortex during the critical period. *The Journal of Neuroscience : the Official Journal of the Society for Neuroscience*, 34(7), 2571–2582. <http://doi.org/10.1523/JNEUROSCI.4600-13.2014>
- Norcia, A. M., & Tyler, C. W. (1985). Spatial frequency sweep VEP: visual acuity during the first year of life. *Vision Research*, 25(10), 1399–1408.
- Nurminen, L., Kilpeläinen, M., Laurinen, P., & Vanni, S. (2009). Area summation in human visual system: psychophysics, fMRI, and modeling. *Journal of Neurophysiology*, 102(5), 2900–2909. <http://doi.org/10.1152/jn.00201.2009>
- Nyíri, G., Freund, T. F., & Somogyi, P. (2001). Input-dependent synaptic targeting of alpha(2)-subunit-containing GABA(A) receptors in synapses of hippocampal pyramidal cells of the rat. *European Journal of Neuroscience*, 13(3), 428–442.

- Oberheim, N. A., Takano, T., Han, X., He, W., Lin, J. H. C., Wang, F., et al. (2009). Uniquely hominid features of adult human astrocytes. *The Journal of Neuroscience : the Official Journal of the Society for Neuroscience*, 29(10), 3276–3287. <http://doi.org/10.1523/JNEUROSCI.4707-08.2009>
- Owens, D. F., & Kriegstein, A. R. (2002). Is there more to gaba than synaptic inhibition? *Nature Reviews Neuroscience*, 3(9), 715–727. <http://doi.org/10.1038/nrn919>
- Owsley, C. (2011). Aging and vision. *Vision Research*, 51(13), 1610–1622. <http://doi.org/10.1016/j.visres.2010.10.020>
- OWSLEY, C., Sekuler, R., & SIEMSEN, D. (1983). Contrast Sensitivity Throughout Adulthood. *Vision Research*, 23(7), 689–699.
- Paoletti, P., Bellone, C., & Zhou, Q. (2013). NMDA receptor subunit diversity: impact on receptor properties, synaptic plasticity and disease, 1–18. <http://doi.org/10.1038/nrn3504>
- Papouin, T., Dunphy, J., Tolman, M., Foley, J. C., & Haydon, P. G. (2017). Astrocytic control of synaptic function. *Philosophical Transactions of the Royal Society of London. Series B, Biological Sciences*, 372(1715), 20160154–8. <http://doi.org/10.1098/rstb.2016.0154>
- Pellegrini-Giampietro, D. E., Bennett, M. V., & Zukin, R. S. (1992). Are Ca(2+)-permeable kainate/AMPA receptors more abundant in immature brain? *Neuroscience Letters*, 144(1-2), 65–69.
- Perea, G., Yang, A., Boyden, E. S., & Sur, M. (2014). Optogenetic astrocyte activation modulates response selectivity of visual cortex neurons in vivo. *Nature Communications*, 5, 3262. <http://doi.org/10.1038/ncomms4262>
- Peters, A., & Sethares, C. (2003). Is there remyelination during aging of the primate central nervous system? *The Journal of Comparative Neurology*, 460(2), 238–254. <http://doi.org/10.1002/cne.10639>
- Peters, A., Moss, M. B., & Sethares, C. (2000). Effects of aging on myelinated nerve fibers in monkey primary visual cortex. *The Journal of Comparative Neurology*, 419(3), 364–376. Retrieved from <http://eutils.ncbi.nlm.nih.gov/entrez/eutils/elink.fcgi?dbfrom=pubmed&id=10723011&retmode=ref&cmd=prlinks>
- Peters, A., Verderosa, A., & Sethares, C. (2008). The neuroglial population in the primary visual cortex of the aging rhesus monkey. *Glia*, 56(11), 1151–1161. <http://doi.org/10.1002/glia.20686>
- Petrini, E. M., Ravasenga, T., Hausrat, T. J., Iurilli, G., Olcese, U., Racine, V., et al. (2014). Synaptic recruitment of gephyrin regulates surface GABAA receptor dynamics for the

- expression of inhibitory LTP. *Nature Communications*, 5, 3921. <http://doi.org/10.1038/ncomms4921>
- Philpot, B. D., Cho, K. K. A., & Bear, M. F. (2007). Obligatory role of NR2A for metaplasticity in visual cortex. *Neuron*, 53(4), 495–502. <http://doi.org/10.1016/j.neuron.2007.01.027>
- Philpot, B. D., Espinosa, J. S., & Bear, M. F. (2003). Evidence for altered NMDA receptor function as a basis for metaplasticity in visual cortex. *Journal of Neuroscience*, 23(13), 5583–5588.
- Philpot, B. D., Sekhar, A. K., Shouval, H. Z., & Bear, M. F. (2001). Visual experience and deprivation bidirectionally modify the composition and function of NMDA receptors in visual cortex. *Neuron*, 29(1), 157–169.
- Pinto, J. G. A., Hornby, K. R., Jones, D. G., & Murphy, K. M. (2010). Developmental changes in GABAergic mechanisms in human visual cortex across the lifespan. *Frontiers in Cellular Neuroscience*, 4, 16. <http://doi.org/10.3389/fncel.2010.00016>
- Pinto, J. G. A., Jones, D. G., Williams, C. K., & Murphy, K. M. (2015). Characterizing synaptic protein development in human visual cortex enables alignment of synaptic age with rat visual cortex. *Frontiers in Neural Circuits*, 9, 3. <http://doi.org/10.3389/fncir.2015.00003>
- PIRCHIO, M., SPINELLI, D., FIORENTINI, A., & Maffei, L. (1978). Infant Contrast Sensitivity Evaluated by Evoked-Potentials. *Brain Research*, 141(1), 179–184.
- Pizzorusso, T. (2002). Reactivation of Ocular Dominance Plasticity in the Adult Visual Cortex. *Science*, 298(5596), 1248–1251. <http://doi.org/10.1126/science.1072699>
- Polat, U., Ma-Naim, T., Belkin, M., & Sagi, D. (2004). Improving vision in adult amblyopia by perceptual learning. *Proceedings of the National Academy of Sciences*, 101(17), 6692–6697. <http://doi.org/10.1073/pnas.0401200101>
- Polat, U., Sagi, D., & Norcia, A. M. (1997). Abnormal long-range spatial interactions in amblyopia. *Vision Research*, 37(6), 737–744.
- Pozo, K., Cingolani, L. A., Bassani, S., Laurent, F., Passafaro, M., & Goda, Y. (2012). $\beta 3$ integrin interacts directly with GluA2 AMPA receptor subunit and regulates AMPA receptor expression in hippocampal neurons. *Proceedings of the National Academy of Sciences of the United States of America*, 109(4), 1323–1328. <http://doi.org/10.1073/pnas.1113736109>
- Prange, O., Wong, T. P., Gerrow, K., Wang, Y. T., & El-Husseini, A. (2004). A balance between excitatory and inhibitory synapses is controlled by PSD-95 and neuroligin. *Proceedings of the National Academy of Sciences*, 101(38), 13915–13920. <http://doi.org/10.1073/pnas.0405939101>

- Priya, A., Johar, K., Nair, B., & Wong-Riley, M. T. T. (2014a). Nuclear respiratory factor 2 regulates the transcription of AMPA receptor subunit GluA2 (Gria2). *BBA - Molecular Cell Research*, 1843(12), 3018–3028. <http://doi.org/10.1016/j.bbamcr.2014.09.006>
- Priya, A., Johar, K., Nair, B., & Wong-Riley, M. T. T. (2014b). Specificity protein 4 (Sp4) regulates the transcription of AMPA receptor subunit GluA2 (Gria2). *BBA - Molecular Cell Research*, 1843(6), 1196–1206. <http://doi.org/10.1016/j.bbamcr.2014.02.008>
- Quinlan, E. M., Olstein, D. H., & Bear, M. F. (1999a). Bidirectional, experience-dependent regulation of N-methyl-D-aspartate receptor subunit composition in the rat visual cortex during postnatal development. *Proceedings of the National Academy of Sciences*, 96(22), 12876–12880.
- Quinlan, E. M., Philpot, B. D., Haganir, R. L., & Bear, M. F. (1999b). Rapid, experience-dependent expression of synaptic NMDA receptors in visual cortex in vivo. *Nature Neuroscience*, 2(4), 352–357. <http://doi.org/10.1038/7263>
- Raiker, S. J., Lee, H., Baldwin, K. T., Duan, Y., Shrager, P., & Giger, R. J. (2010). Oligodendrocyte-Myelin Glycoprotein and Nogo Negatively Regulate Activity-Dependent Synaptic Plasticity. *Journal of Neuroscience*, 30(37), 12432–12445. <http://doi.org/10.1523/JNEUROSCI.0895-10.2010>
- Ranson, A., Sengpiel, F., & Fox, K. (2013). The Role of GluA1 in Ocular Dominance Plasticity in the Mouse Visual Cortex. *Journal of Neuroscience*, 33(38), 15220–15225. <http://doi.org/10.1523/JNEUROSCI.2078-13.2013>
- Roberts, E. B., & Ramoa, A. S. (1999). Enhanced NR2A subunit expression and decreased NMDA receptor decay time at the onset of ocular dominance plasticity in the ferret. *Journal of Neurophysiology*, 81(5), 2587–2591.
- Rosenmund, C., Stern-Bach, Y., & Stevens, C. F. (1998). The tetrameric structure of a glutamate receptor channel. *Science*, 280(5369), 1596–1599. <http://doi.org/10.1126/science.280.5369.1596>
- Rousselet, G. A., Gaspar, C. M., Pernet, C. R., Husk, J. S., Bennett, P. J., & Sekuler, A. B. (2010). Healthy aging delays scalp EEG sensitivity to noise in a face discrimination task. *Frontiers in Psychology*, 1, 19. <http://doi.org/10.3389/fpsyg.2010.00019>
- Rowley, C. D., Sehmbi, M., Bazin, P.-L., Tardif, C. L., Minuzzi, L., Frey, B. N., & Bock, N. A. (2017). Age-related mapping of intracortical myelin from late adolescence to middle adulthood using T 1-weighted MRI. *Human Brain Mapping*, 37, 1573–13. <http://doi.org/10.1002/hbm.23624>

- Sans, N., Vissel, B., Petralia, R. S., Wang, Y. X., Chang, K., Royle, G. A., et al. (2003). Aberrant formation of glutamate receptor complexes in hippocampal neurons of mice lacking the GluR2 AMPA receptor subunit. *Journal of Neuroscience*, 23(28), 9367–9373.
- Sasaki, Y., Nanez, J. E., & Watanabe, T. (2009). Advances in visual perceptual learning and plasticity. *Nature Reviews Neuroscience*, 11(1), 53–60. <http://doi.org/10.1038/nrn2737>
- Schrauf, M., Wist, E. R., & Ehrenstein, W. H. (1999). Development of dynamic vision based on motion contrast. *Experimental Brain Research*, 124(4), 469–473.
- Segalowitz, S. J., Sternin, A., Lewis, T. L., Dywan, J., & Maurer, D. (2017). Electrophysiological evidence of altered visual processing in adults who experienced visual deprivation during infancy. *Developmental Psychobiology*, 59(3), 375–389. <http://doi.org/10.1002/dev.21502>
- Sekuler, R., Hutman, L. P., & Owsley, C. J. (1980). Human aging and spatial vision. *Science*, 209(4462), 1255–1256.
- Sheng, M., Cummings, J., Roldan, L. A., Jan, Y. N., & Jan, L. Y. (1994). Changing subunit composition of heteromeric NMDA receptors during development of rat cortex. *Nature*, 368(6467), 144–147. <http://doi.org/10.1038/368144a0>
- Shepherd, J. D., & Huganir, R. L. (2007). The Cell Biology of Synaptic Plasticity: AMPA Receptor Trafficking. *Annual Review of Cell and Developmental Biology*, 23(1), 613–643. <http://doi.org/10.1146/annurev.cellbio.23.090506.123516>
- Shepherd, J. D., Rumbaugh, G., Wu, J., Chowdhury, S., Plath, N., Kuhl, D., et al. (2006). Arc/Arg3.1 Mediates Homeostatic Synaptic Scaling of AMPA Receptors. *Neuron*, 52(3), 475–484. <http://doi.org/10.1016/j.neuron.2006.08.034>
- Shew, W. L., Yang, H., Petermann, T., Roy, R., & Plenz, D. (2009). Neuronal avalanches imply maximum dynamic range in cortical networks at criticality. *The Journal of Neuroscience : the Official Journal of the Society for Neuroscience*, 29(49), 15595–15600. <http://doi.org/10.1523/JNEUROSCI.3864-09.2009>
- Simic, N., & Rovet, J. (2016). Dorsal and ventral visual streams: Typical and atypical development. *Child Neuropsychology*, 1–14. <http://doi.org/10.1080/09297049.2016.1186616>
- Siu, C. R., Balsor, J. L., Jones, D. G., & Murphy, K. M. (2015). Classic and Golgi Myelin Basic Protein have distinct developmental trajectories in human visual cortex. *Frontiers in Neuroscience*, 9, 138–10. <http://doi.org/10.3389/fnins.2015.00138>
- Siu, C. R., Beshara, S. P., Jones, D. G., & Murphy, K. M. (2017). Development of Glutamatergic Proteins in Human Visual Cortex across the Lifespan. *The Journal of Neuroscience : the*

- Official Journal of the Society for Neuroscience*, 37(25), 6031–6042. <http://doi.org/10.1523/JNEUROSCI.2304-16.2017>
- Smith, A. C. W., Scofield, M. D., & Kalivas, P. W. (2015). The tetrapartite synapse_ Extracellular matrix remodeling contributes to corticoaccumbens plasticity underlying drug addiction. *Brain Research*, 1628(Part A), 29–39. <http://doi.org/10.1016/j.brainres.2015.03.027>
- Smith, A. T., Singh, K. D., Williams, A. L., & Greenlee, M. W. (2001). Estimating receptive field size from fMRI data in human striate and extrastriate visual cortex. *Cerebral Cortex*, 11(12), 1182–1190.
- SOKOL, S., & JONES, K. (1979). Implicit Time of Pattern Evoked-Potentials in Infants - Index of Maturation of Spatial Vision. *Vision Research*, 19(7), 747–755. [http://doi.org/10.1016/0042-6989\(79\)90150-0](http://doi.org/10.1016/0042-6989(79)90150-0)
- Sowell, E. R., Peterson, B. S., Thompson, P. M., Welcome, S. E., Henkenius, A. L., & Toga, A. W. (2003). Mapping cortical change across the human life span. *Nature Neuroscience*, 6(3), 309–315. <http://doi.org/10.1038/nn1008>
- Sowell, E. R., Thompson, P. M., Leonard, C. M., Welcome, S. E., Kan, E., & Toga, A. W. (2004). Longitudinal mapping of cortical thickness and brain growth in normal children. *The Journal of Neuroscience : the Official Journal of the Society for Neuroscience*, 24(38), 8223–8231. <http://doi.org/10.1523/JNEUROSCI.1798-04.2004>
- Stephany, C.-É., Ikrar, T., Nguyen, C., Xu, X., & McGee, A. W. (2016). Nogo Receptor 1 Confines a Disinhibitory Microcircuit to the Critical Period in Visual Cortex. *The Journal of Neuroscience : the Official Journal of the Society for Neuroscience*, 36(43), 11006–11012. <http://doi.org/10.1523/JNEUROSCI.0935-16.2016>
- Sun, Q., & Turrigiano, G. G. (2011). PSD-95 and PSD-93 Play Critical But Distinct Roles in Synaptic Scaling Up and Down. *Journal of Neuroscience*, 31(18), 6800–6808. <http://doi.org/10.1523/JNEUROSCI.5616-10.2011>
- Susilo, Germine, L., & Duchaine, B. (2013). Face recognition ability matures late: evidence from individual differences in young adults. *Journal of Experimental Psychology. Human Perception and Performance*, 39(5), 1212–1217. <http://doi.org/10.1037/a0033469>
- TAKASHIMA, S., Chan, F., Becker, L. E., & Armstrong, D. L. (1980). Morphology of the Developing Visual-Cortex of the Human Infant - a Quantitative and Qualitative Golgi-Study. *Journal of Neuropathology and Experimental Neurology*, 39(4), 487–501.
- Thorn, F., Gwiazda, J., Cruz, A. A., Bauer, J. A., & Held, R. (1994). The development of eye alignment, convergence, and sensory binocularity in young infants. *Investigative Ophthalmology & Visual Science*, 35(2), 544–553.

- Tomassy, G. S., Berger, D. R., Chen, H.-H., Kasthuri, N., Hayworth, K. J., Vercelli, A., et al. (2014). Distinct profiles of myelin distribution along single axons of pyramidal neurons in the neocortex. *Science*, 344(6181), 319–324. <http://doi.org/10.1126/science.1249766>
- Tootell, R. B. H., & Nasr, S. (2017). Columnar Segregation of Magnocellular and Parvocellular Streams in Human Extrastriate Cortex. *Journal of Neuroscience*, 0690–17–71. <http://doi.org/10.1523/JNEUROSCI.0690-17.2017>
- Tretter, V., Jacob, T. C., Mukherjee, J., Fritschy, J.-M., Pangalos, M. N., & Moss, S. J. (2008). The clustering of GABA(A) receptor subtypes at inhibitory synapses is facilitated via the direct binding of receptor alpha 2 subunits to gephyrin. *The Journal of Neuroscience : the Official Journal of the Society for Neuroscience*, 28(6), 1356–1365. <http://doi.org/10.1523/JNEUROSCI.5050-07.2008>
- Tretter, V., Kerschner, B., Milenkovic, I., Ramsden, S. L., Ramerstorfer, J., Saiepour, L., et al. (2011). Molecular basis of the γ -aminobutyric acid A receptor $\alpha 3$ subunit interaction with the clustering protein gephyrin. *The Journal of Biological Chemistry*, 286(43), 37702–37711. <http://doi.org/10.1074/jbc.M111.291336>
- Turrigiano, G. G., & Nelson, S. B. (2004). Homeostatic plasticity in the developing nervous system. *Nature Reviews Neuroscience*, 5(2), 97–107. <http://doi.org/10.1038/nrn1327>
- Tyagarajan, S. K., & Fritschy, J.-M. (2014). Gephyrin: a master regulator of neuronal function? *Nature Publishing Group*, 15(3), 141–156. <http://doi.org/10.1038/nrn3670>
- Tychsen, L., & Lisberger, S. G. (1986). Maldevelopment of visual motion processing in humans who had strabismus with onset in infancy. *Journal of Neuroscience*, 6(9), 2495–2508.
- Van Damme, K., Massie, A., Vandesande, F., & Arckens, L. (2003). Distribution of the AMPA2 glutamate receptor subunit in adult cat visual cortex. *Brain Research*, 960(1-2), 1–8.
- Van Essen, D. C., & Gallant, J. L. (1994). Neural mechanisms of form and motion processing in the primate visual system. *Neuron*, 13(1), 1–10.
- Vicini, S., Ferguson, C., Prybylowski, K., Kralic, J., Morrow, A. L., & Homanics, G. E. (2001). GABA(A) receptor alpha1 subunit deletion prevents developmental changes of inhibitory synaptic currents in cerebellar neurons. *The Journal of Neuroscience : the Official Journal of the Society for Neuroscience*, 21(9), 3009–3016.
- Wake, H., Lee, P. R., & Fields, R. D. (2011). Control of local protein synthesis and initial events in myelination by action potentials. *Science*, 333(6049), 1647–1651. <http://doi.org/10.1126/science.1206998>

- Wattam-Bell, J., Birtles, D., Nyström, P., Hofsten, von, C., Rosander, K., Anker, S., et al. (2010). Reorganization of Global Form and Motion Processing during Human Visual Development. *Current Biology*, 20(5), 411–415. <http://doi.org/10.1016/j.cub.2009.12.020>
- Wiese, S., Karus, M., & Faissner, A. (2012). Astrocytes as a source for extracellular matrix molecules and cytokines. *Frontiers in Pharmacology*, 3, 120. <http://doi.org/10.3389/fphar.2012.00120>
- WIESEL, T. N., & HUBEL, D. H. (1963). SINGLE-CELL RESPONSES IN STRIATE CORTEX OF KITTENS DEPRIVED OF VISION IN ONE EYE. *Journal of Neurophysiology*, 26, 1003–1017.
- Williams, K., Irwin, D. A., Jones, D. G., & Murphy, K. M. (2010). Dramatic Loss of Ube3A Expression during Aging of the Mammalian Cortex. *Frontiers in Aging Neuroscience*, 2, 18. <http://doi.org/10.3389/fnagi.2010.00018>
- Wilson, H. R., Mei, M., Habak, C., & Wilkinson, F. (2011). Visual bandwidths for face orientation increase during healthy aging. *Vision Research*, 51(1), 160–164. <http://doi.org/10.1016/j.visres.2010.10.026>
- Xu, L., Tanigawa, H., & Fujita, I. (2003). Distribution of alpha-amino-3-hydroxy-5-methyl-4-isoxazolepropionate-type glutamate receptor subunits (GluR2/3) along the ventral visual pathway in the monkey. *The Journal of Comparative Neurology*, 456(4), 396–407. <http://doi.org/10.1002/cne.10538>
- Xue, M., Atallah, B. V., & Scanziani, M. (2014). Equalizing excitation-inhibition ratios across visual cortical neurons. *Nature*, 511(7511), 596–600. <http://doi.org/10.1038/nature13321>
- Yashiro, K., & Philpot, B. D. (2008). Regulation of NMDA receptor subunit expression and its implications for LTD, LTP, and metaplasticity. *Neuropharmacology*, 55(7), 1081–1094. <http://doi.org/10.1016/j.neuropharm.2008.07.046>
- Ye, Q., & Miao, Q.-L. (2013). Experience-dependent development of perineuronal nets and chondroitin sulfate proteoglycan receptors in mouse visual cortex. *Matrix Biology*, 32(6), 352–363. <http://doi.org/10.1016/j.matbio.2013.04.001>
- Yoshimura, Y., Ohmura, T., & Komatsu, Y. (2003). Two forms of synaptic plasticity with distinct dependence on age, experience, and NMDA receptor subtype in rat visual cortex. *Journal of Neuroscience*, 23(16), 6557–6566.
- Yu, S., Wang, Y., Li, X., Zhou, Y., & Leventhal, A. G. (2006). Functional degradation of extrastriate visual cortex in senescent rhesus monkeys. *Neuroscience*, 140(3), 1023–1029. <http://doi.org/10.1016/j.neuroscience.2006.01.015>

- Yu, W., Jiang, M., Miralles, C. P., Li, R.-W., Chen, G., & de Blas, A. L. (2007). Gephyrin clustering is required for the stability of GABAergic synapses. *Molecular and Cellular Neuroscience*, 36(4), 484–500. <http://doi.org/10.1016/j.mcn.2007.08.008>
- Zhang, Z., & Sun, Q.-Q. (2011). Development of NMDA NR2 subunits and their roles in critical period maturation of neocortical GABAergic interneurons. *Developmental Neurobiology*, 71(3), 221–245. <http://doi.org/10.1002/dneu.20844>